

**A RESEARCH ON PRODUCTION OPTIMIZATION OF COUPLED SURFACE AND
SUBSURFACE MODEL**

A Thesis

by

SEVAPHOL IEMCHOLVILERT

Submitted to the Office of Graduate Studies of
Texas A&M University
in partial fulfillment of the requirements for the degree of

MASTER OF SCIENCE

Chair of Committee,	Eduardo Gildin
Committee Members,	Ding Zhu
	Yalchin Efendiev
Head of Department,	Daniel Hill

August 2013

Major Subject: Petroleum Engineering

Copyright 2013 Sevaphol Iemcholvilert

ABSTRACT

One of the main objectives in the Oil & Gas Industry is to constantly improve the reservoir management capabilities by using production optimization strategies that can positively impact the so-called net-present value (NPV) of a given project. In order to achieve this goal the industry is faced with the difficult task of maximizing hydrocarbon production and minimizing unwanted fluids, such as water, while sustaining or even enhancing the reservoir recovery factor by handling properly the fluids at surface facilities. A key element in this process is the understanding of the interactions between subsurface and subsurface dynamics in order to provide insightful production strategies which honor reservoir management surface facility constraints. The implementation of the ideal situation of fully coupling surface/subsurface has been hindered by the required computational efforts involved in the process. Consequently, various types of partially coupling that require less computational efforts are practically implemented. Due to importance of coupling surface and subsurface model on production optimization and taking the advantage of advancing computational performance, this research explores the concept of surface and subsurface model couplings and production optimization.

The research aims at demonstrating the role of coupling of surface and subsurface model on production optimization under simple production constraint (i.e. production and injection pressure limit). The normal production prediction runs with various reservoir description (homogeneous-low permeability, homogeneous-high permeability, and heterogeneous permeability) and different fluid properties (dead-oil

PVT and lived-oil PVT) were performed in order to understand the effect of coupling level, and coupling scheme with different reservoir descriptions and fluid properties on production and injection rate prediction. The result shows that for dead-oil PVT, the production rate from different coupling schemes in homogeneous and heterogeneous reservoir is less sensitive than lived-oil PVT cases. For lived-oil PVT, the production rate from different coupling schemes in homogeneous high permeability and heterogeneous permeability are more sensitive than homogeneous low permeability. The production optimization on water flooding under production and injection constraint cases is considered here also.

DEDICATION

To my family and friends

ACKNOWLEDGEMENTS

I would like to thank my committee chair, Dr. Gildin and my committee members, Dr. Zhu and Dr. Efendiev, for their guidance and support throughout the course of this research.

Thanks also go to my friends and colleagues and the department faculty and staff for making my time at Texas A&M University a great experience. I also want to extend my gratitude to PTT Exploration and Production Public Company Limited, my employer, which granted the scholarship and supported me throughout my graduate program. More importantly, I'm really appreciate to be a part of Thai Student Association at TAMU club and would like to say thank you every Thai people in the club for making College station to be like my second home.

Finally, thanks to my mother and father for their encouragement and to my sister for her moral support.

NOMENCLATURE

J	Jacobian Matrix
$J^{(v)}$	Jacobian Matrix at v th Newton - Raphson's Iteration
R	Residual Vector
R^{n+1*}	Residual Vector at * th Newton - Raphson's Iteration
R_f	Residual Vector of the Surface Flow Equation
R_r	Residual Vector of the Subsurface Flow Equation
R_o	Residual Vector of Oil Flow Equation
R_w	Residual Vector of Water Flow Equation
R_g	Residual Vector of Gas Flow Equation
∂x_f	Solution Vector of Newton Linearization of the Surface Flow
∂x_r	Solution Vector of Newton Linearization of the Subsurface Flow
ρ_o	Oil Density
ρ_w	Water Density
ρ_g	Gas Density
ρ_{Go}	Solution Gas Density
k_{ro}	Relative Permeability to Oil
k_{rw}	Relative Permeability to Water
k_{rg}	Relative Permeability to Gas
k	Total Permeability

k_x	Permeability in the X - Direction
k_y	Permeability in the Y - Direction
μ_o	Oil Viscosity
μ_w	Water Viscosity
μ_g	Gas Viscosity
μ_{Go}	Solution Gas Viscosity
ϕ	Porosity
g	Gravitational Acceleration
x	Distance in X - Direction in the Cartesian Coordinate
y	Distance in Y- Direction in the Cartesian Coordinate
z	Distance in Z- Direction in the Cartesian Coordinate
p_o	Oil Phase Pressure
p_w	Water Phase Pressure
p_g	Gas Phase Pressure
S_o	Oil Phase Saturation
S_w	Water Phase Saturation
S_g	Gas Phase Saturation
t	Time
\widetilde{q}_o	Oil Phase Mass Flow Rate
\widetilde{q}_w	Water Phase Mass Flow Rate
\widetilde{q}_g	Gas Phase Mass Flow Rate

q_o^*	Oil Phase Volume Flow Rate
q_w^*	Water Phase Volume Flow Rate
q_g^*	Gas Phase Volume Flow Rate
q_{fg}^*	Volume Flow Rate of Free Gas
P_{cow}	Oil-Water Capillary Pressure
P_{cgo}	Gas-Oil Capillary Pressure
λ_o	Oil Phase Transmissibility
λ_{ox}	Oil Phase Transmissibility in X - Direction
λ_{oy}	Oil Phase Transmissibility in Y - Direction
λ_{oz}	Oil Phase Transmissibility in Z - Direction
λ_w	Water Phase Transmissibility
λ_{wx}	Water Phase Transmissibility in X- Direction
λ_{wy}	Water Phase Transmissibility in Y - Direction
λ_{wz}	Water Phase Transmissibility in Z - Direction
λ_g	Gas Phase Transmissibility
λ_{gx}	Gas Phase Transmissibility in X- Direction
λ_{gy}	Gas Phase Transmissibility in Y- Direction
λ_{gz}	Gas Phase Transmissibility in Z- Direction
γ_o	Oil Phase Hydrostatic Gradient
γ_w	Water Phase Hydrostatic Gradient
γ_g	Gas Phase Hydrostatic Gradient

i, j, k	Subscript Specified the Properties of Superscript at Location (i, j, k)
$i + \frac{1}{2}, j, k$	Subscript Specified the Properties of Superscript Evaluated at Location (i, j, k) and (i+1, j, k)
$i, j + \frac{1}{2}, k$	Subscript Specified the Properties of Superscript Evaluated at Location (i, j, k) and (i, j+1, k)
$i, j, k + \frac{1}{2}$	Subscript Specified the Properties of Superscript Evaluated at Location (i, j, k) and (i, j, k+1)
$i - \frac{1}{2}, j, k$	Subscript Specified the Properties of Superscript Evaluated at Location (i, j, k) and (i-1, j, k)
$i, j - \frac{1}{2}, k$	Subscript Specified the Properties of Superscript Evaluated at Location (i, j, k) and (i, j-1, k)
$i, j, k - \frac{1}{2}$	Subscript Specified the Properties of Superscript Evaluated at Location (i, j, k) and (i, j, k-1)
R_{SO}	Solution Gas - Oil Ratio
B_o	Oil Formation Volume Factor
B_w	Water Formation Volume Factor
B_g	Gas Formation Volume Factor
WI	Peaceman's Well Index
r_o	Equivalent Gridblock Radius
r_w	Wellbore Radius

p_{wf}	Bottomhole Flowing Pressure
h	Reservoir Thickness
s	Skin Factor
p_b	Bubble Point Pressure
U^{n+1}	State Vector of Current Time step
U^{n+1*}	State Vector of Current Time step at *th Newton - Raphson's Iteration
δU	Correction Vector of Newton - Raphson's Linearization
P_{sep}	Separator Pressure
$\left(\frac{dp}{dL}\right)_{elev}$	Pressure Loss Gradient from Elevation Change
$\left(\frac{dp}{dL}\right)_f$	Pressure Loss Gradient from Friction
$\left(\frac{dp}{dL}\right)_{acc}$	Pressure Loss Gradient from Acceleration
g_c	Conversion Factor in Newton's Second Law of Motion
θ	Theta Angle
ρ_m	Density of the Gas/Liquid Mixture in the Pipe Element
ρ_L	Density of Liquid in the Pipe Element
ρ_m	Density of Gas in the Pipe Element
λ_L	Liquid Holdup in the Pipe Element
λ_G	Gas Holdup in the Pipe Element
f	Friction Factor
v	Velocity of Fluid in the Pipe Element

d	Pipe Diameter
$\left(\frac{dv}{dL}\right)$	Acceleration Term
N_{FR}	Froude Number
O^n	Objective Function at Time step n
O	Summation of Objective Function
L	Lagrange Function
d	Discount Factor
r_o	Oil Revenue
r_g	Gas Revenue
c_{pw}	Water Production Cost
c_{iw}	Water Injection Cost
Q_o	Oil Production Rate
Q_w	Water Production Rate
Q_g	Gas Production Rate
Q_{pw}	Water Production Rate
Q_{iw}	Water Injection Rate
x^n	State Variable Vector at Time step n
u^n	Control Vector at Time step n
$c^n(x^{n+1}, u^n)$	Inequality Constraint Function
LB	Lower Bound Value
UB	Upper Bound Value

λ^n	Lagrange Multiplier
u_{opt}^n	Optimal Control Vector
<i>IAM</i>	Integrated Asser Model
<i>BHP</i>	Bottomhole Pressure
<i>THP</i>	Tubing Head Pressure
GOR	Gas-Oil Ratio
<i>NPV</i>	Net Present Value
<i>VLP</i>	Vertical Lift Performance Relationship
<i>IPR</i>	Inflow Performance Relationship
<i>OOIP</i>	Original Oil In-Place

TABLE OF CONTENTS

	Page
ABSTRACT	ii
DEDICATION	iv
ACKNOWLEDGEMENTS	v
NOMENCLATURE	vi
TABLE OF CONTENTS	xiii
LIST OF FIGURES	xvi
LIST OF TABLES	xxiv
1. INTRODUCTION	1
1.1 Objective	3
1.2 Coupling Surface and Subsurface Model	4
1.3 Surface and Subsurface Model Coupling Scheme	5
1.3.1 Explicit Coupling Scheme	5
1.3.2 Implicit Coupling Scheme	6
1.3.3 Fully Implicit Coupling Scheme	6
2. LITERATURE REVIEWS	8
2.1 Advanced Well Modeling	9
2.2 Coupling Surface and Subsurface Model	11
3. SURFACE & SUBSURFACE MODELING AND COUPLING MECHANISMS	14
3.1 Subsurface Modeling	14
3.1.1 Oil Flow Equation Discretization	18
3.1.2 Water Flow Equation Discretization	21
3.1.3 Gas Flow Equation Discretization	23
3.1.4 Treatment of Saturated and Undersaturated State of Reservoir ..	27
3.1.5 Newton-Raphson Linearization	27

	Page
3.2 Multiphase Flow in Wells and Pipes Modeling	32
3.2.1 Pressure Loss in Wells and Pipes Model	34
3.2.2 Two Phases Flow Regimes in Vertical Flow	36
3.2.3 Two Phases Flow Regimes in Horizontal Flow	37
3.2.4 Pressure Gradient Correlations.....	40
3.2.4.1 The Beggs and Brill Method	40
3.2.4.2 The Petroleum Expert 2 Correlation	42
3.3 Surface and Subsurface Model Coupling Mechanism	43
3.3.1 Explicit Coupling Scheme.....	43
3.3.2 Implicit Coupling Scheme.....	46
3.3.3 Fully Implicit Coupling Scheme	49
4. PRODUCTION PREDICTION OF COUPLED SURFACE AND SUBSURFACE MODELS	51
4.1 Surface and Subsurface Simulation Software for Coupling.....	51
4.1.1 Subsurface Simulation Software for Coupling.....	51
4.1.2 Commercial Surface Simulation Software.....	57
4.2 Effect of Various Coupling Level and Scheme with Different Reservoir Descriptions and Fluid Properties on Production Prediction	57
4.2.1 Sensitivity Parameters	58
4.2.2 Study Cases	66
4.3 Effect of the Original Oil In-Place (OOIP) Size	82
4.3.1 Production Scenario	84
4.3.2 Study Cases	84
4.4 Summary	88
5. MATLAB RESERVOIR SIMULATION TOOLBOX MODIFICATION FOR SURFACE AND SUBSURFACE MODEL COUPLING	90
5.1 MRST Fully Implicit Multiphase Solver Routine Modification.....	90
5.1.1 Fast PI Balancing Algorithm.....	93
5.1.2 Modification for Explicit Coupling.....	94
5.1.3 Modification for Implicit Coupling.....	96
5.2 Comparison of Simulation Result from Modified MRST & ECLIPSE100 with Network Options	97
5.2.1 No Coupling Case	98
5.2.2 Implicit Coupling Case.....	100

	Page
5.3 Effect of VLP Table Discretization Scheme on Simulation Result	108
5.3.1 Downstream Production Pressure Discretization	108
5.3.2 Water Cut Discretization	109
5.3.3 Gas-Oil Ratio Discretization	110
5.3.4 Simulation Result Using Different Discretization Scheme	111
6. EFFECT OF COUPLING SCHEME ON PRODUCTION OPTIMIZATION OF COUPLED SURFACE AND SUBSURFACE MODEL	113
6.1 Objective Function Formulation	113
6.2 Gradient Based Optimization Method	115
6.2.1 Gradients with Adjoint Model	116
6.2.2 Sequential Quadratic Programing (SQP)	118
6.3 MRST Module for Finding Gradients with Adjoint Model	120
6.4 Investigation of the Effect of Various Coupling Level and Scheme on Production Optimization	124
6.4.1 Direct Line Drive Water Flooding	129
6.4.1.1 Explicit Coupling Case	129
6.4.1.2 Implicit Coupling Case	131
6.4.1.3 Coupling Surface and Subsurface Model in the Optimization Framework	131
6.4.1.4 Comparison of Explicit and Implicit Coupling Case	135
6.4.2 5-Spots Pattern Water Flooding	148
6.4.2.1 Explicit Coupling Case	148
6.4.2.2 Implicit Coupling Case	149
6.4.2.3 Coupling Surface and Subsurface Model in the Optimization Framework	150
6.4.2.4 Comparison of Explicit and Implicit Coupling Case	152
6.5 Optimization Using Explicit Coupling Model - Prediction Using Implicit Coupling Model	177
6.5.1 Direct Line Drive Water Flooding	177
6.5.2 5-Spots Pattern Water Flooding	178
7. CONCLUSIONS AND RECOMENDATIONS	186
7.1 Summary	186
7.2 Future Works	191
REFERENCES	193

LIST OF FIGURES

	Page
Figure 1 Coupled surface and subsurface model.....	5
Figure 2 Multiphase flow through porous media	15
Figure 3 Flowchart explaining Newton-Raphson method	28
Figure 4 Schematic of production system and associated pressure loss (Source: Beggs (2003)).....	33
Figure 5 Flow regime in vertical flow (Source: Economides (1993))	37
Figure 6 Flow regime in horizontal flow (Source: Economides (1993)).....	39
Figure 7 Explicit coupling scheme.....	45
Figure 8 Implicit coupling scheme.....	48
Figure 9 Fully implicit coupling scheme.....	50
Figure 10 Example of the intersection of wellbore curve and pipeline curve (Source: ECLIPSE100's manual)	52
Figure 11 The example of available add-on module in MRST (Source: MRST's Website).....	56
Figure 12 Oil-Water relative permeability	59
Figure 13 Gas-Oil relative permeability.....	59
Figure 14 Surface model of production and injection facilities	60
Figure 15 Schematic of explicit coupling in every 15 days (Source: AVOCET's manual).....	62
Figure 16 Schematic of explicit coupling in every time step (Source: AVOCET's manual).....	63

	Page
Figure 17 Schematic of implicit coupling in every first three Newton iteration (Source: AVOCET's manual).....	64
Figure 18 The permeability of reservoir model in the case of heterogeneous permeability (left) and homogeneous permeability (right).....	65
Figure 19 Oil production profile and bottomhole pressure of homogeneous high perm – lived oil PVT case.....	67
Figure 20 Water injection profile and bottomhole pressure of homogeneous high perm – lived oil PVT case.....	68
Figure 21 Oil production profile and bottomhole pressure of homogeneous low perm – lived oil PVT case.....	70
Figure 22 IPR of high and low permeability reservoir.....	70
Figure 23 Water injection profile and bottomhole pressure of homogeneous low perm – lived oil PVT case.....	71
Figure 24 Oil production profile and bottomhole pressure of PROD-1 for heterogeneous perm – lived oil PVT case.....	73
Figure 25 Oil production profile and bottomhole pressure of PROD-2 for heterogeneous perm – lived oil PVT case.....	73
Figure 26 Water Injection profile and bottomhole pressure of INJ-1 for heterogeneous perm – lived oil PVT case.....	74
Figure 27 Water Injection profile and bottomhole pressure of INJ-2 for heterogeneous perm – lived oil PVT case.....	74
Figure 28 Oil production profile and bottomhole pressure of homogeneous high perm – dead oil PVT case.....	76
Figure 29 Water injection profile and bottomhole pressure of homogeneous high perm – dead oil PVT case.....	77
Figure 30 Oil production profile and bottomhole pressure of homogeneous low perm – dead oil PVT case.....	78

	Page
Figure 31 Water injection profile and bottomhole pressure of homogeneous low perm – dead oil PVT case	79
Figure 32 Oil production profile and bottomhole pressure of PROD-1 for heterogeneous perm – dead oil PVT case	80
Figure 33 Oil production profile and bottomhole pressure of PROD-2 for heterogeneous perm – dead oil PVT case	81
Figure 34 Water injection profile and bottomhole pressure of INJ-1 for heterogeneous perm – dead oil PVT case	81
Figure 35 Water injection profile and bottomhole pressure of INJ-2 for heterogeneous perm – dead oil PVT case	82
Figure 36 Oil production profile and bottomhole pressure of large OGIP reservoir with homogeneous high perm – live oil PVT case	85
Figure 37 Water injection profile and bottomhole pressure of large OGIP reservoir with homogeneous high perm – live oil PVT case	85
Figure 38 Oil production profile and bottomhole pressure of PROD-1 of large OOIP reservoir with heterogeneous perm – lived oil PVT case	86
Figure 39 Oil production profile and bottomhole pressure of PROD-2 of large OOIP reservoir with heterogeneous perm – lived oil PVT case	87
Figure 40 Water injection profile and bottomhole pressure of INJ-1 of large OOIP reservoir with heterogeneous perm – lived oil PVT case	87
Figure 41 Water injection profile and bottomhole pressure of INJ-2 of large OOIP reservoir with heterogeneous perm – lived oil PVT case	88
Figure 42 Flowchart of MRST fully implicit multiphase solver routine	91
Figure 43 Detailed structure of MRST fully implicit multiphase solver routine	92
Figure 44 Example of Fast PI balancing scheme	93
Figure 45 Detailed structure of modified MRST fully implicit multiphase solver routine for explicit coupling.....	95

	Page
Figure 46 Detailed structure of modified MRST fully implicit multiphase solver routine for implicit coupling	97
Figure 47 Comparison of MRST and ECLIPSE's production and injection profile of no coupling case.....	100
Figure 48 Reservoir simulation model with direct line drive water flooding	103
Figure 49 Reservoir simulation model with 5-spots pattern water flooding.....	103
Figure 50 Comparison of modified MRST and ECLIPSE's production/injection profile of implicit coupling case for direct line drive water flooding.....	105
Figure 51 Comparison of modified MRST and ECLIPSE's injection profile of implicit coupling case for 5-spots water flooding.....	106
Figure 52 Comparison of modified MRST and ECLIPSE's production profile of implicit coupling case for 5-spots water flooding.....	107
Figure 53 VLP of various downstream pressure using linear spacing and geometric spacing	109
Figure 54 VLP of various water cut using linear spacing and geometric spacing.....	110
Figure 55 VLP of various gas-oil ratio using linear spacing and geometric spacing	111
Figure 56 Comparison of production profile of coupling surface and subsurface model using different gas-oil ratio discretization	112
Figure 57 MRST module for finding gradients with adjoint model.....	121
Figure 58 Modified MRST module for finding gradients with adjoint model.....	122
Figure 59 Example of method finding numerical $\frac{\delta BHP}{\delta THP}$	123
Figure 60 Reservoir simulation model with direct line drive water flooding	126
Figure 61 Reservoir simulation model with 5-spots water flooding	126
Figure 62 Comparison of base case and optimized case of direct line drive water flooding production profiles using explicit coupling.....	137

	Page
Figure 63 Comparison of base case and optimized case of direct line drive water flooding production profiles using explicit coupling.....	138
Figure 64 Comparison of base case and optimized case of direct line drive water flooding production profiles using implicit coupling	139
Figure 65 Comparison of base case and optimized case of direct line drive water flooding injection profiles using implicit coupling.....	140
Figure 66 Comparison of no coupled (estimated lower and upper bound) and implicit coupled optimization production profiles for the case of direct line drive water flooding.....	141
Figure 67 Comparison of no coupled (estimated lower and upper bound) and implicit coupled optimization injection profiles for the case of direct line drive water flooding.....	142
Figure 68 Comparison of no coupled (known lower and upper bound) and implicit coupled optimization production profiles for the case of direct line drive water flooding.....	143
Figure 69 Comparison of no coupled (known lower and upper bound) and implicit coupled optimization injection profiles for the case of direct line drive water flooding.....	144
Figure 70 Comparison of explicit coupled and implicit coupled optimization production profiles for the case of direct line drive water flooding	145
Figure 71 Comparison of explicit coupled and implicit coupled optimization injection profiles for the case of direct line drive water flooding.....	146
Figure 72 Comparison of explicit coupled and implicit coupled cumulative production & injection volume and average reservoir pressure for the case of direct line drive water flooding.....	147
Figure 73 Comparison of base case and optimized case of 5-spots pattern water flooding oil production profiles using explicit coupling.....	155
Figure 74 Comparison of base case and optimized case of 5-spots pattern water flooding bottomhole flowing pressure using explicit coupling	156

	Page
Figure 75 Comparison of base case and optimized case of 5-spots pattern water flooding production profiles using explicit coupling	157
Figure 76 Comparison of base case and optimized case of 5-spots pattern water flooding injection profiles using explicit coupling	158
Figure 77 Comparison of base case and optimized case of 5-spots pattern water flooding oil production profiles using implicit coupling	159
Figure 78 Comparison of base case and optimized case of 5-spots pattern water flooding bottomhole production pressure using implicit coupling ..	160
Figure 79 Comparison of base case and optimized case of 5-spots pattern water flooding production profiles using implicit coupling	161
Figure 80 Comparison of base case and optimized case of 5-spots pattern water flooding injection profiles using implicit coupling.....	162
Figure 81 Comparison of no coupled (estimated lower and upper bound) and implicit coupled optimization oil production profiles for the case of 5-spots pattern water flooding	163
Figure 82 Comparison of no coupled (estimated lower and upper bound) and implicit coupled optimization bottomhole production pressure for 5-spots pattern water flooding.....	164
Figure 83 Comparison of no coupled (estimated lower and upper bound) and implicit coupled optimization GOR and water cut for 5-spots pattern water flooding	165
Figure 84 Comparison of no coupled (estimated lower and upper bound) and implicit coupled optimization injection profile for 5-spots pattern water flooding	166
Figure 85 Comparison of no coupled (known lower and upper bound) and implicit coupled optimization oil production profiles for 5-spots pattern water flooding	167
Figure 86 Comparison of no coupled (known lower and upper bound) and implicit coupled optimization bottomhole production pressure for 5-spots pattern water flooding	168

	Page
Figure 87 Comparison of no coupled (known lower and upper bound) and implicit coupled optimization GOR and water cut for 5-spots pattern water flooding	169
Figure 88 Comparison of no coupled (known lower and upper bound) and implicit coupled optimization water injection profile for 5-spots pattern water flooding	170
Figure 89 Comparison of explicit coupled and implicit coupled optimization oil production profiles for 5-spots pattern water flooding	171
Figure 90 Comparison of explicit coupled and implicit coupled optimization bottomhole production pressure for 5-spots pattern water flooding	172
Figure 91 Comparison of explicit coupled and implicit coupled optimization GOR, water cut and pressure for 5-spots pattern water flooding	173
Figure 92 Comparison of explicit coupled and implicit coupled optimization water injection profile for 5-spots pattern water flooding	174
Figure 93 Comparison of explicit coupled and implicit coupled optimization cumulative production and injection volume for 5-spots pattern water flooding	175
Figure 94 Comparison of explicit-implicit coupled and implicit coupled optimization production profiles for the case of direct line drive water flooding	179
Figure 95 Comparison of explicit-implicit coupled and implicit coupled optimization injection profiles for the case of direct line drive water flooding	180
Figure 96 Comparison of explicit-implicit coupled and implicit coupled optimization cumulative production & injection volume and average reservoir pressure for the case of direct line drive water flooding	181
Figure 97 Comparison of explicit-implicit coupled and implicit coupled optimization oil production profiles for the case of 5-spots pattern water flooding	182

	Page
Figure 98 Comparison of explicit-implicit coupled and implicit coupled optimization bottomhole production pressure profiles for the case of 5-spots pattern water flooding	183
Figure 99 Comparison of explicit-implicit coupled and implicit coupled optimization production profiles for the case 5-spots pattern water flooding	184
Figure 100 Comparison of explicit-implicit coupled and implicit coupled optimization injection profiles for the case 5-spots pattern water flooding	185

LIST OF TABLES

		Page
Table 1	Parameter for flow regime determination of Beggs and Brill method.....	41
Table 2	Summary of flow regime and correlation used in Petroleum Expert 2 correlation	42
Table 3	Summary of reservoir simulation model properties used in the 1st phase of the study.....	58
Table 4	Summary of surface facility model properties used in the 1st phase of the study.....	60
Table 5	Summary of parameter varied in the 1st phase of study	61
Table 6	Summary of reservoir simulation model properties used to study the effect of OOIP	83
Table 7	Summary of reservoir simulation model properties used to check the consistency between MRST and ECLIPSE100	98
Table 8	Summary of production strategies used to check the consistency between MRST and ECLIPSE100.....	99
Table 9	Summary of reservoir simulation model properties used to check the consistency between modified MRST and ECLIPSE100 & Network Option.....	101
Table 10	Summary of production strategy and surface model properties used to check the consistency between modified MRST and ECLIPSE100 & Network Option for direct line drive & 5-spots water flooding	102
Table 11	Reservoir simulation model properties for production optimization.....	125
Table 12	Fluid properties for production optimization	125
Table 13	Summary of cost and revenue assumption for production optimization ...	128

	Page
Table 14 Summary of lower bound and upper bound of upstream injection pressure and downstream production pressure	128
Table 15 Lower and upper bound of bottomhole production and injection pressures.....	132
Table 16 Estimated lower and upper bound of bottomhole production and injection pressures.....	134
Table 17 Summary of difference of total cumulative production and injection volume of production optimization using different coupling schemes.....	136
Table 18 Estimated lower and upper bound of bottomhole production and injection pressures.....	150
Table 19 Lower and upper bound of bottomhole production and injection pressures.....	152
Table 20 Summary of difference of total cumulative production and injection volume of production optimization using different coupling schemes.....	154
Table 21 Summary of computational time using in production optimization	176

1. INTRODUCTION

Production optimization has always become an important step in Oil & Gas field development production. Production optimization plays an important role in reservoir management improvement through finding the production strategies that leads to maximum so-called net-present value (NPV) of a given project. The NPV maximization can be done by minimizing undesirable fluid and maximizing hydrocarbon production by controlling surface production facility. One of the important elements to achieve this goal is the understanding of the connections and interactions between subsurface and surface dynamics so as to deliver insightful production strategies which honor reservoir management surface facility constraints. Interaction of subsurface and surface dynamics can be taken into account by coupling the surface and subsurface model.

Coupled surface and subsurface model can be done by using several options of coupling mechanism. The general concept of coupling surface and subsurface model is to link the surface and subsurface model by passing control parameter at the coupling point such as bottomhole flowing pressure and flow rate back and forth between surface and subsurface model. There are three main coupling mechanisms used in Oil & Gas industry, explicit coupling, implicit coupling, and fully implicit coupling. The fully implicit coupling mechanism is rarely used in Oil & Gas industry since this coupling scheme is the most complicated and computational expensive coupling scheme. The surface and subsurface model is treated as one domain such that the system of equations

of surface flow and system of equations of subsurface flow are solved simultaneously. The root cause of complexity and computational expensive of fully implicit coupling mechanism is treating the surface flow and subsurface flow to be a single system of equation. This can be done by treating nodes of surface facility as additional grid block of reservoir model which increase the number of unknown parameter in Newton Raphson linearization. The system of equations is solved simultaneously by Newton Raphson linearization which requires modification of original residual and jacobian matrix.

The practical coupling mechanisms used in the industry are implicit and explicit coupling mechanism. These two coupling mechanisms are different from fully implicit coupling as the surface and subsurface are treated as different domain. The major difference between explicit and implicit coupling mechanism is the treatment of well boundary condition of subsurface model. The well boundary condition for explicit coupling will be treated explicitly by obtaining it from surface and subsurface model balancing in the beginning of the time step while for the implicit coupling; surface and subsurface model are balanced in almost every Newton iteration step of Newton Raphson linearization process for solving the system of equation of subsurface model. These two mechanisms require less computational effort and have less structure complexity. Consequently, this research will focus on only implicit and explicit coupling mechanisms.

After the coupled surface and subsurface model with explicit and implicit coupling option is developed. The effect of coupling mechanism with several setting of

reservoir and fluid properties on normal production prediction can be investigated and use to design the case for production optimization to illustrate the importance of choosing coupling mechanism.

1.1. Objective

The popularity and importance of the application of coupled surface and subsurface models for production optimization is the motivation for this research. Since there are several choices to do coupling and each coupling mechanisms have their advantage and disadvantage. Consequently, the objective of this project is to investigate various surface and subsurface model coupling mechanisms applied in the Oil&Gas Industry. To this end, we will investigate the effect of various coupling levels, and coupling schemes on production optimization results and give recommendations on the critical point of coupling. To accomplish this objective, two main phases are to be completed. First, we construct a simple coupling model of water flooding scenario by using programming software (i.e. MATLAB®) or commercial software (i.e. ECLIPSE100 & Network option). The model obtained in this first task will be used to investigate the effect of various coupling levels, and coupling schemes with different reservoir descriptions and fluid properties on normal production prediction. In the second phase, the result from the first phase will be used to design the production optimization cases and resulting in recommendations on the critical point of coupling. The production & injection rate and economic results will be used as indicators on effectiveness of the various coupling mechanism discussed here.

1.2. Coupling Surface and Subsurface Model

In general, surface and subsurface models are modeled separately and treated as two different domains. The subsurface model is normally referred to reservoir simulation model and the surface model is referred to production network simulation. To make a realistic reservoir performance prediction in reservoir simulation, it is often necessary to connect the surface and subsurface model together in order to ensure that all of the production constraints from surface facilities are obeyed. Connecting of surface and subsurface models can be done by a process known as “Coupling”. The concept of coupling is shown in the Figure 1. The parameter that we use to connect surface and subsurface models is called control parameter. The “Coupling” can be done by passing the control parameter back and forth between surface and subsurface models. Normally, the control parameter used in “Coupling” is bottomhole pressure (BHP), tubinghead pressure (THP), and flow rate depend on where the coupling point and control parameter are used.

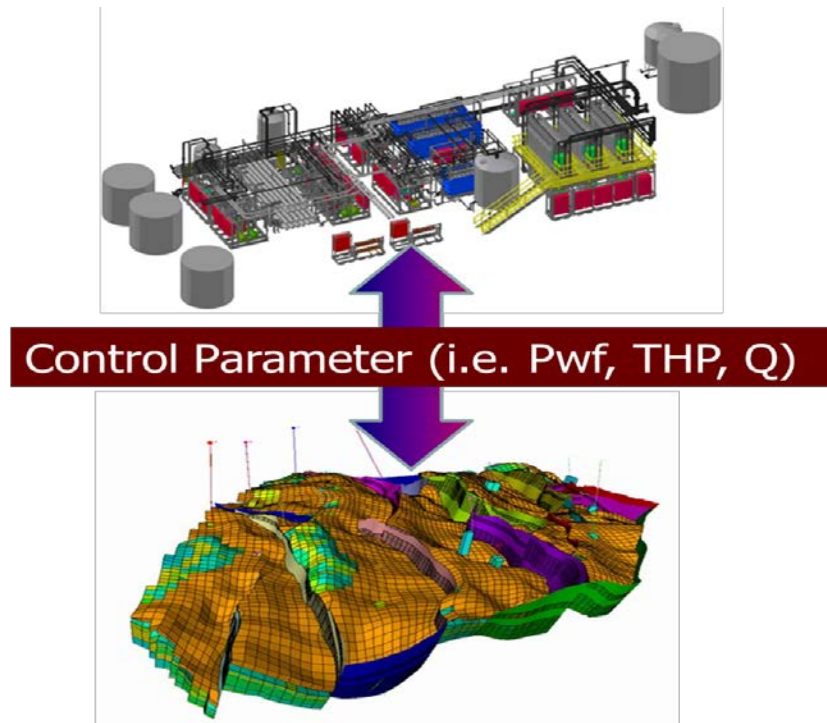


Figure 1: Coupled surface and subsurface model

1.3. Surface and Subsurface Model Coupling Scheme

There are three different types of coupling scheme that are generally used in the petroleum industry.

1.3.1. Explicit Coupling Scheme

The surface and subsurface are treated as different domain (domain decomposition) and the iterative process is simplified such that the boundary condition for subsurface model is treated explicitly. The subsurface model and surface model are solved at different time steps. Given the production rate from previous time step, the

pressure drop across surface facilities is calculated to give the value of bottomhole pressure (BHP). The BHP and well block pressure at the beginning of the time step will be used as input for well rate calculation. The iterative loop will be continued until the solution of well rate calculation and surface model is converged. The converged BHP will be used as boundary condition for subsurface model to solve for the production rate at current time step. It can be said that the system (surface and subsurface model) is balanced at the beginning of the time step to calculate the boundary condition for subsurface model, after subsurface model run the well rate will not consistent with the well rate at the beginning of the time step as the gridblock condition is changed.

1.3.2. Implicit Coupling Scheme

The surface and subsurface are treated as different domain as same as the explicit coupling method but the subsurface model becomes a part of the Newton iterative process. The implicit method can lead to high computational time. So, the domain decomposition technique is use to accelerate the convergence speed. The main idea of this technique is to separate subsurface domain into reservoir subdomain and well subdomain. The well subdomains contain just only small portion of subsurface model and only the well subdomain will be include in first iterative loop to find boundary condition for the remaining part of reservoir subdomain.

1.3.3. Fully Implicit Coupling Scheme

The surface and subsurface model is treated as one domain such that the system of equations of surface facility and system of equations of subsurface flow are solved simultaneously by considering nodes of surface facility as additional grid block of

reservoir model. Normally, the system of equation will be linearized and solved by Newton iteration which requires the knowledge of derivatives to form a Jacobian matrix (J). The set of matrix below shows the general structure of Newton linearization ($\partial x = J^{-1}R$)

$$\begin{bmatrix} \partial x_f \\ \partial x_r \end{bmatrix} = \begin{bmatrix} A_f & \dots \\ \dots & A_r \end{bmatrix}^{-1} \begin{bmatrix} R_f \\ R_r \end{bmatrix}$$

The R_f and R_r represent subvector of Residual vector while the A_f and A_r represent submatrix of Jacobian matrix derived from the system of equation of the surface model and subsurface model, respectively. The vector ∂x_f & ∂x_r represent subvector of the solution vector of Newton linearization of the surface and subsurface model equations. In each Newton iteration step, the vector ∂x_f and ∂x_r will be solved. The iterative process will be stopped when Newton iteration is converged.

2. LITERATURE REVIEWS

In this session, we briefly review the field developments in two main areas: advanced well modeling and coupling surface and subsurface models. They will set the background material for the developments in this thesis.

In addition to advanced well modeling, there have been developments of coupling surface and subsurface model. Normally, the surface and subsurface model are decoupled from each other for the sake of simplification. The surface and subsurface model are decoupled at well boundary condition. The importance of coupled model is pointed out here. In history matching process, there is no issue of inconsistent well boundary conditions between surface and subsurface model because the well boundary conditions (well production rate or bottomhole flowing pressure) is known (from hard data such as production test and pressure test). However, in the predictive processes, the well boundary condition is unknown and depends on reservoir behavior and surface facility performance. This may lead to inconsistent of well boundary conditions between surface and subsurface model because it is possible that either reservoir deliverability or surface facility performance cannot deliver the specified well boundary condition.

Moreover, coupling surface and subsurface model can play a major role in field production optimization. Normally, the subsurface model is only used in the reservoir performance optimization. The surface model is used as a tool for surface facility capability optimization. Both of these aspects have the common goal of production optimization. However, using the models separately does not guarantee that both aspects

will be achieved. Consequently, the coupling is necessary in field production optimization.

To take an advantage of coupled models, many authors have presented method for simultaneous solving the system of equation of surface and subsurface model. Some of publications are presented in these sections.

2.1. Advanced Well Modeling

In the past decade, there have been several developments of advanced well modeling which can be viewed a precursor of coupling surface and subsurface models. The model is mainly used in order to support the invention of multilateral wells, horizontal wells and even intelligence wells which has complex well configurations.

Holmes (1983) presented fully implicit three dimensional black oil simulator that use three variables in each well instead of single variable (bottomhole pressure). The two additional variables are used to describe fluid content in the wellbore which can be used for crossflow calculation in the wellbore. This model is a good starting point to consider the effect of surface facility dynamic (although it is just wellbore model) on subsurface model.

Stone et al. (1989) created a fully implicit three phases, three dimensional dead-oil thermal numerical model that coupling wellbore and tubing model with reservoir model. Reservoir mass and energy balance, transport equation in pipe (energy, momentum, and mass balance) were solved simultaneously using Newton iteration. The model faces some stability issues. The time step size is too small when the flow in

wellbore cannot reach quasi steady-state. The flow regime calculation is unstable in the transition lead to convergence problem.

Holmes et al. (1998) established a more comprehensive model from the work in 1983. The model can determine pressure lost due to friction and able to determine more accurate crossflow. The model is fully coupled, implicit three phases, three dimensional black oil numerical that fully couple segmented wellbore and tubing with reservoir model. The system of equations comprise 3 phases (oil, gas, and water) mass balance equations, hydraulic equation for calculating pressure lost in each segment, and constraint equations. Four variables are included for each well segmented. The concept can be extended to compositional simulator. The system of equations is linearized by using Newton-Raphson scheme. The continuous & differentiable of the pressure loss and flow rate correlation is necessary condition for implicit numerical calculation. The continuity requirement rules out many of the correlations which based on flow regime as they tend to be discontinuous across the flow regime boundaries. The enhanced version of previous work is the thermal simulation with multisegment well which incorporates heat transfer equation.

2.2. Coupling Surface and Subsurface Model

Dempsey et al. (1971) published the coupling of a simple surface and gas/water subsurface model. The model is explicit couple at time step level. Although the author does not mention that the reason of using selected flow in pipe correlation regarding stability issue, it can be observed that the flow in pipe correlation used in the study are all continuous. (Surface piping-Eaton, Production string-Modified Hagedon and Brown, Griffith for bubble flow).

Emanuel and Ranney (1981) presented the coupling of complex surface and three dimensional black oil reservoir models. The author use implicit couple at time step level technique to solve the system of equation (Surface and Production string - Beggs and Brill, Orkiszewski).

Litvak and Darlow (1995) published the rigorous procedure for the determination of well rate from surface pipeline network and tubinghead pressure constraint. They claim that the procedure is implemented in an industrial compositional reservoir simulator and it's applicable with black oil simulator.

Fang and Lo (1996) presented the gas-lifted production optimization of scheme for integrated reservoir simulation model and production network model with multiple field limits. The author aims to develop well-management scheme that can optimize oil production rate under general conditions with multiple facility limits. The author developed practical well-management scheme using the simplex/separable programming technique which they claim that it is much faster than gradient - based approach (i.e. linear programming).

Several authors tried to integrate commercial reservoir simulator (such as ECLIPSE) with commercial production network simulator (such as FORGAS and NetOpt) using Parallel Virtual Machine interface as a controller to pass the information between these two program. The level of coupling is varied from time step level to Newton iteration level (Hepguler et al. 1997; Trick 1998).

Hayder et al. (2006) used the commercial production network simulator (GAP) which has the production optimization algorithm available and this is capable of optimization of the flow rate under production constraint. GAP can be used to couple an in-house reservoir simulation program by using RESOLVE as a controller. It shows that the coupled model shows the improvement in reduction of water cut while the oil production rate is not significantly different compare to the uncoupled model.

Another important method for coupling the surface and subsurface model is the Integrate Asset Model (IAM) is define as the model that integrates reservoir, wells, surface infrastructure, and process facilities—as well as the asset's operating parameters, financial metrics, and economic conditions—into a single production management environment. It has gained widely acceptance for production integration and optimization as we can see several recently publication. Wickens and Jonge (2006) use IAM for risk management in production forecasting. Ursini et al. (2010) use IAM to couple dynamic oil reservoirs with surface facilities model for an onshore Algerian asset in order to account for pressure interaction between reservoir and surface facility, bottleneck and constraint identification, mixing of difference produced fluid. Gonzalez et al. (2010) build a fully compositional IAM for a giant gas-condensate field and it can

be used for manage the production schedule and liquid production optimization. The application of IAM is not limited to reservoir production management and optimization. Okafor (2011) shows the application of IAM for the flow assurance problem.

3. SUBSURFACE & SURFACE MODELING AND COUPLING MECHANISMS

In this chapter, the fundamental equations and theory related to surface & subsurface modeling and coupling mechanism are explained. The subsurface model used in this study is the black oil multiphase reservoir simulation model which simulates the flow of fluid in three phases (Oil, Gas, and Water). The derivation of three phases flow equations in reservoir system are shown in this chapter. The in-depth derivation of multiphase flow equation can be found from the textbooks by Ertekin (2001) and Chen et al. (2006). For surface model, the multiphase flow in pipe model is used in this study. The flow regime in vertical & horizontal pipe and related pressure lost correlations are described in a brief detail.

3.1. Subsurface Modeling

In this section we discuss the black oil formulation of three phases flow (oil gas, and water) in reservoir engineering. The black oil formulation is derived from mass-conservation equations and Darcy's equation in form of partial differential equations (PDE's). Most of equation presented here is mostly based on the textbook by Ertekin (2001) and Chen et al. (2006).

Assume that there are oil, gas, and water phases flow through the porous media which has permeability k , porosity ϕ , oil saturation S_o , water saturation S_w , and gas saturation S_g as shown in the Figure 2. The oil, gas and water phases have

density ρ_o, ρ_g , and ρ_w , respectively. The viscosity of oil, gas and water are μ_o, μ_g , and μ_w , respectively.

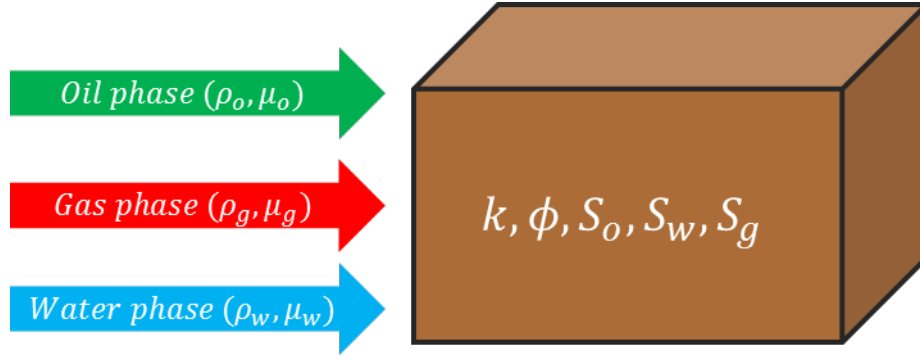


Figure 2: Multiphase flow through porous media

The oil, gas and water flow equation can be derived using the concept of material balance which states that the mass of inflow stream is equal to mass of outflow stream and accumulation. Combining the material balance equations and Darcy's equation yield the oil, water and gas flow equation which can be used to describe the flow of multiphase through the porous media. The partial differential equation of three phases flow is shown below

Oil Flow Equation

$$\nabla \cdot \left[\frac{\rho_o k_{ro} k}{\mu_o} (\nabla p_o - \rho_o g \nabla z) \right] = \frac{\partial(\rho_o \phi S_o)}{\partial t} + \tilde{q}_o \quad (1)$$

Water Flow Equation

$$\nabla \cdot \left[\frac{\rho_w k_{rw} k}{\mu_w} (\nabla p_w - \rho_w g \nabla z) \right] = \frac{\partial(\rho_w \phi S_w)}{\partial t} + \tilde{q}_w \quad (2)$$

Gas Flow Equation

$$\nabla \cdot \left[\frac{\rho_{Go} k_{ro} k}{\mu_{Go}} (\nabla p_o - \rho_o g \nabla z) + \frac{\rho_g k_{rg} k}{\mu_g} (\nabla p_g - \rho_g g \nabla z) \right] = \frac{\partial ((\rho_{Go} S_o + \rho_g S_g) \phi)}{\partial t} + \widetilde{q}_g \quad (3)$$

where $S_o + S_w + S_g = 1$, $P_{cow} = P_o - P_w$ and $P_{cgo} = P_g - P_o$

The term on the left side of flow equations represent the different of mass flowing in and out while on the right side of the flow equations represent the accumulation term and external sink/ source (\widetilde{q}). The unit of equation (1), (2), and (3) above is mass flow/unit volume.

Dividing the equation (1), (2), and (3) by ρ_{STC} and use the definition of $B = V_{rc}/V_{STC}$

Oil Flow Equation

$$\nabla \cdot [\lambda_o (\nabla p_o - \gamma_o \nabla z)] = \frac{\partial (\frac{\phi S_o}{B_o})}{\partial t} + q_o^* \quad (4)$$

Water Flow Equation

$$\nabla \cdot [\lambda_w (\nabla p_w - \gamma_w \nabla z)] = \frac{\partial (\frac{\phi S_w}{B_w})}{\partial t} + q_w^* \quad (5)$$

Gas Flow Equation

$$\nabla \cdot [\lambda_g (\nabla p_g - \gamma_g \nabla z) + R_{SO} \lambda_o (\nabla p_o - \gamma_o \nabla z)] = \frac{\partial (\frac{\phi R_{SO} S_o}{B_o} + \frac{\phi S_g}{B_g})}{\partial t} + q_g^* + q_o^* R_{SO} \quad (6)$$

where $\lambda_o = \frac{k_{ro} k}{B_o \mu_o}$, $\lambda_w = \frac{k_{rw} k}{B_w \mu_w}$, $\lambda_g = \frac{k_{rg} k}{B_g \mu_g}$, and $R_{SO} = W_G \rho_o / W_o \rho_g$

The ∇ operator is gradient operator and it stand for $\frac{\partial}{\partial x} + \frac{\partial}{\partial y} + \frac{\partial}{\partial z}$ operation for the space in 3D-Cartesian coordinate. In addition, we can impose three constraint equations $S_o + S_w + S_g = 1$, $P_{cow} = P_o - P_w$ and $P_{cgo} = P_g - P_o$ into the equations (4) to (5). The equations become

Oil Flow Equation

$$\begin{aligned} \frac{\partial}{\partial x} \left(\lambda_{ox} \left(\frac{\partial p_o}{\partial x} - \gamma_o \frac{\partial z}{\partial x} \right) \right) + \frac{\partial}{\partial y} \left(\lambda_{oy} \left(\frac{\partial p_o}{\partial y} - \gamma_o \frac{\partial z}{\partial y} \right) \right) + \frac{\partial}{\partial z} \left(\lambda_{oz} \left(\frac{\partial p_o}{\partial z} - \gamma_o \frac{\partial z}{\partial z} \right) \right) \\ = \frac{\partial \left(\frac{\phi(1 - S_w - S_g)}{B_o} \right)}{\partial t} + q_o^* \end{aligned} \quad (7)$$

Water Flow Equation

$$\begin{aligned} \frac{\partial}{\partial x} \left(\lambda_{wx} \left(\frac{\partial p_o}{\partial x} - \frac{\partial p_{cow}}{\partial x} - \gamma_w \frac{\partial z}{\partial x} \right) \right) + \frac{\partial}{\partial y} \left(\lambda_{wy} \left(\frac{\partial p_o}{\partial y} - \frac{\partial p_{cow}}{\partial y} - \gamma_w \frac{\partial z}{\partial y} \right) \right) \\ + \frac{\partial}{\partial z} \left(\lambda_{wz} \left(\frac{\partial p_o}{\partial z} - \frac{\partial p_{cow}}{\partial z} - \gamma_w \frac{\partial z}{\partial z} \right) \right) = \frac{\partial \left(\frac{\phi S_w}{B_w} \right)}{\partial t} + q_w^* \end{aligned} \quad (8)$$

Gas Flow Equation

$$\begin{aligned} \frac{\partial}{\partial x} \left(\lambda_{ox} R_{so} \left(\frac{\partial p_o}{\partial x} - \gamma_o \frac{\partial z}{\partial x} \right) \right) + \frac{\partial}{\partial y} \left(\lambda_{oy} R_{so} \left(\frac{\partial p_o}{\partial y} - \gamma_o \frac{\partial z}{\partial y} \right) \right) + \frac{\partial}{\partial z} \left(\lambda_{oz} R_{so} \left(\frac{\partial p_o}{\partial z} - \gamma_o \frac{\partial z}{\partial z} \right) \right) \\ + \frac{\partial}{\partial x} \left(\lambda_{gx} \left(\frac{\partial p_g}{\partial x} - \frac{\partial p_{cgo}}{\partial x} - \gamma_g \frac{\partial z}{\partial x} \right) \right) + \frac{\partial}{\partial y} \left(\lambda_{gy} \left(\frac{\partial p_g}{\partial y} - \frac{\partial p_{cgo}}{\partial y} - \gamma_g \frac{\partial z}{\partial y} \right) \right) \\ + \frac{\partial}{\partial z} \left(\lambda_{gz} \left(\frac{\partial p_g}{\partial z} - \frac{\partial p_{cgo}}{\partial z} - \gamma_g \frac{\partial z}{\partial z} \right) \right) = \frac{\partial \left(\frac{\phi R_{so}(1 - S_w - S_g)}{B_o} + \frac{\phi S_g}{B_g} \right)}{\partial t} + q_g^* \end{aligned} \quad (9)$$

In order to solve the system of equations ((7), (8), and (9)) numerically, Accurate discretization method such as finite differences, finite volumes, or finite elements need to be applied. Here we will work with the block – centered finite difference which connected to the finite volume discretization methodology.

3.1.1. Oil Flow Equation Discretization

The left hand side and right hand side of oil flow equation can be discretized . The discretization of each term in each side is explained here. For discretization of the left hand side terms, the case that the depth of top and the bottom layer does not change with x and y the term $\gamma \frac{\partial z}{\partial x}$ and $\gamma \frac{\partial z}{\partial y}$ becomes zero. The discretization of left hand side terms of the equations is as follow

$$\frac{\partial}{\partial x} \left(\lambda_{ox} \left(\frac{\partial p_o}{\partial x} - \gamma_o \frac{\partial z}{\partial x} \right) \right) \approx \frac{1}{\Delta x_i} \left(\lambda_{o_{i+\frac{1}{2},j,k}} \frac{p_{o_{i+1,j,k}} - p_{o_{i,j,k}}}{\Delta x_i^+} + \lambda_{o_{i-\frac{1}{2},j,k}} \frac{p_{o_{i-1,j,k}} - p_{o_{i,j,k}}}{\Delta x_i^-} \right) \quad (10)$$

$$\frac{\partial}{\partial y} \left(\lambda_{oy} \left(\frac{\partial p_o}{\partial y} - \gamma_o \frac{\partial z}{\partial y} \right) \right) \approx \frac{1}{\Delta y_i} \left(\lambda_{o_{i,j+\frac{1}{2},k}} \frac{p_{o_{i,j+1,k}} - p_{o_{i,j,k}}}{\Delta y_i^+} + \lambda_{o_{i,j-\frac{1}{2},k}} \frac{p_{o_{i,j-1,k}} - p_{o_{i,j,k}}}{\Delta y_i^-} \right) \quad (11)$$

$$\begin{aligned} \frac{\partial}{\partial z} \left(\lambda_{oz} \left(\frac{\partial p_o}{\partial z} - \gamma_o \frac{\partial z}{\partial z} \right) \right) \\ \approx \frac{1}{\Delta z_i} \left(\lambda_{o_{i,j,k+\frac{1}{2}}} \frac{p_{o_{i,j,k+1}} - p_{o_{i,j,k}}}{\Delta z_i^+} + \lambda_{o_{i,j,k-\frac{1}{2}}} \frac{p_{o_{i,j,k-1}} - p_{o_{i,j,k}}}{\Delta z_i^-} \right. \\ \left. - \lambda_{o_{i,j,k+\frac{1}{2}}} \gamma_{o_{i,j,k+\frac{1}{2}}} \frac{z_{i,j,k+1} - z_{i,j,k}}{\Delta z_i^+} - \lambda_{o_{i,j,k-\frac{1}{2}}} \gamma_{o_{i,j,k-\frac{1}{2}}} \frac{z_{i,j,k-1} - z_{i,j,k}}{\Delta z_i^-} \right) \end{aligned} \quad (12)$$

The subscript $i + 1, j, k$ stand for the property of the adjacent gridblock in positive direction while $i - 1, j, k$ stand for the property of the adjacent gridblock in negative direction. The subscript $i + \frac{1}{2}, j, k$ indicates that it is average properties of two adjacent gridlocks in positive x direction while the subscription $i - \frac{1}{2}, j, k$ defines that it is average properties of two adjacent gridlocks in negative x direction. The term Δx_i^+ is the distance between the center of two adjacent gridblock in positive x direction and Δx_i^- in negative x direction. The same convention is applied with y and z direction.

Putting together the equation (10), (11), and (12), we have the left hand side term of discretized oil flow equation.

$$\begin{aligned}
& \frac{\partial}{\partial x} \left(\lambda_{ox} \left(\frac{\partial p_o}{\partial x} - \gamma_o \frac{\partial z}{\partial x} \right) \right) + \frac{\partial}{\partial y} \left(\lambda_{oy} \left(\frac{\partial p_o}{\partial y} - \gamma_o \frac{\partial z}{\partial y} \right) \right) + \frac{\partial}{\partial z} \left(\lambda_{oz} \left(\frac{\partial p_o}{\partial z} - \gamma_o \frac{\partial z}{\partial z} \right) \right) \\
& \approx \frac{1}{\Delta x_i} \left(\lambda_{o_{i+\frac{1}{2},j,k}} \frac{p_{o_{i+1,j,k}} - p_{o_{i,j,k}}}{\Delta x_i^+} + \lambda_{o_{i-\frac{1}{2},j,k}} \frac{p_{o_{i-1,j,k}} - p_{o_{i,j,k}}}{\Delta x_i^-} \right) \\
& + \frac{1}{\Delta y_i} \left(\lambda_{o_{i,j+\frac{1}{2},k}} \frac{p_{o_{i,j+1,k}} - p_{o_{i,j,k}}}{\Delta y_i^+} + \lambda_{o_{i,j-\frac{1}{2},k}} \frac{p_{o_{i,j-1,k}} - p_{o_{i,j,k}}}{\Delta y_i^-} \right) \\
& + \frac{1}{\Delta z_i} \left(\lambda_{o_{i,j,k+\frac{1}{2}}} \frac{p_{o_{i,j,k+1}} - p_{o_{i,j,k}}}{\Delta z_i^+} + \lambda_{o_{i,j,k-\frac{1}{2}}} \frac{p_{o_{i,j,k-1}} - p_{o_{i,j,k}}}{\Delta z_i^-} \right) \\
& - \lambda_{o_{i,j,k+\frac{1}{2}}} \gamma_{o_{i,j,k+\frac{1}{2}}} \frac{z_{i,j,k+1} - z_{i,j,k}}{\Delta z_i^+} - \lambda_{o_{i,j,k-\frac{1}{2}}} \gamma_{o_{i,j,k-\frac{1}{2}}} \frac{z_{i,j,k-1} - z_{i,j,k}}{\Delta z_i^-}
\end{aligned} \tag{13}$$

For discretization of the right hand side terms, consider term $\frac{\partial \left(\frac{\phi(1-S_w-S_g)}{B_o} \right)}{\partial t}$, it can

be expanded in several ways but has to guarantee the material balance. For this research, the accumulation term is expanded as follow (Ertekin 2001)

$$\begin{aligned}
\frac{\partial \left(\frac{\phi(1-S_w-S_g)}{B_o} \right)}{\partial t} &= \left[(1 - S_w - S_g)^n (b_o^{n+1} \phi' + \phi^n b_o') \Delta_t P_o - (\phi b_o)^{n+1} \Delta_t S_w - \right. \\
& \left. \phi b_o n + 1 \Delta_t S_g \right]
\end{aligned} \tag{14}$$

where

$$\begin{aligned}
b_o &= \frac{1}{B_o}, \quad b_o' = \frac{(b_o^{n+1} - b_o^n)}{p_o^{n+1} - p_o^n}, \quad \phi' = \frac{(\phi^{n+1} - \phi^n)}{p_o^{n+1} - p_o^n}, \\
\Delta_t P_o &= \frac{p_o^{n+1} - p_o^n}{\Delta t}, \quad \Delta_t S_w = \frac{S_w^{n+1} - S_w^n}{\Delta t}, \quad \text{and} \quad \Delta_t S_g = \frac{S_g^{n+1} - S_g^n}{\Delta t}
\end{aligned}$$

For sink/source term q_o^* , we can treat it by using Peaceman's equation (Ertekin 2001).

$$q_o^* = WI_o(p_{o_{i,j,k}}^{n+1} - p_{wf}) \quad (15)$$

where WI_o is defined as follow

$$WI_o = -\frac{2\pi k_{r_o} \sqrt{k_x k_y} h}{\mu_o B_o [\ln(r_o/r_w) + s]} \quad (16)$$

k_{r_o} is relative permeability, k_x is permeability in x-direction, k_y is permeability in y-direction, h is thickness of grid block, and r_w is wellbore radius

The parameter r_o is equivalent grid block radius. At this radius, the pressure at steady-state in the reservoir is equal to the well-block pressure. The equivalent wellbore radius can be calculated as follow

$$r_o = 0.28 \frac{\left\{ \left[\left(\frac{k_y}{k_x} \right)^{\frac{1}{2}} (\Delta x)^2 \right] + \left[\left(\frac{k_x}{k_y} \right)^{\frac{1}{2}} (\Delta y)^2 \right] \right\}^{\frac{1}{2}}}{\left(\frac{k_y}{k_x} \right)^{1/4} + \left(\frac{k_x}{k_y} \right)^{1/4}} \quad (17)$$

Finally, combining equation (14) and (15), we have the right hand side terms of discretized oil flow equation.

$$\begin{aligned}
& \frac{\partial \left(\frac{\phi(1 - S_w - S_g)}{B_o} \right)}{\partial t} + q_o^* \\
& = [(1 - S_w - S_g)^n (b_o^{n+1} \phi' + \phi^n b_o') \Delta_t P_o - (\phi b_o)^{n+1} \Delta_t S_w \\
& \quad - (\phi b_o)^{n+1} \Delta_t S_g] + W I_o (p_{o_{i,j,k}}^{n+1} - p_{wf})
\end{aligned} \tag{18}$$

3.1.2. Water Flow Equation Discretization

The discretization of the left hand side terms of water flow equation can be done in the same way as the discretization of oil flow equation.

$$\frac{\partial}{\partial x} \left(\lambda_{wx} \left(\frac{\partial p_o}{\partial x} - \frac{\partial p_{cow}}{\partial x} - \gamma_w \frac{\partial z}{\partial x} \right) \right) \approx \frac{1}{\Delta x_i} \left(\lambda_{w_{i+\frac{1}{2},j,k}} \frac{p_{o_{i+1,j,k}} - p_{o_{i,j,k}}}{\Delta x_i^+} + \lambda_{w_{i-\frac{1}{2},j,k}} \frac{p_{o_{i-1,j,k}} - p_{o_{i,j,k}}}{\Delta x_i^-} \right) \tag{19}$$

$$\frac{\partial}{\partial y} \left(\lambda_{wy} \left(\frac{\partial p_o}{\partial y} - \frac{\partial p_{cow}}{\partial y} - \gamma_w \frac{\partial z}{\partial y} \right) \right) \approx \frac{1}{\Delta y_i} \left(\lambda_{w_{i,j+\frac{1}{2},k}} \frac{p_{o_{i,j+1,k}} - p_{o_{i,j,k}}}{\Delta y_i^+} + \lambda_{w_{i,j-\frac{1}{2},k}} \frac{p_{o_{i,j-1,k}} - p_{o_{i,j,k}}}{\Delta y_i^-} \right) \tag{20}$$

$$\begin{aligned}
& \frac{\partial}{\partial z} \left(\lambda_{wz} \left(\frac{\partial p_o}{\partial z} - \frac{\partial p_{cow}}{\partial z} - \gamma_w \frac{\partial z}{\partial z} \right) \right) \\
& \approx \frac{1}{\Delta z_i} \left(\lambda_{w_{i,j,k+\frac{1}{2}}} \frac{p_{o_{i,j,k+1}} - p_{o_{i,j,k}}}{\Delta z_i^+} + \lambda_{w_{i,j,k-\frac{1}{2}}} \frac{p_{o_{i,j,k-1}} - p_{o_{i,j,k}}}{\Delta z_i^-} \right. \\
& \quad \left. - \lambda_{w_{i,j,k+\frac{1}{2}}} \gamma_w \frac{z_{i,j,k+1} - z_{i,j,k}}{\Delta z_i^+} - \lambda_{w_{i,j,k-\frac{1}{2}}} \gamma_w \frac{z_{i,j,k-1} - z_{i,j,k}}{\Delta z_i^-} \right)
\end{aligned} \tag{21}$$

Putting together the equation (19), (20), and (21), we have the left hand side term of discretized water flow equation.

$$\begin{aligned}
& \frac{\partial}{\partial x} \left(\lambda_{wx} \left(\frac{\partial p_o}{\partial x} - \frac{\partial p_{cow}}{\partial x} - \gamma_w \frac{\partial z}{\partial x} \right) \right) + \frac{\partial}{\partial y} \left(\lambda_{wy} \left(\frac{\partial p_o}{\partial y} - \frac{\partial p_{cow}}{\partial y} - \gamma_w \frac{\partial z}{\partial y} \right) \right) \\
& + \frac{\partial}{\partial z} \left(\lambda_{wz} \left(\frac{\partial p_o}{\partial z} - \frac{\partial p_{cow}}{\partial z} - \gamma_w \frac{\partial z}{\partial z} \right) \right) \\
& \approx \frac{1}{\Delta x_i} \left(\lambda_{w_{i+\frac{1}{2},j,k}} \frac{p_{o_{i+1,j,k}} - p_{o_{i,j,k}}}{\Delta x_i^+} + \lambda_{w_{i-\frac{1}{2},j,k}} \frac{p_{o_{i-1,j,k}} - p_{o_{i,j,k}}}{\Delta x_i^-} \right) \\
& + \frac{1}{\Delta y_i} \left(\lambda_{w_{i,j+\frac{1}{2},k}} \frac{p_{o_{i,j+1,k}} - p_{o_{i,j,k}}}{\Delta y_i^+} + \lambda_{w_{i,j-\frac{1}{2},k}} \frac{p_{o_{i,j-1,k}} - p_{o_{i,j,k}}}{\Delta y_i^-} \right) \\
& + \frac{1}{\Delta z_i} \left(\lambda_{w_{i,j,k+\frac{1}{2}}} \frac{p_{o_{i,j,k+1}} - p_{o_{i,j,k}}}{\Delta z_i^+} + \lambda_{w_{i,j,k-\frac{1}{2}}} \frac{p_{o_{i,j,k-1}} - p_{o_{i,j,k}}}{\Delta z_i^-} \right) \\
& - \lambda_{w_{i,j,k+\frac{1}{2}}} \gamma_w \frac{z_{i,j,k+1} - z_{i,j,k}}{\Delta z_i^+} - \lambda_{w_{i,j,k-\frac{1}{2}}} \gamma_w \frac{z_{i,j,k-1} - z_{i,j,k}}{\Delta z_i^-}
\end{aligned} \tag{22}$$

For discretization of the right hand side terms, consider term $\frac{\partial(\frac{\phi S_w}{B_w})}{\partial t}$, it can be expanded in several ways but has to guarantee the material balance. For this research, the accumulation term is expanded as follow (Ertekin 2001)

$$\frac{\partial(\frac{\phi S_w}{B_w})}{\partial t} = S_w^n [b_w^{n+1} \phi' + \phi^n b_w'] \Delta_t P_o + [\phi^{n+1} b_w^{n+1}] \Delta_t S_w \tag{23}$$

For sink/source term q_w^* , we can treat it by using Peaceman's equation.

$$q_w^* = W I_w (p_{w_{i,j,k}}^{n+1} - p_{wf}) \tag{24}$$

The definition of $W I_w$ is the same definition of $W I_o$ in the equation (15) but use the water properties instead of oil properties.

Finally, combining equation (23) and (24), we have the right hand side terms of discretized water flow equation.

$$\frac{\partial(\frac{\phi S_w}{B_w})}{\partial t} + q_w^* = S_w^n [b_w^{n+1} \phi' + \phi^n b_w'] \Delta_t P_o + [\phi^{n+1} b_w^{n+1}] \Delta_t S_w + W I_w (p_w^{n+1} - p_{wf}) \quad (25)$$

3.1.3. Gas Flow Equation Discretization

For discretization of the left hand side terms, the case that the depth of top and the bottom layer does not change with x and y the term $\gamma \frac{\partial z}{\partial x}$ and $\gamma \frac{\partial z}{\partial y}$ becomes zero. The

discretization of left side of the free gas flow terms in x-direction $\frac{\partial}{\partial x} \left(\lambda_{gx} \left(\frac{\partial p_o}{\partial x} - \frac{\partial p_{cgo}}{\partial x} - \gamma g \partial z \partial x \right) \right)$, y - direction $\frac{\partial}{\partial y} \left(\lambda_{gy} \left(\frac{\partial p_o}{\partial y} - \frac{\partial p_{cgo}}{\partial y} - \gamma g \partial z \partial y \right) \right)$, and z - direction

$\frac{\partial}{\partial z} \left(\lambda_{gz} \left(\frac{\partial p_o}{\partial z} - \frac{\partial p_{cgo}}{\partial z} - \gamma g \frac{\partial z}{\partial z} \right) \right)$ can be done in the same way as discretization of left side

of the oil flow terms. Comparing gas flow equation with oil flow equation, there are additional three more terms which represent solution gas flow in x-direction

$\frac{\partial}{\partial x} \left(\lambda_{ox} R_{SO} \left(\frac{\partial p_o}{\partial x} - \gamma_o \frac{\partial z}{\partial x} \right) \right)$, y-direction $\frac{\partial}{\partial y} \left(\lambda_{oy} R_{SO} \left(\frac{\partial p_o}{\partial y} - \gamma_o \frac{\partial z}{\partial y} \right) \right)$, and z-direction

$\frac{\partial}{\partial z} \left(\lambda_{oz} R_{SO} \left(\frac{\partial p_o}{\partial z} - \gamma_o \frac{\partial z}{\partial z} \right) \right)$. These three additional terms can be discretized as follow

$$\begin{aligned} & \frac{\partial}{\partial x} \left(\lambda_{ox} R_{SO} \left(\frac{\partial p_o}{\partial x} - \gamma_o \frac{\partial z}{\partial x} \right) \right) \\ & \approx \frac{1}{\Delta x_i} \left((R_{SO} \lambda_o)_{i+\frac{1}{2},j,k} \frac{p_{o,i+1,j,k} - p_{o,i,j,k}}{\Delta x_i^+} \right. \\ & \quad \left. + (R_{SO} \lambda_o)_{i-\frac{1}{2},j,k} \frac{p_{o,i-1,j,k} - p_{o,i,j,k}}{\Delta x_i^-} \right) \end{aligned} \quad (26)$$

$$\begin{aligned}
& \frac{\partial}{\partial y} \left(\lambda_{oy} R_{SO} \left(\frac{\partial p_o}{\partial y} - \gamma_o \frac{\partial z}{\partial y} \right) \right) \\
& \approx \frac{1}{\Delta y_i} \left((R_{SO} \lambda_o)_{i,j+\frac{1}{2},k} \frac{p_{o,i,j+1,k} - p_{o,i,j,k}}{\Delta y_i^+} \right. \\
& \quad \left. + (R_{SO} \lambda_o)_{i,j-\frac{1}{2},k} \frac{p_{o,i,j-1,k} - p_{o,i,j,k}}{\Delta y_i^-} \right)
\end{aligned} \tag{27}$$

$$\begin{aligned}
& \frac{\partial}{\partial z} \left(\lambda_{oz} R_{SO} \left(\frac{\partial p_o}{\partial z} - \gamma_o \frac{\partial z}{\partial z} \right) \right) \\
& \approx \frac{1}{\Delta z_i} \left((R_{SO} \lambda_o)_{i,j,k+\frac{1}{2}} \frac{p_{o,i,j,k+1} - p_{o,i,j,k}}{\Delta z_i^+} \right. \\
& \quad + (R_{SO} \lambda_o)_{i,j,k-\frac{1}{2}} \frac{p_{o,i,j,k-1} - p_{o,i,j,k}}{\Delta z_i^-} \\
& \quad - (R_{SO} \lambda_o)_{i,j,k+\frac{1}{2}} \gamma_{o,i,j,k+\frac{1}{2}} \frac{z_{i,j,k+1} - z_{i,j,k}}{\Delta z_i^+} \\
& \quad \left. - (R_{SO} \lambda_o)_{i,j,k-\frac{1}{2}} \gamma_{o,i,j,k-\frac{1}{2}} \frac{z_{i,j,k-1} - z_{i,j,k}}{\Delta z_i^-} \right)
\end{aligned} \tag{28}$$

Putting together the equation (26), (27), (28), and discretized free gas flow terms, we have the left hand side term of discretized gas flow equation.

$$\begin{aligned}
& \frac{\partial}{\partial x} \left(\lambda_{ox} R_{So} \left(\frac{\partial p_o}{\partial x} - \gamma_o \frac{\partial z}{\partial x} \right) \right) + \frac{\partial}{\partial y} \left(\lambda_{oy} R_{So} \left(\frac{\partial p_o}{\partial y} - \gamma_o \frac{\partial z}{\partial y} \right) \right) + \frac{\partial}{\partial z} \left(\lambda_{oz} R_{So} \left(\frac{\partial p_o}{\partial z} - \gamma_o \frac{\partial z}{\partial z} \right) \right) \\
& + \frac{\partial}{\partial x} \left(\lambda_{gx} \left(\frac{\partial p_g}{\partial x} - \frac{\partial p_{cgo}}{\partial x} - \gamma_g \frac{\partial z}{\partial x} \right) \right) + \frac{\partial}{\partial y} \left(\lambda_{gy} \left(\frac{\partial p_g}{\partial y} - \frac{\partial p_{cgo}}{\partial y} - \gamma_g \frac{\partial z}{\partial y} \right) \right) \\
& + \frac{\partial}{\partial z} \left(\lambda_{gz} \left(\frac{\partial p_g}{\partial z} - \frac{\partial p_{cgo}}{\partial z} - \gamma_g \frac{\partial z}{\partial z} \right) \right) \\
& \approx \frac{1}{\Delta x_i} \left((R_{So} \lambda_o)_{i+\frac{1}{2},j,k} \frac{p_{oi+1,j,k} - p_{oi,j,k}}{\Delta x_i^+} + (R_{So} \lambda_o)_{i-\frac{1}{2},j,k} \frac{p_{oi-1,j,k} - p_{oi,j,k}}{\Delta x_i^-} \right) \\
& + \frac{1}{\Delta y_i} \left((R_{So} \lambda_o)_{i,j+\frac{1}{2},k} \frac{p_{oi,j+1,k} - p_{oi,j,k}}{\Delta y_i^+} + (R_{So} \lambda_o)_{i,j-\frac{1}{2},k} \frac{p_{oi,j-1,k} - p_{oi,j,k}}{\Delta y_i^-} \right) \\
& + \frac{1}{\Delta z_i} \left((R_{So} \lambda_o)_{i,j,k+\frac{1}{2}} \frac{p_{oi,j,k+1} - p_{oi,j,k}}{\Delta z_i^+} + (R_{So} \lambda_o)_{i,j,k-\frac{1}{2}} \frac{p_{oi,j,k-1} - p_{oi,j,k}}{\Delta z_i^-} \right) \\
& - (R_{So} \lambda_o)_{i,j,k+\frac{1}{2}} \gamma_o \frac{z_{i,j,k+1} - z_{i,j,k}}{\Delta z_i^+} \\
& - (R_{So} \lambda_o)_{i,j,k-\frac{1}{2}} \gamma_o \frac{z_{i,j,k-1} - z_{i,j,k}}{\Delta z_i^-} \\
& + \frac{1}{\Delta x_i} \left(\lambda_{g_{i+\frac{1}{2},j,k}} \frac{p_{oi+1,j,k} - p_{oi,j,k}}{\Delta x_i^+} + \lambda_{g_{i-\frac{1}{2},j,k}} \frac{p_{oi-1,j,k} - p_{oi,j,k}}{\Delta x_i^-} \right) \\
& + \frac{1}{\Delta y_i} \left(\lambda_{g_{i,j+\frac{1}{2},k}} \frac{p_{oi,j+1,k} - p_{oi,j,k}}{\Delta y_i^+} + \lambda_{g_{i,j-\frac{1}{2},k}} \frac{p_{oi,j-1,k} - p_{oi,j,k}}{\Delta y_i^-} \right) \\
& + \frac{1}{\Delta z_i} \left(\lambda_{w_{i,j,k+\frac{1}{2}}} \frac{p_{oi,j,k+1} - p_{oi,j,k}}{\Delta z_i^+} + \lambda_{w_{i,j,k-\frac{1}{2}}} \frac{p_{oi,j,k-1} - p_{oi,j,k}}{\Delta z_i^-} \right) \\
& - \lambda_{w_{i,j,k+\frac{1}{2}}} \gamma_w \frac{z_{i,j,k+1} - z_{i,j,k}}{\Delta z_i^+} - \lambda_{w_{i,j,k-\frac{1}{2}}} \gamma_w \frac{z_{i,j,k-1} - z_{i,j,k}}{\Delta z_i^-}
\end{aligned} \tag{29}$$

Consider term $\frac{\partial \left(\frac{\phi R_{SO}(1-S_w-S_g)}{B_o} + \frac{\phi S_g}{B_g} \right)}{\partial t}$ in the right hand side terms, it can be

expanded in several ways but has to guarantee the material balance. For this research, the accumulation term is expanded as follow (Ertekin 2001)

$$\begin{aligned} & \frac{\partial \left(\frac{\phi R_{SO}(1-S_w-S_g)}{B_o} + \frac{\phi S_g}{B_g} \right)}{\partial t} \\ &= \{(1-S_w-S_g)^n [(b_o^{n+1}\phi' + \phi^n b_o')R_{SO}^n + R'_{SO}(\phi b_o)^{n+1}] \\ &+ S_g^n [b_g^{n+1}\phi' + \phi^n b_g']\} \Delta_t P_o - R_{SO}^{n+1} (b_o \phi)^{n+1} \Delta_t S_w + [(b_g \phi)^{n+1} \\ &- R_{SO}^{n+1} (b_o \phi)^{n+1}] \Delta_t S_g \end{aligned} \quad (30)$$

For sink/source term q_g^*

$$q_g^* = q_{fg}^{*n+1} + R_{SO}^{n+1} q_o^{n+1} = WI_g (p_{g_{i,j,k}}^{n+1} - p_{wf}) + R_{SO}^{n+1} WI_o (p_{g_{i,j,k}}^{n+1} - p_{wf}) \quad (31)$$

The definition of WI_g is the same definition of WI_o in the equation (15) but use the gas properties instead of oil properties.

Finally, combining equation (30) and (31), we have the right hand side terms of discretized gas flow equation.

$$\begin{aligned} & \frac{\partial \left(\frac{\phi R_{SO}(1-S_w-S_g)}{B_o} + \frac{\phi S_g}{B_g} \right)}{\partial t} + q_g^* = \{(1-S_w-S_g)^n [(b_o^{n+1}\phi' + \phi^n b_o')R_S^n + R'_S(\phi b_o)^{n+1}] + \\ & S_g^n [b_g^{n+1}\phi' + \phi^n b_g']\} \Delta_t P_o - R_{SO}^{n+1} (b_o \phi)^{n+1} \Delta_t S_w + [(b_g \phi)^{n+1} \\ & - R_{SO}^{n+1} (b_o \phi)^{n+1}] \Delta_t S_g + \\ & WI_g (p_{g_{i,j,k}}^{n+1} - p_{wf}) + R_S^{n+1} WI_o (p_{g_{i,j,k}}^{n+1} - p_{wf}) \end{aligned} \quad (32)$$

3.1.4. Treatment of Saturated and Undersaturated State of Reservoir

In undersaturated state of reservoir, there is no free gas phase present in the reservoir and the reservoir pressure is higher than the bubble point pressure. Hence, the constraint conditions are

$$\begin{aligned} S_w^{n+1} + S_o^{n+1} &= 1 \text{ and } S_g^{n+1} = 0 \\ p_o^{n+1} &> p_b^{n+1} \end{aligned} \tag{33}$$

where p_b^{n+1} is bubble point pressure

In saturated state of reservoir, the reservoir pressure is above or equal to the initial bubble point pressure and free gas phase comes out from the oil phase. The constraint conditions can be written as follows

$$\begin{aligned} S_w^{n+1} + S_o^{n+1} + S_g^{n+1} &= 1 \\ p_o^{n+1} &= p_b^{n+1} \end{aligned} \tag{34}$$

3.1.5. Newton-Raphson Linearization

Since oil, water, and gas discretization equations above are nonlinear in terms of primary unknowns which are p^{n+1} , S_w^{n+1} , and S_g^{n+1} . The set of nonlinear equations can be linearized by Newton-Raphson method such that the system of equations can be solved iteratively by a linear solver. The implementation step of Newton-Raphson method is shown in a form of flowchart in Figure 3.

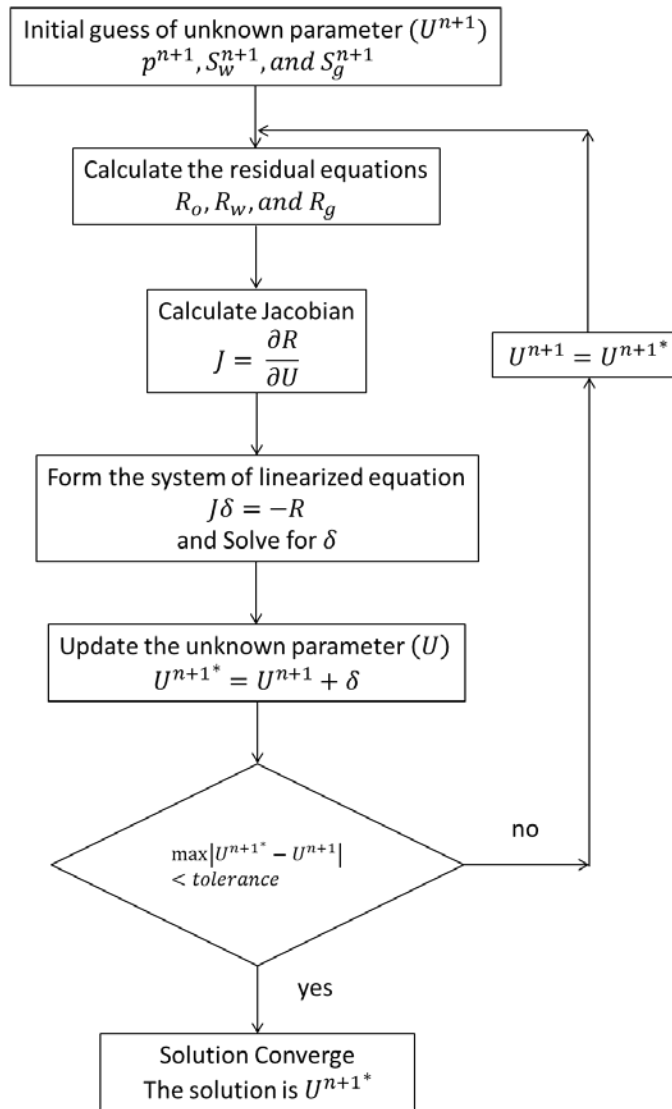


Figure 3: Flowchart explaining Newton-Raphson method

Oil, Water, and Gas Discretization Equations can be formulated in term of residual equations (R). The residual equations are simply the left hand side terms minus the right hand side term of flow equation of each phase.

Residual of Oil Discretization Equation

$$\begin{aligned}
R_o = & \frac{1}{\Delta x_i} \left(\lambda_{o_{i+\frac{1}{2},j,k}} \frac{p_{o_{i+1,j,k}} - p_{o_{i,j,k}}}{\Delta x_i^+} + \lambda_{o_{i-\frac{1}{2},j,k}} \frac{p_{o_{i-1,j,k}} - p_{o_{i,j,k}}}{\Delta x_i^-} \right) \\
& + \frac{1}{\Delta y_i} \left(\lambda_{o_{i,j+\frac{1}{2},k}} \frac{p_{o_{i,j+1,k}} - p_{o_{i,j,k}}}{\Delta y_i^+} + \lambda_{o_{i,j-\frac{1}{2},k}} \frac{p_{o_{i,j-1,k}} - p_{o_{i,j,k}}}{\Delta y_i^-} \right) \\
& + \frac{1}{\Delta z_i} \left(\lambda_{o_{i,j,k+\frac{1}{2}}} \frac{p_{o_{i,j,k+1}} - p_{o_{i,j,k}}}{\Delta z_i^+} + \lambda_{i,j,k-\frac{1}{2}} \frac{p_{o_{i,j,k-1}} - p_{o_{i,j,k}}}{\Delta z_i^-} \right) \\
& - \lambda_{o_{i,j,k+\frac{1}{2}}} \gamma_{o_{i,j,k+\frac{1}{2}}} \frac{z_{i,j,k+1} - z_{i,j,k}}{\Delta z_i^+} - \lambda_{o_{i,j,k-\frac{1}{2}}} \gamma_{o_{i,j,k-\frac{1}{2}}} \frac{z_{i,j,k-1} - z_{i,j,k}}{\Delta z_i^-} \\
& - [(1 - S_w - S_g)^n (b_o^{n+1} \phi' + \phi^n b_o') \Delta_t P_o - (\phi b_o)^{n+1} \Delta_t S_w \\
& - (\phi b_o)^{n+1} \Delta_t S_g] - W I_o (p_{o_{i,j,k}}^{n+1} - p_{wf})
\end{aligned} \tag{34}$$

Residual of Water Discretization Equation

$$\begin{aligned}
R_w = & \frac{1}{\Delta x_i} \left(\lambda_{w_{i+\frac{1}{2},j,k}} \frac{p_{o_{i+1,j,k}} - p_{o_{i,j,k}}}{\Delta x_i^+} + \lambda_{w_{i-\frac{1}{2},j,k}} \frac{p_{o_{i-1,j,k}} - p_{o_{i,j,k}}}{\Delta x_i^-} \right) \\
& + \frac{1}{\Delta y_i} \left(\lambda_{w_{i,j+\frac{1}{2},k}} \frac{p_{o_{i,j+1,k}} - p_{o_{i,j,k}}}{\Delta y_i^+} + \lambda_{w_{i,j-\frac{1}{2},k}} \frac{p_{o_{i,j-1,k}} - p_{o_{i,j,k}}}{\Delta y_i^-} \right) \\
& + \frac{1}{\Delta z_i} \left(\lambda_{w_{i,j,k+\frac{1}{2}}} \frac{p_{o_{i,j,k+1}} - p_{o_{i,j,k}}}{\Delta z_i^+} + \lambda_{w_{i,j,k-\frac{1}{2}}} \frac{p_{o_{i,j,k-1}} - p_{o_{i,j,k}}}{\Delta z_i^-} \right) \\
& - \lambda_{w_{i,j,k+\frac{1}{2}}} \gamma_{w_{i,j,k+\frac{1}{2}}} \frac{z_{i,j,k+1} - z_{i,j,k}}{\Delta z_i^+} - \lambda_{w_{i,j,k-\frac{1}{2}}} \gamma_{w_{i,j,k-\frac{1}{2}}} \frac{z_{i,j,k-1} - z_{i,j,k}}{\Delta z_i^-} \\
& - [S_w^n [b_w^{n+1} \phi' + \phi^n b_w'] \Delta_t P_o + [\phi^{n+1} b_w^{n+1}] \Delta_t S_w] - W I_w (p_{w_{i,j,k}}^{n+1} - p_{wf})
\end{aligned} \tag{35}$$

Residual of Gas Discretization Equation

$$\begin{aligned}
R_g = & \frac{1}{\Delta x_i} \left((R_{SO}\lambda_o)_{i+\frac{1}{2},j,k} \frac{p_{oi+1,j,k} - p_{oi,j,k}}{\Delta x_i^+} + (R_{SO}\lambda_o)_{i-\frac{1}{2},j,k} \frac{p_{oi-1,j,k} - p_{oi,j,k}}{\Delta x_i^-} \right) \\
& + \frac{1}{\Delta y_i} \left((R_{SO}\lambda_o)_{i,j+\frac{1}{2},k} \frac{p_{oi,j+1,k} - p_{oi,j,k}}{\Delta y_i^+} \right. \\
& \left. + (R_{SO}\lambda_o)_{i,j-\frac{1}{2},k} \frac{p_{oi,j-1,k} - p_{oi,j,k}}{\Delta y_i^-} \right) \\
& + \frac{1}{\Delta z_i} \left((R_{SO}\lambda_o)_{i,j,k+\frac{1}{2}} \frac{p_{oi,j,k+1} - p_{oi,j,k}}{\Delta z_i^+} \right. \\
& \left. + (R_{SO}\lambda_o)_{i,j,k-\frac{1}{2}} \frac{p_{oi,j,k-1} - p_{oi,j,k}}{\Delta z_i^-} \right. \\
& \left. - (R_{SO}\lambda_o)_{i,j,k+\frac{1}{2}} \gamma_{oi,j,k+\frac{1}{2}} \frac{z_{i,j,k+1} - z_{i,j,k}}{\Delta z_i^+} \right. \\
& \left. - (R_{SO}\lambda_o)_{i,j,k-\frac{1}{2}} \gamma_{oi,j,k-\frac{1}{2}} \frac{z_{i,j,k-1} - z_{i,j,k}}{\Delta z_i^-} \right) \\
& + \frac{1}{\Delta x_i} \left(\lambda_{g_{i+\frac{1}{2},j,k}} \frac{p_{oi+1,j,k} - p_{oi,j,k}}{\Delta x_i^+} + \lambda_{g_{i-\frac{1}{2},j,k}} \frac{p_{oi-1,j,k} - p_{oi,j,k}}{\Delta x_i^-} \right) \\
& + \frac{1}{\Delta y_i} \left(\lambda_{g_{i,j+\frac{1}{2},k}} \frac{p_{oi,j+1,k} - p_{oi,j,k}}{\Delta y_i^+} + \lambda_{g_{i,j-\frac{1}{2},k}} \frac{p_{oi,j-1,k} - p_{oi,j,k}}{\Delta y_i^-} \right) \\
& + \frac{1}{\Delta z_i} \left(\lambda_{w_{i,j,k+\frac{1}{2}}} \frac{p_{oi,j,k+1} - p_{oi,j,k}}{\Delta z_i^+} + \lambda_{w_{i,j,k-\frac{1}{2}}} \frac{p_{oi,j,k-1} - p_{oi,j,k}}{\Delta z_i^-} \right. \\
& \left. - \lambda_{w_{i,j,k+\frac{1}{2}}} \gamma_{w_{i,j,k+\frac{1}{2}}} \frac{z_{i,j,k+1} - z_{i,j,k}}{\Delta z_i^+} - \lambda_{w_{i,j,k-\frac{1}{2}}} \gamma_{w_{i,j,k-\frac{1}{2}}} \frac{z_{i,j,k-1} - z_{i,j,k}}{\Delta z_i^-} \right) \\
& - \left\{ (1 - S_w - S_g)^n [(b_o^{n+1}\phi' + \phi^n b_o')R_S^n + R_S'(\phi b_o)^{n+1}] \right. \\
& \left. + S_g^n [b_g^{n+1}\phi' + \phi^n b_g'] \Delta_t P_o - R_S^{n+1} (b_o \phi)^{n+1} \Delta_t S_w \right. \\
& \left. + [(b_g \phi)^{n+1} - R_S^{n+1} (b_o \phi)^{n+1}] \Delta_t S_g \right\} - W I_g (p_{g_{i,j,k}}^{n+1} - p_{wf}) \\
& - R_S^{n+1} W I_o (p_{g_{i,j,k}}^{n+1} - p_{wf})
\end{aligned} \tag{36}$$

After the residual of oil water and gas flow equation are formulated. The jacobian $J = \frac{\partial R}{\partial U}$ can be calculated in order to form the linearized equation for solving the unknown parameter. The problem can be set up as follow

Define residual vector R and unknown vector U

$$\begin{aligned} U &= (p, S_w, S_g)^T \\ R &= (R_o, R_w, R_g)^T \end{aligned} \tag{37}$$

Jacobian matrix can be formulated as follow

$$J = \frac{\partial R}{\partial U} = \begin{bmatrix} \frac{\partial R_o}{\partial p} & \frac{\partial R_o}{\partial S_w} & \frac{\partial R_o}{\partial S_g} \\ \frac{\partial R_w}{\partial p} & \frac{\partial R_w}{\partial S_w} & \frac{\partial R_w}{\partial S_g} \\ \frac{\partial R_g}{\partial p} & \frac{\partial R_g}{\partial S_w} & \frac{\partial R_g}{\partial S_g} \end{bmatrix} \tag{38}$$

Newton-Raphson Iteration

$$\begin{aligned} J^{n+1*} \delta U &= -R^{n+1*} \\ U^{n+1^{*+1}} &= U^{n+1*} + \delta U \end{aligned} \tag{39}$$

The Newton-Raphson iteration will be continued until the solutions are converged. When the solution is converged the norm of δU will approach to zero. Consequently, in practical, the Newton-Raphson iteration will be stopped when norm of δU is smaller than some small tolerance value.

3.2. Multiphase Flow in Wells and Pipes Modeling

Most of producing oil and gas reservoir are operated under multiphase flow condition. The producing fluid mostly contains oil, gas, and in some cases there may even be producing water. Hence, the basic knowledge of multiphase flow in wells and pipes are of primary importance in identifying the total producing fluid at the surface facilities. The basic knowledge of multiphase flow in wells and pipes presented here. For more detail, there are many references on this subject. For this study, we will base on the textbook by Economides (1993) and Beggs (2003).

One of an important part in coupled surface and subsurface modeling is the determination of interaction of producing fluid with surface facilities in term of pressure loss. The pressure of producing fluid is loss when flow thru wells and pipes. The presence of liquid and gas in flow in pipes and wells complicate the pressure loss calculation. As the pressure changes, the phase changes occur resulting in changes of fluid densities, viscosities, and volume of each phase. In addition, temperature can be changes when the fluid flows along pipes and wells. In order to precisely identify the changing of properties of fluid and predict the pressure loss multiphase flow in wells and pipes modeling is needed.

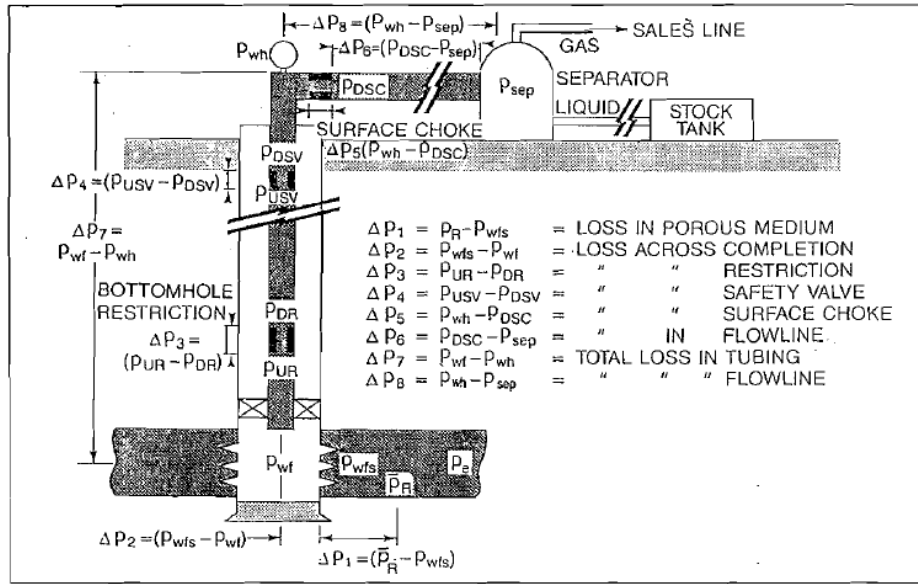


Figure 4: Schematic of production system and associated pressure loss (Source: Beggs (2003))

The Figure 4 is taken from Beggs (2003) give a good explanation of the production system and its pressure lost along the production system. The estimation of bottomhole flowing pressure P_{wf} can be calculate in the following forms

$$P_{sep} + \Delta P_7 + \Delta P_6 + \Delta P_5 + \Delta P_4 + \Delta P_3 + \Delta P_2 = P_{wf} \quad (40)$$

The producing fluid flow from bottomhole with bottomhole flowing pressure P_{wf} thru the completion, flow restriction, and safety valve in the well resulting in pressure loss ΔP_2 , ΔP_3 , and ΔP_4 , respectively. After that the producing fluid pressure is loss when flow thru tubing. The pressure loss in tubing is represented by ΔP_7 . When the fluid reach the wellhead, it will flow thru the surface choke, if one existed and then thru the flowline connected to separator. The pressure loss across the surface choke and flow line

are represented by ΔP_5 and ΔP_6 , respectively. The fluid pressure after reach the separator is equal to P_{sep} .

In a simple production system, it may contain just only two main component of pressure loss which is pressure loss in pipeline and tubing. In this section, the overview of multiphase flow in pipes and wells will be presented.

3.2.1. Pressure Loss in Wells and Pipes Model

The pressure loss is generally expressed in a form of pressure gradient. For multiphase flow in wells and pipes, there are three main components of the pressure loss gradient.

$$\frac{dp}{dL} = \left(\frac{dp}{dL}\right)_{elev} + \left(\frac{dp}{dL}\right)_f + \left(\frac{dp}{dL}\right)_{acc} \quad (41)$$

Elevation Change Component $\left(\frac{dp}{dL}\right)_{elev}$ represents pressure loss due to potential energy or elevation change. It's also known as hydrostatic component,

$$\left(\frac{dp}{dL}\right)_{elev} = \frac{g}{g_c} \rho_m \sin\theta, \quad (42)$$

where ρ_m is the density of the gas/liquid mixture in the pipe element. In the case of no slippage, the mixture density can be calculated by following equation.

$$\begin{aligned} \rho_m &= \rho_L \lambda_L + \rho_G \lambda_G, \text{ and} \\ \lambda_L &= \frac{q_L}{q_L + q_g} \text{ and } \lambda_G = 1 - \lambda_L, \end{aligned} \quad (43)$$

λ_L is known as liquid holdup and λ_g is gas hold up. The liquid hold up and gas hold up is a function of liquid flow rate q_L and gas flow rate q_g .

Friction Component $\left(\frac{dp}{dL}\right)_f$ represents pressure loss due to friction forces

$$\left(\frac{dp}{dL}\right)_f = \frac{(f\rho v^2)_f}{2g_c d}, \quad (44)$$

where d is pipe diameter, f is friction factor, ρ is the density of fluid, and v is the velocity of fluid. The way that these parameters are defined and evaluated is different by different sources, each which introduces different assumptions.

Finally, the acceleration component, $\left(\frac{dp}{dL}\right)_{acc}$, represents pressure loss due to kinetic energy changes, as

$$\left(\frac{dp}{dL}\right)_{acc} = \frac{(\rho v dv)_k}{g_c dL}, \quad (45)$$

where ρ is density, v is velocity, and $\frac{dv}{dL}$ is acceleration term

Some of pressure loss correlations completely ignore the acceleration component. Moreover, when this term is considered, various assumptions are made to simplify the procedure to determine the acceleration component. It can be said that the major considerations of developing pressure gradient correlation are basically the assumption in development of liquid hold-up prediction and friction factor.

3.2.2. Two Phases Flow Regimes in Vertical Flow

The flow regime is a qualitative property of phase distribution. For gas-liquid vertical upward flow, there are four flow regimes that can occur. The figure described each flow regime is shown in the Figure 5. A brief description of each flow regime is shown below

- Bubble flow: The liquid phase flow as a continuous phase with dispersed bubble of gas phase.
- Slug flow: The gas phase has higher velocity than gas phase in bubble flow. The gas bubbles coalesce into large bubbles which entirely filled the pipe cross section, known as Taylor bubble. The slugs of liquid that contain many small bubbles of gas are in between the large gas bubble.
- Churn flow: As gas phase keep flowing at further higher gas rate, the large bubbles become unstable and collapse resulting in both liquid phase and gas phase dispersion and highly turbulent flow. Churn flow is characterized by oscillatory motion of liquid flow.
- Annular flow: At very high gas phase rate, gas becomes the continuous phase and flow in the middle of the pipe. The liquid phase flow as annulus coating surface of the pipe and with liquid droplets dispersed in the continuous gas phase.

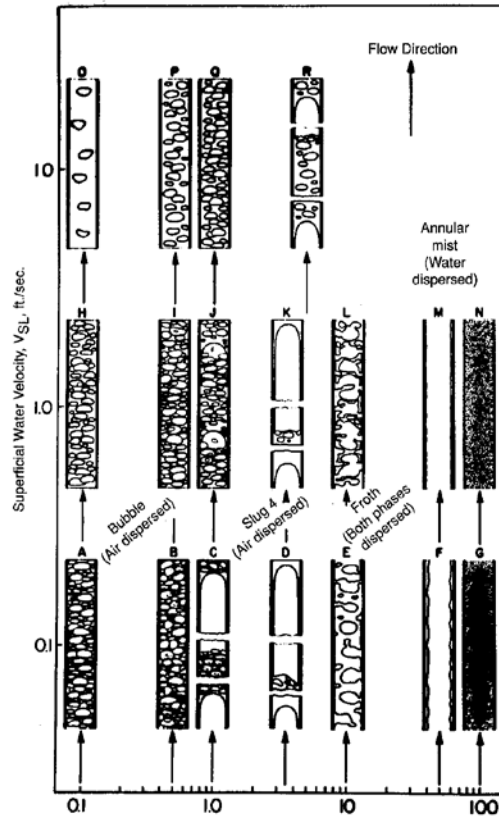


Figure 5: Flow regime in vertical flow (Source: Economides (1993))

3.2.3. Two Phases Flow Regimes in Horizontal Flow

For horizontal flow, the flow regime does not affect the pressure drop as significantly as it does in vertical flow. However, in some pressure correlation, the flow regime is considered and can effect production operation. The obvious example is the occurrence of slug flow which can affect the designing of separators to handle the large volume of liquid contained in a slug and some of special equipment such as slug catchers. The flow regime of horizontal flow is shown in the Figure 6. The flow regime can be classified into three types of regimes, as described below

- Segregated flow: The segregated flow occurs when gas and liquid phases are flow almost separately. It can be classified further as being stratified smooth, stratified wavy or ripple flow, and annular.
 - Stratified smooth flow describes the flow that gas phase flow in the top part of horizontal pipe while liquid phase flow in the bottom part of the pipe with a smooth interface between the phases. The stratified smooth occurs at low flow rate of both phases;
 - Stratified wavy flow describes the flow that gas phase flow in the top part of horizontal pipe while liquid phase flow in the bottom part of the pipe with wavy interface between the phases. This regime occurs when the gas rate is high;
 - Annular flow occurs when gas and liquid rate are both high and consist of an annulus of liquid coating the wall of pipe with continuous flow of gas phase with liquid droplets in the middle of the pipe.
- Intermittent flow: The segregated flow consist of two type of flow which are plug flow and slug flow
 - Plug flow consists of large gas bubbles flow along the top of the pipe which is otherwise filled with liquid;
 - Slug flow is the flow that large liquid slug alternating with bubble of gas at high velocity that fill almost the entire pipe.

- Distributive flow: It can be classified further as being bubble flow and mist flow
 - Bubble flow: the bubble flow for horizontal pipe is different from bubble flow in vertical pipe in that the gas bubble in horizontal flow will be concentrate at the top part of the pipe;
 - Mist flow consists of continuous gas phase flow with liquid droplets. This flow regime occur when gas rates is high and low liquid flow rates. Most of the time, annular flow and mist flow are indistinguishable.

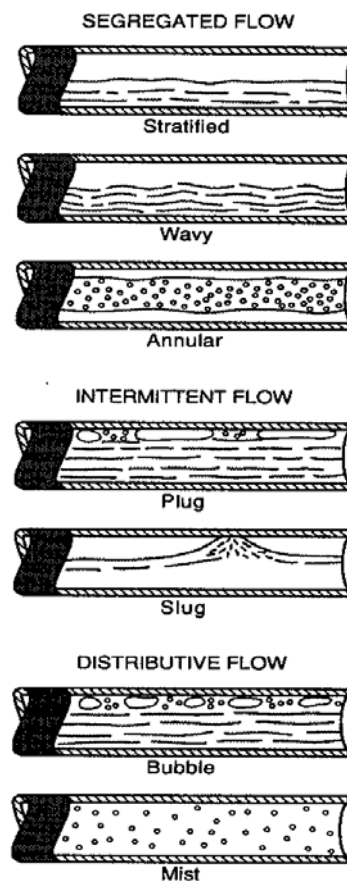


Figure 6: Flow regime in horizontal flow (Source: Economides(1993))

3.2.4. Pressure Gradient Correlations

In this section, the pressure drop correlations used in this thesis are described. As pointed out before, there are different methodologies to determine the pressure drop.

3.2.4.1. The Beggs and Brill Method

In Beggs and Brill, the correlation is developed from experimental data. It's different from other correlations such that it's applicable to any pipe inclination and flow direction. The Beggs and Brill method includes flow regime into pressure gradient calculation which affect the liquid hold-up and average density calculation. This method determines the flow regime that would occur if the pipeline is perfectly horizontal and then make a correction to account for the change of holdup behavior with inclination. Although, the method gives good results for pipeline calculations, it was observed that it slightly over-predict pressure gradient in vertical wells in some cases. In this study, the Beggs and Brill method is used to calculated pressure loss of water injection and production fluids in pipeline. The flow regime determination of the Beggs and Brill method based on the following parameters summarized in Table1.

Parameter	Correlation
N_{FR}	$\frac{u_m^2}{gD}$
λ_L	$\frac{u_{sl}}{u_m}$
L_1	$316\lambda_L^{0.302}$
L_2	$0.0009252\lambda_L^{-2.4684}$
L_3	$0.10\lambda_L^{-1.4516}$
L_4	$0.5\lambda_L^{-6.738}$

Table 1: Parameter for flow regime determination of Beggs and Brill method

Segregated flow exists if

$$\lambda_l < 0.01 \text{ and } N_{FR} < L_1 \text{ or } \lambda_l \geq 0.01 \text{ and } N_{FR} < L_2$$

Transition flow exists when

$$\lambda_l \geq 0.01 \text{ and } L_2 < N_{FR} \leq L_3$$

Intermittent flow occurs when

$$0.01 \leq \lambda_l < 0.4 \text{ and } L_3 < N_{FR} \leq L_1 \text{ or } \lambda_l \geq 0.4 \text{ and } L_3 < N_{FR} \leq L_4$$

Distributed flow occur if

$$\lambda_l < 0.4 \text{ and } N_{FR} \geq L_1 \text{ or } \lambda_l \geq 0.4 \text{ and } N_{FR} > L_4$$

3.2.4.2. The Petroleum Experts 2 Correlation

The Petroleum Experts 2 correlation is a pressure lost correlation developed by Petroleum Experts Company. The Petroleum Expert 2 correlation is an extended work of Petroleum Expert 1 correlation which includes the features of the Petroleum Expert 1 correlation and adds original work on predicting low-rate VLP and well stability (PROSPER's manual).

Unfortunately, there was no publication about the correlation found. However, based on Prosper's manual, Petroleum Expert Correlation combines the best features of existing correlations. The Hagedorn & Brown correlation Gould et al flow map is used in slug flow and Duns and Ros correlation for mist flow. A combination of slug and mist results is used for transition regime. The manual also mention that the correlation has been tested with several high flow rate wells and gave good estimate of pressure drops. The table below summarizes the correlations used for each flow regime.

Flow Regime	Correlation
Bubble flow	Wallis and Griffith
Slug flow	Hagedorn and Brown
Transition flow	Dun and Ros
Annular Mist flow	Dun and Ros

Table 2: Summary of flow regime and correlation used in Petroleum Expert 2 correlation

3.3. Surface and Subsurface Model Coupling Mechanism

As pointed before, the core idea in the coupling surface/subsurface flows stem from the choice of mechanism used to compute the “correct” bottomhole pressure coming from the reservoir material balance equation and the equation coming from the theory of flow in pipes.

In this session, we explore the three main schemes used in the coupling surface and subsurface model. The idea here is to summarize each of the advantages and disadvantages of the three different coupling schemes. Their application to a reservoir model will be done in the next chapter.

3.3.1. Explicit Coupling Scheme

In this scheme, the surface and subsurface are treated as different domain (domain decomposition) and the iterative process is simplified such that the boundary condition for subsurface model is treated explicitly. The subsurface model and surface model are solved at different time steps. The procedure for explicit coupling is explained below

- In the first timestep of simulation, the controlling parameter (i.e. BHP) will be guessed at the best knowledge of user while in the later timestep, surface model calculates the pressure loss and solves for controlling parameter at the beginning of time step. Let’s assume function g is the function that uses to calculate the pressure loss. The controlling parameter (i.e. BHP) can be calculated as follow

$$BHP = g(Q, P)$$

where BHP is bottomhole flowing pressure, Q is flow rate, and P is upstream injection pressure or downstream production pressure.

- Pass the controlling parameters (i.e. BHP) to subsurface model for well rate calculation using Peaceman's equation (Equation (15)). Let's assume f is the function of Peaceman's equation. The well rate can be calculated as follow

$$Q_{well} = f(BHP, P_{res})$$

where BHP is bottomhole flowing pressure, Q_{well} is well flow rate, and P_{res} is reservoir pressure.

- Check that the solutions of well rate calculation (Q_{well}) and surface model (Q) are converged or not. These process is called balancing process.
- If “Y”, use controlling parameters as well boundary condition to solve the subsurface model (Equation (39): linearized oil, water, and gas discretization equations) and proceed to the next time step
- If “N”, repeat the process until the solutions of well rate calculation and surface model are converged

The explicit coupling balances the surface and subsurface in time step level. The frequency can be varied. The main advantage of applying explicit coupling scheme is that it requires less computation effort than any other coupling schemes. Also it has high flexibility in terms of using different surface and subsurface simulation software to perform coupling. However, this may introduce inaccuracies in bottomhole flowing

pressure (BHP) because the surface and subsurface model are balanced at the beginning of the time step whereas the reservoir and fluid properties used in the balancing step are taken from previous time step of simulation. The flow chart of explicit coupling scheme is shown in Figure 7.

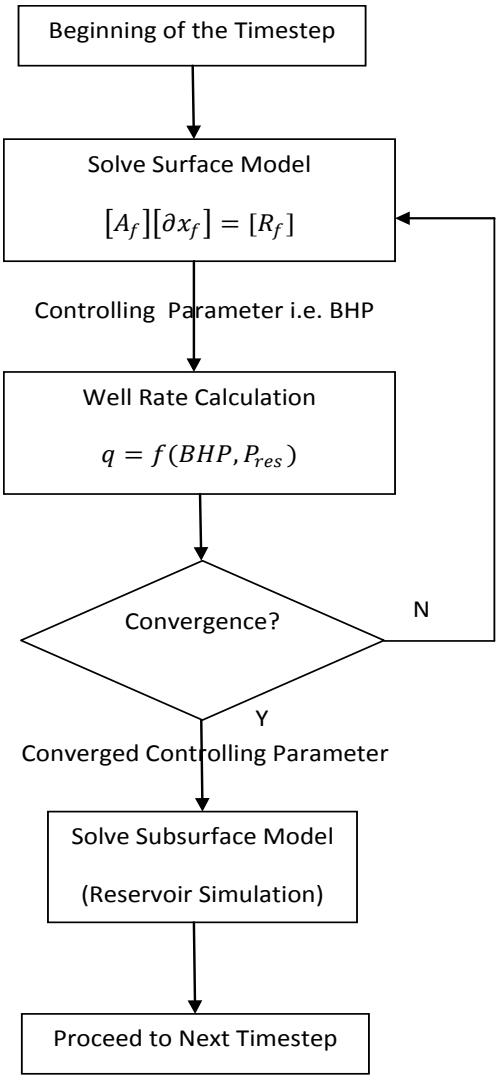


Figure 7: Explicit coupling scheme

3.3.2. *Implicit Coupling Scheme*

This coupling scheme is a variant of the explicit method in which the surface and subsurface are treated as different domain but the subsurface model becomes a part of the Newton iterative process.

The procedure for implicit coupling is explained below

- In the first timestep of simulation, the controlling parameter (i.e. BHP) will be guessed at the best knowledge of user while in the later timestep, surface model calculates the pressure loss and solves for controlling parameter using the input in the beginning of newton iteration. Let's assume function g is the function that uses to calculate the pressure loss. The controlling parameter (i.e. BHP) can be calculated as follow

$$BHP = g(Q, P)$$

where BHP is bottomhole flowing pressure, Q is flow rate, and P is upstream injection pressure or downstream production pressure.

- Pass the controlling parameters (i.e. BHP) to subsurface model for well rate calculation using Peaceman's equation (Equation (15)). Let's assume f is the function of Peaceman's equation. The well rate can be calculated as follow

$$Q_{well} = f(BHP, P_{res})$$

where BHP is bottomhole flowing pressure, Q_{well} is well flow rate, and P_{res} is reservoir pressure.

- Check that the solutions of well rate calculation (Q_{well}) and surface model (Q) are converged or not. These process is called balancing process.
- Use converged controlling parameter (i.e. BHP) as well boundary condition to solve the subsurface model (Equation (39)): linearized oil, water, and gas discretization equations)
- Check that the Newton iteration solution is converged or not
- If “Y”, proceed to the next time step
- If “N”, repeat the process until the Newton iteration solution is converged or it meets the maximum number of Newton iteration that require balancing step

The implicit coupling balances the surface and subsurface in Newton iteration level. The updating frequency can be varied. This coupling scheme requires higher computational effort than explicit coupling scheme as it associates the iterative calculation at time step level. This coupling scheme also has some flexibility in term of using different surface and subsurface simulation software to perform coupling because it requires an access to the Newton iteration step in subsurface simulation software. However, the error in control parameter estimation (i.e. BHP) rooted from applying the implicit coupling scheme is smaller than the explicit coupling scheme because the surface and subsurface model are balanced in several Newton iteration steps so that the reservoir and fluid properties used in the balancing is updated every Newton step. The flow chart of implicit coupling scheme is shown in Figure 8.

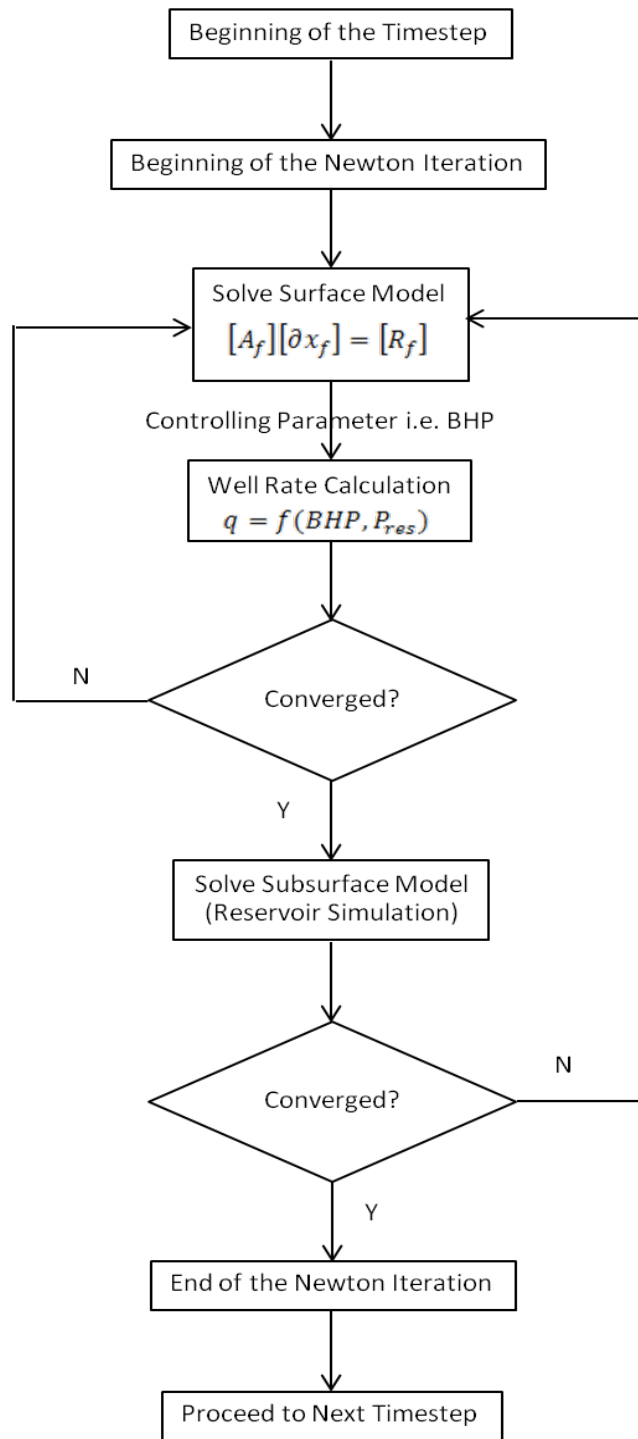


Figure 8: Implicit coupling scheme

3.3.3. Fully Implicit Coupling Scheme

In this scheme, the surface and subsurface model are treated as one domain such that the system of equations of surface facility and system of equations of subsurface facility are solved simultaneously by considering nodes of surface facility as additional grid block of reservoir model. The example of combining system of equation of surface and subsurface model is depicted again here.

$$\begin{bmatrix} \partial x_f \\ \partial x_r \end{bmatrix} = \begin{bmatrix} A_f & \dots \\ \dots & A_r \end{bmatrix}^{-1} \begin{bmatrix} R_f \\ R_r \end{bmatrix}$$

The process of fully implicit coupling scheme is explained below

- The system of equation of surface model and system of equation of subsurface model are combined and solved simultaneously.
- Check that the Newton iteration is converged or not
- If “Y”, proceed to the next time step
- If “N”, repeat the process until the Newton iteration is converged

The fully implicit coupling scheme is the most computational expensive and complicated scheme because it has to be formulated in such a way that the system of equation of surface and subsurface model to a single system of equation. However, it is the “correct way” to coupling because all of the unknown parameters (i.e. reservoir pressure, saturation, and bottomhole pressure) are solved simultaneously and resulting in accurate solution. The flow chart of implicit coupling scheme is shown in Figure 9.

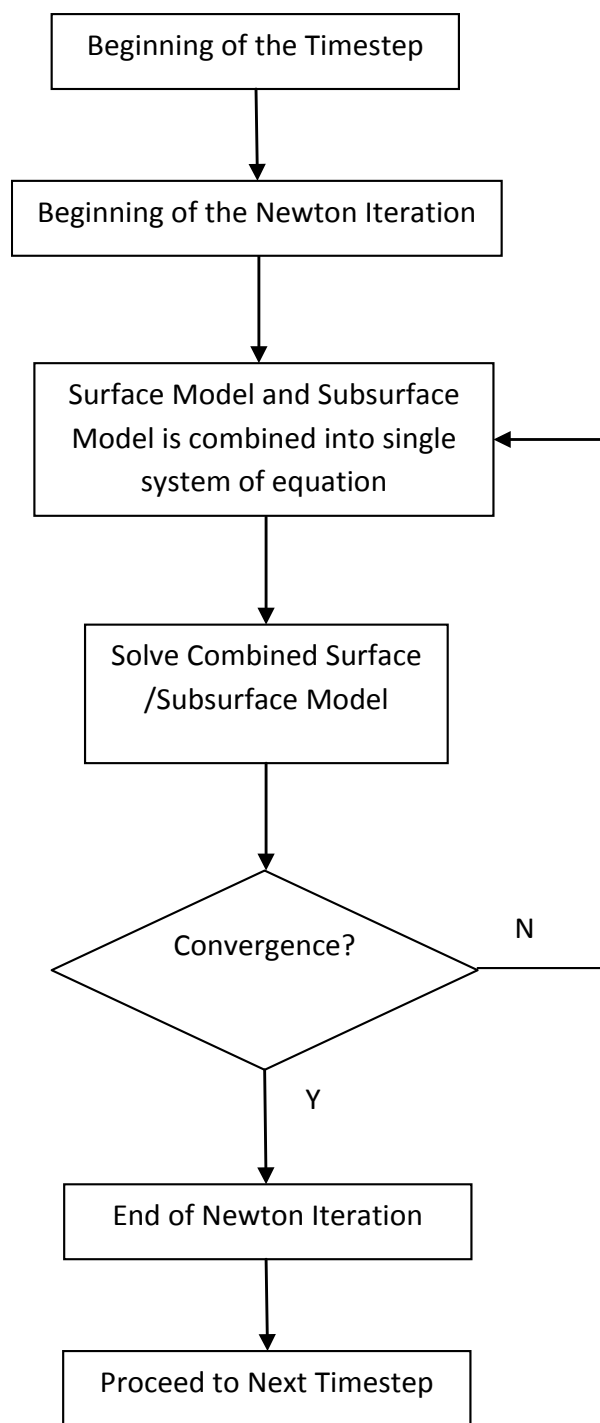


Figure 9: Fully implicit coupling scheme

4. PRODUCTION PREDICTION OF COUPLED SURFACE AND SUBSURFACE MODELS

This chapter presents the results of the investigation of the effect of various coupling levels, and coupling schemes with different reservoir descriptions and fluid properties on production prediction using commercial and in-house simulators developed as part of this project. We start by introducing commercial tools used to couple surface and subsurface model. Then, we show how the in-house simulator can be used in the coupling in the next chapter.

4.1. Surface and Subsurface Simulation Software for Coupling

There are several tools that can be used in coupling surface and subsurface model. The coupling can be done either using commercial software or in-house software. This section will show general overview the Surface and Subsurface Model Coupling Tools used in this study.

4.1.1. Subsurface Simulation Software for Coupling

ECLIPSE 100 & Network Option: ECLIPSE 100 is commercial black oil reservoir simulation software developed by Schlumberger. ECLIPSE 100 alone can simulate the flow of oil, gas, and water phases in subsurface model or reservoir models. Combining with Network Option with ECLIPSE 100 make us to be able to coupling surface and subsurface models.

The way ECLIPSE 100 & Network Option works is that surface models can be represented by simple pressure lost across production and injection network. It can be

input into the program in a form of Outflow Performance tables or Vertical Lift Performance (VLP) tables. The VLP table is the calculated pressure lost across surface models for various flow rate, water cut and GOR that can be generated from production software such as OLGA and PROSPER. For this study, the production software used to generate VLP tables is PROSPER. ECLIPSE 100 & Network Option can find the solution at coupling points by query wellbore curve from ECLIPSE 100 reservoir simulation run and pipeline curve from inputs in the VLP table. The solution is at the intersection of wellbore curve and pipeline curve. The step to find the solution at coupling points is called network balancing. The Figure 10 shows an example of wellbore curve, pipeline curve, and their intersection which is the solution of the coupling point.

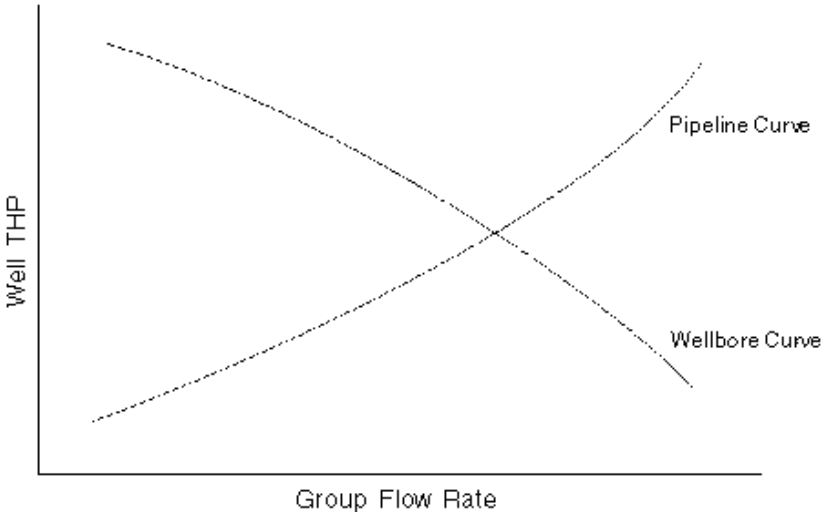


**Figure 10: Example of the intersection of wellbore curve and pipeline curve
(Source: ECLIPSE100's manual)**

ECLIPSE100 & Network Option have several level and frequency of network balancing which allow us to vary coupling level and coupling scheme from loose coupling (i.e. Explicit coupling for every specified time step) to tight coupling (i.e. implicit coupling for every specified Newton iteration). The production and injection network can be setup using the ECLIPSE multi-level grouping hierarchy which allows connecting several production wells or group to its “parent” in the grouping tree by pipeline.

The advantage of using ECLIPSE100 & Network Option as a coupling tool stem from its simplicity because we do not need to deal with several software connection as it just requires only just VLP tables and ECLIPSE deck file with a small modification for doing the coupling using ECLIPSE100 & Network Option. However, there are several drawbacks in using ECLIPSE100 & Network Option. The first drawback is the flexibility of the coupling point. ECLIPSE100 & Network Option has only one option of coupling point which is at wellhead of wells. Secondly, the only allowable control parameter at the most upstream point of the production and injection network is pressure. Moreover, ECLIPSE100 & Network Option cannot be used for production optimization using upstream and downstream (such as tubing head pressure) as control parameter. Lastly, it lacks of an option to visualize and analyze the solution at coupling points. Due to some of these drawbacks, this thesis will concentrate in using different tools for getting more accurate and flexible coupling mechanism which suit with the objective of this study.

Another subsurface simulation that we use in this study is MRST which stand for MATLAB® Reservoir Simulation Toolbox which is an open source code based on a high-level language and interactive environment for numerical computation, visualization, and programming known as MATLAB®. The whole package of MRST consists of two main parts. First part is MRST core which offers a complete set of routines and data structures for creating, manipulating, and visualizing grids and physical properties. MRST assume all grids to be fully unstructured and the toolbox has a particular focus on the corner-point format which widely used in the petroleum industry.

The add-on modules are the second part. This part contains several advanced solvers and tools written as additional scripts and functions that extend, complement, and override existing MRST features. Based on MRST Version 2012b released on the 20th of December, 2012, this part consist several useful features include routine for reading and processing industry-standard input decks (i.e. ECLIPSE input deck files), grid coarsening and upscaling routine, flow diagnostic routine, fully-implicit multiphase solver routine, etc. The example of add-on module is shown in the Figure 11. The routine that will be used and modified to support the coupling is the fully-implicit multiphase solver routine. The structure of fully-implicit multiphase solver routine and detail of modification will be explained in the next chapter.

The advantage of using MRST as a reservoir simulator is that the routine is an open source code with well-organized structure. It is feasible to do the modification of the code without deteriorating flexibility of the routine. Moreover, as mentioned before,

MRST also provide routine for reading and processing industry-standard input decks which are applicable with ECLIPSE input deck files. Consequently, we can guarantee that the input is consistent with the input we use in ECLIPSE100. The result of normal reservoir simulation without coupling from MRST and ECLIPSE 100 is considerably closed and consistent. The result of the comparison will be shown in the next chapter.

Although, there are several advantages of using MRST as a reservoir simulator, some disadvantages hinder its full applicability in the coupling surface/subsurface model. First, MRST is developed based on MATLAB® language which is not highly optimized in terms of computing time. MRST takes considerable more time than ECLIPSE100 to finish the run. The reservoir model with large number of grids can cause a very long simulation run time. In addition, based on the current release, the fully-implicit multiphase solver routine does not provide an adaptive time step feature. Consequently, using large time step size in the beginning of reservoir simulation run may causes divergence of the solution.

Modules

Starting from the 2011a release, MRST has been divided into core functionality and add-on modules, where the latter is defined as a set of functions and scripts that extend or modify the existing capabilities of MRST. A module may use all features of the core toolbox and may, optionally, depend on other modules.

Advanced solvers

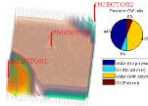
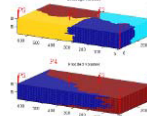
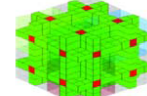
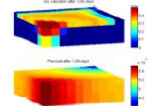
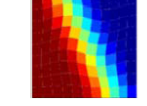
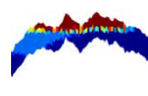
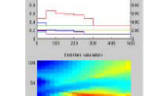
	<p>Fully implicit solvers</p> <p>This module contains a set of fully implicit solvers for a variety of flow problems. The module uses automatic differentiation to calculate Jacobians which makes prototyping of new models faster.</p> <p>Read more..</p> <p>In MRST: <code>mrstModule add ad-fi</code></p>		<p>Flow diagnostics</p> <p>The flow diagnostics module contains utilities and examples demonstrating tracer partitioning and testing of upscaling qu</p> <p>Read more..</p> <p>In MRST: <code>mrstModule add diagnostics</code></p>
	<p>Multiscale mixed finite elements</p> <p>The module implements the multiscale mixed finite-element (MsMFE) method applied to unstructured grids in 3D.</p> <p>Read more..</p> <p>In MRST: <code>mrstModule add msmfe</code></p>		<p>Multiscale finite volumes</p> <p>The module implements the multiscale finite-volume (MsFV) method applied to unstructured grids in 3D.</p> <p>Read more..</p> <p>In MRST: <code>mrstModule add msfv</code></p>
	<p>IMPES solver</p> <p>This module contains an implementation of a pressure/transport solver using an Implicit Pressure, Explicit Saturation (IMPES) strategy for compressible black-oil flow.</p> <p>Read more...</p> <p>In MRST: <code>mrstModule add impes</code></p>		<p>MPFA</p> <p>The module implements the MPFA-O scheme, which is an example of a multipoint flux-approximation scheme that emp more degrees of freedom to ensure a consistent discretizati with reduced grid-orientation effects.</p> <p>In MRST: <code>mrstModule add mpfa</code></p>
	<p>Numerical CO₂ laboratory</p> <p>The module contains tools and scripts for fast and accurate simulation of CO₂ migration based upon a vertically integrated model as well as routines for interacting with publicly available datasets.</p> <p>Read more..</p>		<p>Adjoint formulations</p> <p>This module implements strategies for production optimisati based on adjoint formulations. This enables for instance net present value optimization constrained by the bottom hole pressure in wells.</p> <p>In MRST: <code>mrstModule add adjoints</code></p>

Figure 11: The example of available add-on module in MRST (Source: MRST's Website)

4.1.2. Commercial Surface Simulation Software

PROSPER is a commercial software developed by Petroleum Expert Limited. PROSPER stand for Production and System Performance analysis software. PROSPER provides the way to predict tubing and pipeline hydraulics with accuracy and speed. PROSPER can generate VLP tables that contain information of pressure lost in tubing and pipeline under various parameter sensitivity such as upstream injection pressure, downstream production pressure, water cut, and gas-oil ratio.

As mentioned before, ECLIPSE 100 & Network Option use VLP tables generated by PROSPER to represent the pressure lost in production and injection network. For the case of using MRST as a reservoir simulator choice, the VLP tables generated by PROSPER can also be used to represent the pressure lost in production and injection network.

4.2. Effect of Various Coupling Level and Scheme with Different Reservoir

Descriptions and Fluid Properties on Production Prediction

This phase of study is aimed to thoroughly understand the effect of the permeability and fluid properties with different coupling levels, and coupling schemes before moving to the 2nd Phase of study that include the production optimization performance.

4.2.1. Sensitivity Parameters

In order to, demonstrate each of these coupling mechanism capabilities; we will develop our finding based on the reservoir model as described in Table 3. This general reservoir simulation model will be used during the entire this phase of the study.

Reservoir Simulation Model Properties	Value	Unit
NX:NY:NZ (homogeneous)	45:45:6	
NX:NY:NZ (heterogeneous)	45:45:2	
Grid size (homogeneous)	20 x 20 x 1	ft
Grid size (heterogeneous)	20 x 20 x 3	ft
Porosity	20	%
Initial Water Saturation	10	%
Initial Oil Saturation	90	%
SCAL	Figure 12 & 13	
Production Scenario	Direct line drive	
Reservoir pressure	3000	psia
Reservoir depth	3000	ft

Table 3: Summary of reservoir simulation model properties used in the 1st phase of the study

In addition to the Table 3 summarized the general reservoir properties, the relative permeability relationships of gas-oil, and oil-water are shown in the Figures 12 and 13. The general surface facility model properties used in the 1st Phase of study is summarized in the Table 4.

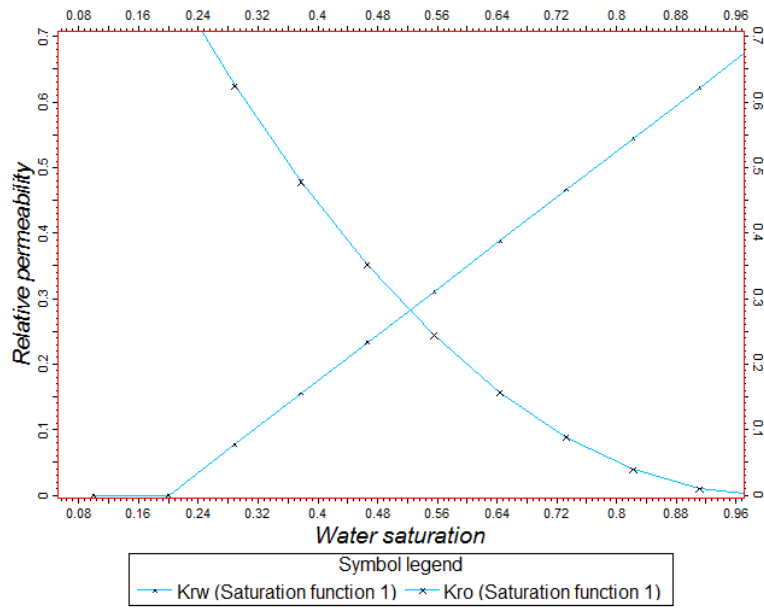


Figure 12: Oil-Water relative permeability

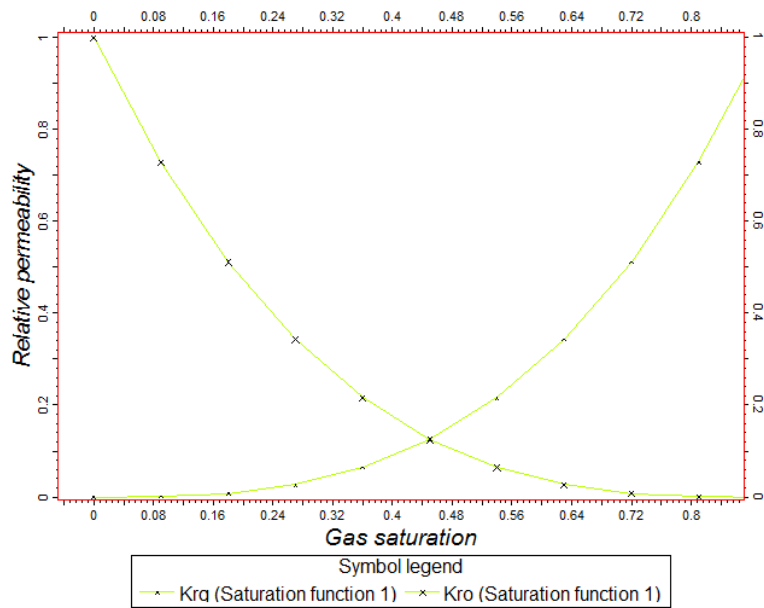


Figure 13: Gas-Oil relative permeability

Surface Facility Model Properties	Value	Unit
Production Tubing Size (ID)	6	in
Production Tubing Length	3000	ft
Injection Tubing Size (ID)	6	in
Injection Tubing Length	3000	ft
Surface Pipeline Size (ID)	6	in
Surface Pipeline Length	3280	ft
Downstream Production Pressure	100	psig
Upstream Injection Pressure	3000	psig

Table 4: Summary of surface facility model properties used in the 1st phase of the study

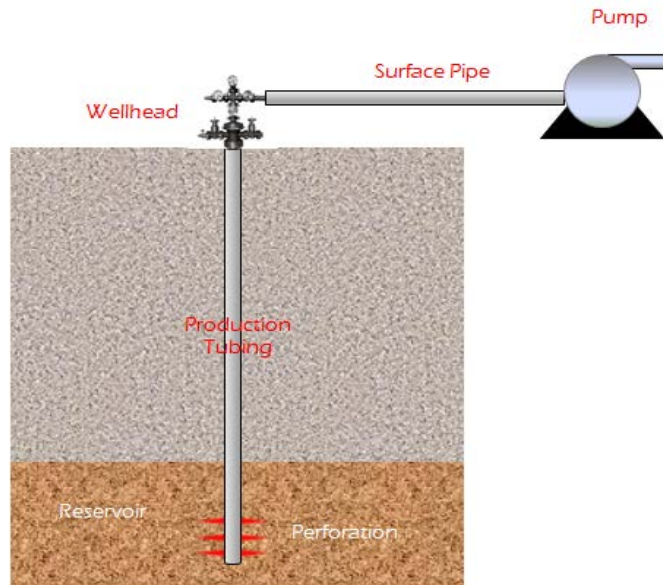


Figure 14: Surface model of production and injection facilities

- Production scenario

The example of the surface model of production and injection used in 1st phase of study is shown in the Figure 14. The coupling point of the models is at wellhead. The production scenario used to demonstrate the several level of coupling was chosen as a direct line drive waterflooding with two production and two injection wells at each corner of the reservoir model. The upstream pressure (pumping head pressure) of water injection is given at 3000 psi and the downstream pressure of production is at 100 psi.

There are three main types of parameter that we consider: Coupling scheme and frequency, reservoir description, and fluid properties. The summary of parameter varied in the 1st phase of study is shown in the Table 5.

Coupling scheme and frequency	Explicit Coupling Every 15 Days	Explicit Coupling Every Timestep	Implicit Coupling First 3 Newton Iteration
Reservoir Description	Homogeneous - High Perm	Homogeneous - Low Perm	Heterogeneous
Fluid Properties	Dead oil	Lived oil	

Table 5: Summary of parameter varied in the 1st phase of study

- Coupling scheme and frequency

As mentioned before the coupling mechanism that we consider in this study is explicit and implicit coupling. Consequently, there are three main types of coupling scheme and frequency that we consider in this study.

- Explicit coupling for every 15 days: The surface model is balanced at the beginning of each time step that starts after 15 days interval has elapsed since the previous balancing calculation. The diagram for this type of coupling is shown in the Figure 15. The figure shows that the simulation starts at 0 day. In the beginning of the time step of $T = 0$ day, the surface model will be balanced before the 1st Newton iteration and proceed to the next time step under the same well target until it reaches the next 15 days. The process will be repeated until it reaches the end of the prediction time.

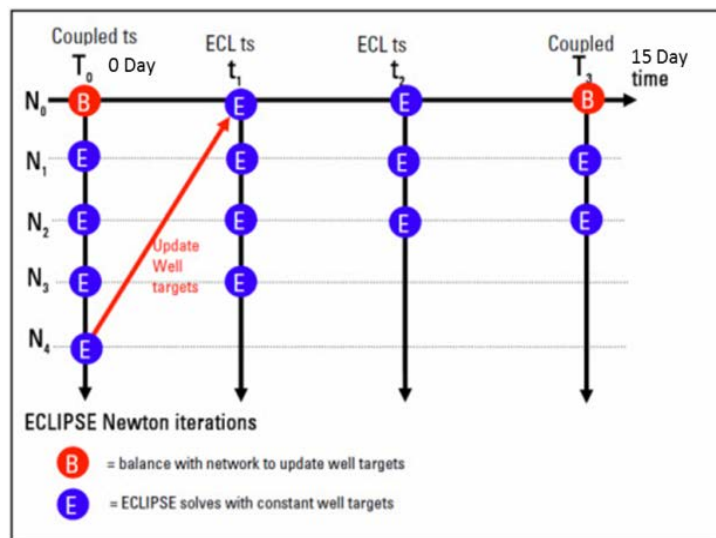


Figure 15: Schematic of explicit coupling in every 15 days (Source: AVOCET's manual)

- Explicit coupling for every time step: The surface model is balanced at the beginning of every time step (before the 1st Newton iteration) since the previous balancing calculation. The diagram for this type of coupling is

shown in the Figure 16. The figure shows that the simulation starts at 0 day. In the beginning of the time step of $T = 0$ day, the surface model will be balanced before the 1st Newton iteration and proceed to the next time step. The process will be repeated until it reaches the end of prediction time.

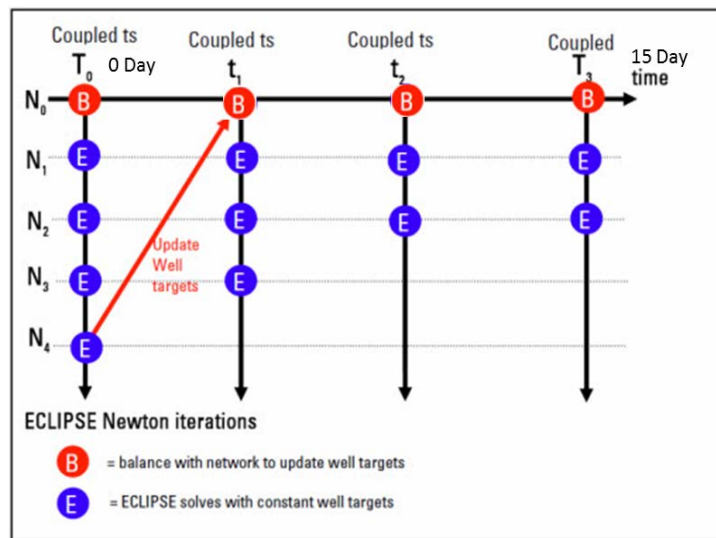


Figure 16: Schematic of explicit coupling in every time step (Source: AVOCET's manual)

- Implicit coupling for every first 3 Newton iteration: The network will be balanced in each of the first three Newton iterations of every time step. The diagram for this type of coupling is shown in the Figure 17. The figure shows that the simulation starts at 0 day. In the beginning of the time step of 0 day, the surface model will be balanced at zero th Newton iteration (before the 1st Newton iteration) to second Newton iteration and proceed to the next time step. The process will be repeated until reach the end of prediction time.

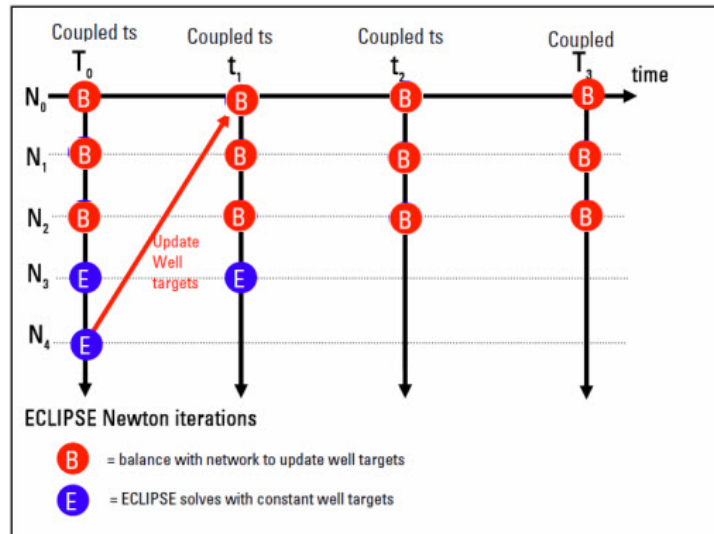


Figure 17: Schematic of explicit coupling in every first three Newton iteration (Source: AVOCET's manual)

- Reservoir descriptions

In this phase of study various reservoir properties (i.e. permeability) are considered. There are three main types of reservoir descriptions that we include in the coupling study.

- Homogeneous high permeability: for the case of homogeneous high permeability, the reservoir model has permeability about 550 md with ratio of vertical permeability and horizontal permeability ($k_v:k_h$ ratio) about 0.1.
- Homogeneous low permeability: for the case of Homogeneous Low Permeability, the reservoir model has permeability about 50 md with $k_v:k_h$ ratio about 0.1.

- Heterogeneous permeability: the reservoir model has average permeability about 250 md with kv:kh ratio about 0.1. The permeability range is 30 – 5000 md with high permeability zone in the northwest of the reservoir model.

The figures of reservoir model of the heterogeneous and homogeneous permeability cases are shown in the Figure 18.

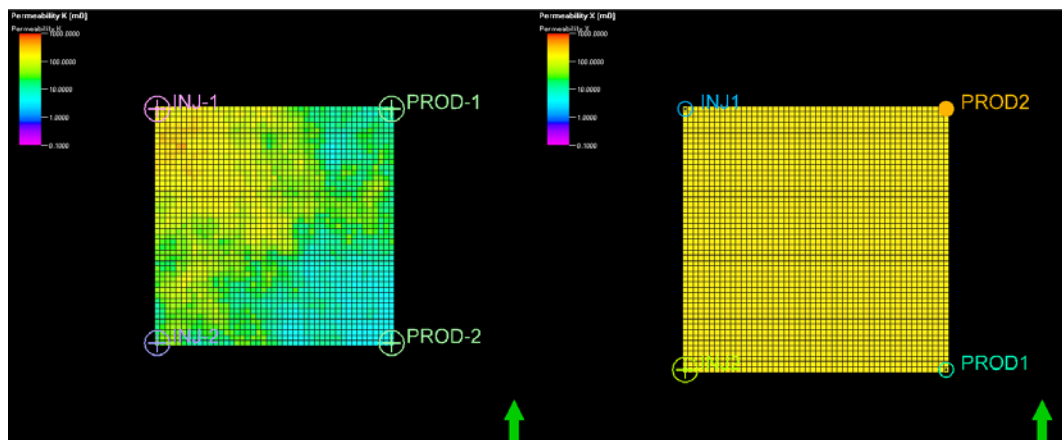


Figure 18: The permeability of reservoir model in the case of heterogeneous permeability (left) and homogeneous permeability (right)

- Fluid properties: There are two main types of fluid properties that we consider.

Dead Oil PVT:

- Oil density 30 API
- Gas gravity 0.664 sg air
- Solution GOR 0.09 MSCF/STB

Lived Oil PVT

- Oil density 40 API

- Gas gravity 0.664 sg air
- Solution GOR 1.5 MSCF/STB

4.2.2. Study Cases

In total, there are eighteen cases to be ran and analyzed, in order to understand the effect of each parameter on the production prediction. The results of each different coupling scheme and frequency on the same reservoir description and fluid property will be analyzed together to compare the differences in prediction of the production and injection rates.

- Case 1: Homogeneous high permeability – lived oil PVT

Figure 19 shows the production profile of well “PROD1”. The production profile of two production wells (PROD1 & PROD2) are the same. Consequently, the only one production profile will be shown here. The dash line represents oil production rate and the solid line represents bottomhole flowing pressure. Three different line colors represent three different coupling schemes and frequencies. The figure shows that in the case of explicit coupling for every 15 days the oil production rate is lower than the other cases in the first 15 days as the bottomhole flowing pressure is higher than the other cases in the first 15 days. This can be explained by following reason: for explicit coupling, the surface and subsurface model are not completely balanced. Consequently, the bottomhole flowing pressure obtained from the balancing is not the actual value of bottomhole flowing pressure for that time step which causes discrepancies in the final result.

The balanced pressure in the first time step will be used as the well control target for the whole period of 15 days of the production prediction. For the case of explicit coupling for every time step and implicit coupling, the results are almost the same because of the bottomhole flowing pressures of these two cases are closed to each other which it implies that the explicit coupling for every time step gives acceptable balancing of surface and subsurface model.

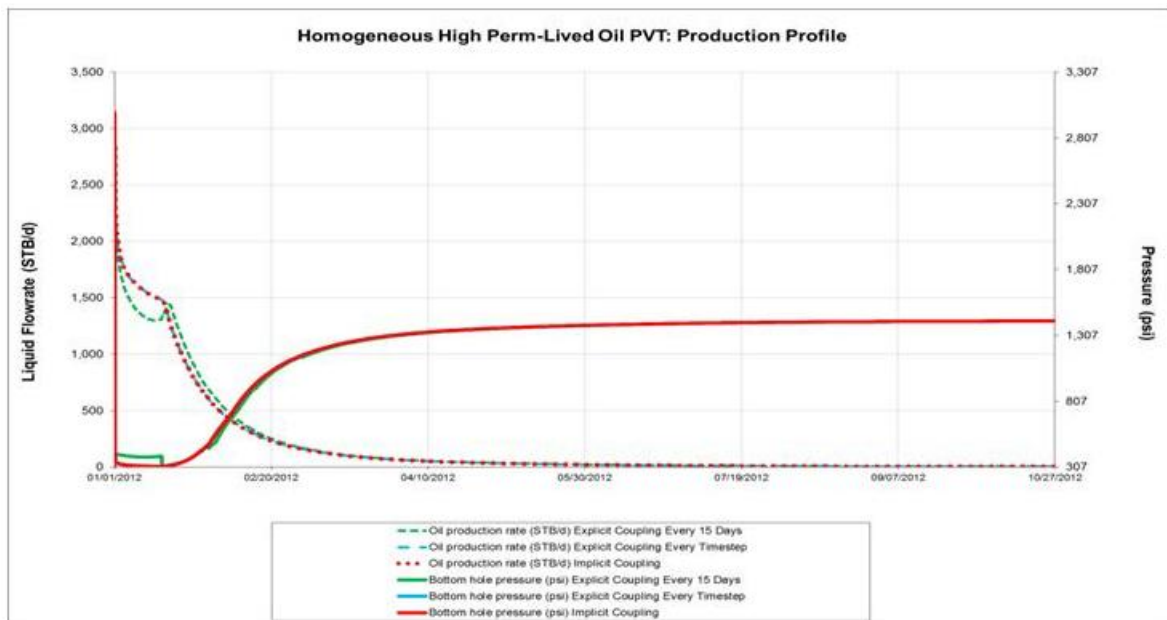


Figure 19: Oil production profile and bottomhole pressure of homogeneous high perm – lived oil PVT case

Figure 20 shows the injection profile of well “INJ1”. The only one injection profile will be shown here because the injection profile of two injection wells are the same. The dash line represents water injection rate and the solid line represents bottomhole flowing pressure. Three different line colors represent three different

coupling schemes and frequencies. The figure shows that in the case of explicit coupling every 15 days, the water injection rate is lower than the other case in the first 15 days as the bottomhole flowing pressure is lower than the other case in the first 15 days. This occurs as in the production profile case because for explicit coupling, the surface and subsurface model are not completely balanced.

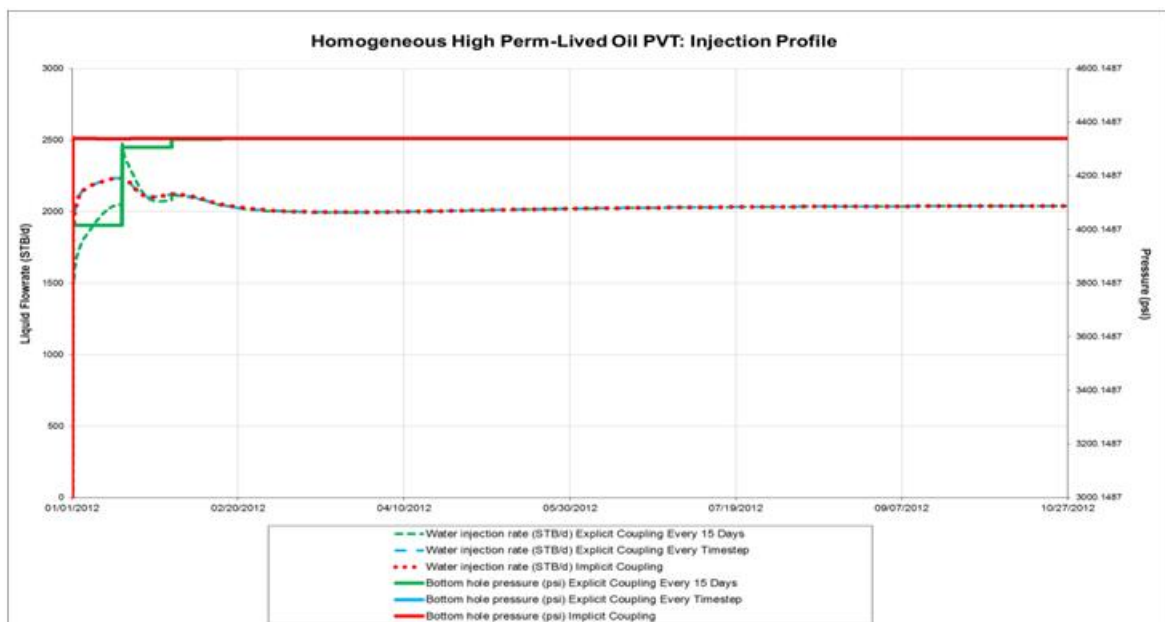


Figure 20: Water injection profile and bottomhole pressure of homogeneous high perm – lived oil PVT case

It can be noticed that the oil production rate of the first 15 days of the explicit coupling case every 15 days is not only lower than the other cases but it's also dramatically decline. This because the water injection rate of the case is lower than the other cases resulting in much lower reservoir pressure and lead to high rate of production decline.

- Case 2: Homogeneous low permeability – lived oil PVT

The production and injection profile of two production wells and two injection wells for the case homogeneous low permeability – lived oil PVT are the same. So, the production and injection profile from only one production and injection well will be shown here.

The production profile shown in Figure 21 shows demonstrates similar results as the homogeneous high permeability – lived oil PVT case. The figure shows that in the case of explicit coupling every 15 days, the oil production rate is lower than the other cases in the beginning period of production, because the bottomhole flowing pressure is higher than the other case in that period. However, the difference of the production rate is less obvious than the case of homogeneous high permeability – lived oil PVT. This implies that in the lower permeability reservoir case, the changing of bottomhole flowing pressure has less effect on the change of production rate. This can be explained by Nodal analysis. The IPR curve of low and high permeability cases is shown in the Figure 22. The line with number 0 represent the IPR of low permeability case while the line with number 1 represent the IPR of high permeability. It obviously shows that for the case of low permeability when the pressure change from 1500 psi to 750 psi the production rate is changed just only 200 STB/D while for the case of high permeability the production rate is changed about 1000 STB/D.

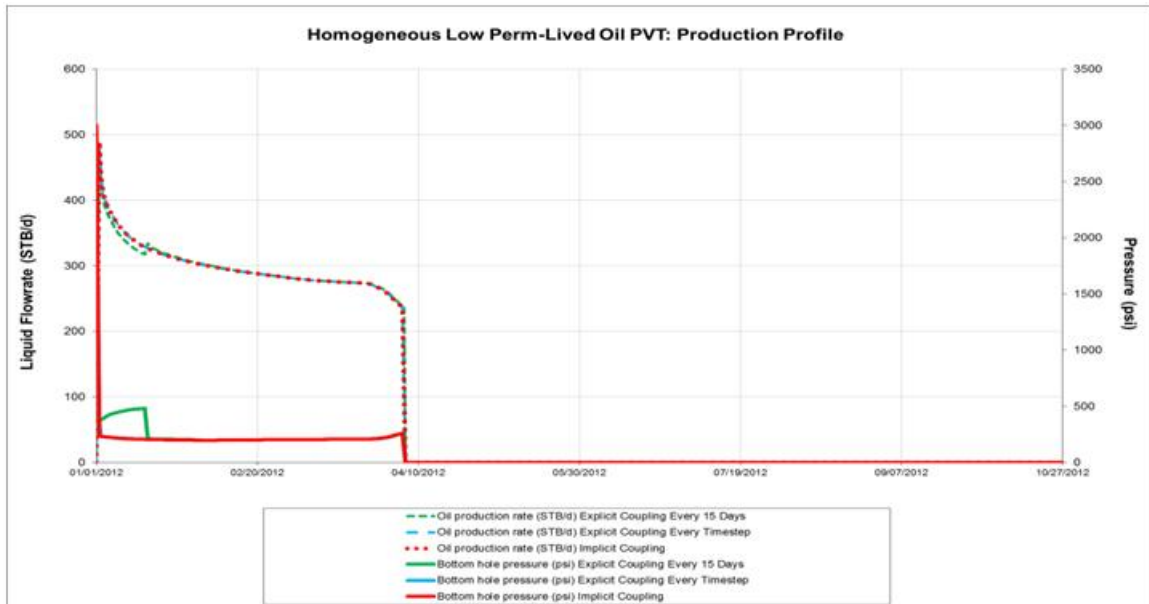


Figure 21: Oil production profile and bottomhole pressure of homogeneous low perm – lived oil PVT case

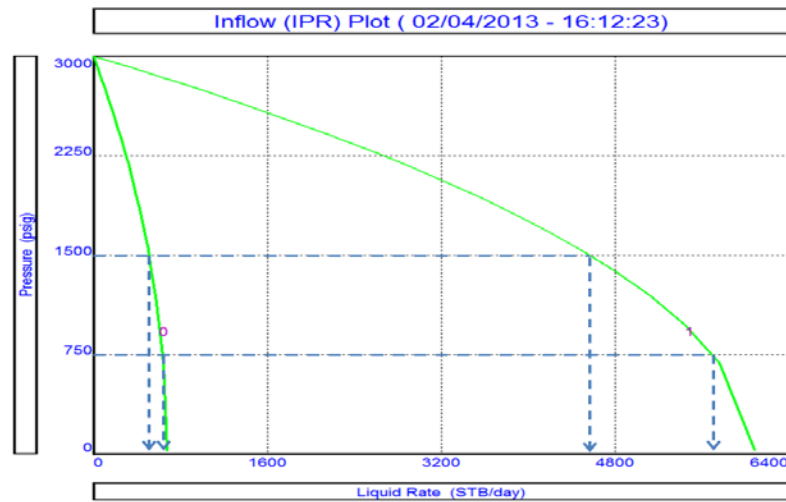


Figure 22: IPR of high and low permeability reservoir

Also for the injection profile, the same trends can be experienced with the injection rate. Figure 23 shows that in the case of explicit coupling for every 15 days, the water injection rate is lower than the other cases in the first 15 days as the bottomhole flowing pressure is lower than the other cases in the first 15 days.

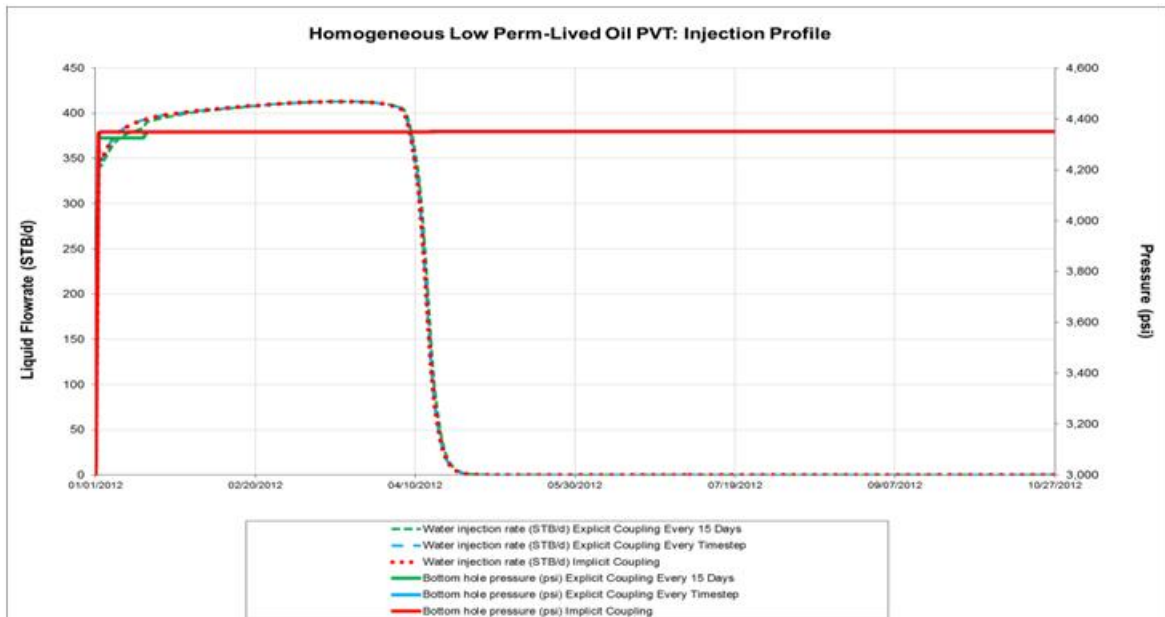


Figure 23: Water injection profile and bottomhole pressure of homogeneous low perm – lived oil PVT case

- Case 3: Heterogeneous permeability – lived oil PVT

For the case of heterogeneous permeability, the production and injection profile of the two production injection well are different as they are placed in the different permeability zones. The injection well “INJ-1” and the production well “PROD-1” are in the high permeability zone while the injection well “INJ-2” and the production well “PROD-2” are in the low permeability zone. This explained why under the same

conditions of production and injection, the injection rate of well “INJ-1” is higher than “INJ-2” and the production rate of “PROD-1” higher than “PROD-2”.

For production profile, it can be observed from Figures 24 and 25 that the oil production rate of both “PROD-1” and “PROD-2” wells in the case of explicit coupling for every 15 days is lower than the other cases in the first 15 days because of bottomhole flowing pressure difference resulting from incomplete balancing of surface and subsurface model. However, the production rate in the first 15 days does not show much trend of decline because the injection rates of two injection wells are relatively constant. For the production profile, both “PROD-1” and “PROD-2” well in the case of explicit coupling for every time step and implicit coupling, the production rate over all production period are almost the same because the bottomhole flowing pressure of these two cases are closed to each other.

For injection profiles of both two injection wells which shown in the Figures 26 and 27, the water injection rate in the first 15 Days of the case of explicit coupling for every 15 days is lower than the other cases but it's relatively constant. After the first 15 days, the reservoir pressure of the case explicit coupling for every 15days is lower than the other cases and the bottomhole flowing pressure get closer to the other case resulting in a small peak in injection rate in a short period and decline rapidly to a constant injection rate.

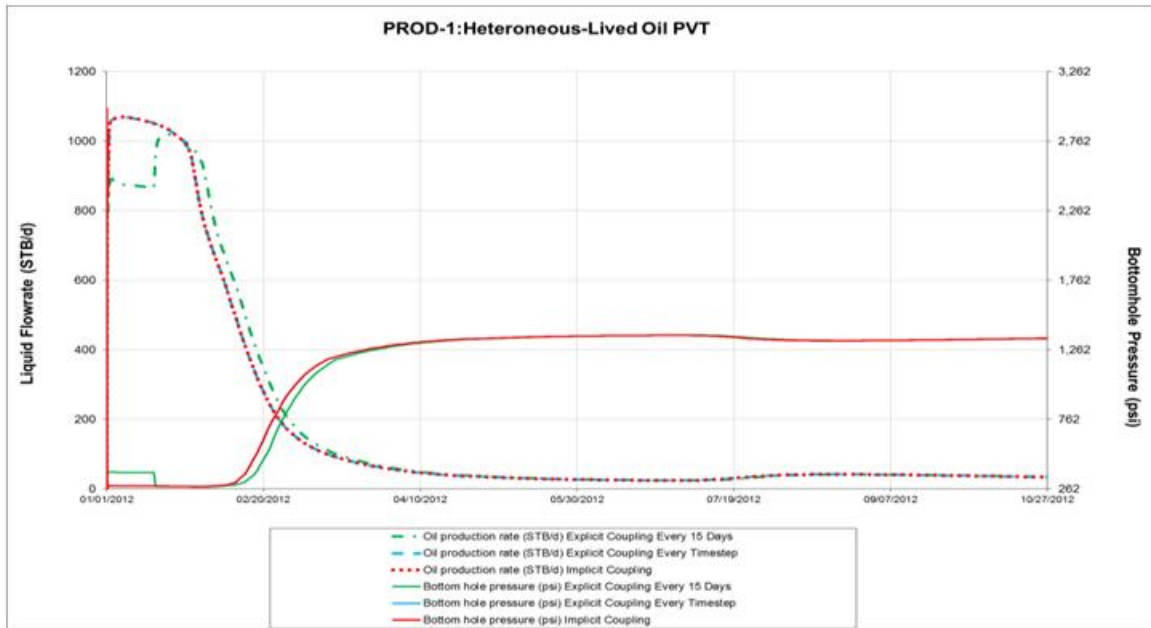


Figure 24: Oil production profile and bottomhole pressure of PROD-1 for heterogeneous perm – lived oil PVT case

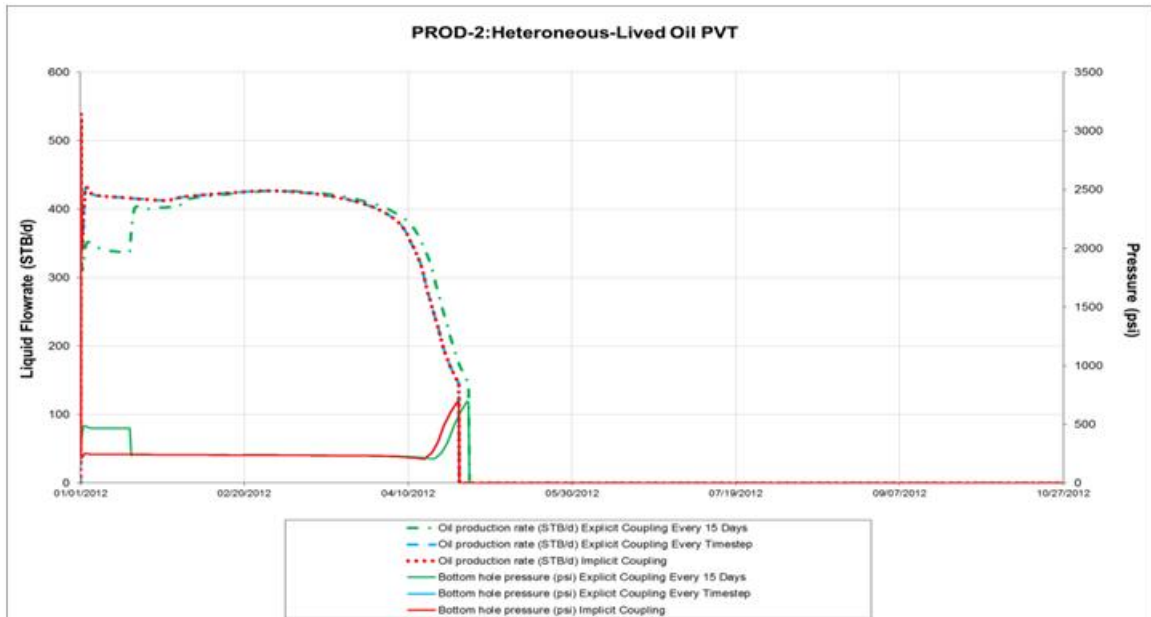


Figure 25: Oil production profile and bottomhole pressure of PROD-2 for heterogeneous perm – lived oil PVT case

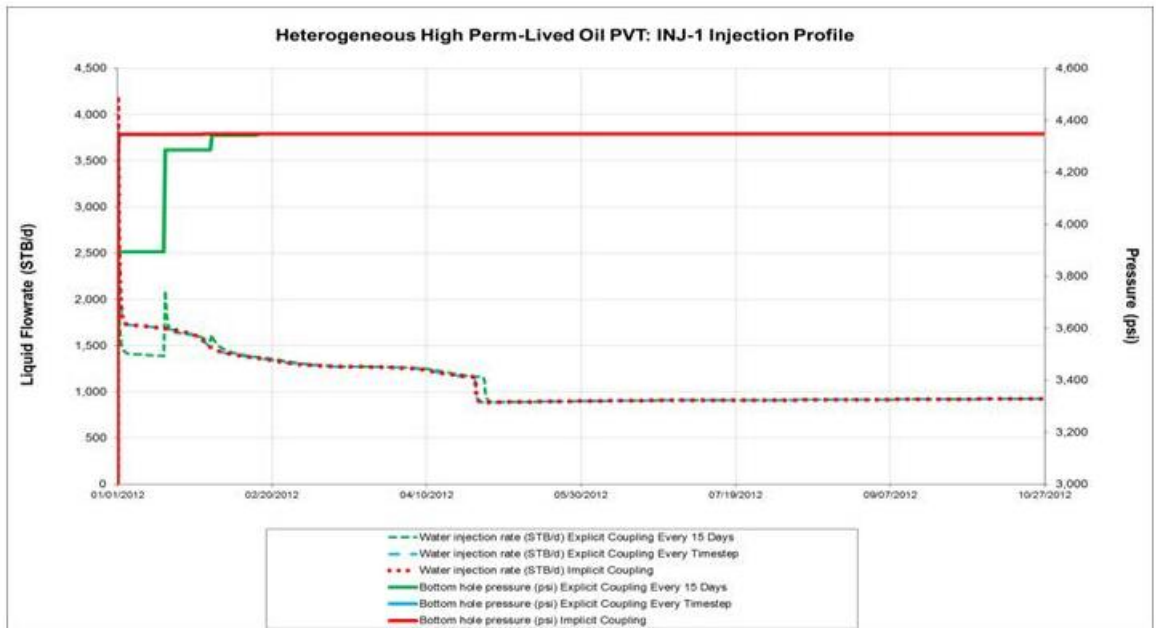


Figure 26: Water Injection profile and bottomhole pressure of INJ-1 for heterogeneous perm – lived oil PVT case

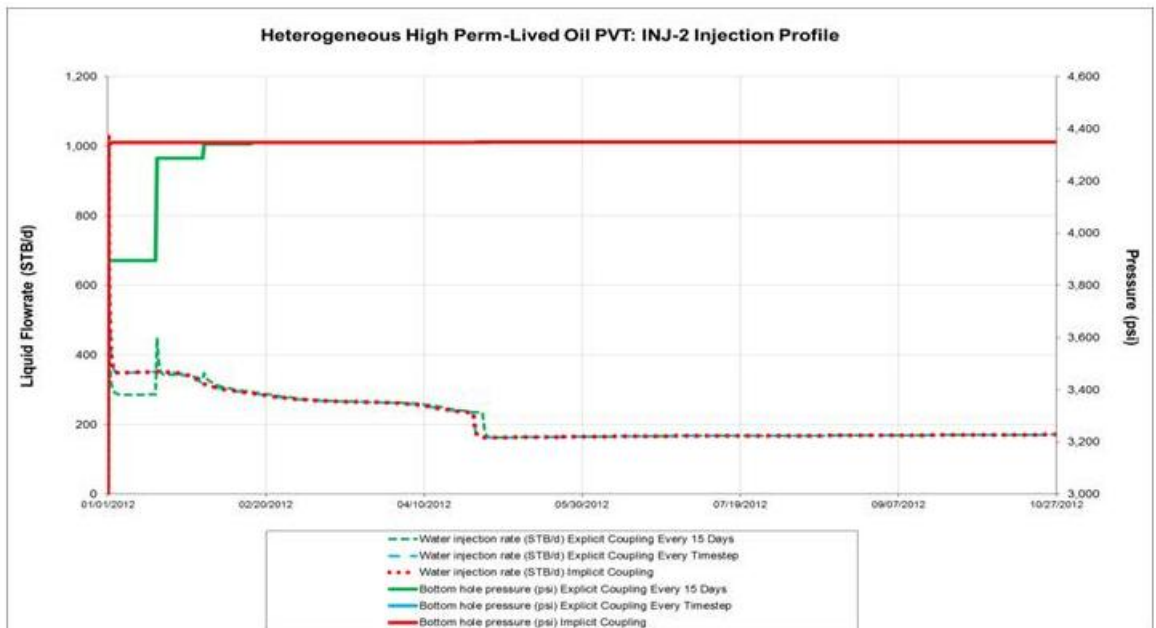


Figure 27: Water Injection profile and bottomhole pressure of INJ-2 for heterogeneous perm – lived oil PVT case

- Case 4: Homogeneous high permeability – dead oil PVT

The production profile of two production wells (PROD1 & PROD2) are the same. Consequently, the only one production profile will be shown here. Figure 28 shows the production profile of “PROD1”. It can be seen that the oil production rate of different coupling scheme and frequency are the same because the bottomhole flowing pressure of each cases are indifferent and the rate of injection are the same for all cases.

The injection profile of two production wells (INJ1 & INJ2) are the same. Consequently, the only one injection profile will be shown here. The injection profile in Figure 29 shows no different between various types of coupling although the bottomhole flowing pressure for the case of explicit coupling for every 15 days shows a bit of difference. It is not significant to affect the injection rate.

The reason that the bottomhole flowing pressure for all the cases is the same can be easily explained by the fact that the IPR of dead oil PVT is a straight line (due to very low amount of gas phase flow). So, it does not require several time step (for explicit coupling) or Newton iteration (for implicit coupling) to get an actual balancing point between surface and subsurface model (The detail of finding balancing point between surface and subsurface model can be found the section 5). In addition, fluid properties such as oil density, gas density, and GOR of the dead oil PVT of oil production stream do not change significantly over the whole production period. This cause pressure lost and production rate relationship in the production facility (tubing head to downstream) to be the same over the time till before the water breakthrough. This is the reason that the frequency of coupling does not cause bottomhole flowing pressure differences. After

water breakthrough, WOR keep increasing but it does not affect pressure lost in the production facility get it results in slight changes of pressure lost and production rate relationship. Consequently, the bottomhole flowing pressure of different coupling cases are the same.

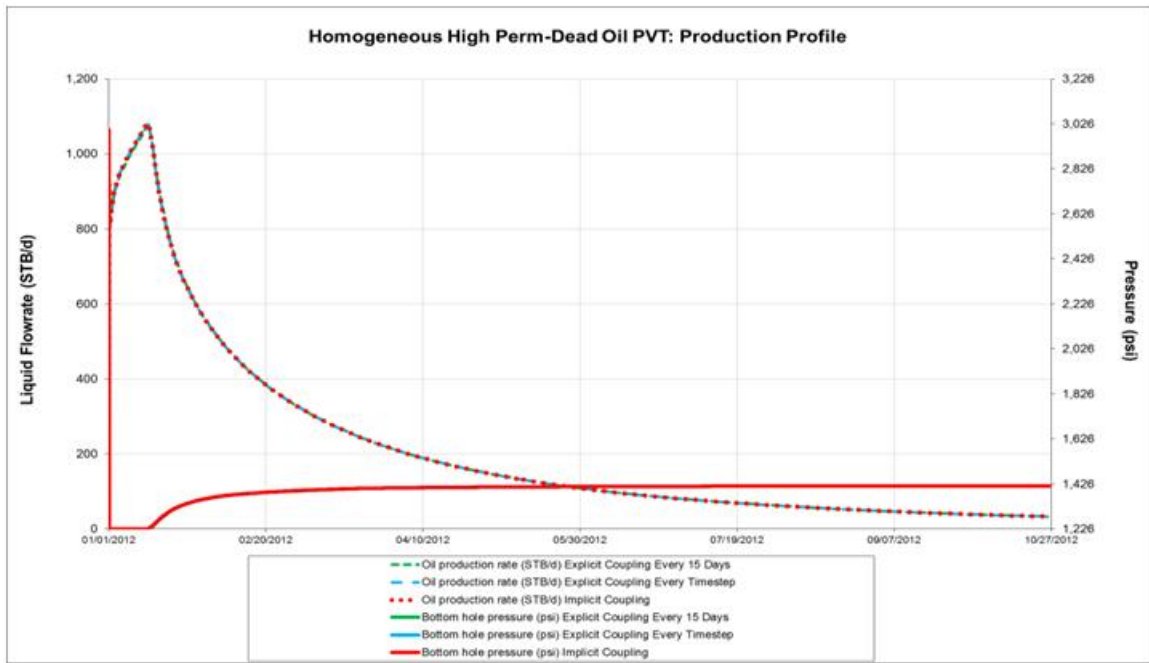


Figure 28: Oil production profile and bottomhole pressure of homogeneous high perm – dead oil PVT case

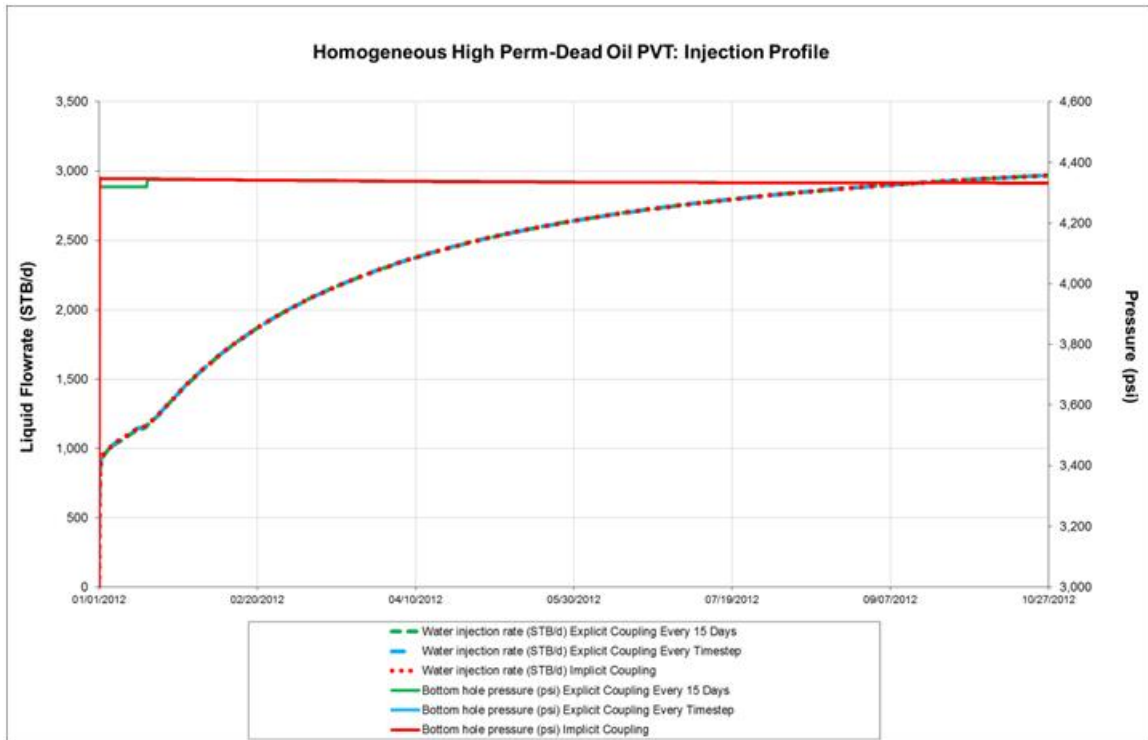


Figure 29: Water injection profile and bottomhole pressure of homogeneous high perm – dead oil PVT case

- Case 5: Homogeneous low permeability – dead oil PVT

For the case of homogeneous low permeability – dead oil, the results in Figures 30 and 31 show the same trend as the homogeneous high permeability – dead oil case. To this end, there is no difference in production profile and bottomhole flowing pressure between various types of coupling. This can be explained by the same reason mentioned in the case of homogeneous high permeability – dead oil PVT case. However, the rate of production of the case of low permeability is lower than the case of high permeability because the reservoir has lower productivity.

The same observations can be achieved with the injection profile. It also shows no difference between various types of coupling of comparing high and low permeability cases: moreover, the injection rate of the case of low permeability is lower than the case of high permeability because of lower permeability.

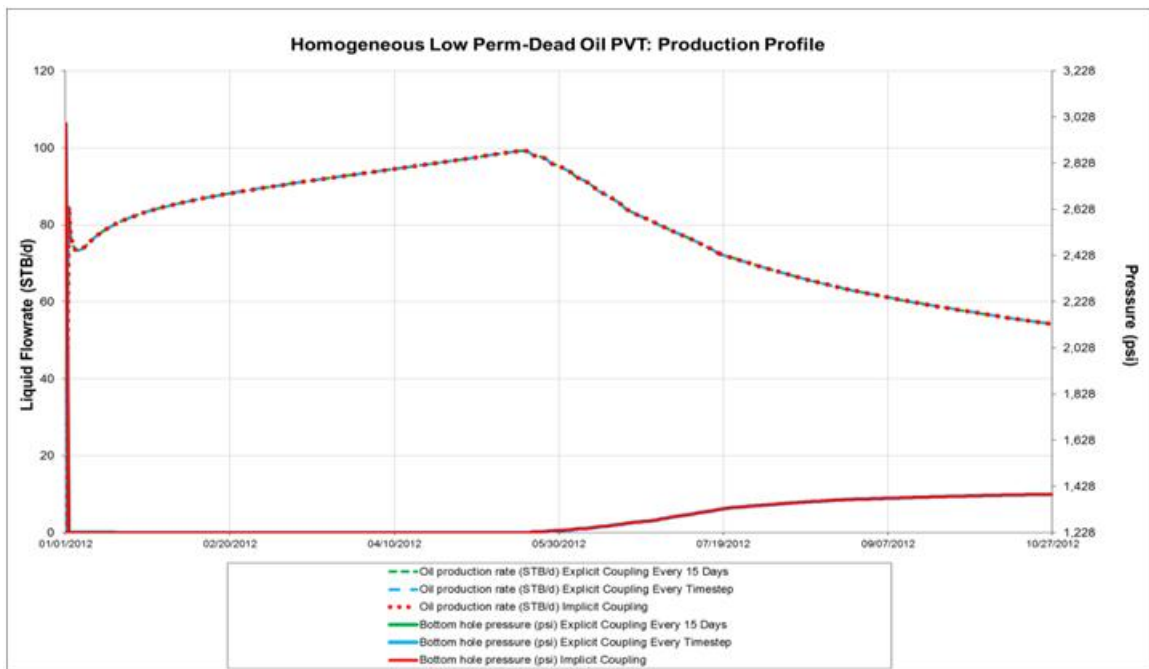


Figure 30: Oil production profile and bottomhole pressure of homogeneous low perm – dead oil PVT case

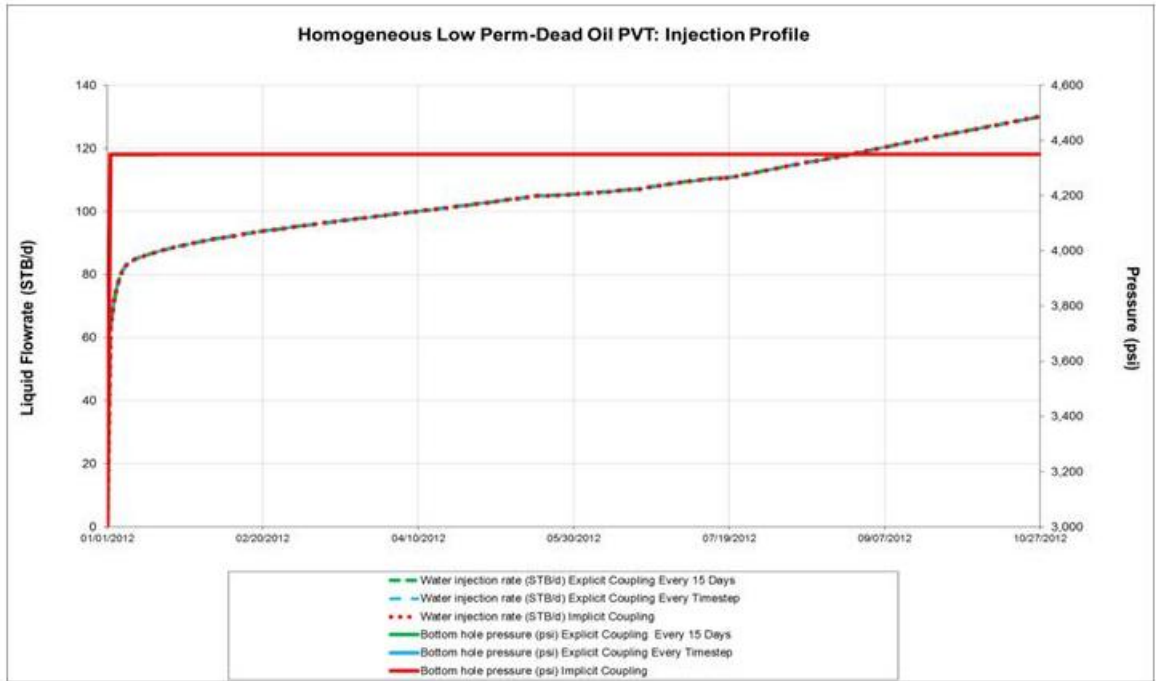


Figure 31: Water injection profile and bottomhole pressure of homogeneous low perm – dead oil PVT case

- Case 6: Heterogeneous permeability – dead oil PVT

The difference of permeability causes the production profile of the well “PROD-1” and “PROD-2” to be different. The production rate of “PROD-1” is higher because the well locates in the high perm zone. This also occurs with injection wells. The injection well “INJ-1” has higher injection rate than “INJ-2”.

Figure 32 and Figure 33 show that there are not differences between various types of coupling in production profile and bottomhole flowing pressure. The reason is the same as explained before. The same thing occurs with the injection profile in Figures 34 and 35. It also shows no different between various types of coupling although the

bottomhole flowing pressure for the case of explicit coupling for every 15days shows a bit of difference. It is not significant to affect the injection rate.

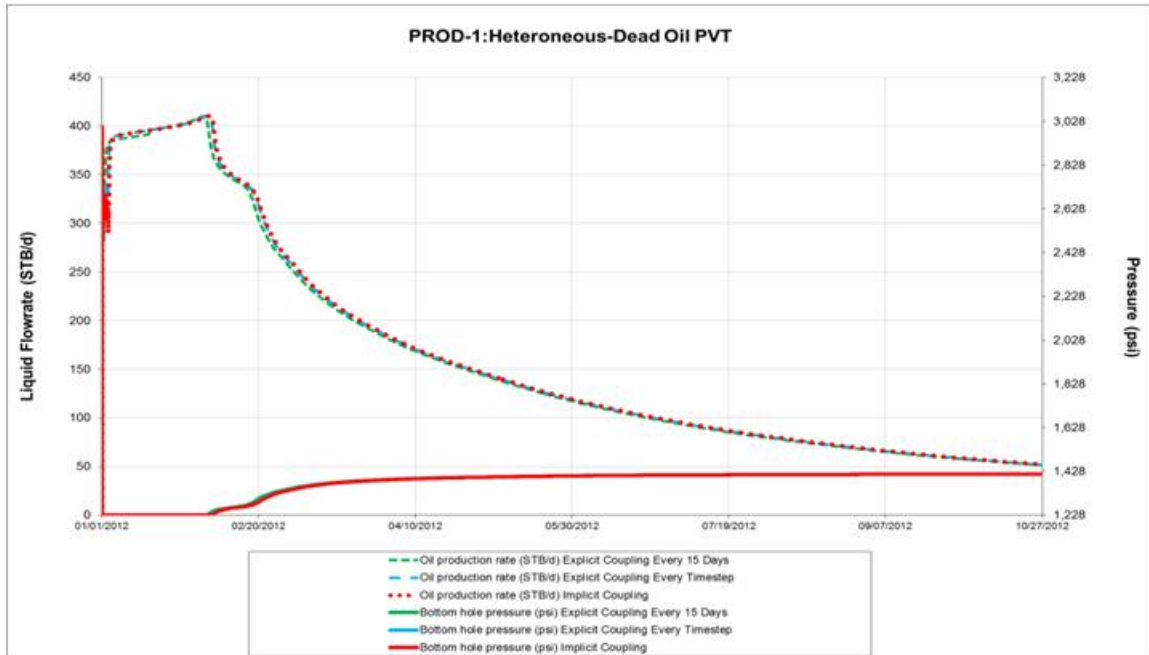


Figure 32: Oil production profile and bottomhole pressure of PROD-1 for heterogeneous perm – dead oil PVT case

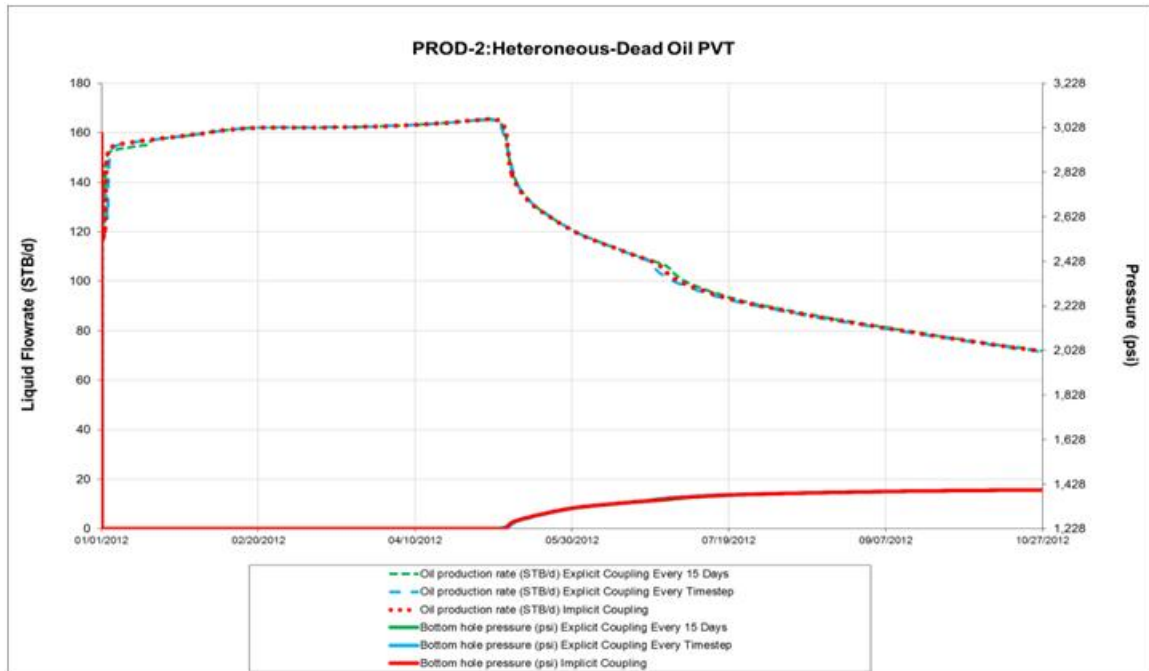


Figure 33: Oil production profile and bottomhole pressure of PROD-2 for heterogeneous perm – dead oil PVT case

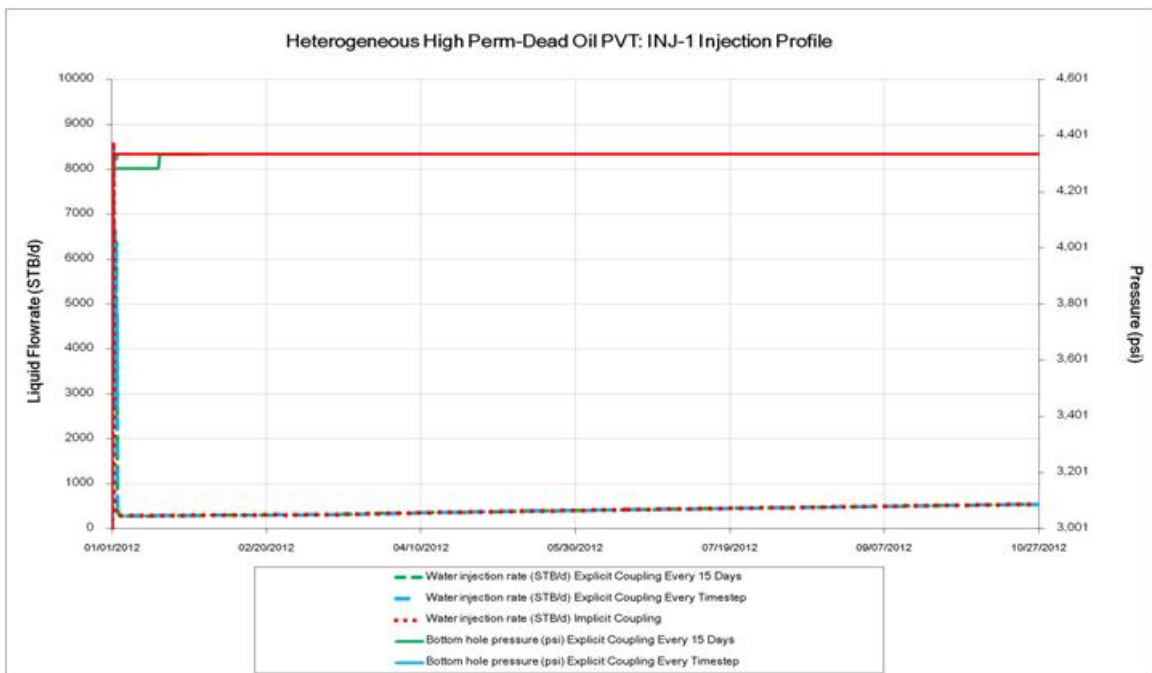


Figure 34: Water injection profile and bottomhole pressure of INJ-1 for heterogeneous perm – dead oil PVT case

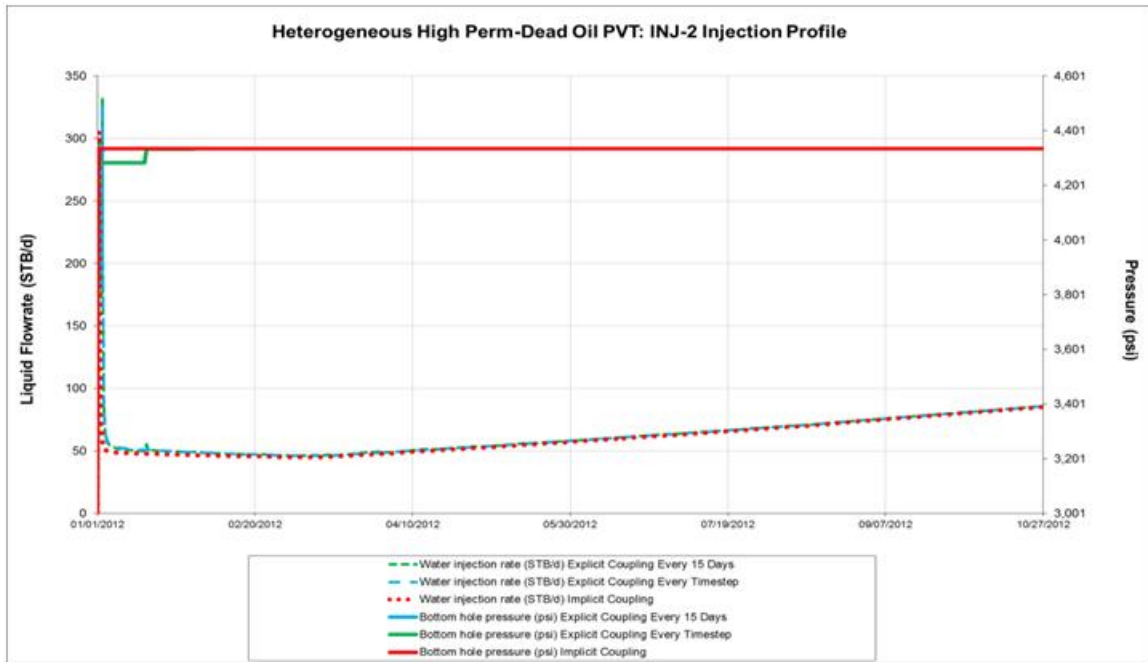


Figure 35: Water injection profile and bottomhole pressure of INJ-2 for heterogeneous perm – dead oil PVT case

All the case run, the bottomhole production pressure is increased because the water is breakthrough at the production well.

4.3. Effect of the Original Oil In-Place (OOIP) Size

This part aims to illustrate the effect of system size or, in another word the size of the OOIP with different coupling levels, and coupling schemes. The size of the reservoir can has an effect on production prediction with different coupling level, and coupling scheme because under the same production strategy in a small system (i.e. small OOP), the reservoir conditions (i.e. pressure, saturations) are changed much faster than the system or reservoir that has large OOIP. The dynamics of the reservoir condition

especially in an early time of production for coupling level and coupling scheme like explicit coupling can lead to balancing error and resulting in different production profile. The general reservoir simulation model properties used to study the effect of system size is summarized in the Table 6.

Reservoir Simulation Model Properties	Value	Unit
NX:NY:NZ (homogeneous)	23:23:6	
NX:NY:NZ (heterogeneous)	23:23:6	
Grid size (homogeneous)	350 x 350 x 5	ft
Grid size (heterogeneous)	350 x 350 x 5	ft
Porosity	20	%
Initial Water Saturation	10	%
Initial Oil Saturation	90	%
SCAL	Gas-Oil & Oil-Water	
Production Scenario	Direct line drive water flooding	
Reservoir pressure	3000	psia
Reservoir depth	3000	ft

Table 6: Summary of reservoir simulation model properties used to study the effect of OOIP

It can be seen that all of the reservoir simulation model properties are the same as in previous section except the grid size and the number of grid these changes affect the size of reservoir and resulting in larger OOIP about 400 times than the reservoir simulation model in the previous section. From now on the reservoir simulation model in this section will be called large OOIP reservoir and the reservoir simulation model in previous section will be called small OOIP reservoir. The rock & fluid properties and

surface models description used in this section are the same as the properties that used in previous section.

4.3.1. Production Scenario

The production scenario used here is the same as in the previous section namely the direct line drive waterflooding with 2 production and 2 injection wells at each corner of the reservoir model. The upstream pressure (pumping head pressure) of water injection is 3000 psi and the downstream pressure of production is 100 psi which exactly the same as production.

4.3.2. Study Cases

In this section, some of the obvious cases are shown here to illustrate the effect of size of OOIP. There are two cases presented here.

- Case 1: Homogeneous high permeability – lived oil PVT

Figures 36 and 37 show production and injection profile for the case of large OOIP reservoir. Comparing with Figures 19 and 20 which represent the case of small OOIP, the production and injection profile of large OOIP case show that the coupling level and scheme have less effect on the production and injection rate differences.

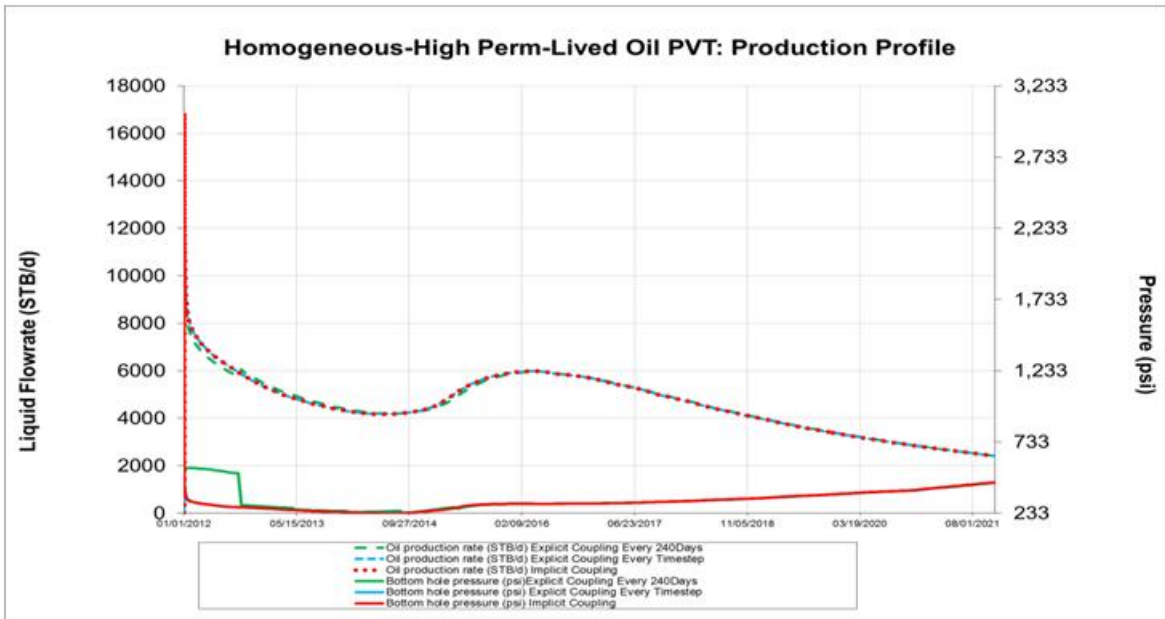


Figure 36: Oil production profile and bottomhole pressure of large OOIP reservoir with homogeneous high perm – live oil PVT case

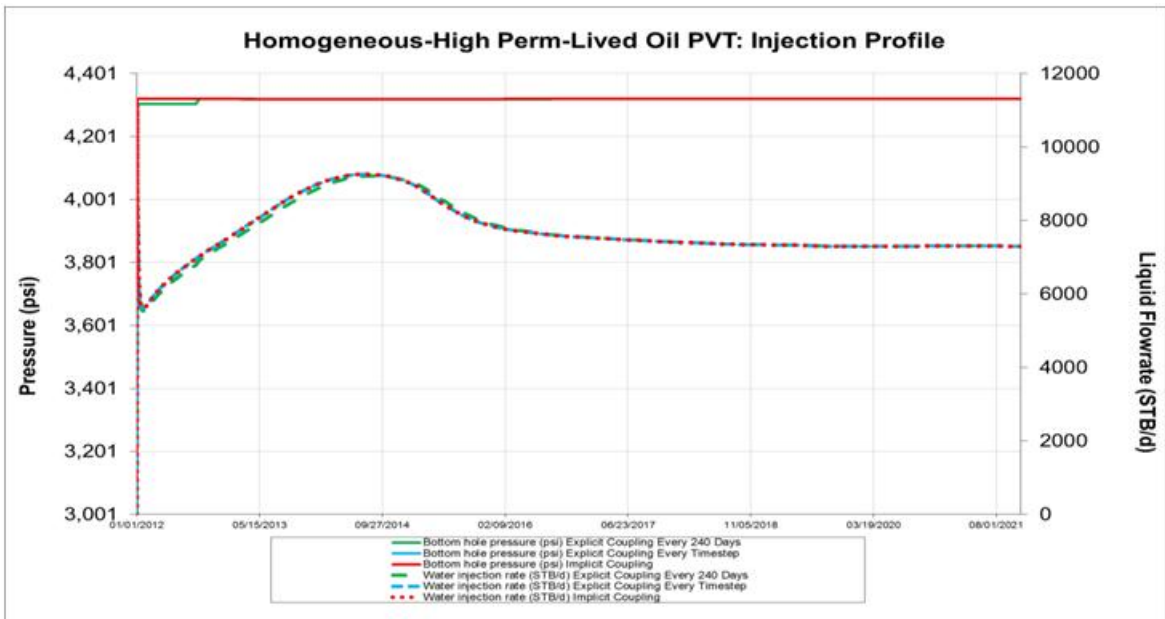


Figure 37: Water injection profile and bottomhole pressure of large OOIP reservoir with homogeneous high perm – live oil PVT case

- Case 2: Heterogeneous permeability – lived oil PVT

Another explicit case to show the effect of the size of reservoir is heterogeneous – lived oil PVT case. Figures 38, 39, 40, and 41 show production and injection profiles for the case of large OOIP for heterogeneous permeability – lived oil PVT case. The production and injection profile of different coupling level and coupling scheme of small OOIP reservoir shown in the previous section (Figures 24, 25, 26, and 27) are different while for large OOIP reservoir that shown in this section shows just only small difference in production and injection rate.

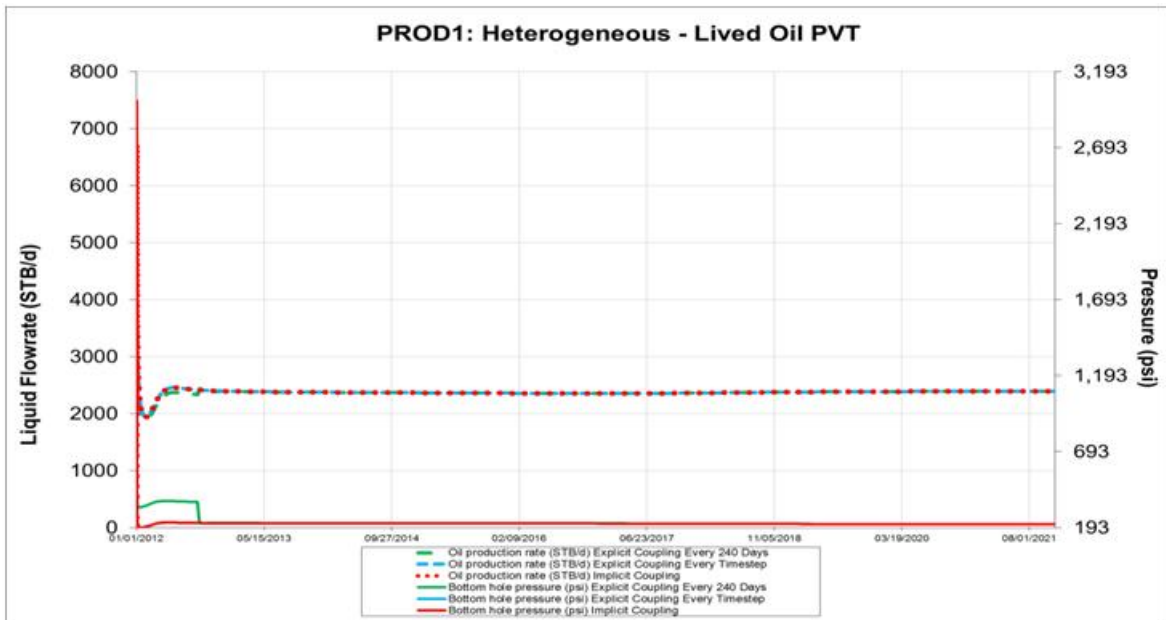


Figure 38: Oil production profile and bottomhole pressure of PROD-1 of large OOIP reservoir with heterogeneous perm – lived oil PVT case

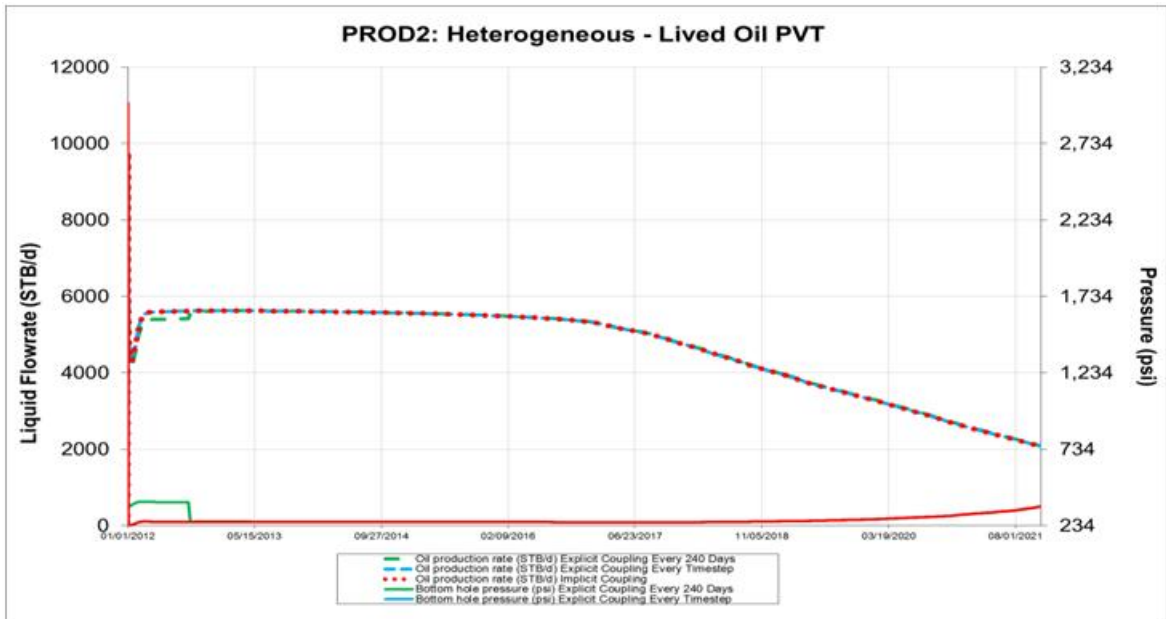


Figure 39: Oil production profile and bottomhole pressure of PROD-2 of large OOIP reservoir with heterogeneous perm – lived oil PVT case

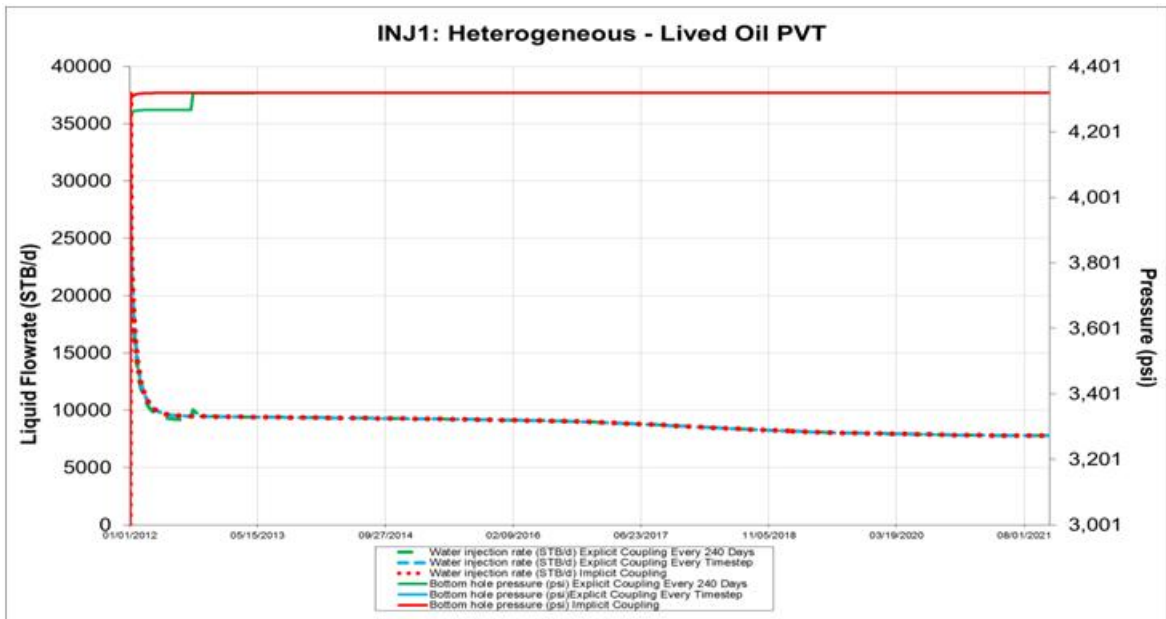


Figure 40: Water injection profile and bottomhole pressure of INJ-1 of large OOIP reservoir with heterogeneous perm – lived oil PVT case

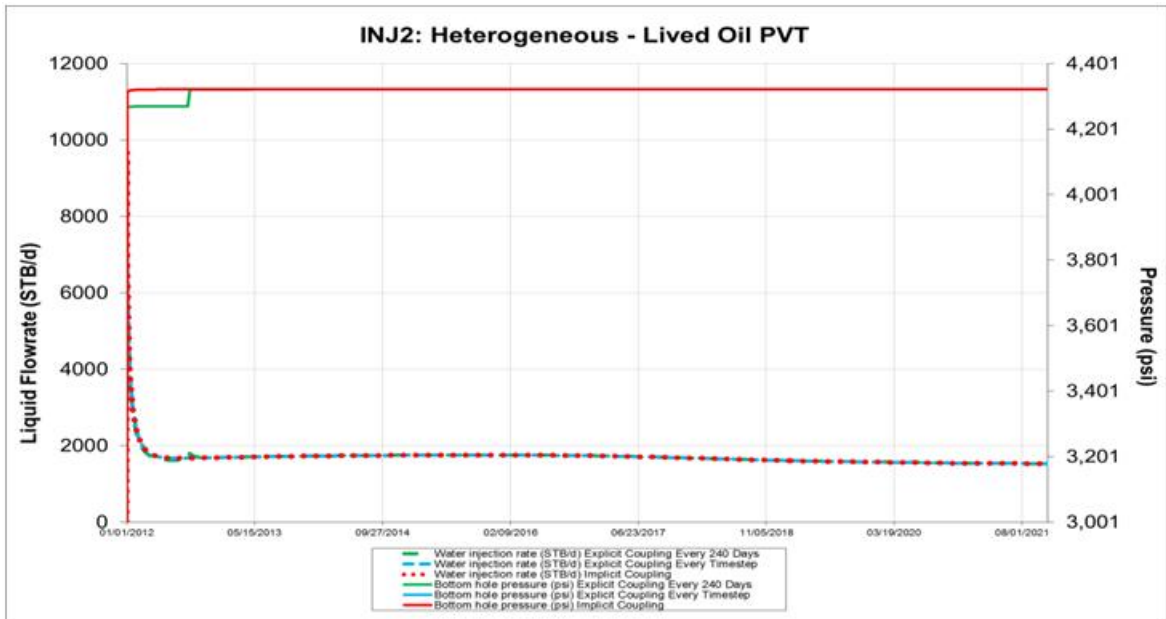


Figure 41: Water injection profile and bottomhole pressure of INJ-2 of large OOIP reservoir with heterogeneous perm – lived oil PVT case

4.4. Summary

- For dead oil PVT, the coupling schemes have less effect on the production and injection profile than Lived Oil PVT.
- For lived oil PVT, the production prediction of homogeneous high permeability and heterogeneous permeability reservoir using different coupling schemes is more sensitive than the production and injection prediction of homogeneous low perm.
- The production prediction difference between explicit coupling at every specified time step and explicit coupling at every time step is significant.
- The production prediction difference between explicit coupling at every time step and implicit coupling at every first 3 Newton iterations is not significant because the coupling point of ECLIPSE100 with Network Option is at wellhead which mean that

the pressure loss from flow in the well is solved simultaneously with subsurface model plus the order of pressure loss in the surface pipe is order of tenth compare to the order of pressure lost in the well which is order of thousandth. Consequently, the difference of pressure loss in surface pipe between explicit coupling for every timestep and implicit coupling scheme are not significant.

- Under the same production strategy, the production and injection profile of the reservoir that has smaller OOIP tend to show more different in production and injection profile when different coupling schemes are used.

5. MATLAB RESERVOIR SIMULATION TOOLBOX MODIFICATION FOR SURFACE AND SUBSURFACE MODEL COUPLING

As discussed in the previous chapter, there are several advantages of using ECLIPSE 100 & Network Option to run the coupled surface and subsurface models. However, ECLIPSE 100 & Network Option does not provide the way to make the production optimization using upstream injection pressure and downstream production pressure as control parameters. A modification to the MRST is developed in order to create the functionality that ECLIPSE 100 & Network Option does not support. In this chapter, we will explain how to modify the MRST code and compare the result with ECLIPSE 100 & Network Option. Moreover, the effect of generated VLP table on the result is also analyzed and limitations of modified MRST code are presented.

5.1. MRST Fully Implicit Multiphase Solver Routine Modification

Based on the original work of MRST, the MATLAB® code for setting up the problem can be divided into three main parts. The first part is to call the routine for reading and processing ECLIPSE input deck files. The second part is to call the fully implicit multiphase solver routine. Most of the code modification works are focused on this part. The last part of MATLAB® code is to post-process the solution from the second part. The flowchart of the original work of MRST is shown in the Figure 42. The detail of fully implicit multiphase solver routine is shown in the Figure 43. In this

section, we will show the parameter associated with the coupling and which MRST models in the fully implicit multiphase solver routine are modified.

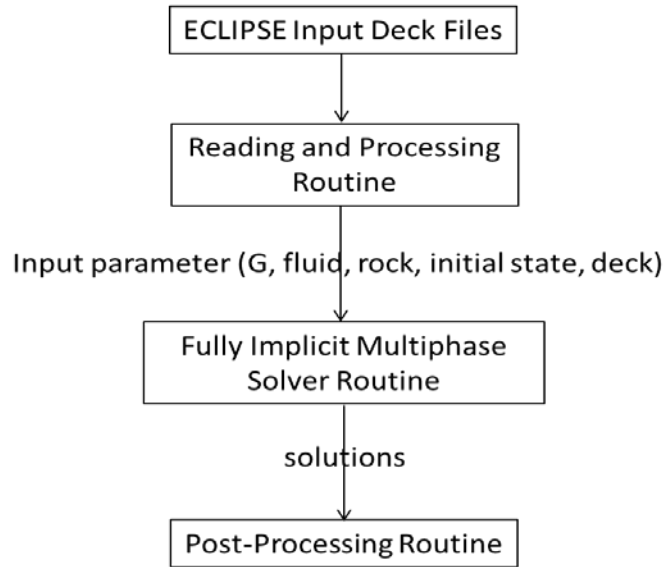


Figure 42: Flowchart of MRST fully implicit multiphase solver routine

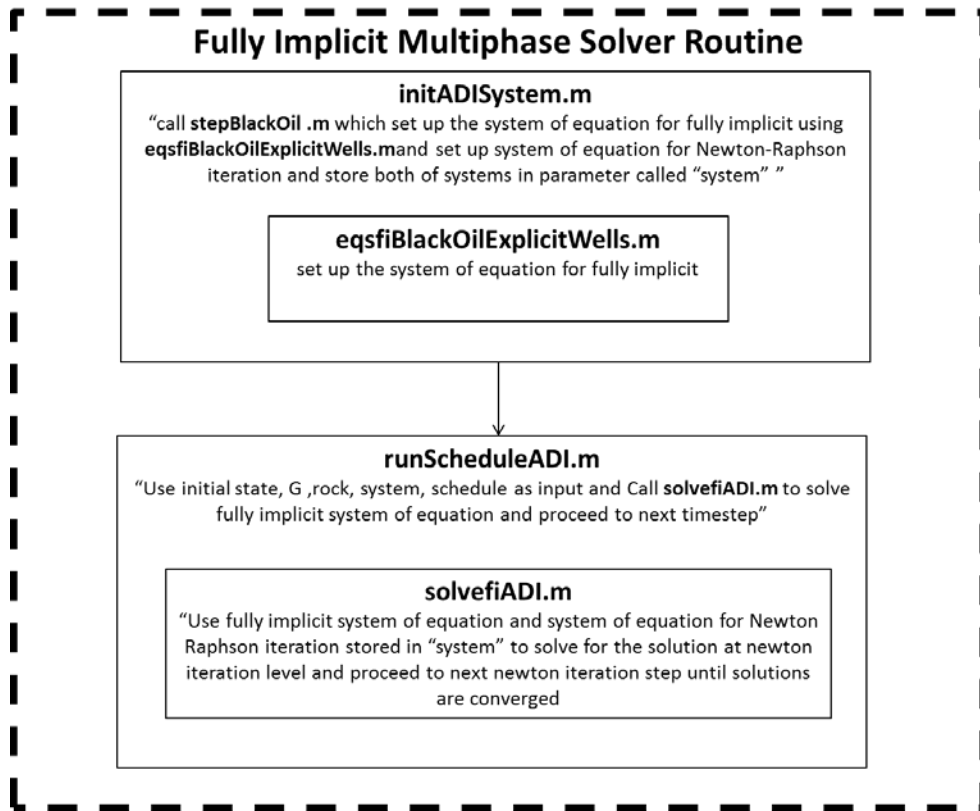


Figure 43: Detailed structure of MRST fully implicit multiphase solver routine

As discussed in the previous chapter, one of important part of the implicit and explicit couplings is the balancing algorithm. The function of balancing algorithm is to find the balancing point of the Inflow Performance Relationship (IPR) obtained from reservoir simulation and Outflow Performance Relationship (OPR) obtained from VLP table generated from PROSPER. When the balancing point is found, the bottomhole flowing pressure at the balancing point will be used as control parameter for the reservoir simulation run. The balancing algorithm that was implemented in fully implicit multiphase solver routine modification is pretty similar to the balancing algorithm called

Fast PI that is used in ECLIPSE 100 & Network Option. The detail is presented in the next subsection below

5.1.1. Fast PI Balancing Algorithm

The fast PI coupling method is a non-iterative network-balancing process. The steps worked in the algorithm are shown below.

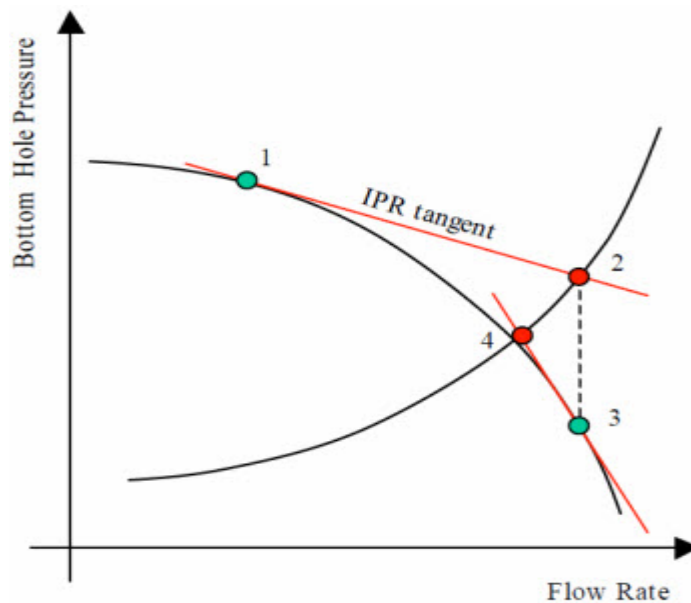


Figure 44: Example of Fast PI balancing scheme

Step of Fast PI Balancing Algorithm

- Start with the current operating point (point No.1 of Figure 44) which is obtained from the previous time step or Newton iteration. For the first time step for explicit coupling or first Newton iteration for implicit coupling, the current operating point is guessed to the best of user knowledge.

- Query for the well linear IPR curve which tangent with the current operating point in the following form:

$$Q = M(B) + A$$

where M is slope of the well linear IPR at current operating point, B is the bottomhole flowing pressure, and Q is flow rate

- Calculate water cut and GOR from the solution of previous time step (in another words they are water cut and GOR of the beginning of current time step) and use them to interpolate VLP table.
- Find intercept (point No.2 of Figure 44) between well linear IPR and interpolated VLP.
- Use BHP at intercept as control parameter for reservoir simulation run at current time step for explicit coupling or Newton iteration for implicit coupling.
- For implicit coupling, the process can be done iteratively to get more accurate BHP (point No.3 of Figure 44)-(point No.4 of Figure 44).

5.1.2. Modification for Explicit Coupling

The structure of fully implicit multiphase solver routine after the modification for explicit coupling is shown in the Figure 45. The additional function called “*explicitCoup.m*” is included into “*runScheduleADI.m*”. The function of “*explicitCoup.m*” is the same as the function of Fast PI algorithm. It uses the operating point from the last time step to query for well linear IPR, and it uses water cut and GOR to interpolate the VLP table. The intersection between well linear IPR and interpolated

VLP table yield the bottomhole flowing pressure that will be used as the control for current time step.

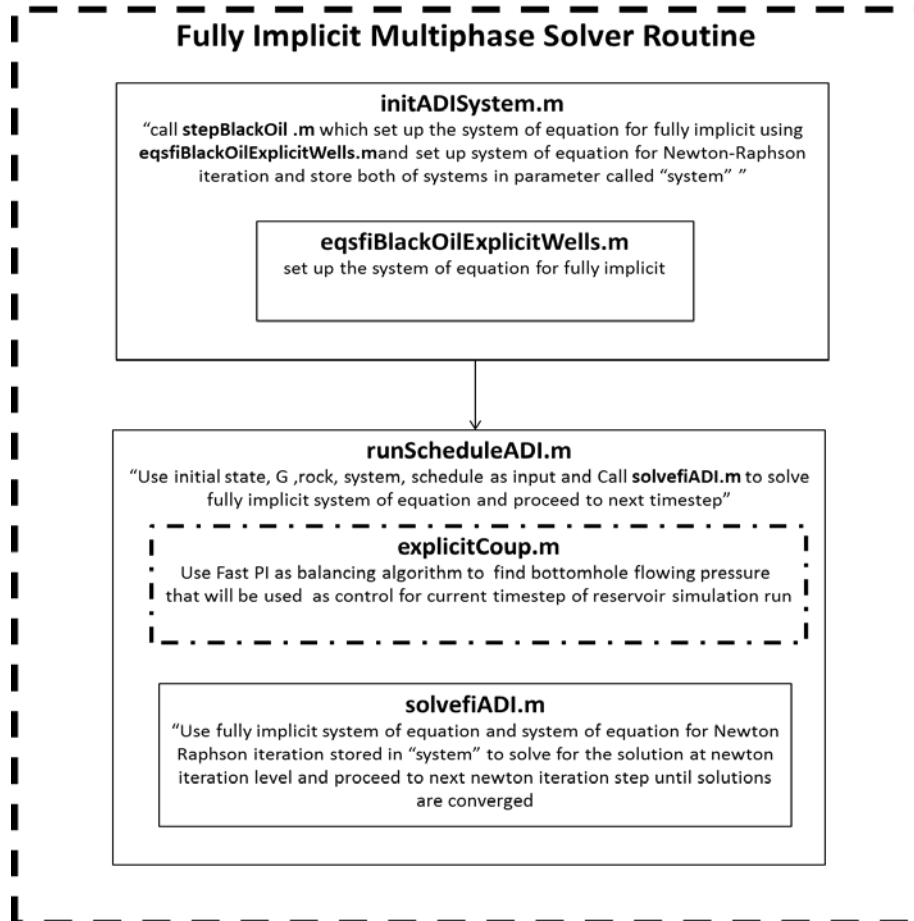


Figure 45: Detailed structure of modified MRST fully implicit multiphase solver routine for explicit coupling

5.1.3. Modification for Implicit Coupling

The structure of fully implicit multiphase solver routine after the modification for implicit coupling is shown in the Figure 46. For the implicit coupling case, the “*eqsfiBlackOilExplicitWells.m*” function is changed to “*eqsfiBlackOilExplicitWellsIm.m*”. The description of the “*eqsfiBlackOilExplicitWellsIm.m*” is pretty much the same as the description of “*eqsfiBlackOilExplicitWells.m*” except that it has an additional function that work like Fast PI balancing algorithm. It uses operating point from the last Newton iteration to query for well linear IPR, and uses water cut and GOR from the last time step to interpolate the VLP table. The intersection between well linear IPR and interpolated VLP table yield the bottomhole flowing pressure that will be used as the control for current Newton iteration.

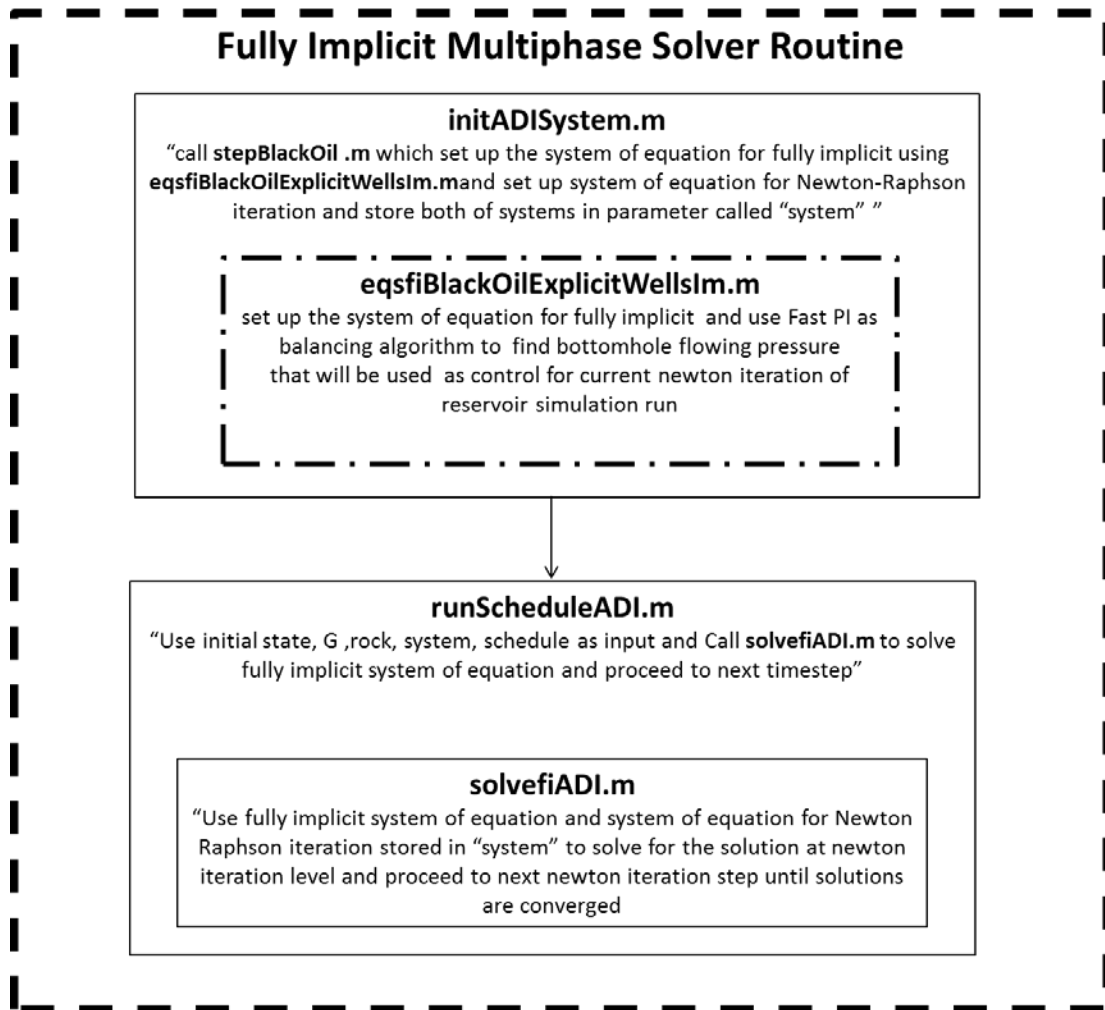


Figure 46: Detailed structure of modified MRST fully implicit multiphase solver routine for implicit coupling

5.2. Comparison of Simulation Result from Modified MRST & ECLIPSE100 with Network Options

This section will show the simulation run results in the case of no coupling, explicit coupling and implicit coupling in order to check the consistency of the result from the modified MRST and the ECLIPSE100+Network Option.

5.2.1. No Coupling Case

The reservoir description and production strategy of the no coupling case is summarized in the Tables 7 and 8.

Reservoir Simulation Model Properties	Value	Unit
NX:NY:NZ (homogeneous)	23:23:6	
Grid size (homogeneous)	350 x 350 x 5	ft
Permeability	350	md
Porosity	20	%
Initial Water Saturation	10	%
Initial Oil Saturation	90	%
Production Scenario	Direct line drive water flooding	
Reservoir pressure	3000	psia
Reservoir depth	3000	ft

Table 7: Summary of reservoir simulation model properties used to check the consistency between MRST and ECLIPSE100

Production Strategy	Value	Unit
Bottomhole flowing pressure	400	psi
Bottomhole injection pressure	4300	psi

Table 8: Summary of production strategies used to check the consistency between MRST and ECLIPSE100

The comparison of the result of no coupling case for MRST & ECLIPSE100 is shown in the Figure 47. It can be seen that the result from MRST & ECLIPSE100 is very similar except in the very early period of the production that MRST gives higher production and injection rate. This occurs because the production and injection profile of ECLIPSE100 is an averaged production rate. In the very early time of the simulation, ECLIPSE100 normally reduce time step into smaller interval than report time step and the production rate and injection rate of the report time step is the result of the averaged production and injection rate from every smaller interval.

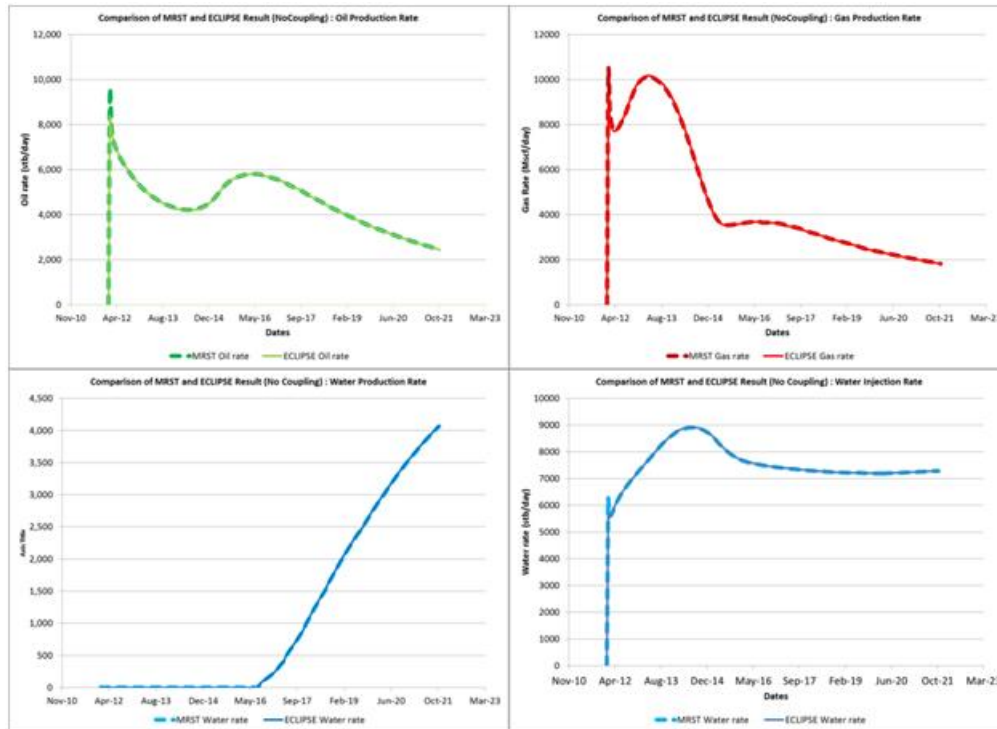


Figure 47: Comparison of MRST and ECLIPSE's production and injection profile of no coupling case

5.2.2. *Implicit Coupling Case*

In this section, we consider the consistency of the production and injection profile result from modified MRST and ECLIPSE100 & Network Option for the cases of implicit coupling only. The reason that we compare the result from MRST and ECLIPSE100 & Network Option only implicit coupling case is because ECLIPSE100 & Network Option use coupling point at tubing head. The tubing is treated as a part of reservoir model and the pressure lost in the tubing will be solved simultaneously with reservoir simulation model. This gives the same effect as implicit coupling at the

bottomhole. The reservoir description and production strategy of no coupling case is summarized in the Tables 9 and 10.

Reservoir Simulation Model Properties	Value	unit
NX:NY:NZ (homogeneous)	23:23:6	
Grid size (homogeneous)	350 x 350 x 5	ft
Permeability	350	md
Porosity	20	%
Initial Water Saturation	10	%
Initial Oil Saturation	90	%
Production Scenario	Direct line drive water flooding & 5-spots water flooding	
Reservoir pressure	3000	psia
Reservoir depth	3000	ft

Table 9: Summary of reservoir simulation model properties used to check the consistency between modified MRST and ECLIPSE100 & Network Option

Surface Facility Model Properties	Value	unit
Production Tubing Size (ID) / Injection Tubing Size (ID)	7.5	in
Production Tubing Length/ Injection Tubing Length	3000	ft
Surface Pipeline Size (ID)	7.5	in
Surface Pipeline Length	3280	ft
Downstream Production Pressure	260 (direct line drive case) 220 (5-spots case)	psia
Upstream Injection Pressure	4666 (direct line drive case) 3000 (5-spots case)	psia

Table 10: Summary of production strategy and surface model properties used to check the consistency between modified MRST and ECLIPSE100 & Network Option for direct line drive & 5-spots water flooding

The production scenario that will be used to check the consistencies between modified MRST and ECLIPSE100 & Network Option are the same configuration from the previous section. For the sake of completeness, the reservoir models are depicted again in Figures 48 and 49.

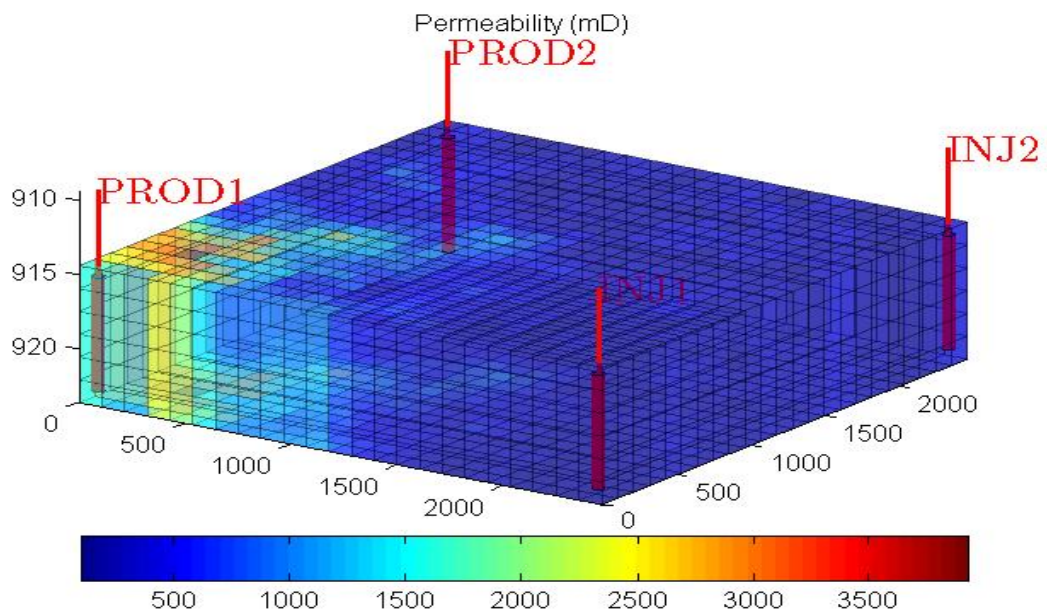


Figure 48: Reservoir simulation model with direct line drive water flooding

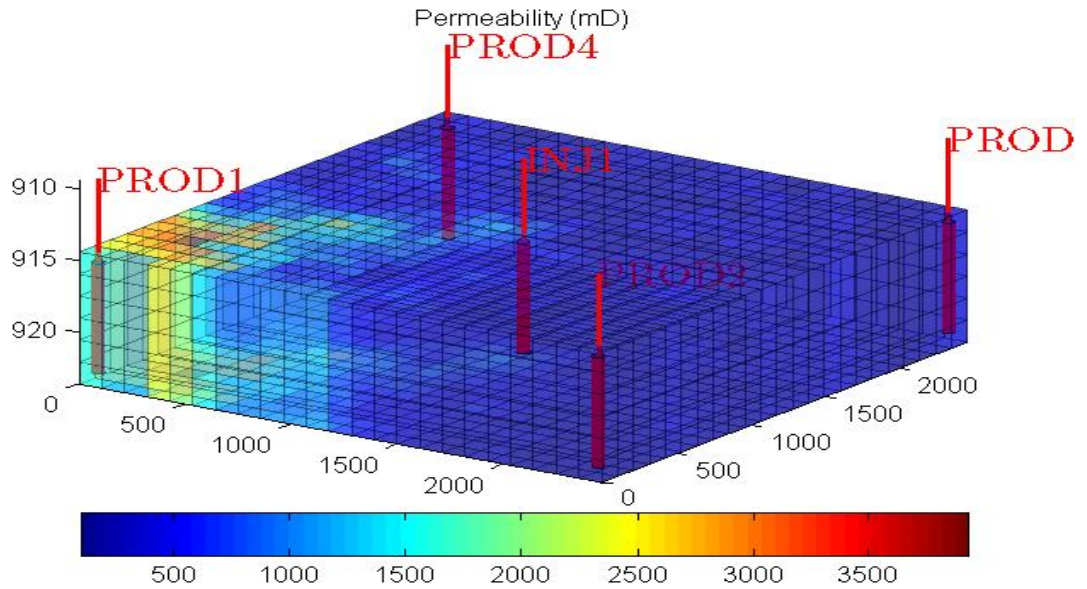


Figure 49: Reservoir simulation model with 5-spots pattern water flooding

The comparison of the modified MRST & ECLIPSE100 with Network Option results for direct line drive waterflooding is shown in the Figure 50. The dash line represents the result of well PROD1 & INJ1 and solid line represents the result of PROD2 & INJ2. The red line shows the result of modified MRST and blue line shows the result of ECLIPSE100 & Network Option. It can be seen both simulators yeild similar results, and the only difference stem from the production and injection rate between the modified MRST & ECLIPSE100 with Network Options in the early time of the simulation. This indeed the same results as obtained before for the no coupling scheme. A small different of the result is caused by the difference of bottomhole pressure.

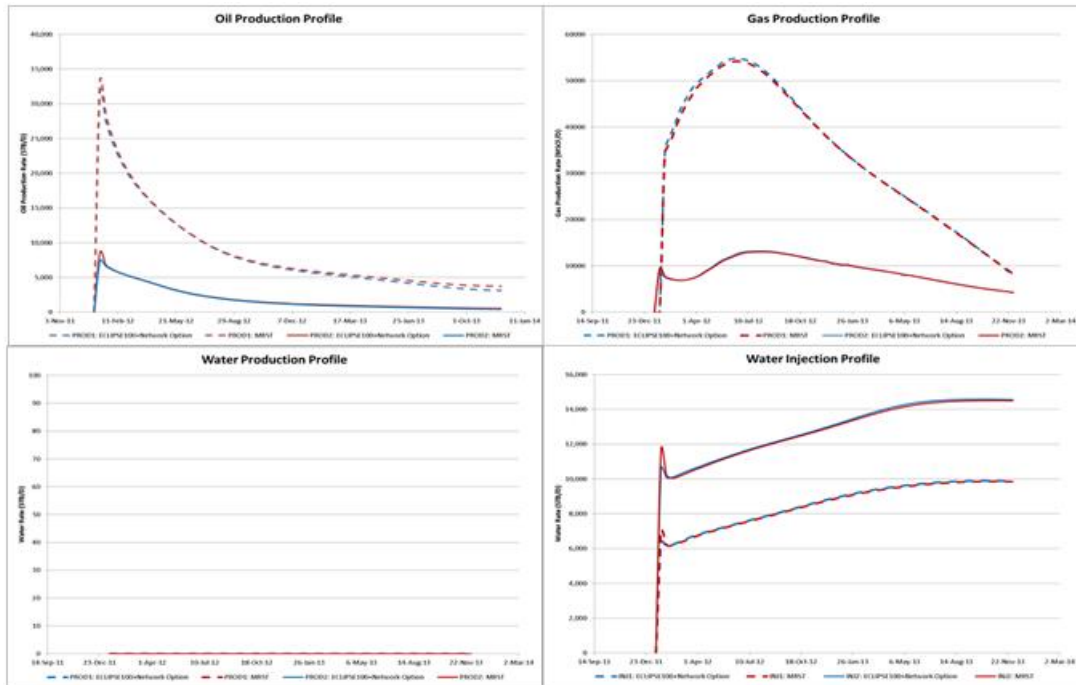


Figure 50: Comparison of modified MRST and ECLIPSE's production/injection profile of implicit coupling case for direct line drive water flooding

The comparisons of the injection and production profiles for the 5-spots pattern water flooding are shown in the Figures 51 and 52, respectively. The result of PROD-1 is shown separately from the other production wells in order to avoid confusion of axis scale because the well has very high production rate compare to the other wells. The solid line represents the result from modified MRST and the dash line represents the result from ECLIPSE100 & Network Option. The difference of production and injection rate between modified MRST & ECLIPSE100 & Network Options in the early time of simulation also occurs here. There is a small difference in injection and production rates which rooted from the different bottomhole pressure for both cases.

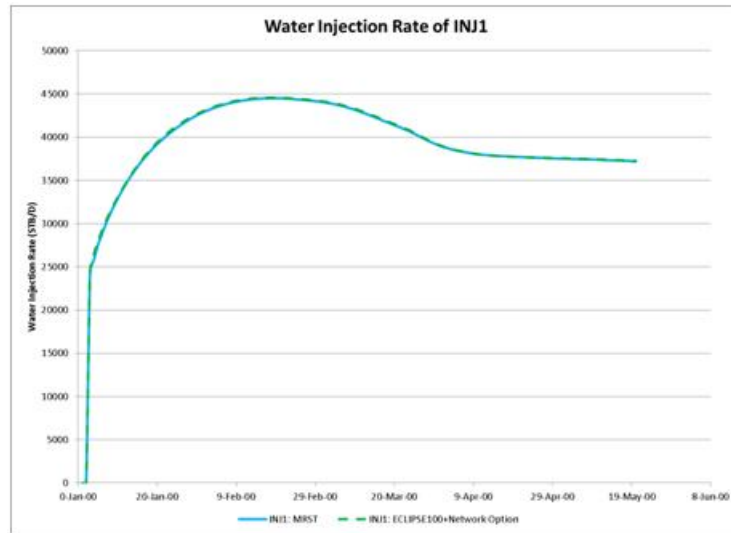


Figure 51: Comparison of modified MRST and ECLIPSE’s injection profile of implicit coupling case for 5-spots water flooding

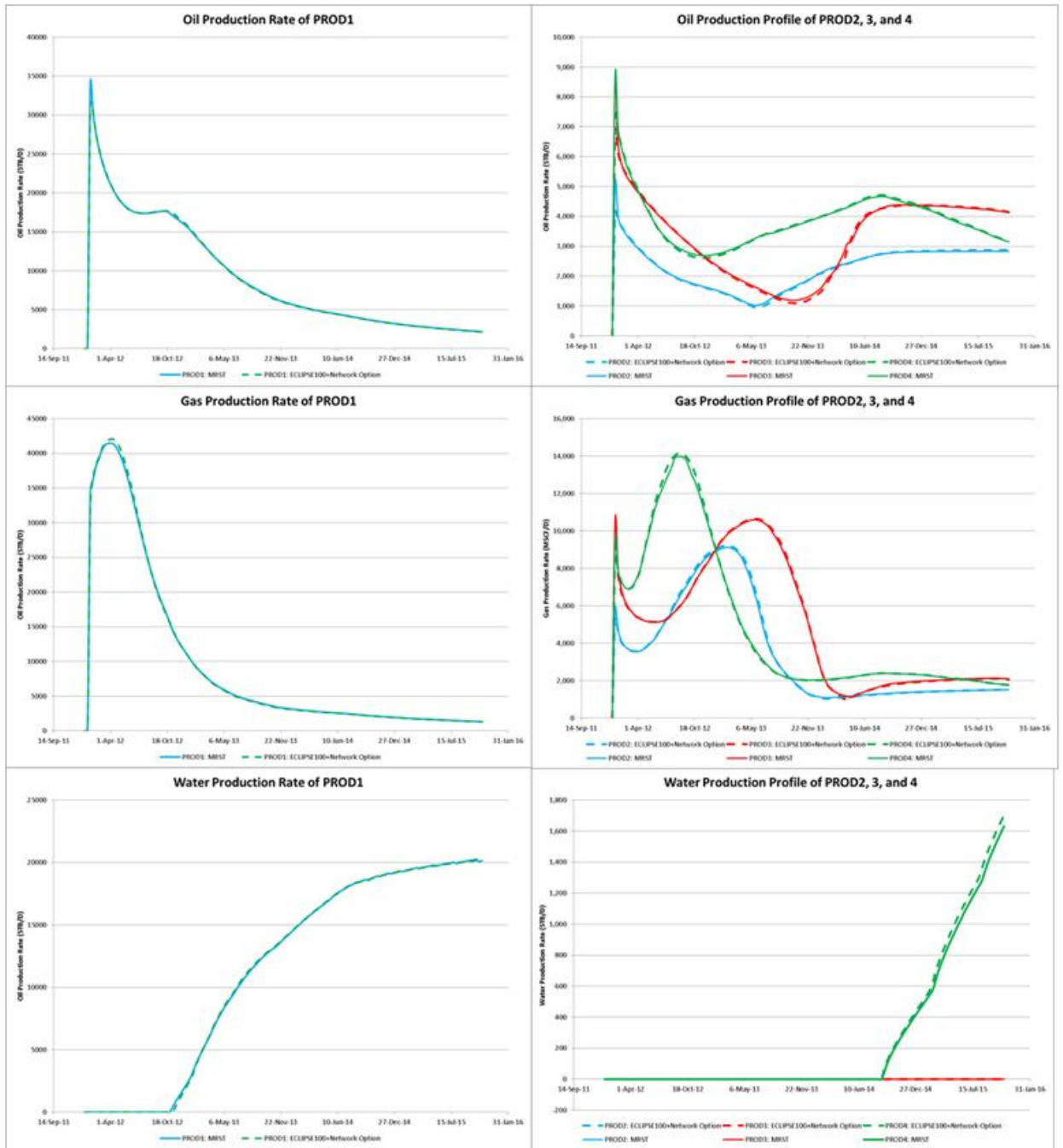


Figure 52: Comparison of modified MRST and ECLIPSE’s production profile of implicit coupling case for 5-spots water flooding

5.3. Effect of VLP Table Discretization Scheme on Simulation Result

As discussed before that the pressure lost in production and injection stream can be represented in form of VLP tables. The pressures lost versus flow rates for specified range of downstream production pressure, gas-oil ratio, and water cut are generated by PROSPER and export into a table format. In PROSPER, there are several options to discretize the range of upstream pressure, gas-oil ratio, and water cut. However, the discretization scheme that will be considered here are linear spacing (equally spacing) and geometric spacing.

5.3.1. Downstream Production Pressure Discretization

Figure 53 shows the comparison of VLP curves using different discretization schemes for the downstream pressure. The plot on left hand side is VLP curve of various downstream pressures discretized by using linear spacing while the plot on the right hand side use geometric spacing. It can be seen that the relationship between upstream pressures and VLP curves are closed to linear relationship. Consequently, the discretization scheme does not affect the accuracy of VLP table interpolation and simulation result.

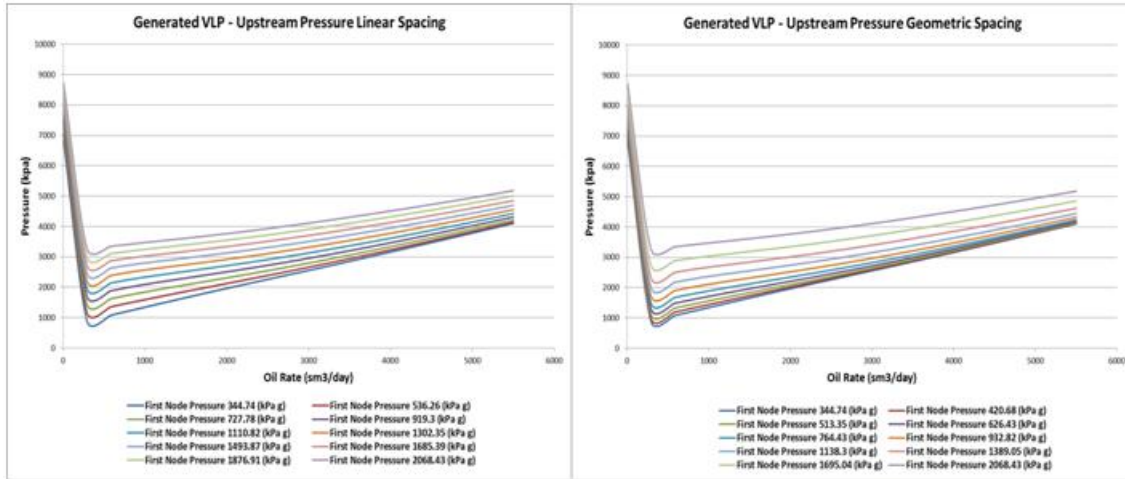


Figure 53: VLP of various downstream pressure using linear spacing and geometric spacing

5.3.2. Water Cut Discretization

Figure 54 shows the comparison of VLP curves using different discretization scheme to discretize water cut. The plot on left hand side is VLP curve of various water cut discretized by using linear spacing while the plot on right hand side use geometric spacing. It can be seen that for geometric spacing case poorly represent the change of VLP curves with water cut because there is large gap between VLP curve at 60% water cut and VLP curve at 100% water cut which can cause more interpolation error than the case of linear spacing. Hence, linear spacing is recommended discretization scheme for water cut.

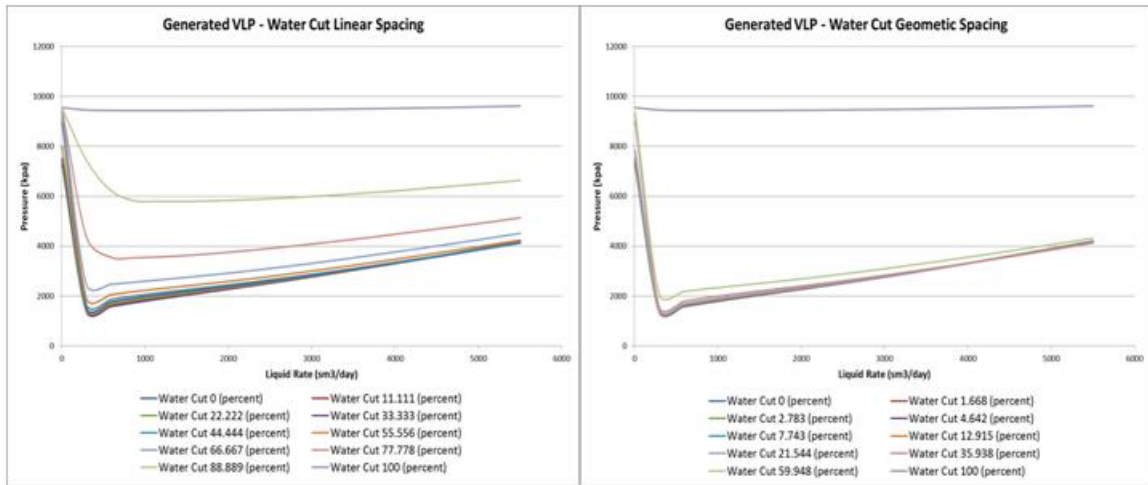


Figure 54: VLP of various water cut using linear spacing and geometric spacing

5.3.3. Gas-Oil Ratio Discretization

Similarly, we show in Figure 55, the different discretization scheme for the gas-oil ratio. The plot shows that gas-oil ratio discretization using geometric spacing is better to represent the changes of VLP curve with gas-oil ratio than the linear spacing case. This is due to the fact that there is large gap of VLP curve at low gas-oil ratio in the linear spacing case. Consequently, the geometric spacing is recommended for gas-oil ratio discretization.

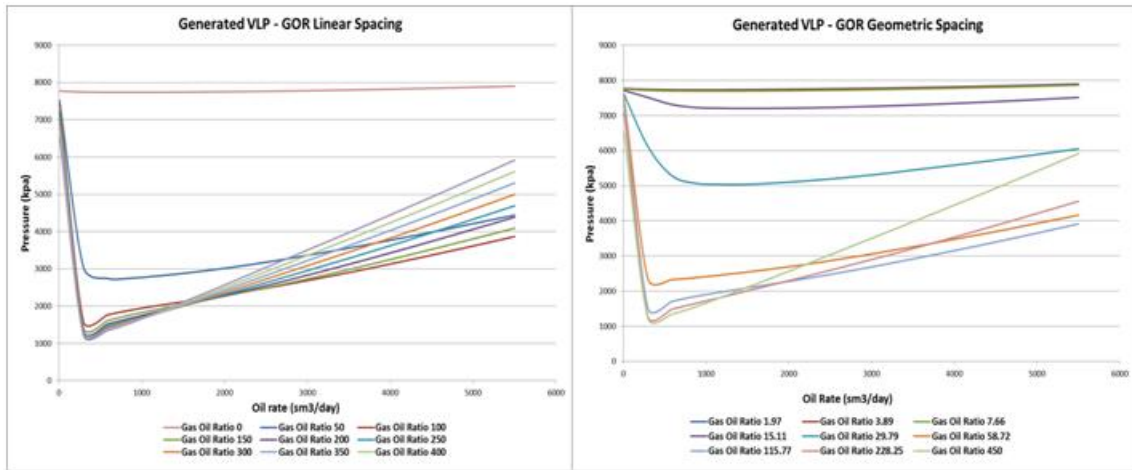


Figure 55: VLP of various gas-oil ratio using linear spacing and geometric spacing

5.3.4. Simulation Result Using Different Discretization Scheme

Figure 56 shows the comparison of simulation results for well PROD1 using coupled surface and subsurface model for 5-spots water flooding scenario presented in the previous sections. Here, we use different gas-oil ratio discretization schemes to generate the VLP tables for coupling surface and subsurface model. The plot on the top-left and top-right show the oil and gas production profiles, respectively. The plot on the bottom-left and bottom-right of Figure 56 show bottomhole flowing pressure and gas-oil ratio. The blue solid line represents the case that use geometric spacing gas-oil ratio and the red dash line represents the case that use linear spacing gas-oil ratio. It can be seen that the bottomhole production pressure between two cases are different and resulting in different oil and gas production profile. It can be seen that the case of the linear spacing overestimate the bottomhole flowing pressure.

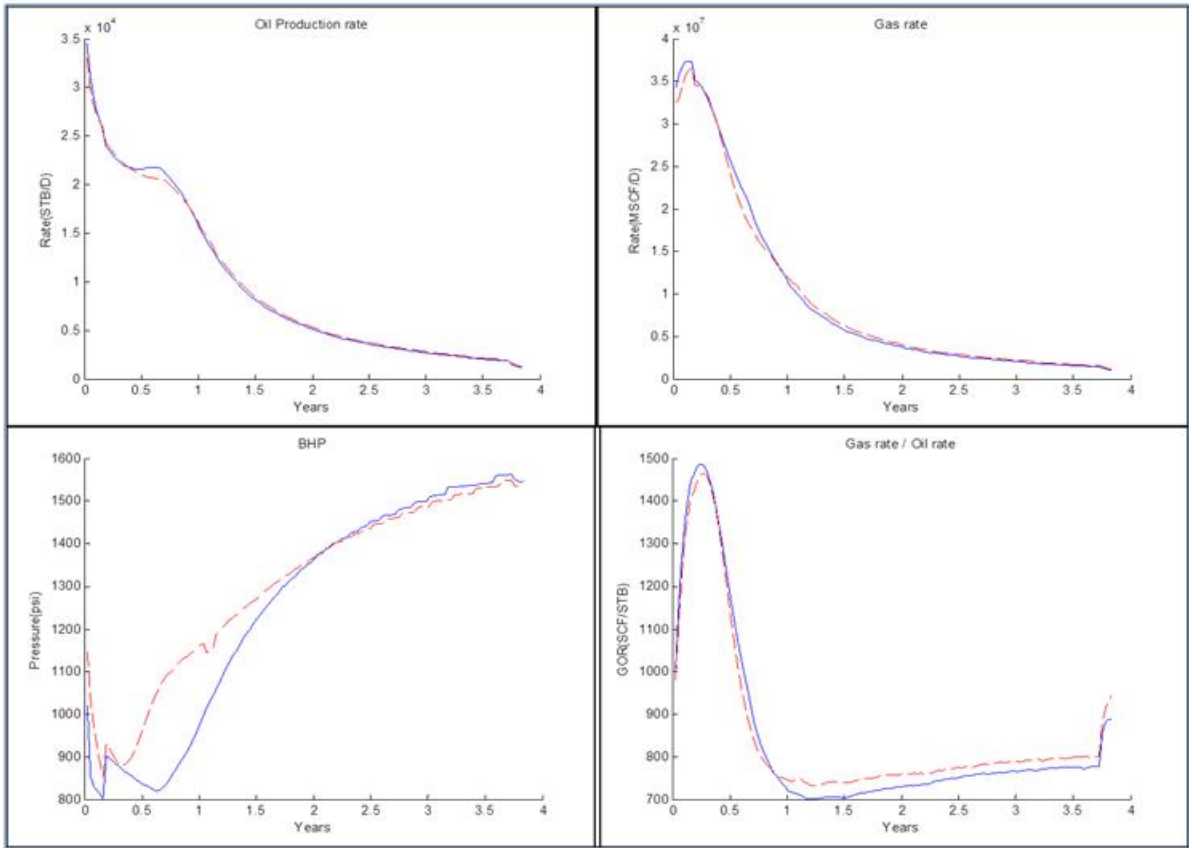


Figure 56: Comparison of production profile of coupling surface and subsurface model using different gas-oil ratio discretization

6. EFFECT OF COUPLING SCHEME ON PRODUCTION OPTIMIZATION OF COUPLED SURFACE AND SUBSURFACE MODEL

In this section, the theory and procedure of performing production optimization of coupled surface and subsurface model using gradient based optimization are explained. In the standard subsurface model production optimization framework, the optimal control parameters are mostly described in terms of well rates and bottomhole flowing pressures. The coupled surface and subsurface model production optimization can be perform in similar fashion except that the optimal control will be in the form of upstream and downstream pressures. The objective function used in here is Net Present Value (NPV). The detailed objective function formulation, gradient computation via adjoint model, and the surface and subsurface production optimization problem will be discuss in this section.

6.1. Objective Function Formulation

In production optimization process, we usually set the objective function as NPV, which can be defined as function of the total oil and gas revenue subtract by total injection and production costs and then multiply by a discount factor which used to discount future cash flows to the present value. The objective function O can be formulated as follow.

$$O^n = \left\{ \frac{\Delta t}{(1+d)^{\frac{n\Delta t}{T}}} \left(- \sum_{j=1}^{N_w} r_o Q_{o,j,n} - \sum_{j=1}^{N_w} r_g Q_{g,j,n} + \sum_{j=1}^{N_w} c_{pw} Q_{pw,j,n} + \sum_{j=1}^{N_w} c_{iw} Q_{iw,j,n} \right) \right\} \quad (45)$$

where d is discount factor, n is number of current time step, and Δt is time step size

r_o is Oil revenue, r_g is Gas revenue, c_{pw} is Water production cost, and c_{iw} is Water injection cost

Q_o is Oil production rate, Q_g is Gas production rate, Q_{pw} is Water production rate, and Q_{iw} is Water injection rate

In this formula, the oil, gas, and water production rate is set to be negative while the water injection is set to be positive. Consequently, the oil and gas revenue is positive and water production and injection cost term is negative. The control that we use in this study is upstream injection & downstream production pressure and terms $Q_o, Q_g, Q_{pw},$ and Q_{iw} are function of them and state variables (P, Sw, and Sg). The function above can be written in accumulative form as follow

$$O = \sum_{n=0}^{N-1} O^n(x^n, u^n) \quad (46)$$

where x^n is state variable vector (P, Sw, and Sg) at time step n

u^n is control vector which is upstream injection & downstream production pressure for this study

What we can do in optimization is to maximize the objective function P or minimize the negative of objective function O . In this study, we choose to minimize the negative of objective function J. Thus, the problem can be formulated as follow

$$\min -O = -\sum_{n=0}^{N-1} O^n(x^n, u^n) \quad (47)$$

The objective function is subjected to

$$g^n(x^{n+1}, x^n, u^n) = 0, x^0 = x_0(\text{initial condition})$$

$$c^n(x^{n+1}, u^n) \leq 0, LB \leq u^n \leq UB$$

The problem is a constrained optimization problem, where the constrained term is $g^n(x^{n+1}, x^n, u^n)$, which are the coupled surface and reservoir simulation function for each grid block at each time step. The governing equation is stated as follow

$$g^n(x^{n+1}, x^n, u^n) = R_{o,g,w} = 0 \quad (48)$$

where $R_{o,g,w}$ are the Residual of oil, gas and water discretization equations

6.2. Gradient Based Optimization Method

To solve the problem mentioned in the previous section, there are two main categories of existing optimization algorithm. First, stochastic algorithms like Simulated Annealing and Genetic Algorithm. Second is gradient-based algorithm for example, Steepest Descent and Quasi – Newton Algorithm. The first one normally requires a large number of forward simulation runs because the algorithm uses stochastic process, the algorithm is not suit with time consuming model like reservoir simulation with large number of grid block. The second one does not require a lot of forward simulation run but the optimization solution might not be a global solution. In practice, the number of grid block of reservoir simulation is large which may require several hours to finish one run of forward simulation.

Consequently, the stochastic algorithm does not suit with production optimization using reservoir simulation. The feasible option to solve the optimization problem is gradient-based algorithm. Although, the gradient-based algorithm does not always give global solution, it can improve the whole system of production effectiveness.

There are several ways to find gradient for example, gradients from numerical perturbation method and gradients with adjoint model. In this thesis, the gradients with adjoint model method are selected.

6.2.1. Gradients with Adjoint Model

Finding gradients with adjoint model is more effective way than numerical perturbation. The objective function is modified by adding the constrained term with Lagrange multiplier(λ^{n+1}). The modified objective function becomes

$$\bar{O} = -\sum_{n=0}^{N-1}[O^n(x^n, u^n) + \lambda^{n+1}g^n(x^{n+1}, x^n, u^n)] \quad (49)$$

The vector λ^n is called Lagrange multiplier vector which one Lagrange multiplier is required for each constraint with which the cost function (J^n) is augmented.

Lets

$$L^n = O^n(x^n, u^n) + \lambda^{n+1}g^n(x^{n+1}, x^n, u^n) \quad (50)$$

We can obtain first order partial derivation of \bar{J} in term of x^{n+1}, x^n, u^n , and λ^{n+1}

$$\delta\bar{O} = \sum_{n=1}^{N-1}\left(\frac{\partial L^n}{\partial x^n}\right)\delta x^n + \sum_{n=0}^{N-1}\left(\frac{\partial L^n}{\partial x^{n+1}}\right)\delta x^{n+1} + \sum_{n=0}^{N-1}\left(\frac{\partial L^n}{\partial u^n}\right)\delta u^n + \sum_{n=0}^{N-1}\left(\frac{\partial L^n}{\partial \lambda^{n+1}}\right)\delta \lambda^{n+1} \quad (51)$$

And thus we can rearrange the equation above

$$\delta\bar{O} = \sum_{n=1}^{N-1}\left(\frac{\partial L^{n-1}}{\partial x^n} + \frac{\partial L^n}{\partial x^n}\right)\delta x^n + \sum_{n=0}^{N-1}\left(\frac{\partial L^n}{\partial u^n}\right)\delta u^n + \sum_{n=0}^{N-1}\left(\frac{\partial L^n}{\partial \lambda^{n+1}}\right)\delta \lambda^{n+1} + \left(\frac{\partial L^{N-1}}{\partial x^N}\right)\delta x^N \quad (52)$$

According to constrain condition, we can notice that the term $\frac{\partial L^n}{\partial \lambda^{n+1}} = 0$

If we impose the following term to be zero

$$\frac{\partial L^{N-1}}{\partial x^N} = 0 \text{ and } \frac{\partial L^{n-1}}{\partial x^n} + \frac{\partial L^n}{\partial x^n} = 0 \quad (53)$$

then the equation(52) becomes

$$\delta\bar{O} = \sum_{n=0}^{N-1} \left(\frac{\partial L^n}{\partial u^n} \right) \delta u^n = \sum_{n=0}^{N-1} \left(\frac{\partial J^n}{\partial u^n} + (\lambda^{n+1}) \frac{\partial g^n}{\partial u^n} \right) \delta u^n \quad (54)$$

The term $\frac{\partial L^{N-1}}{\partial x^N} = 0$ is called final condition. We can manipulate the equation (53) by

substitute term $L^n = O^n(x^n, u^n) + \lambda^{n+1} g^n(x^{n+1}, x^n, u^n)$

$$\frac{\partial L^{n-1}}{\partial x^n} + \frac{\partial L^n}{\partial x^n} = 0$$

$$\begin{aligned} & \frac{\partial(O^{n-1}(x^{n-1}, u^{n-1}) + \lambda^n g^{n-1}(x^n, x^{n-1}, u^{n-1}))}{\partial x^n} \\ & + \frac{\partial(O^n(x^n, u^n) + \lambda^{n+1} g^n(x^{n+1}, x^n, u^n))}{\partial x^n} = 0 \end{aligned}$$

$$(\lambda^n)^T \left(\frac{\partial g^{n-1}}{\partial x^n} \right) = -(\lambda^{n+1})^T \frac{\partial g^n}{\partial x^n} - \frac{\partial O^n}{\partial x^n}$$

(55)

We can use final condition to get λ^N and use equation above to compute backward to get all λ^n , for all n:

$$\lambda^N = \left[\frac{\partial O^{N-1}}{\partial x^N} \right] \left[\frac{\partial g^{N-1}}{\partial x^N} \right]^{-1} \quad (56)$$

$$\lambda^n = - \left[\frac{\partial O^n}{\partial x^n} + (\lambda^{n+1}) \frac{\partial g^n}{\partial x^n} \right] \left[\frac{\partial g^{n-1}}{\partial x^n} \right]^{-1} \quad (57)$$

After all of Lagrange multipliers are calculated, the gradient vector $\frac{\delta \bar{J}}{\delta u^n}$ can be found by substituting all of calculated Lagrange multipliers into equation (54).

$$\frac{\delta \bar{O}}{\delta u^n} = \sum_{n=0}^{N-1} \left(\frac{\partial O^n}{\partial u^n} + (\lambda^{n+1}) \frac{\partial g^n}{\partial u^n} \right) \quad (58)$$

The calculated gradient $\frac{\delta \bar{O}}{\delta u^n}$ can be used with any gradient - based optimization algorithm to find an optimal control u_{opt}^n .

The gradient – based optimization algorithm used in this study is Sequential Quadratic Programming (SQP). It is a popular algorithm for solving non-linearly constrained problems. This approach is a generalization of Newton’s method for case of no non-linearly constrained condition.

6.2.2. *Sequential Quadratic Programming (SQP)*

Let $f(x)$ be objective function and the set of problem is to minimize $f(x)$

$$\text{Minimize } f(x)$$

the objective function is subjected to

$$g(x) = 0 \tag{59}$$

The method for solving the problem above can be derived by applying Newton’s method. The Lagrangian for the problem is

$$L(x, \lambda) = f(x) - \lambda^T g(x) \tag{60}$$

The first-order optimality condition

$$\nabla L(x, \lambda) = 0 \tag{61}$$

The formula for Newton’s method

$$\begin{pmatrix} x_{k+1} \\ \lambda_{k+1} \end{pmatrix} = \begin{pmatrix} x_k \\ \lambda_k \end{pmatrix} + \begin{pmatrix} p_k \\ v_k \end{pmatrix} \tag{62}$$

where p_k and v_k can be obtained from the solution of the following linear system.

$$\nabla^2 L(x_k, \lambda_k) \begin{pmatrix} p_k \\ v_k \end{pmatrix} = - \nabla L(x_k, \lambda_k) \tag{63}$$

This linear system has the form

$$\begin{pmatrix} \nabla_{xx}^2 L(x_k, \lambda_k) & -\nabla g(x_k) \\ -\nabla g(x_k)^T & 0 \end{pmatrix} \begin{pmatrix} p_k \\ v_k \end{pmatrix} = \begin{pmatrix} -\nabla_x L(x_k, \lambda_k) \\ g(x_k) \end{pmatrix} \quad (64)$$

This system of equations represents the first order optimality condition for the following optimization problem

$$\begin{aligned} \text{Minimize} \quad & q(p) = \frac{1}{2} p^T [\nabla_{xx}^2 L(x_k, \lambda_k)] p + p^T [\nabla_x L(x_k, \lambda_k)] \\ \text{Subjected to} \quad & [\nabla g(x_k)]^T p + g(x_k) = 0 \end{aligned}$$

This optimization problem is a quadratic program (the minimization of a quadratic function subject to linear constraints) where the quadratic function is the Taylor series approximation of Lagrangian at (x_k, λ_k) and the linear constraint is linear approximation of $g(x_k + p) = 0$. For unconstrained problem, the formula for Newton's method relate to the minimization of a quadratic approximation to the objective function. At each iteration, a quadratic program is solved to obtain $\begin{pmatrix} p_k \\ v_k \end{pmatrix}$ and used to update $\begin{pmatrix} x_k \\ \lambda_k \end{pmatrix}$.

6.3. MRST Module for Finding Gradients with Adjoint Model

In this study MRST module for finding gradients with adjoint model is used to calculate the gradients and provide the gradients to MATLAB® function called “fmincon”. The “sqp” option which is Sequential Quadratic Programming option is selected to be an algorithm to solve the optimization problem.

However, the MRST module for finding gradients with adjoint model is designed for the model that use well rate or bottomhole flowing pressure as controls. Some modification is needed to modify the module to be able to optimize the model when using downstream production and upstream injection pressure as controls.

This section will show a brief detail of MRST module for finding gradients with adjoint model and modification. The structure of MRST module for finding gradients with adjoint model before modification is shown in the Figure 57.

In the modification the function that will be modified is "runAdjointADI.m". The structure of MRST module after modification is shown in the Figure 58. The concept of modification is simply base on chain rule of differentiation.

let THP be upstream injection pressure or downstream production pressure control, BHP be bottomhole pressure control and $\frac{\delta \bar{O}}{\delta BHP}$ be gradients of objective function with respect to bottomhole pressure control. We can find $\frac{\delta \bar{O}}{\delta THP}$ by applying chain rule of differentiation as follow

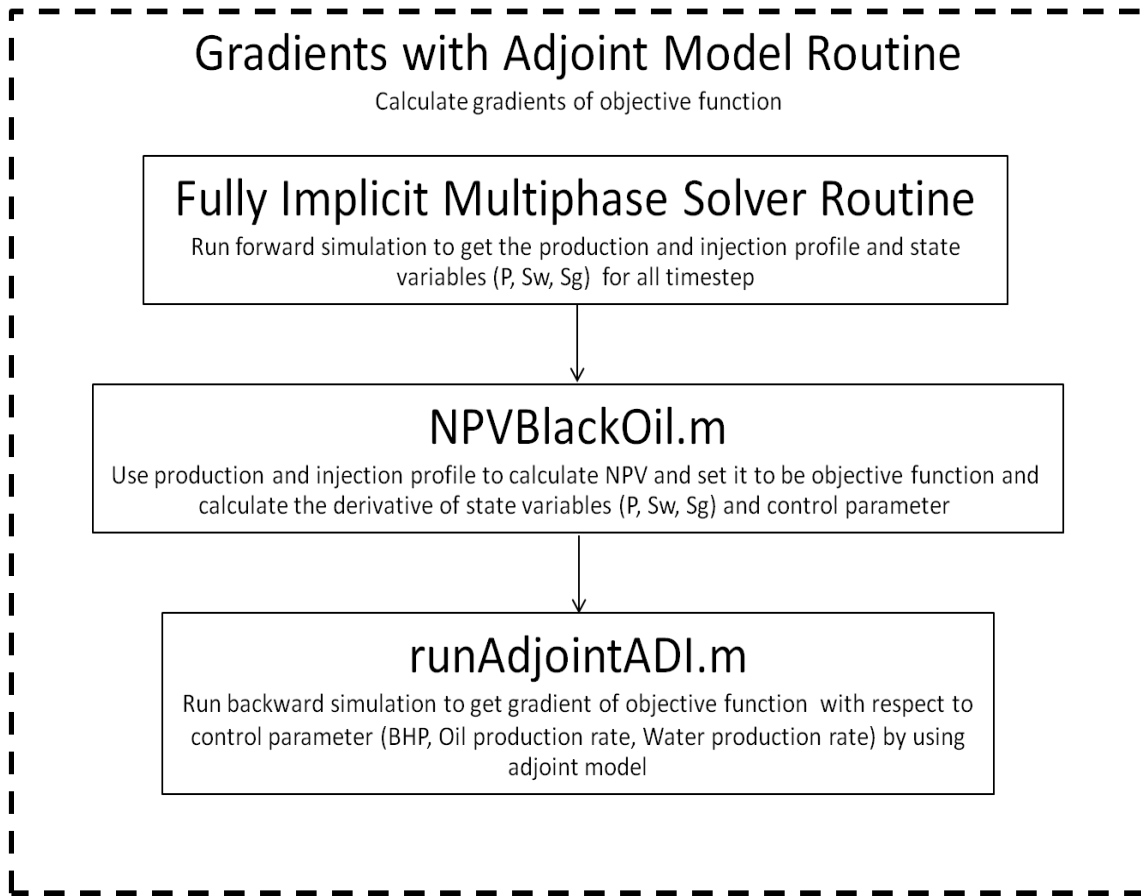


Figure 57: MRST module for finding gradients with adjoint model

$$\frac{\delta \bar{O}}{\delta THP} = \frac{\delta \bar{O}}{\delta BHP} \frac{\delta BHP}{\delta THP} \quad (65)$$

The function of "delbhpdelthp.m" is to calculate the term $\frac{\delta BHP}{\delta THP}$. The "delbhpdelthp.m" is added into "runAdjointADI.m" in order to modified the gradients calculated from original function of "runAdjointADI.m" to be the gradient of objective function with respect to upstream pressure for case of injection and downstream pressure for production.

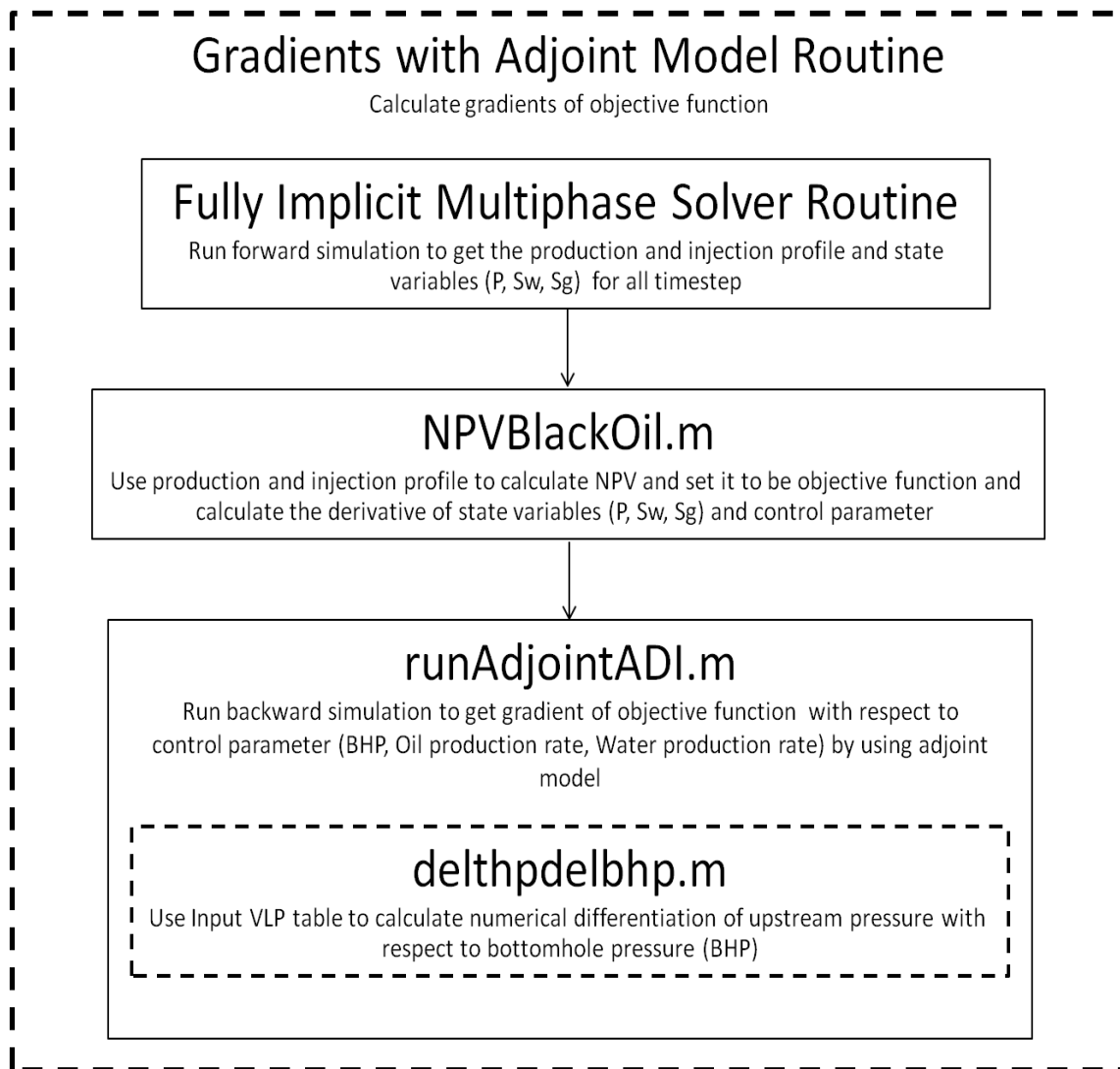


Figure 58: Modified MRST module for finding gradients with adjoint model

As the surface model is in form of VLP table, the relationship between bottomhole pressure and downstream production pressure is discrete. Consequently, the term $\frac{\delta BHP}{\delta THP}$ can be calculated by numerical method. The Figure 59 shows how to find the term $\frac{\delta BHP}{\delta THP}$ numerically. Assume that the VLP table has pressure loss and rate relationship

for two different downstream production pressure (DPP1 and DPP2). The intersection of DPP1's curve and DPP2's curve with IPR curve gives the bottomhole pressure A and B, respectively. The numerical $\frac{\delta BHP}{\delta THP}$ can be found by following equation

$$\frac{\delta BHP}{\delta THP} = \frac{A-B}{DPP1-DPP2} \quad (66)$$

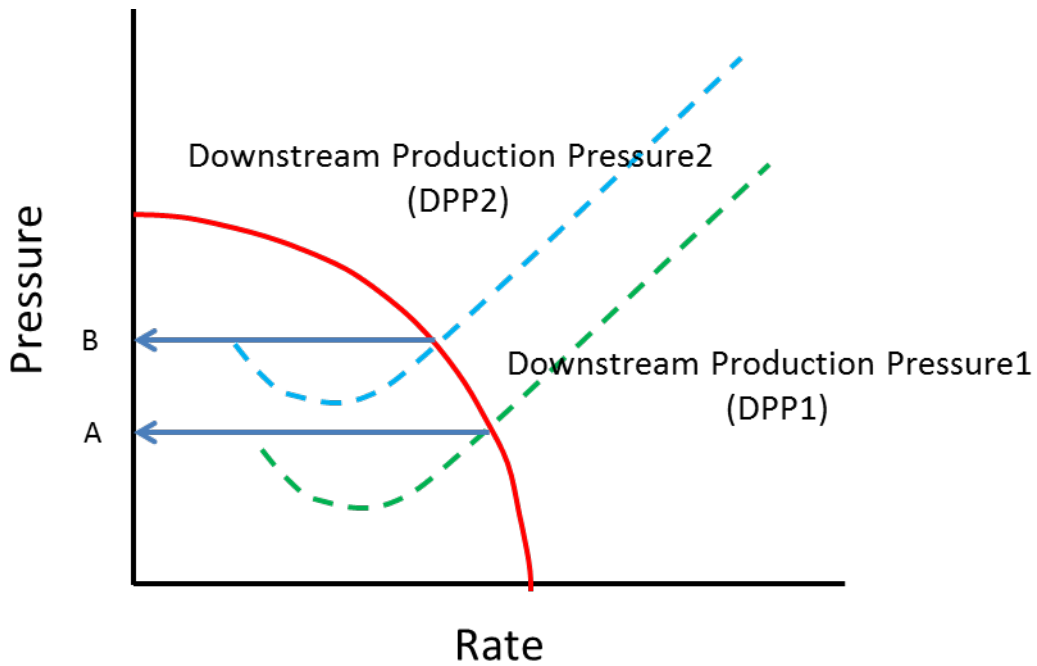


Figure 59: Example of method finding numerical $\frac{\delta BHP}{\delta THP}$

6.4. Investigation of the Effect of Various Coupling Level and Scheme on Production Optimization

The goal of a study in the 2nd phase of the study is to investigate the effect of the coupling mechanisms on the production optimization framework in order to infer the best coupling level for the optimization setup. Also we seek for the recommendation for coupling surface and subsurface models in production optimization. One of important step in this phase of study is the selection of fluid and reservoir properties, and production strategies. The properties should be selected in such a way that we can observe difference in the final result of the optimization process to figure out how much the coupling scheme can affect the production optimization result.

In this section, the gradients with the adjoint model and the sequential quadratic programming algorithm mentioned in previous section will be used to optimize the selected fluid properties, reservoir properties, and production strategies. According to the finding in the first phase of this study, the reservoir properties that give obvious different result between the different coupling schemes are reservoir properties which have heterogeneity and high permeability. Fluid with dynamic properties tends to give observable different result. Consequently, for fluid properties, lived oil PVT will yield better results than dead oil PVT. This leads to the use of the reservoir and fluid properties as summarized in Table 11 and 12.

The production strategies that will be considered here are the direct line drive water flooding and the 5-spots patterns water flooding. Figures 60 and 61 show the reservoir model with production and injection wells for direct line drive water flooding

and 5-spots pattern water flooding, respectively. The figures show that for both production scenario cases, there is at least one production well that deliberately locates in the high permeability zone in order to emphasize the effect of the high permeability, as described before.

Reservoir Simulation Model Properties	Value	Unit
NX:NY:NZ	23:23:6	
Grid size	350 x 350 x 5	ft
Permeability	Heterogeneous	md
Porosity	20	%
Initial Water Saturation	10	%
Initial Oil Saturation	90	%
Reservoir pressure	3000	psia
Reservoir depth	3000	ft

Table 11: Reservoir simulation model properties for production optimization

Fluid Properties	Value	Unit
Type of fluid	Lived oil	-
Oil Density	40	API
Gas Gravity	0.664	Sg air
Solution GOR	1.5	MSCF/STB

Table 12: Fluid properties for production optimization

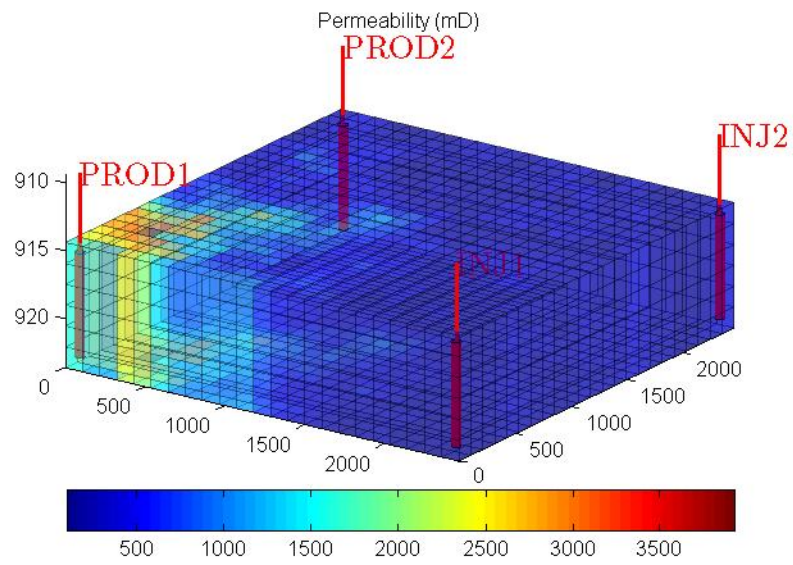


Figure 60: Reservoir simulation model with direct line drive water flooding

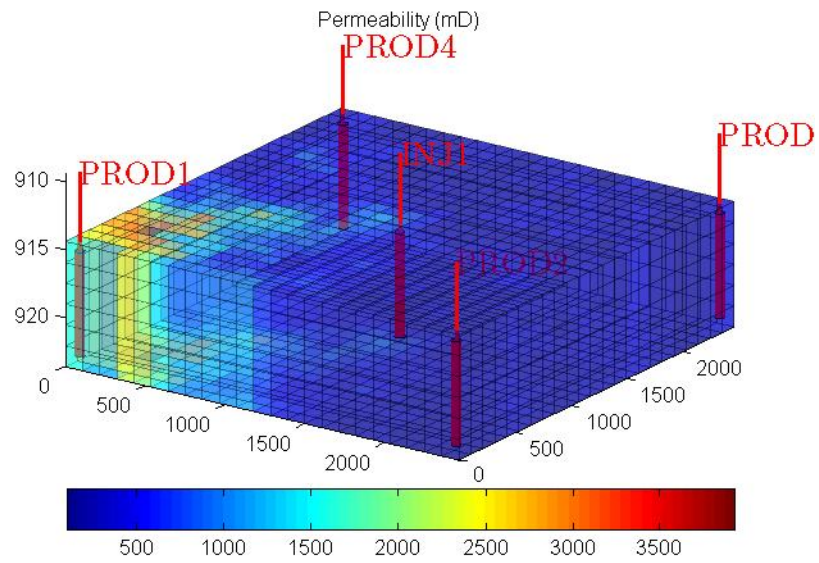


Figure 61: Reservoir simulation model with 5-spots water flooding

The production scenario of direct line drive water flooding case is pretty much the same as the production scenario of heterogeneous case in section 4 except that the production wells are located in the high permeability zone instead of the injection wells in order to emphasize the effect of high permeability.

The direct line drive water flooding production scenario can be expected that the water from injection wells could not breakthrough the production wells as the injection wells are in the low permeability zone. On the other hand, the 5-spots pattern water flooding production scenario is supposed to have some water breakthrough at the production wells, especially PROD1 since there is high permeability path between PROD1 and INJ1.

The objective function in equation (45) is NPV and it is associated with oil price, gas price, water production cost and water injection cost. In order to make the equation (45) to be completed, we need to specify the values of the cost and revenue. The summary of cost and revenue assumption used to calculate NPV is summarized in the Table 13.

Parameter	Value	Unit
Oil Price	100	US/STB
Gas Price	15	US/MSCF
Water Injection Cost	10	US/STB
Water Production Cost	10	US/STB

Table 13: Summary of cost and revenue assumption for production optimization

The production and injection constraints imposed in the production optimization problem here is the lower and upper bound of upstream injection pressure and downstream production pressure which are caused by the production and injection facility limits. The summary of the lower and upper bound of upstream injection pressure and downstream production pressure used in these production optimization problems are summarized in the Table 14.

Parameter	Lower bound	Upper bound
Upstream injection pressure	2666 psi	3666 psi
Downstream production pressure	203 psi	406 psi

Table 14: Summary of lower bound and upper bound of upstream injection pressure and downstream production pressure

Each production and injection well is assumed to be connected to the surface pipeline and can be controlled independently by downstream production pressure and upstream injection pressure. The well and surface pipeline specifications of both water flooding optimization cases are the same as the well and surface pipeline specification used in Table 10 of section 5.

6.4.1. Direct Line Drive Water Flooding

For direct line drive water flooding, there are two injection wells (INJ1 and INJ2) and two production wells (PROD1 and PROD2). All the wells are fully perforated. The upstream injection pressure and downstream production pressure for the base case run is controlled at 3000 psi and 220 psi, respectively, for the whole time of production timespan. This case is a representative case of low pressure support from water flooding because the injection wells are in low permeability zone and the direct line drive water flooding production scenario is expected to be produced without water breakthrough at the production wells. This implies that the water flooding could not provide a strong pressure support. The production optimization using explicit coupling, implicit coupling, and no coupling for direct line drive water flooding production optimization are presented in the following subsection.

6.4.1.1. Explicit Coupling Case

In the explicit coupling case, there is a term of timing that is used in production optimization process called optimization time step. The meaning of optimization time step is the time that the control parameters (for this problem, they are upstream injection pressure and downstream production pressure) can be changed to minimized (or

maximized) the objective function. In an explicit coupling case, the optimization time step and the surface and subsurface model balancing time step are the same and it occurs periodically (every specified interval of time). For the case of direct line drive water flooding, the total production time is 1000 days and the optimization and balancing time step size is set to be 20 days. Consequently, there will be 50 optimization and balancing time steps. The comparison of production profile of the base case and optimized case is shown in the Figure 62. The red line represents the result of optimized case while the blue line represents the result of base case. The PROD1 and PROD2 production profiles are represented by solid line and dash line respectively. The same notation is used for injection profile shown in the Figure 63. It can be seen that after the production optimization run, the control of downstream production pressure of both production wells are changed to 406 psi which is the upper bound value for 280 days and then go down to 206 psi which is the lower bound value for the rest of production period. The upstream injection pressure of both injection wells also changes to upper bound in the early period of production and then go down to lower bound in the middle and late period of production. The improvement of production in the optimized case is resulting from maintaining the reservoir pressure in the early time of production by reducing gas production and increasing water injection rate. In the middle and late time of production, the water injection can be reduced since the reservoir still has driving energy from the gas that was not produced in the early time of production. The optimized case improves the NPV to 11.3 billion USD as compared to the base case NPV by 0.7 billion USD.

6.4.1.2. Implicit Coupling Case

For the implicit coupling case, the optimization time step and the surface and subsurface model balancing time step are the same and occur every time step, namely every 10 days. Consequently, there will 100 optimization and balancing time steps. The comparison of the base case and optimized case of production and injection profile are shown in the Figures 64 and 65, respectively. The control of upstream injection pressure and downstream production pressure after optimization is pretty much the same as the explicit coupling case except that the high upstream injection pressure and downstream production pressure period is shorter than the implicit case. The NPV of the base case using implicit coupling is about 10.5 billion USD while the optimized case increase the NPV to 11.2 billion USD.

6.4.1.3. Coupling Surface and Subsurface Model in the Optimization Framework

This section aims to illustrate the importance of using coupled surface and subsurface model in production optimization. The production optimization of no coupled model or standalone reservoir simulation model can be achieved by using bottomhole production and injection pressures as control parameters. All of reservoir description is the same as the one that used in the coupled model.

In a real situation, the possible lowest and highest bottomhole production and injection pressure can be estimated using nodal analysis. The possible highest bottomhole production and injection pressure occurs when the wells produce/inject at the highest downstream production pressure/upstream injection pressure and reservoir pressure is maintained at initial reservoir pressure. The lowest bottomhole injection

pressure can be estimated by the same method but use lowest upstream injection pressure and reservoir pressure at low pressure. The possible lowest bottomhole production pressure is assumed to be equal to abandonment pressure, which in our example is 400 psi. The summary of estimated lower and upper bound of bottomhole production and injection pressures is shown in the Table 15.

Parameter	Lower Bound	Upper Bound
INJ1: Bottomhole Injection Pressure	3871 psi	4926 psi
INJ2: Bottomhole Injection Pressure	3871 psi	4926 psi
PROD1: Bottomhole Production Pressure	400 psi	2050 psi
PROD2: Bottomhole Production Pressure	400 psi	850 psi

Table 15: Lower and upper bound of bottomhole production and injection pressures

Figures 66 and 67 show the comparison of production optimization results of coupled and no coupled case. The red line represents the implicit coupling case and the blue line represents the no coupling case. It can be seen that the bottomhole production pressure of the two cases is obviously different. The bottomhole production pressures of no-coupling case are at maximum allowable pressure or upper bound which higher than the maximum bottomhole production pressure of implicit coupling case and maintain at this value from the day one of production and keep constant about one year and eight months for PROD1 and about one year and six months for PROD2. Then, they drop to the lower bound value for the rest of production period while the bottomhole production

pressures of implicit coupling case are gradually reduced as the gas oil-ratio increase and then suddenly drop due to reducing of downstream production pressure. For injection profiles, the bottomhole injection pressures of two injection wells in the case of no coupling are at maximum allowable pressures for a longer time than the case of implicit coupling and drop to lower bound about at the same time that the bottomhole production pressures of two production wells are dropped resulting in different injection rate profiles. The difference of bottomhole production/injection pressures impacts the oil and gas production profile and it causes NPV of no coupling case to be higher than implicit coupling case about 1.8 billion USD.

We also ran a different setup by using assumption that we know the minimum and maximum of bottomhole pressure results from the optimization using implicit coupling. The lower and upper bound of bottomhole production and injection pressures are set to be equal to minimum and maximum of bottomhole pressure result of production optimization using implicit coupling. The summary of lower and upper bound of bottomhole production and injection pressures used in production optimization of standalone reservoir simulation model is shown in Table 16.

Parameter	Lower Bound	Upper Bound
INJ1: Bottomhole Injection Pressure	3971 psi	4974 psi
INJ2: Bottomhole Injection Pressure	3971 psi	4974 psi
PROD1: Bottomhole Production Pressure	305 psi	1029 psi
PROD2: Bottomhole Production Pressure	303 psi	644 psi

Table 16: Estimated lower and upper bound of bottomhole production and injection pressures

Although the bottomhole production pressures and production profiles of the two production wells of no coupling (with known lower and upper bound) and implicit coupling case are still different as shown in Figure 68, it can be seen from the Figures 68 and 69 that the production and injection profiles are much more similar than the case of no-coupling with estimated lower and upper bound. The NPV of no coupling case with known bound is 11.49 billion USD which is higher than the implicit coupling case NPV about 0.3 billion USD.

The differences of no coupling and coupling case will be more visible when water breakthrough the production well which will be shown in the case of 5-spots pattern water flooding.

6.4.1.4. Comparison of Explicit and Implicit Coupling Case

The Figures 70 and 71 show the comparison of explicit coupling and implicit coupling results of optimization. The blue line represents the case of production optimization using implicit coupling while the red line denotes the explicit coupling. As mentioned before that the optimal control of upstream injection pressure and downstream production pressure of explicit and implicit coupling are a little bit different. However, the bottomhole flowing pressures of production wells between implicit and explicit coupling are obviously different in the early date of production since the surface and subsurface model of explicit coupling case are not fully balanced resulting in different oil production and gas production rate in that period of time. The differences of oil and gas production rate affect the average reservoir pressure.

After the first balancing time step, the bottomhole production pressures of explicit coupling case are getting closed to implicit coupling case because the well linear IPR is queried from more realistic operating point. Moreover, the bottomhole production pressure profiles after the first balancing time step of explicit coupling and implicit coupling cases have quite the same trend because gas-oil ratio profile which influence the outflow performance relationship and reservoir pressure (in Figure 72) which influence the inflow performance relationship of the both implicit and explicit cases are relatively similar.

The reason that the average reservoir pressure and gas-oil ratio of difference coupling cases are fairly similar can be explained as follow; the reservoir pressure depletions of the two cases are similar (same trend but different value) and assimilate to

normal depletion trend because the water flooding can provide only a small pressure support. The similarity of reservoir pressure depletions effects gas-oil ratio profiles of the two different coupling cases to be fairly similar. The plot of comparison of average reservoir pressure can be found in the Figure 72.

Moreover, the optimized NPV of these two coupling schemes is not much different since the total volume of oil and gas production and water injection are not much different. The summary of difference of cumulative production and injection is concluded in the Table 17. The plot of cumulative production and injection volume comparison can be found in the Figure 72.

Parameter	Value	Unit
Difference of Cumulative Oil Production	-81.0	MSTB
Difference of Cumulative Gas Production	125.5	MMSCF
Difference of Cumulative Water Injection	80.1	MSTB

Table 17: Summary of difference of total cumulative production and injection volume of production optimization using different coupling schemes

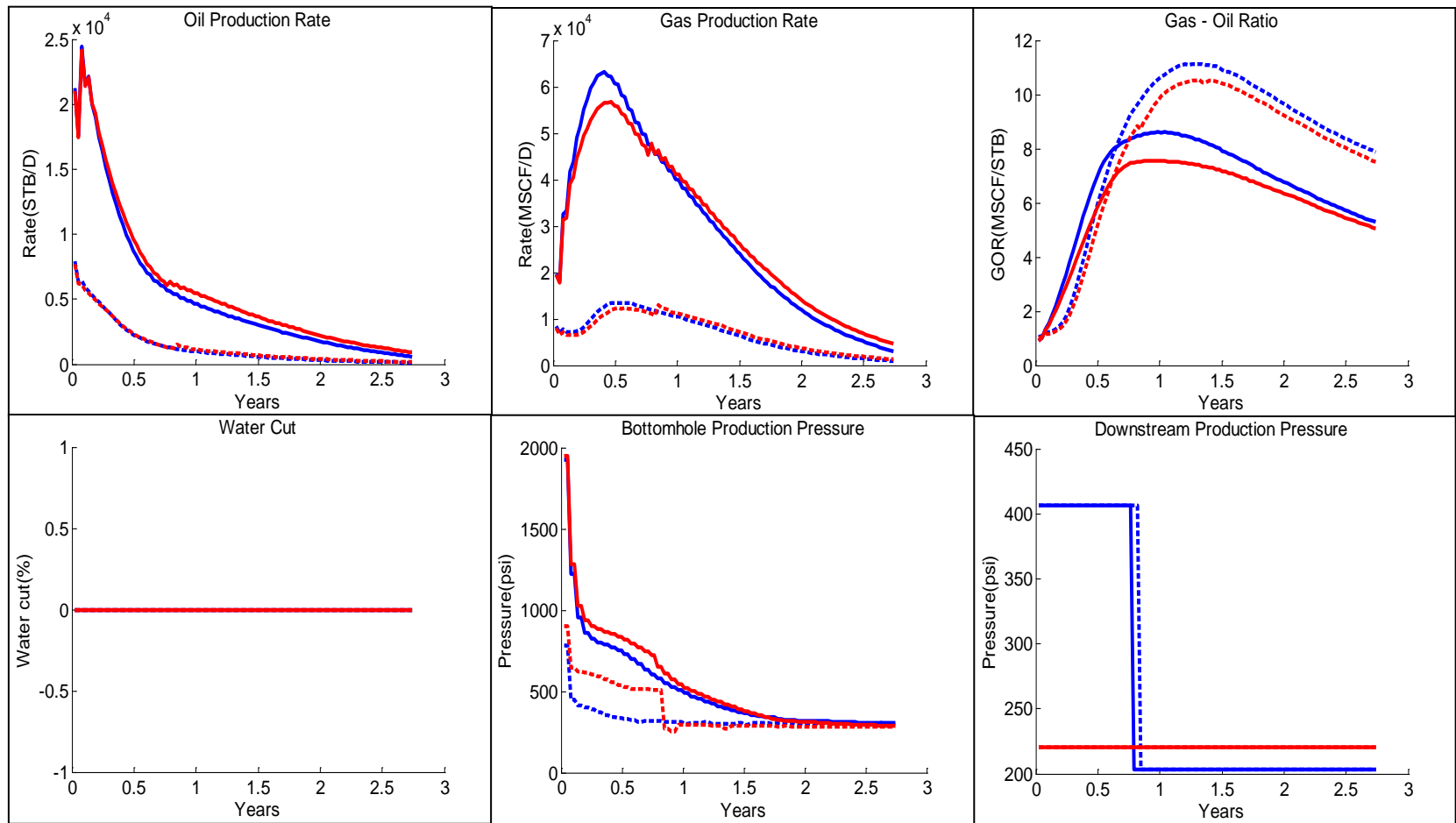


Figure 62: Comparison of base case and optimized case of direct line drive water flooding production profiles using explicit coupling

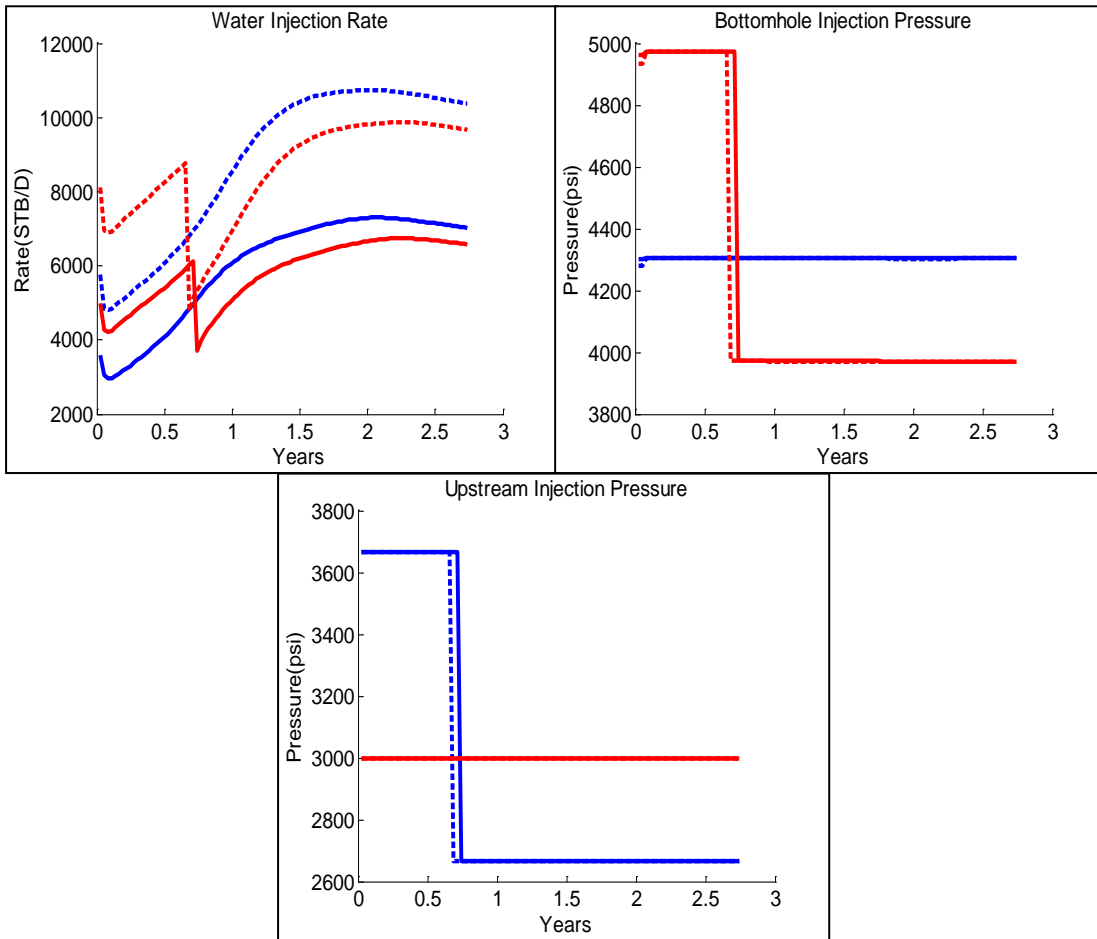


Figure 63: Comparison of base case and optimized case of direct line drive water flooding production profiles using explicit coupling

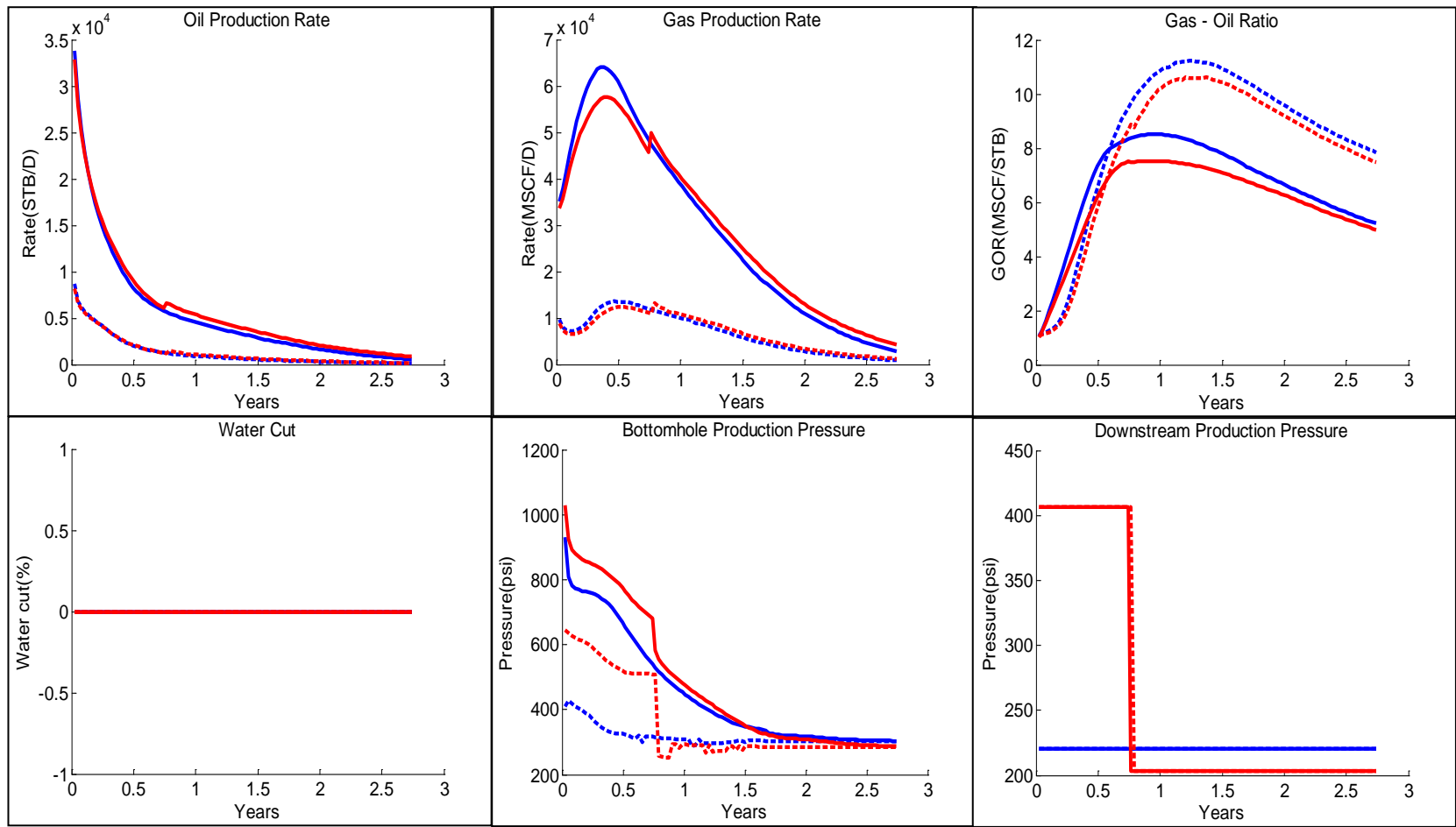


Figure 64: Comparison of base case and optimized case of direct line drive water flooding production profiles using implicit coupling

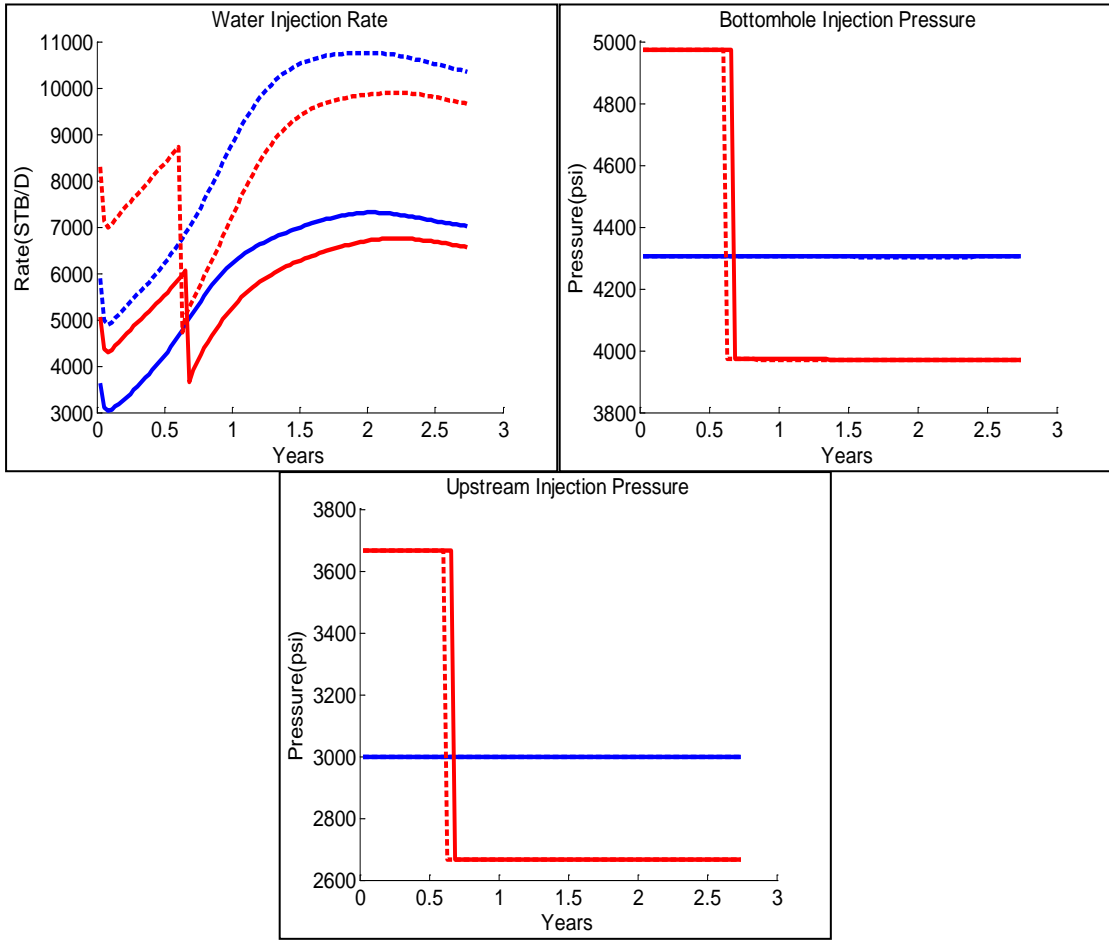


Figure 65: Comparison of base case and optimized case of direct line drive water flooding injection profiles using implicit coupling

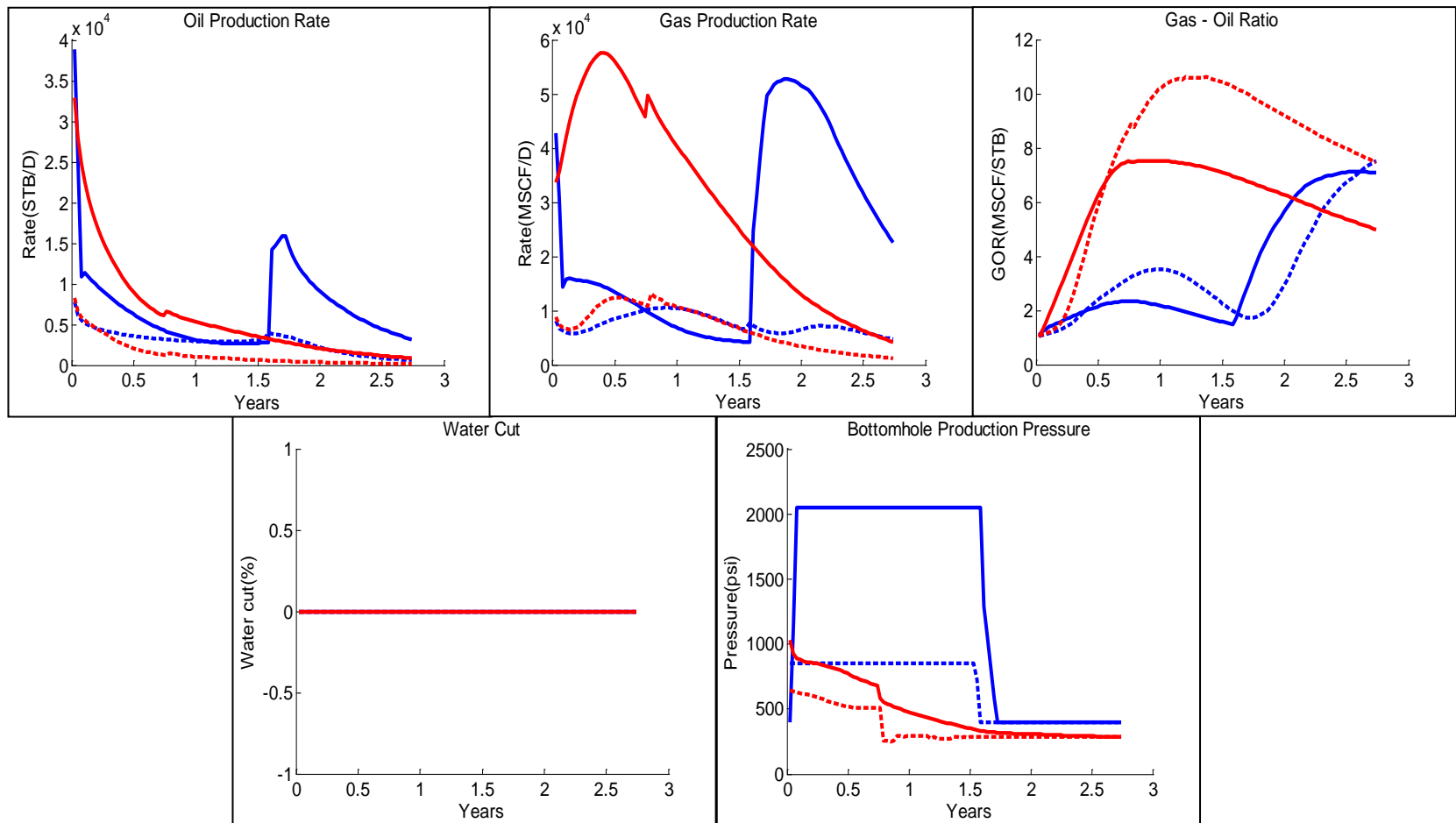


Figure 66: Comparison of no coupled (estimated lower and upper bound) and implicit coupled optimization production profiles for the case of direct line drive water flooding

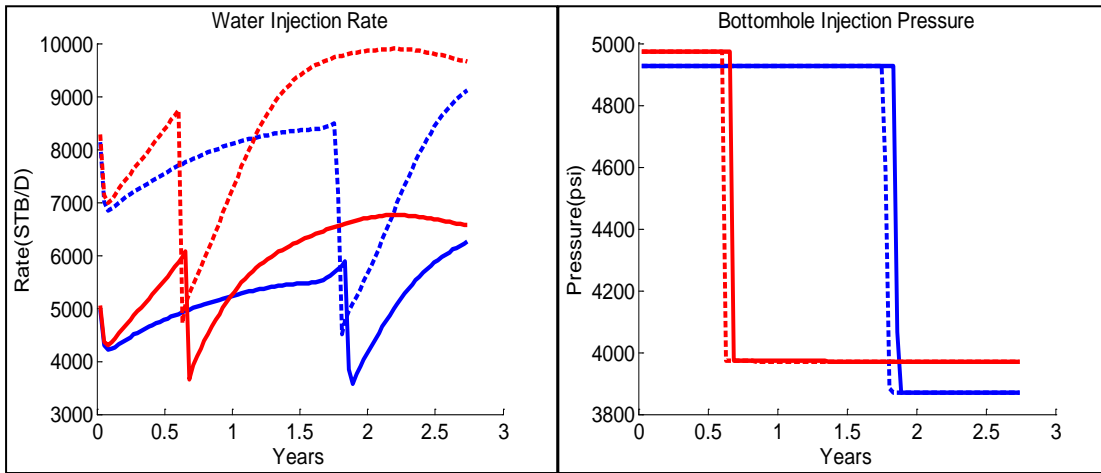


Figure 67: Comparison of no coupled (estimated lower and upper bound) and implicit coupled optimization injection profiles for the case of direct line drive water flooding

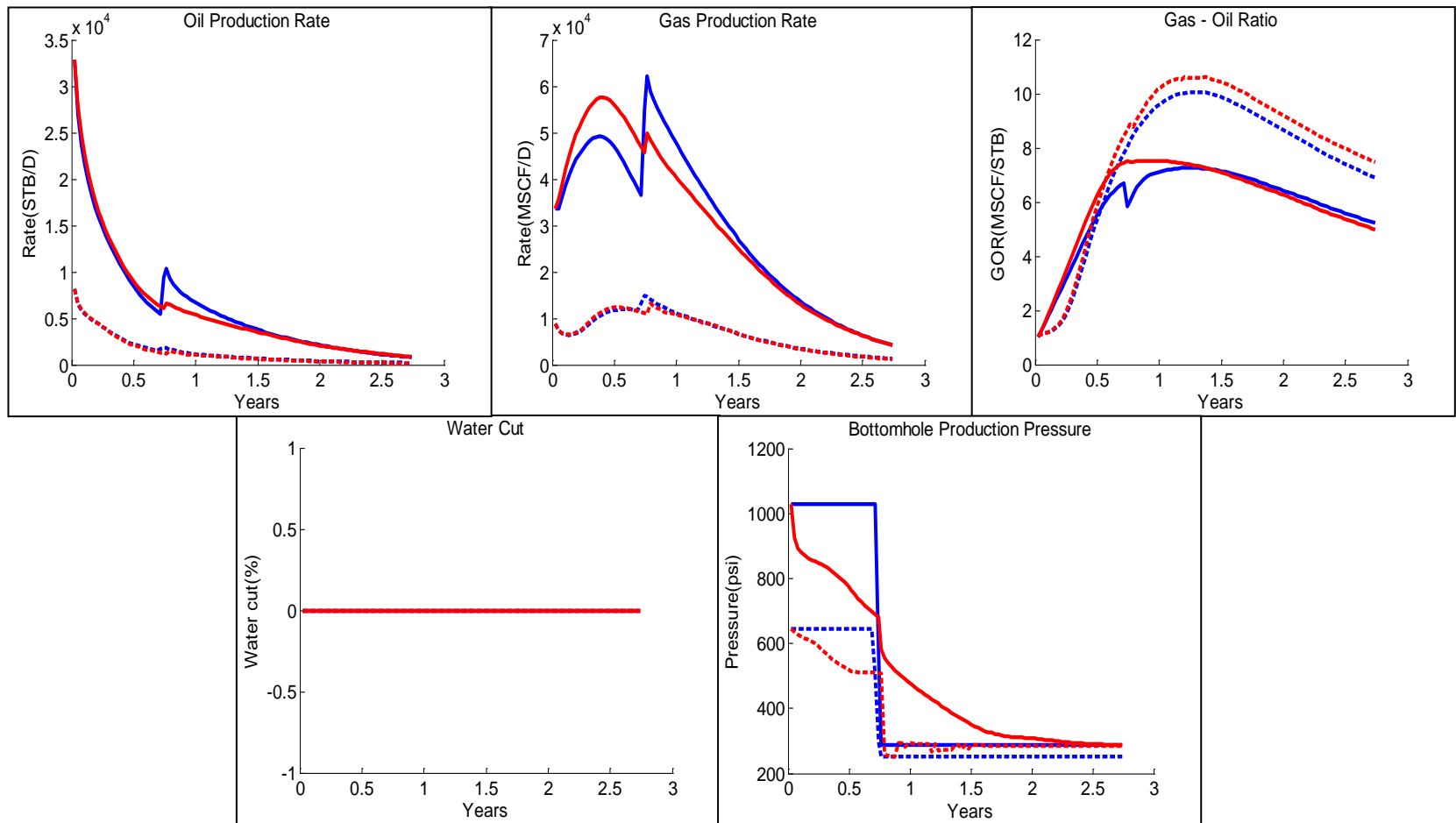


Figure 68: Comparison of no coupled (known lower and upper bound) and implicit coupled optimization production profiles for the case of direct line drive water flooding

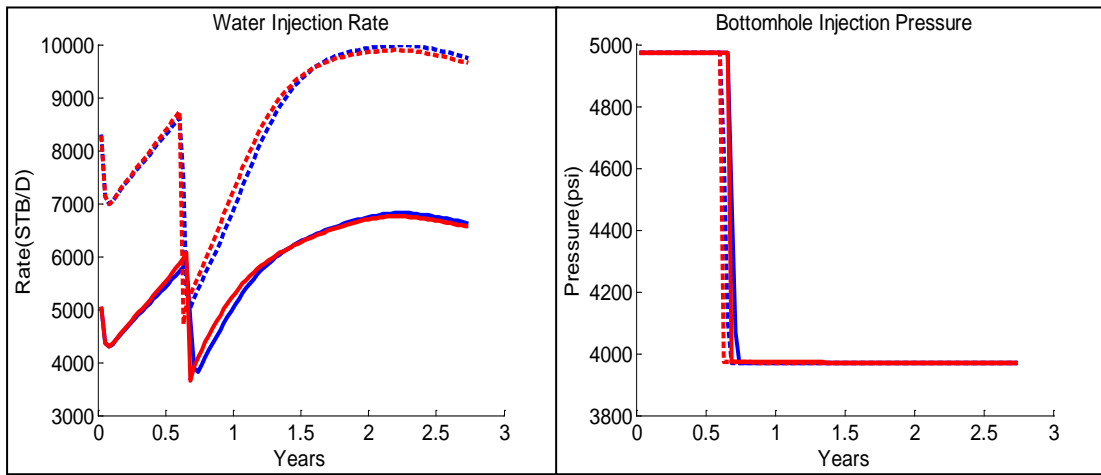


Figure 69: Comparison of no coupled (known lower and upper bound) and implicit coupled optimization injection profiles for the case of direct line drive water flooding

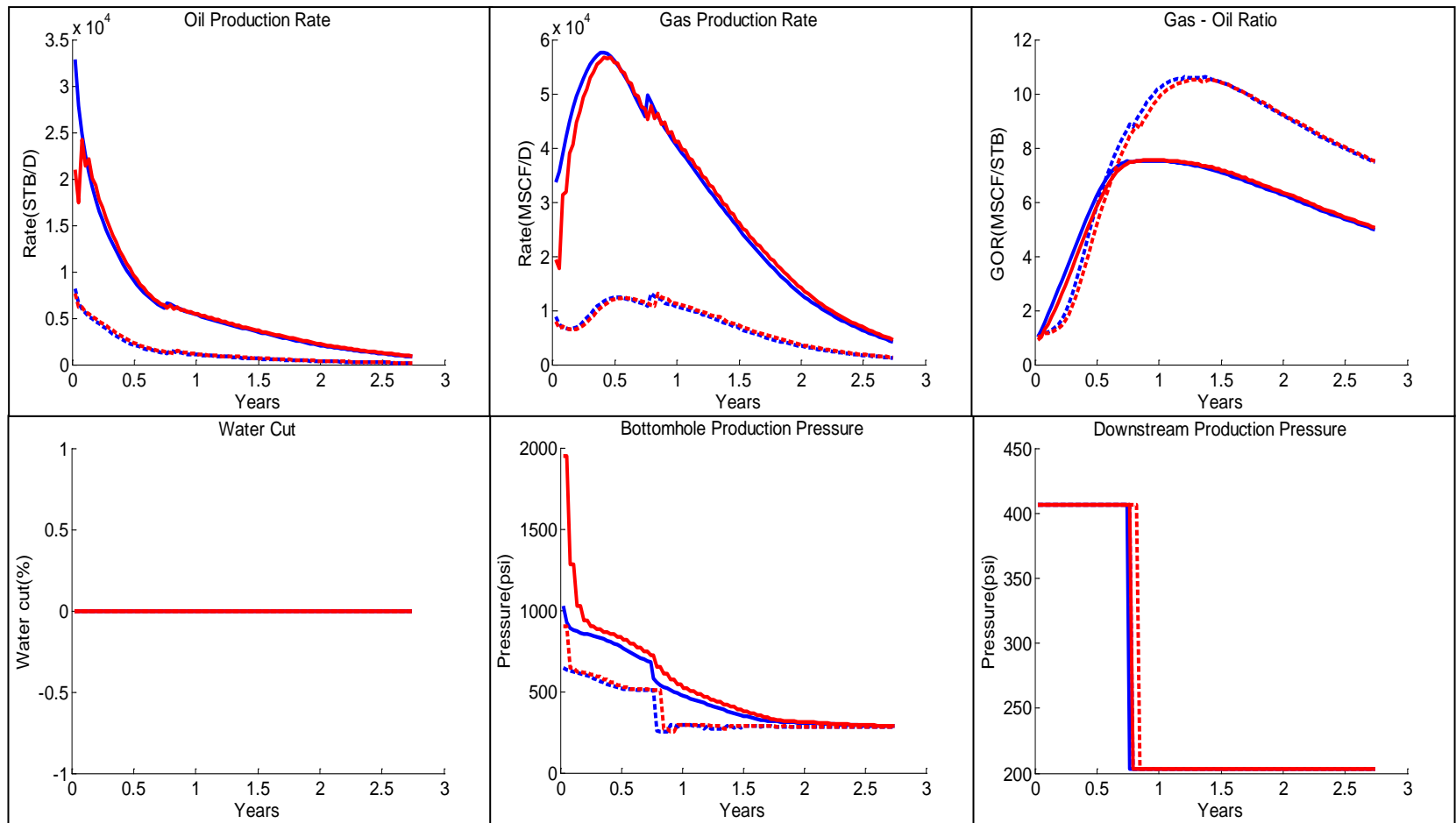


Figure 70: Comparison of explicit coupled and implicit coupled optimization production profiles for the case of direct line drive water flooding

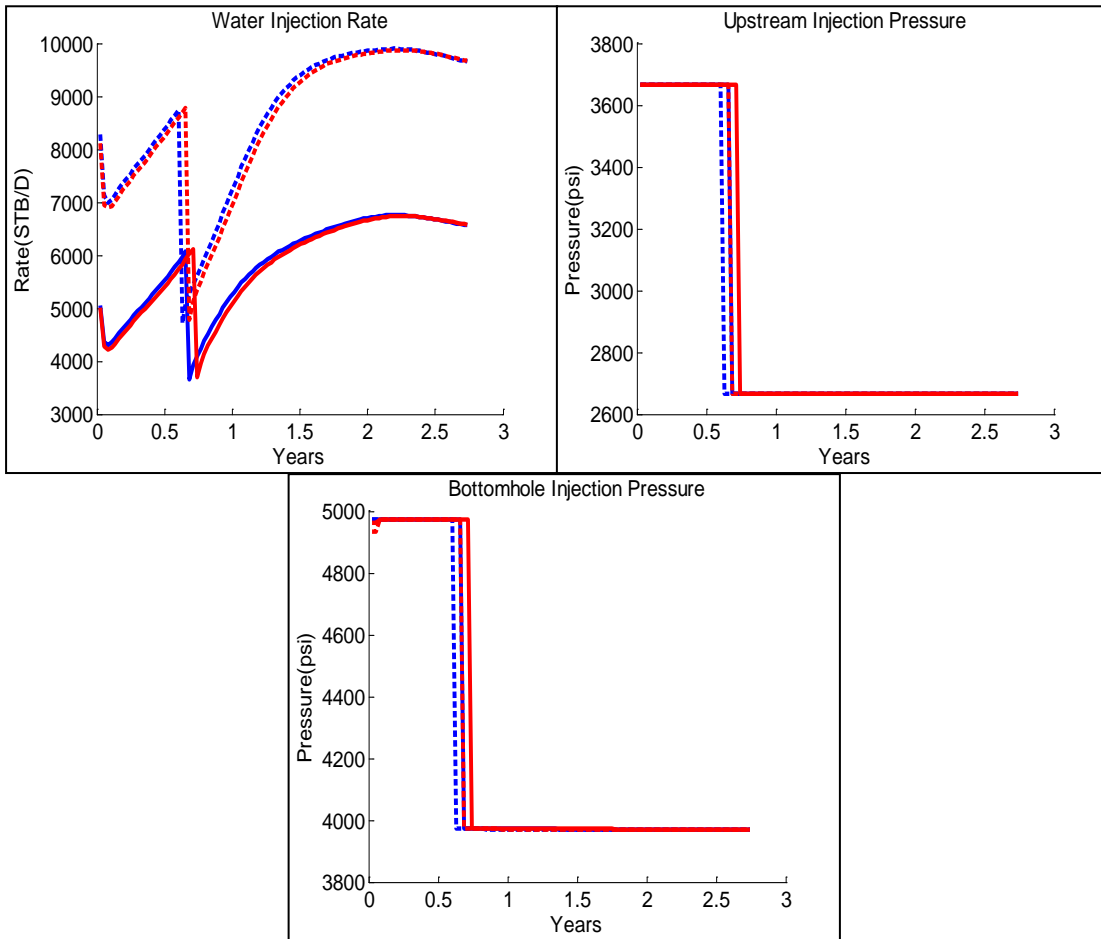


Figure 71: Comparison of explicit coupled and implicit coupled optimization injection profiles for the case of direct line drive water flooding

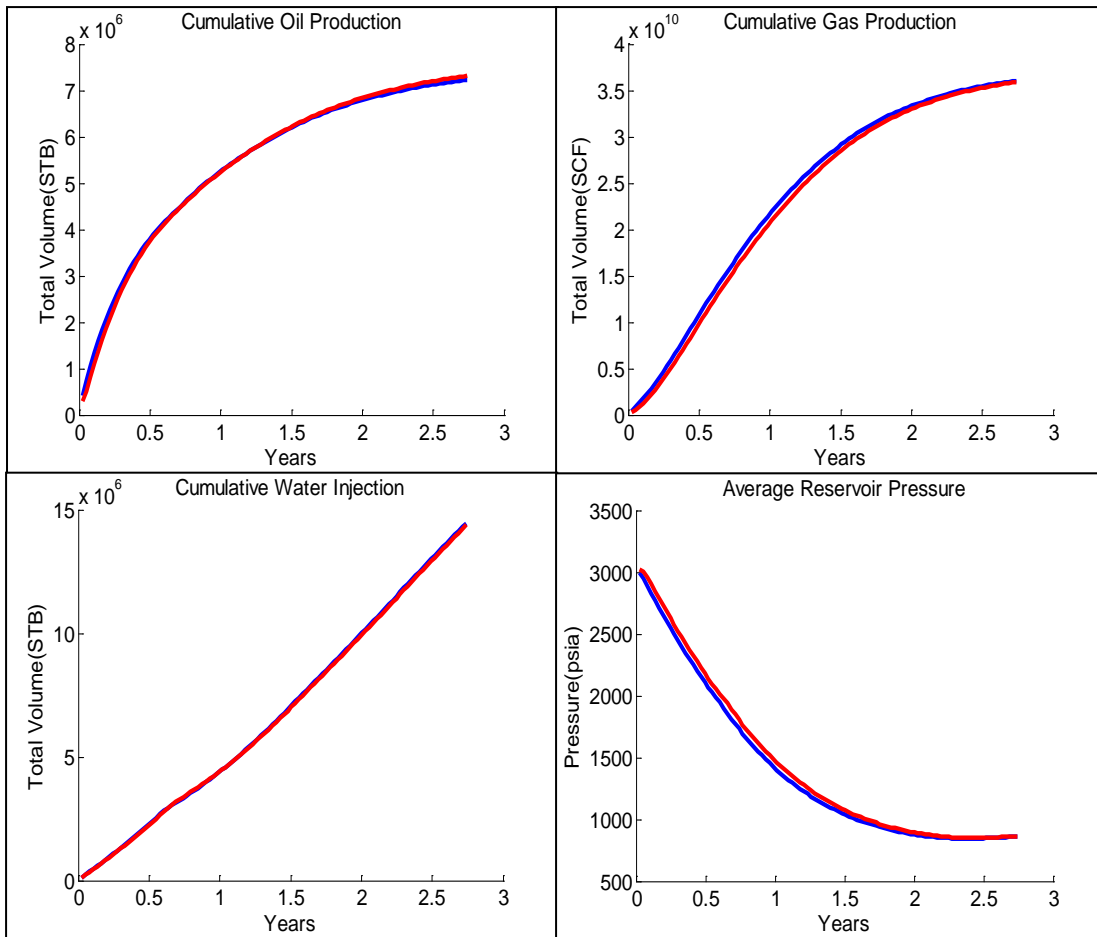


Figure 72: Comparison of explicit coupled and implicit coupled cumulative production & injection volume and average reservoir pressure for the case of direct line drive water flooding

6.4.2. 5-Spots Pattern Water Flooding

The 5-spots pattern water flooding consists of four production wells (PROD1, PROD2, PROD3, and PROD4) and one injection well (INJ1). The wells are assumed to be fully perforated. As same as the direct line drive water flooding, the upstream injection pressure and downstream production pressure for base case are controlled at 3000 psi and 220 psi for the whole time of injection and production. This production scenario represents the case that the water flooding has a strong effect on reservoir pressure because the injection well is in the high permeability zone such that the injected water can effectively flood the remaining oil. The results of 5-spots pattern water flooding with various coupling scheme and no coupling are presented and analyzed to observe the effect of different coupling scheme on production optimization.

6.4.2.1. Explicit Coupling Case

The total time of production of 5-spots pattern water flooding is 1400 days. The optimization and balancing time step used here is 50 days. Consequently, there will be 28 optimization and balancing time step. The oil production profile and bottomhole production pressure of each production wells are shown in the Figures 73 and 74, respectively. The red line represents the optimized case and the blue line represents the base case. The Figure 75 shows comparison of base case and optimize case of the other production results. It can be seen that the downstream production pressure of PROD1 (solid red line) is changed to the maximum value to delay the water breakthrough while the pressure for the other production wells is changed to minimum value to maximize the oil production rate. Although the bottomhole production pressure of the optimized

case in the early time of production is higher than the base case and water breakthrough faster than the base case, the oil production profile of all four production wells of optimized case clearly shows the improvement of oil production rate because higher volume of water can be injected and flooded more remaining oil out of reservoir. The comparison of injection rate of the base case and the optimized case can be found in the Figure 76. The upstream injection pressure of optimized case (red line) is changed from the base case (blue line) to the upper bound and goes down to the lower bound around 50 days before end of four years of production. The NPV of optimized case is 26.19 billion USD which improve from the base case by 2.76 billion USD.

6.4.2.2. Implicit Coupling Case

For implicit coupling case, the size of simulation time step is 10 days. Consequently, the number of optimization time step and balancing time step is 140. The Figures 77 and 78 show the comparison of base case and optimized case oil production profile and bottomhole production pressure. The Figure 79 illustrates the comparison of base case and optimized case of the other production results. The optimized case is represented by the red line while the blue line represents the base case. It can be seen that the characteristic of production profiles of implicit coupling case are pretty much the same as explicit coupling case results. For injection side, the comparison of injection rate of the base case and the optimized case can be found in the Figure 80. The rate of water injection of optimized case is higher than the base case. The production improvement of implicit coupling case can be explained by the same reasons as it explained in explicit

coupling case. The NPV of optimized case is 26.27 billion USD which improve form the base case by 2.76 billion USD.

6.4.2.3. Coupling Surface and Subsurface Model in the Optimization Framework

In the previous section (direct line drive water flooding), the importance of coupled model for production optimization is presented. It can be seen that in the case of direct line drive water flooding, there is no water breakthrough at production wells. In this section, the results will show you how the water breakthrough can affect the difference between using coupled surface and subsurface model and no coupled model for production optimization results.

The estimation of lower and upper bound of bottomhole production and injection pressure can be done in the same fashion as mentioned the previous section. The summary of estimated lower and upper bound of bottomhole production and injection pressures is shown in the Table 18.

Parameter	Lower Bound	Upper Bound
INJ1 : Bottomhole Injection Pressure	3871 psi	4962 psi
PROD1: Bottomhole Production Pressure	400 psi	2050 psi
PROD2: Bottomhole Production Pressure	400 psi	710 psi
PROD3: Bottomhole Production Pressure	400 psi	965 psi
PROD4: Bottomhole Production Pressure	400 psi	850 psi

Table 18: Estimated lower and upper bound of bottomhole production and injection pressures

The Figures 81 and 82 show the oil production profile and bottomhole production pressure of no coupling and implicit coupling optimization case. It can be observed that the oil production profiles and bottomhole production pressures of the two cases are totally different. The bottomhole production pressure of PROD1 is increased to the maximum allowable pressure since the early time of production in order to delay the water breakthrough while the bottomhole production pressure of the other wells are changed to the minimum allowable or lower bound pressure to maximize the oil production. The difference of bottomhole production pressures of no coupling case and implicit coupling case causes the production profiles of the two cases to be different.

The Figure 83 shows the comparison of gas-oil ratio and water cut of no coupling and implicit coupling cases. The case of no coupling obviously produces lower gas-oil ratio which imply that most of the reservoir energy is preserved. This explains the reason why the water injection rate of the no coupling case is lower than the implicit coupling case although the bottomhole injection pressures of the both cases are quite identical. The injection profile of no coupling and implicit coupling can be found in the Figure 84.

As same as the direct line drive water flooding, another no coupling case can be ran based on assumption that we know and use the minimum and maximum of bottomhole pressure result of production optimization using implicit coupling as lower and upper bound of bottomhole production and injection pressures. The summary of lower and upper bound of bottomhole production and injection pressures used in production optimization of standalone reservoir simulation model is shown in Table 19.

Parameter	Lower Bound	Upper Bound
INJ1 : Bottomhole Injection Pressure	3949 psi	4938 psi
PROD1: Bottomhole Production Pressure	802 psi	1563 psi
PROD2: Bottomhole Production Pressure	320 psi	411 psi
PROD3: Bottomhole Production Pressure	343 psi	427 psi
PROD4: Bottomhole Production Pressure	352 psi	617 psi

Table 19: Lower and upper bound of bottomhole production and injection pressures

Although the bottomhole production pressure and oil production profiles of the production wells of no coupling (with known lower and upper bound) and implicit coupling case are still have obvious differences as shown in Figures 85, 86 and 87, it can be seen that the production and injection profiles are much more similar than the case of no coupling with estimated lower and upper bound. The water injection profiles in the Figure 88 also show that the water injection rate of no coupling case with known lower and upper bound the water injection profile, The NPV of no coupling case with known bound is 11.49 billion USD which different from the implicit coupling case NPV about 0.3 billion USD.

6.4.2.4. Comparison of Explicit and Implicit Coupling Case

The comparison of explicit coupling and implicit coupling of oil production profile and bottomhole production pressure in each well are shown in the Figures 89 and 90. The blue line represents the case of production optimization using implicit coupling while the red line denotes the explicit coupling. The Figure 91 shows gas-oil ratio, water

cut profiles, downstream production pressure controls and average reservoir pressure of the two different coupling cases. Although the downstream production pressure controls of each production well of two difference coupling schemes which is shown in the Figure 91 are quite the same, it can be seen that in the first time step of production the oil production rate of all production wells of explicit coupling are less than the case of implicit coupling because of higher bottomhole production pressure. After the first time step, the bottomhole production pressures of two different coupling schemes are significantly different. As mentioned before that the bottomhole production pressure is obtained from the intersection of well linear inflow performance relationship and outflow performance relationship. The well linear inflow performance is related to the reservoir pressure while the outflow relationship is subjected to composition of the fluid flow in pipe (i.e. gas-oil ratio and water cut). It can be seen from Figure 91 that the shape of gas-oil ratio profiles and average reservoir pressure profiles are quiet similar but they are shifted. Consequently, the shape of bottomhole production pressure profiles of the two different coupling schemes are quite the same but shifted. The difference of reservoir pressure and bottomhole production pressure affect the production profiles of oil and gas to be different.

In the late time, the oil production rates of explicit coupling and implicit coupling are pretty much the same because the bottomhole production pressures and reservoir pressures of the two cases are getting closed.

In the Figure 92, the upstream injection pressure control of injection well of two difference coupling schemes is similar but the injection profile shows some differences

in the early period of production since the oil production wells of implicit coupling produce at higher rate cause the reservoir pressure to be lower and resulting in higher injection rate. In the late time of production, the injection rate of explicit coupling case is higher because the reservoir pressure of explicit coupling case is increased more than the reservoir pressure of implicit coupling case.

Although the oil production, gas production, and water production profiles of different coupling scheme of each well are different, the total cumulative production profiles are not much different as they are shown in the Figure 93. The summary of difference of total cumulative production and injection volume of production optimization using different coupling schemes is shown in the Table 20. The optimized NPV of these two coupling scheme is not much different since the total volume of oil, gas, and water production and water injection are not much different.

Parameter	Value	Unit
Difference of Cumulative Oil Production	128.6	MSTB
Difference of Cumulative Gas Production	100.3	MMSCF
Difference of Cumulative Water Production	226.1	MSTB
Difference of Cumulative Water Injection	448.7	MSTB

Table 20: Summary of difference of total cumulative production and injection volume of production optimization using different coupling schemes

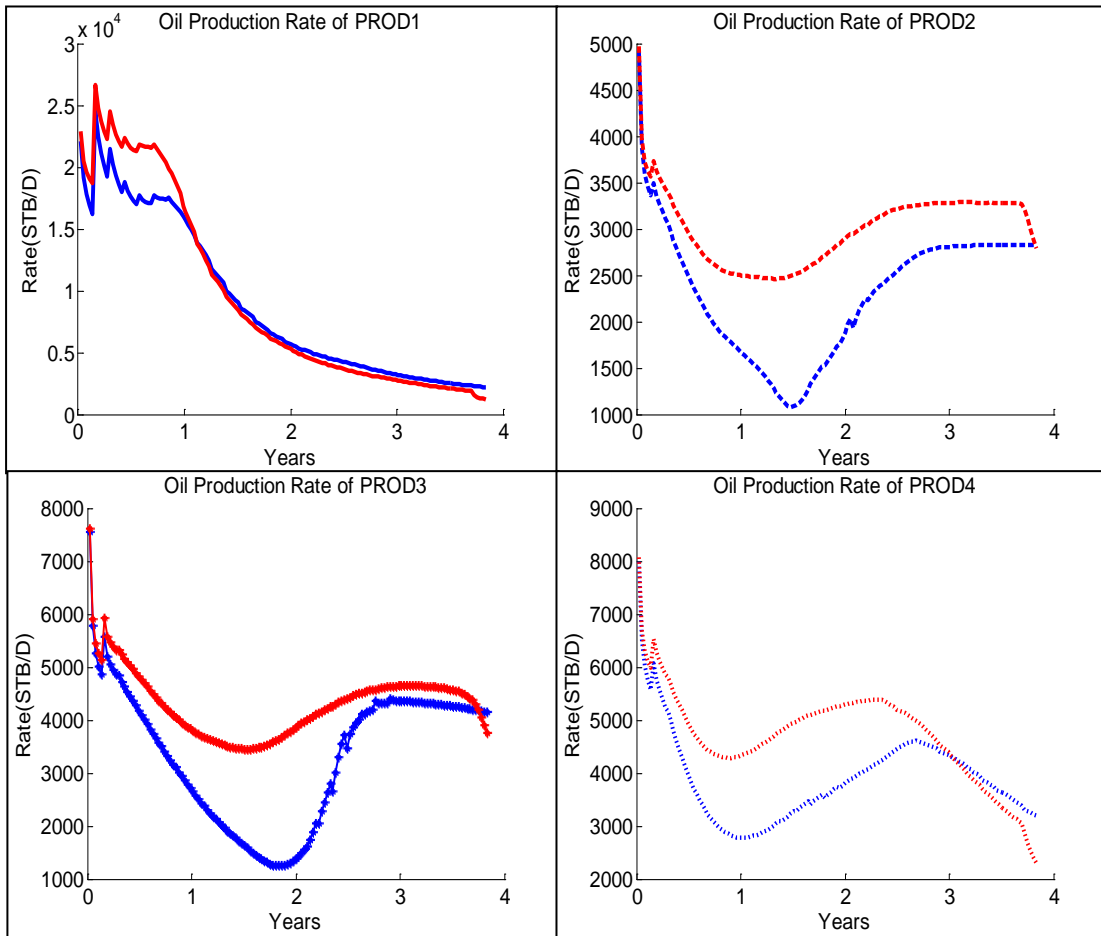


Figure 73: Comparison of base case and optimized case of 5-spots pattern water flooding oil production profiles using explicit coupling

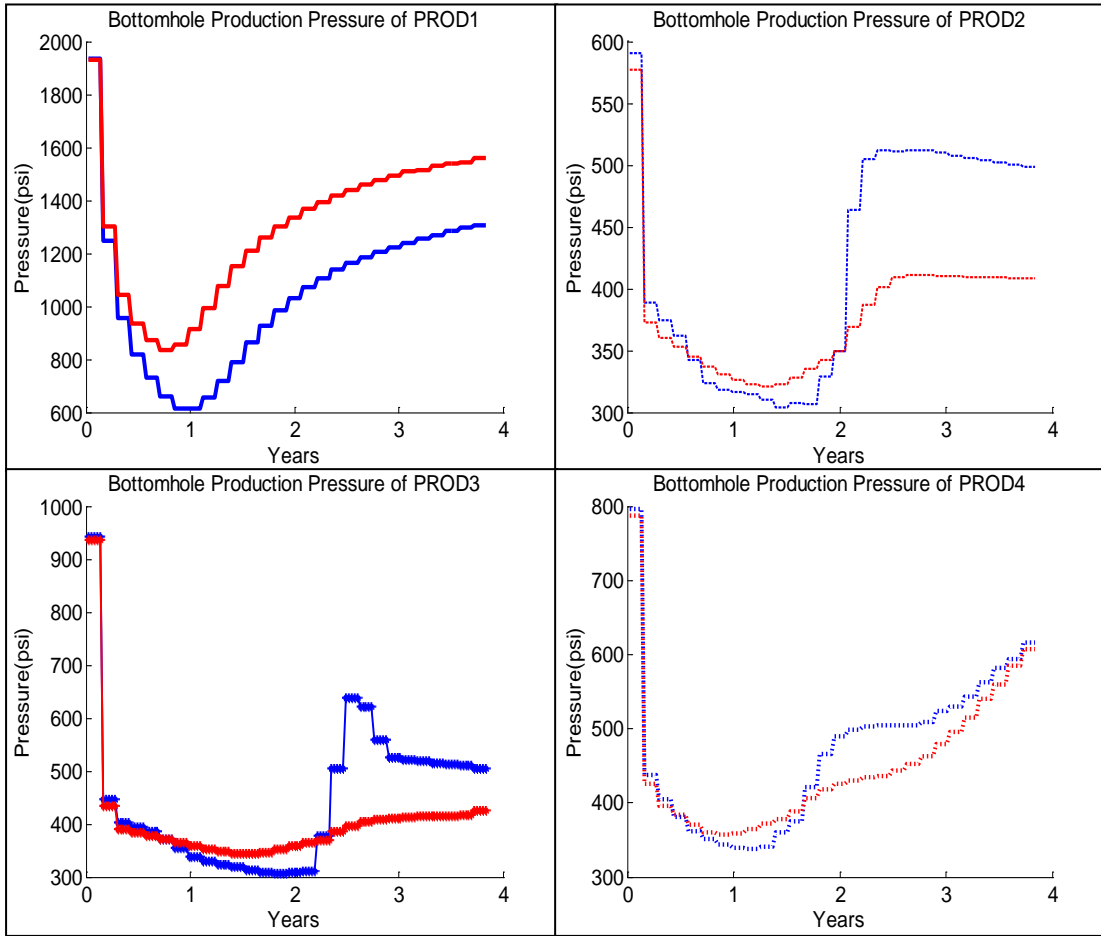


Figure 74: Comparison of base case and optimized case of 5-spots pattern water flooding bottomhole flowing pressure using explicit coupling

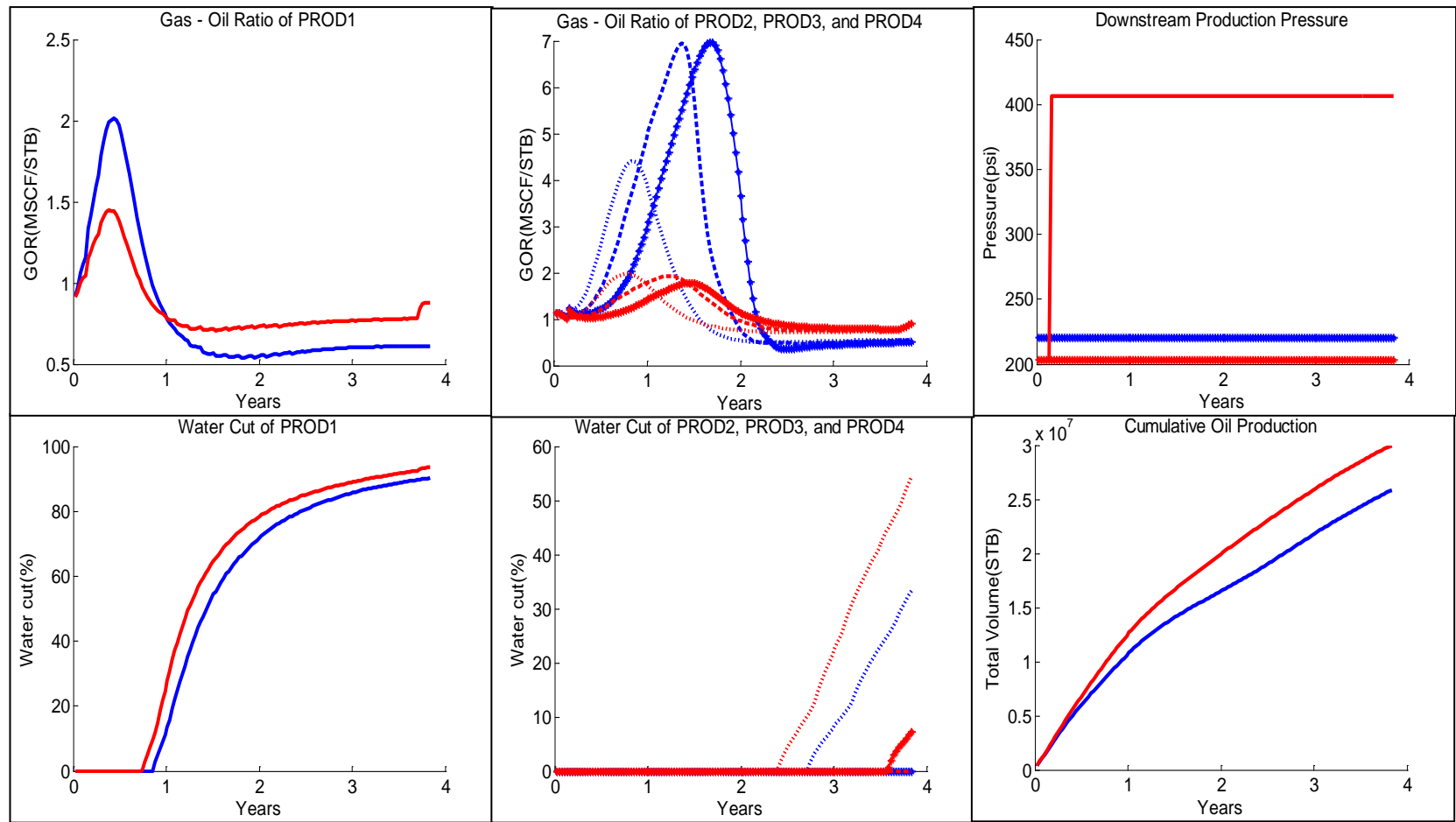


Figure 75: Comparison of base case and optimized case of 5-spots pattern water flooding production profiles using explicit coupling

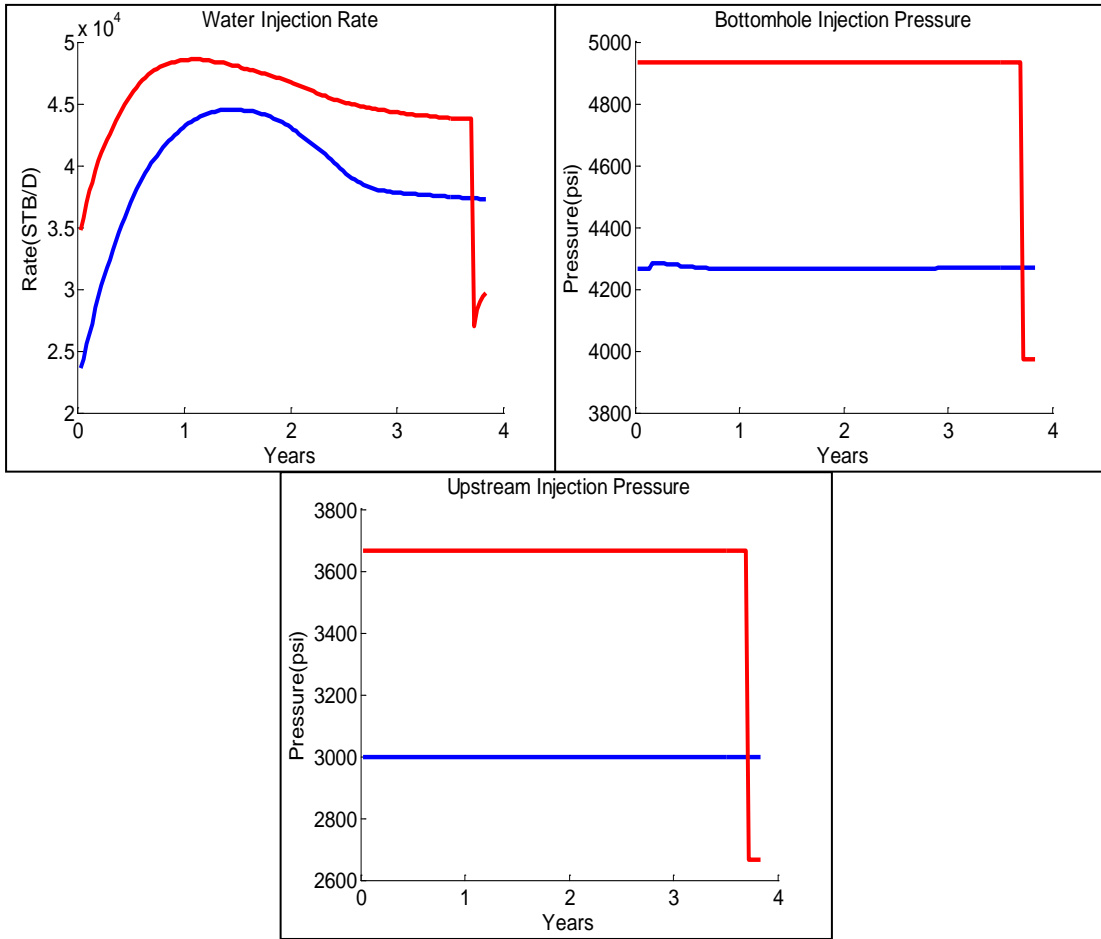


Figure 76: Comparison of base case and optimized case of 5-spots pattern water flooding injection profiles using explicit coupling

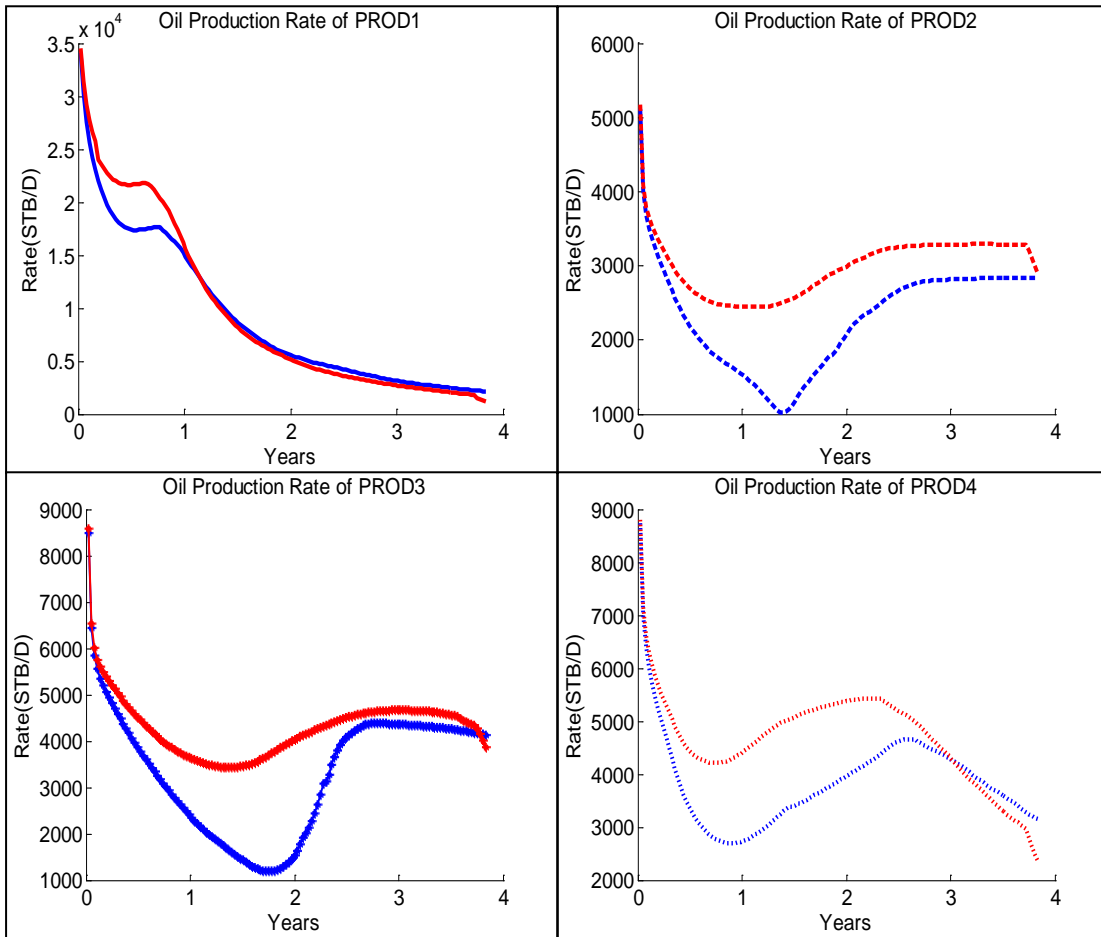


Figure 77: Comparison of base case and optimized case of 5-spots pattern water flooding oil production profiles using implicit coupling

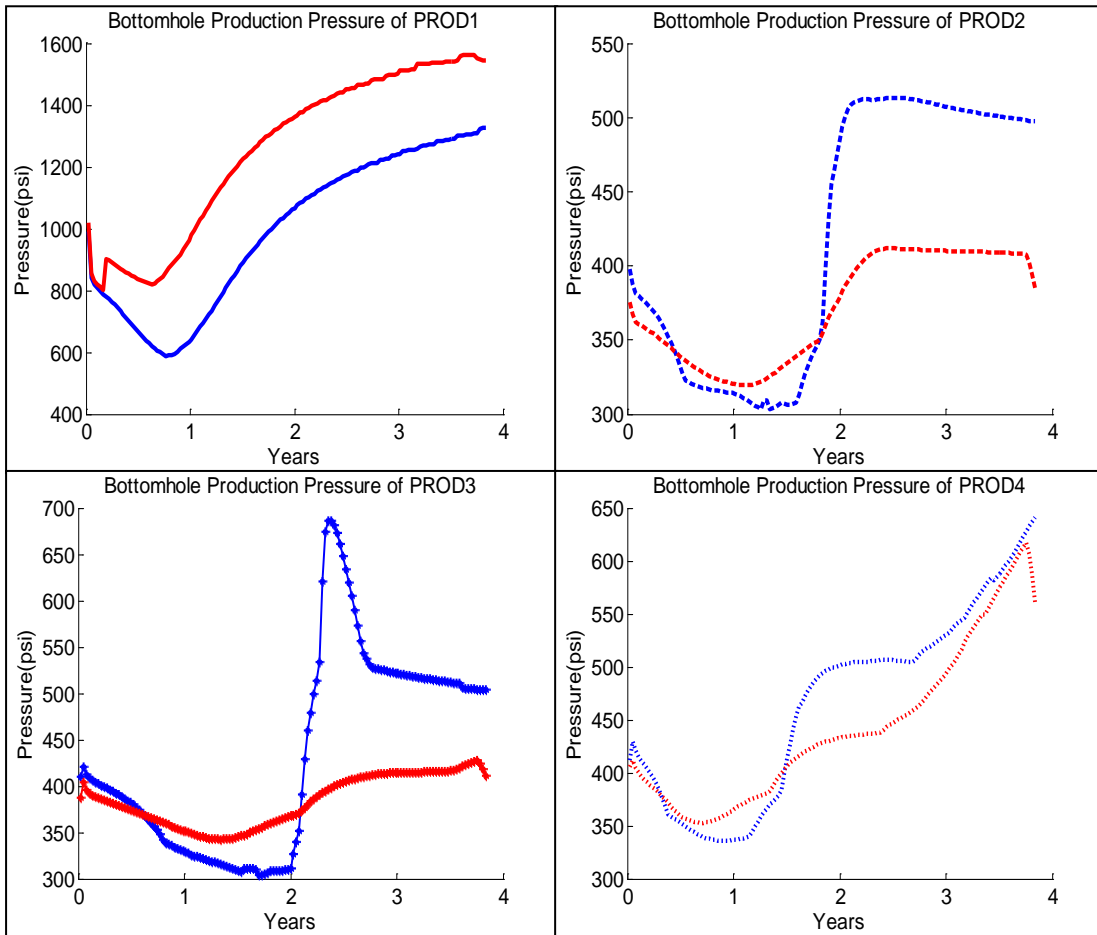


Figure 78: Comparison of base case and optimized case of 5-spots pattern water flooding bottomhole production pressure using implicit coupling

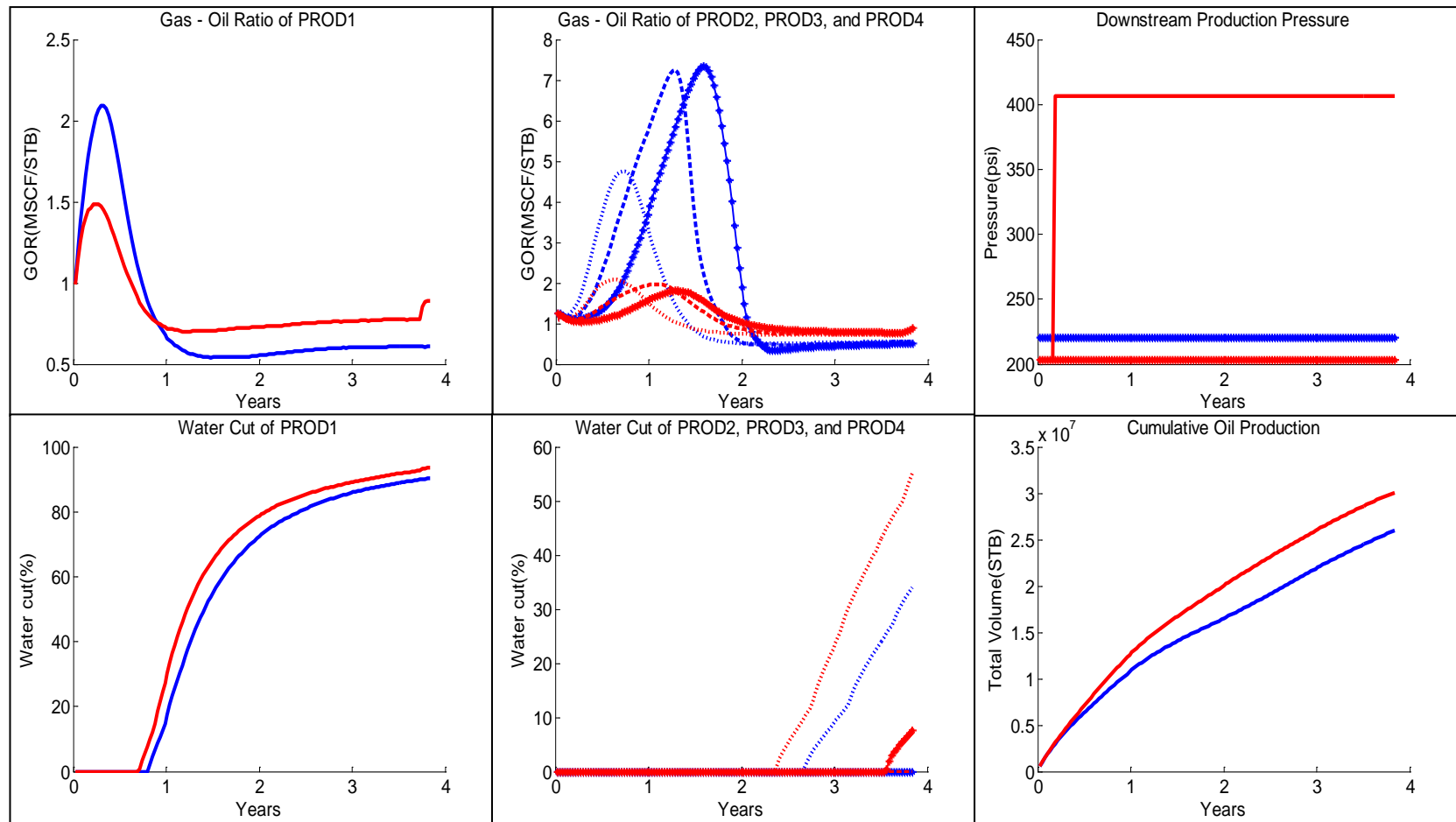


Figure 79: Comparison of base case and optimized case of 5-spots pattern water flooding production profiles using implicit coupling

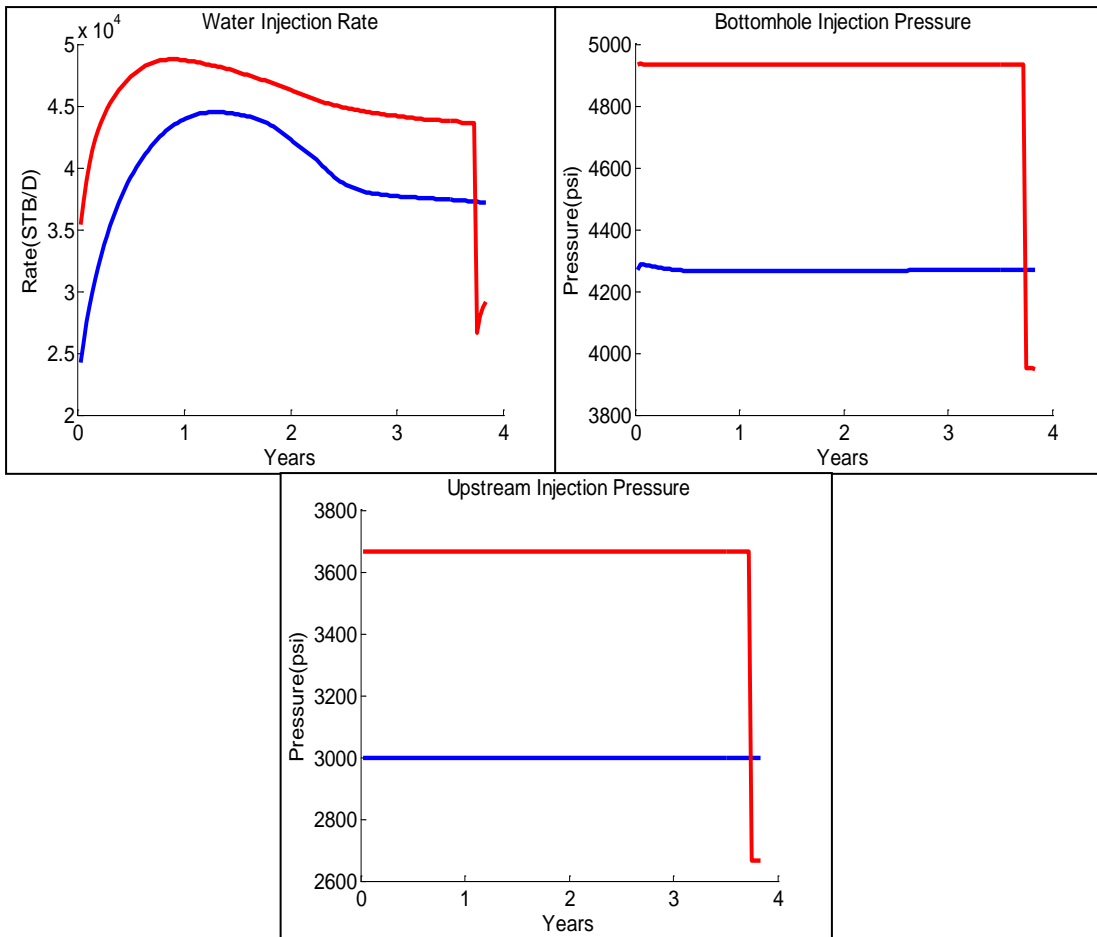


Figure 80: Comparison of base case and optimized case of 5-spots pattern water flooding injection profiles using implicit coupling

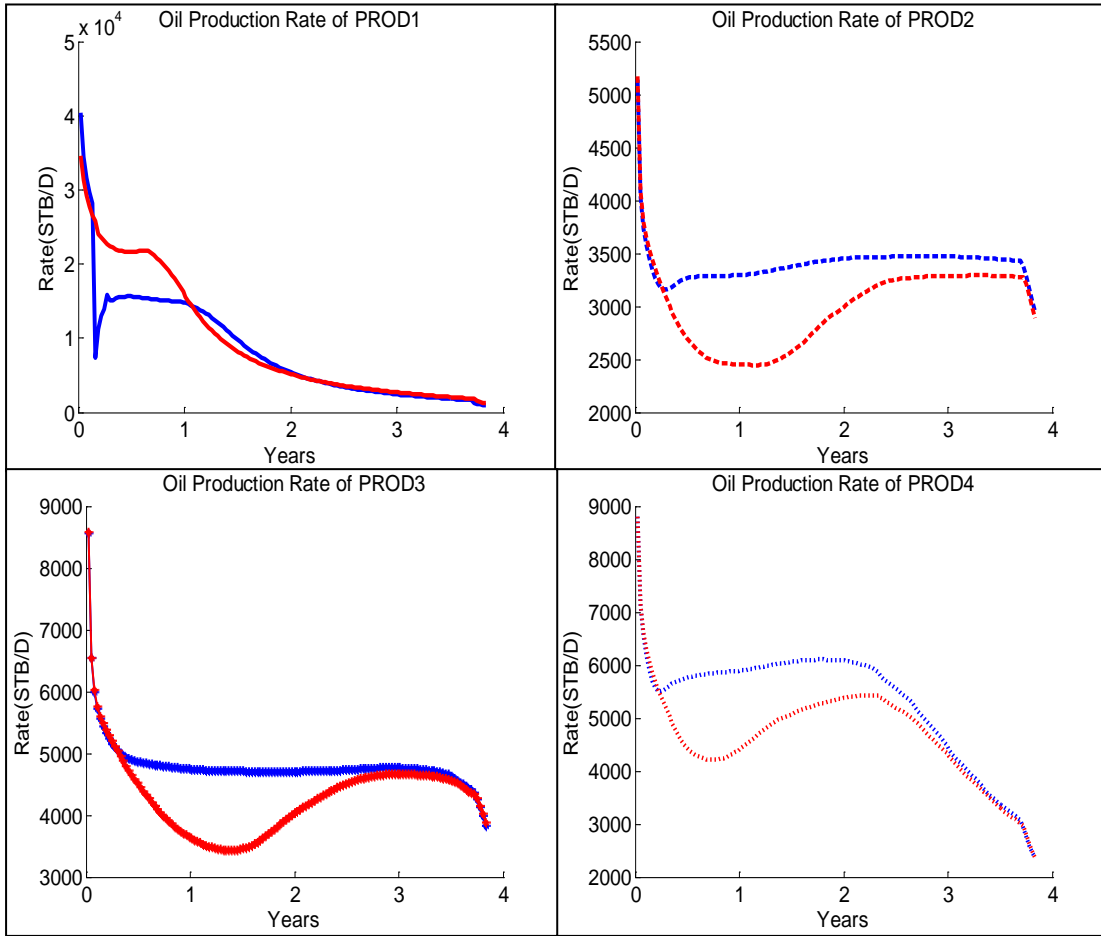


Figure 81: Comparison of no coupled (estimated lower and upper bound) and implicit coupled optimization oil production profiles for the case of 5-spots pattern water flooding

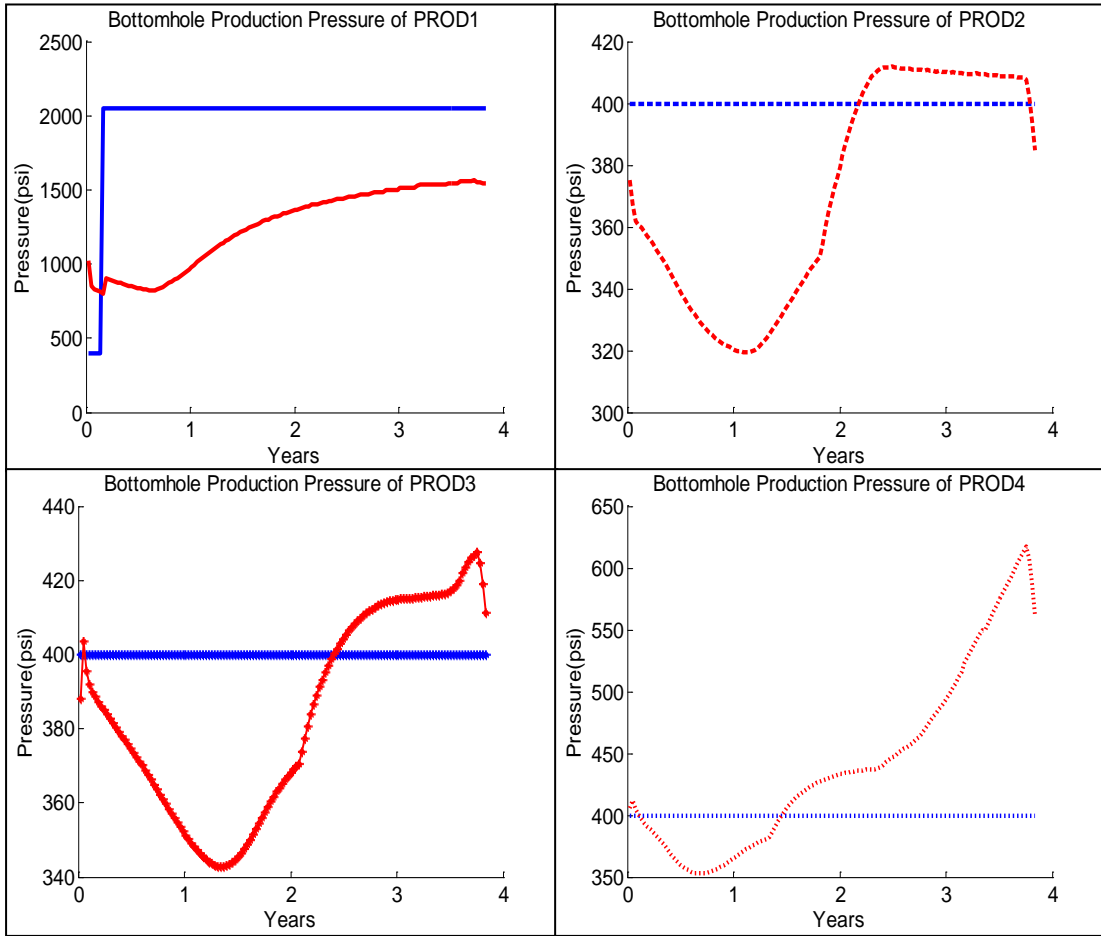


Figure 82: Comparison of no coupled (estimated lower and upper bound) and implicit coupled optimization bottomhole production pressure for 5-spots pattern water flooding

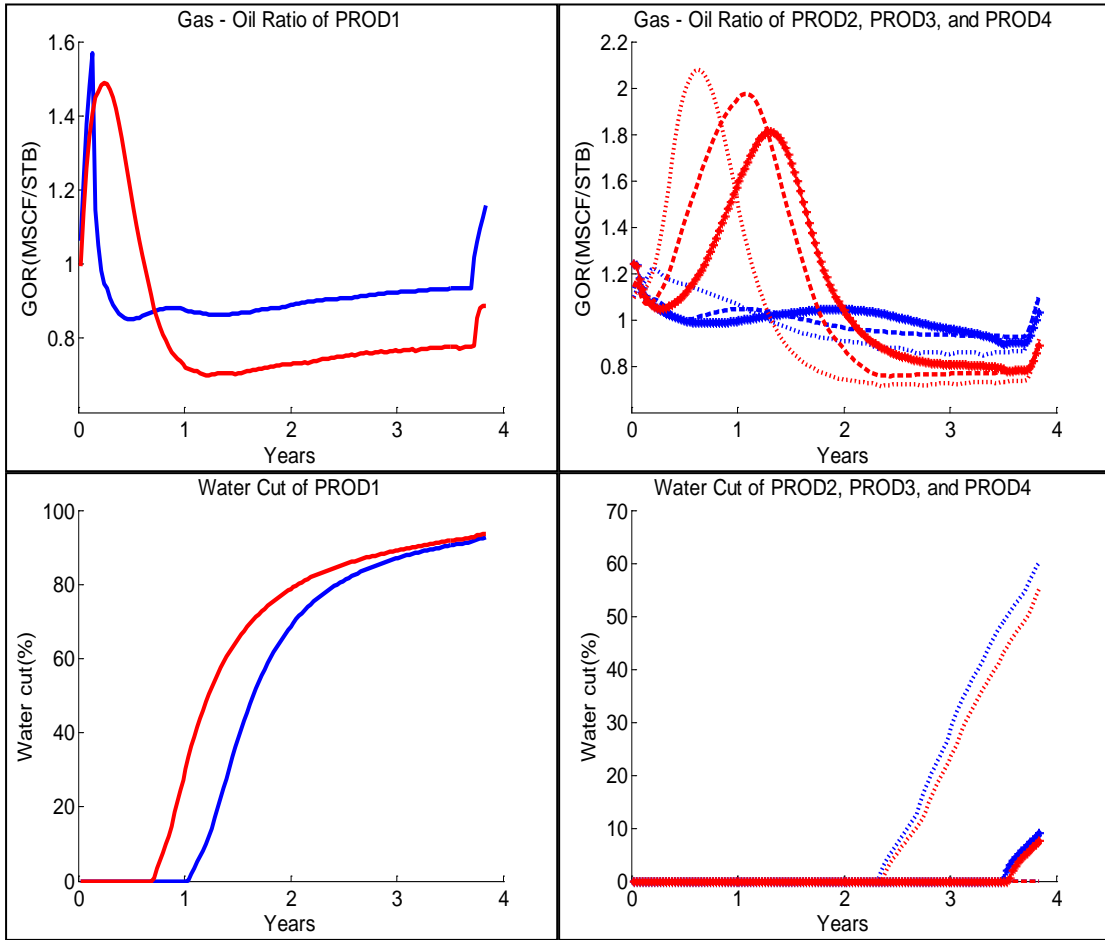


Figure 83: Comparison of no coupled (estimated lower and upper bound) and implicit coupled optimization GOR and water cut for 5-spots pattern water flooding

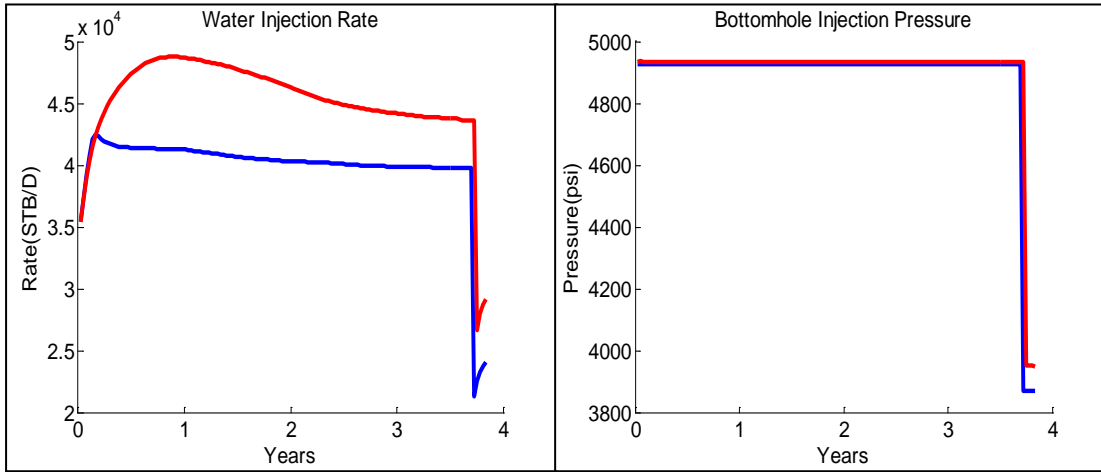


Figure 84: Comparison of no coupled (estimated lower and upper bound) and implicit coupled optimization injection profile for 5-spots pattern water flooding

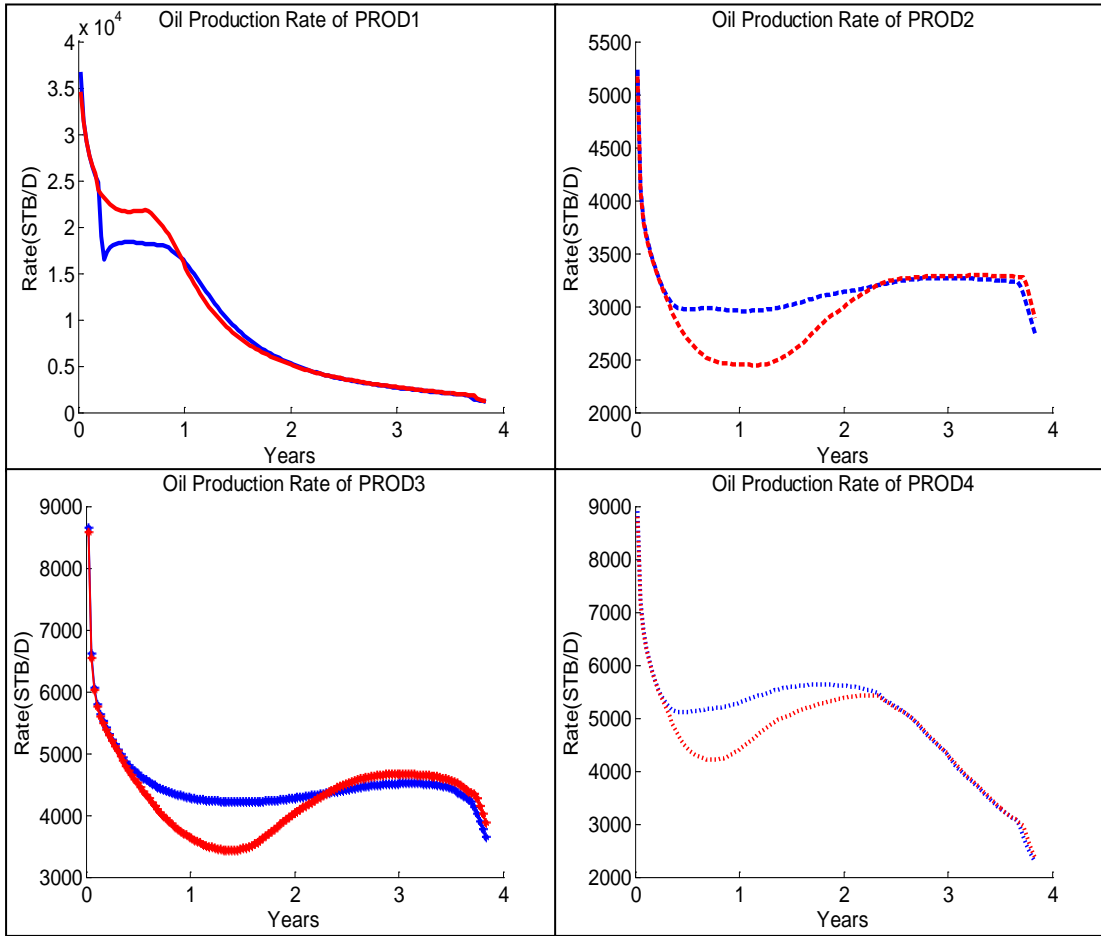


Figure 85: Comparison of no coupled (known lower and upper bound) and implicit coupled optimization oil production profiles for 5-spots pattern water flooding

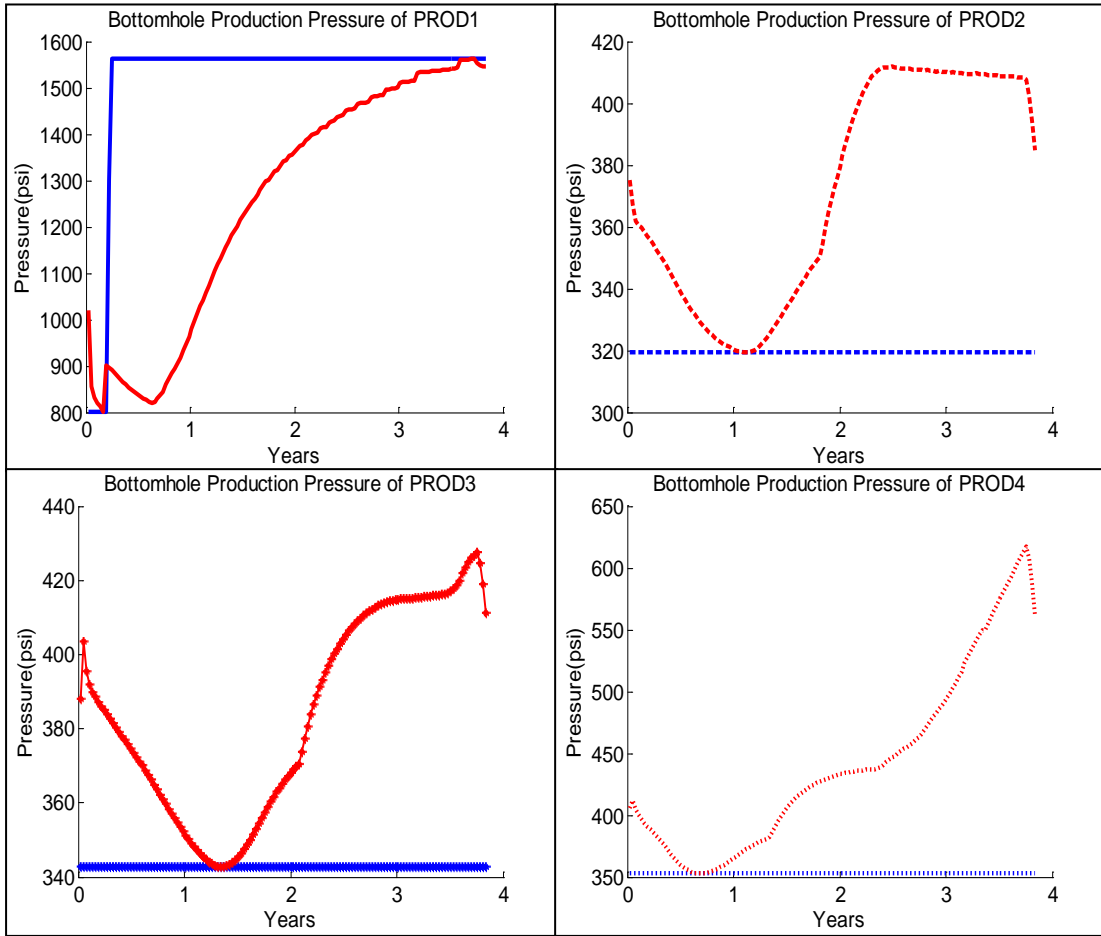


Figure 86: Comparison of no coupled (known lower and upper bound) and implicit coupled optimization bottomhole production pressure for 5-spots pattern water flooding

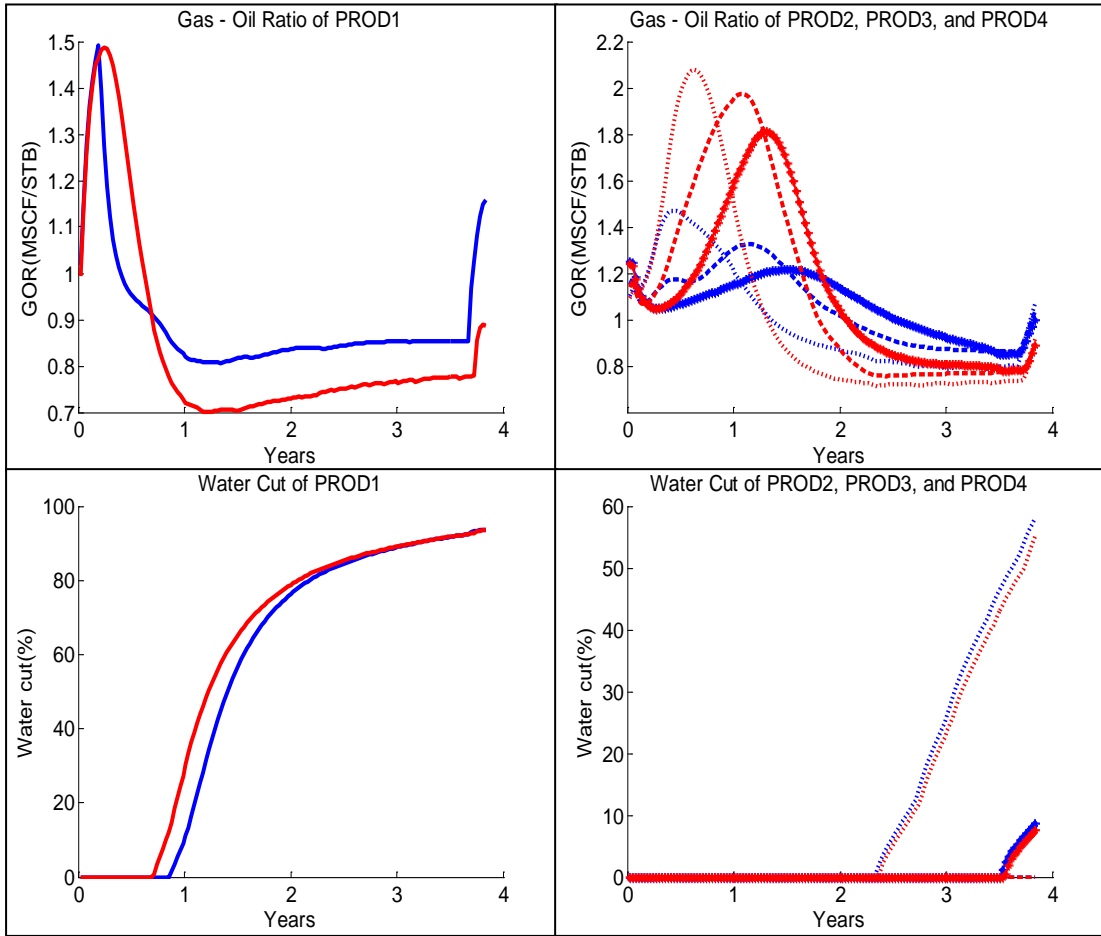


Figure 87: Comparison of no coupled (known lower and upper bound) and implicit coupled optimization GOR and water cut for 5-spots pattern water flooding

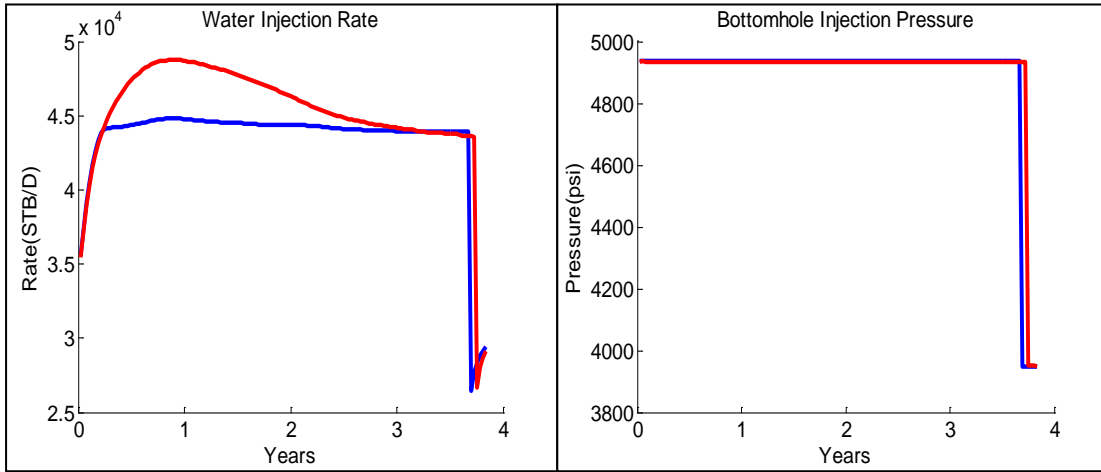


Figure 88: Comparison of no coupled (known lower and upper bound) and implicit coupled optimization water injection profile for 5-spots pattern water flooding

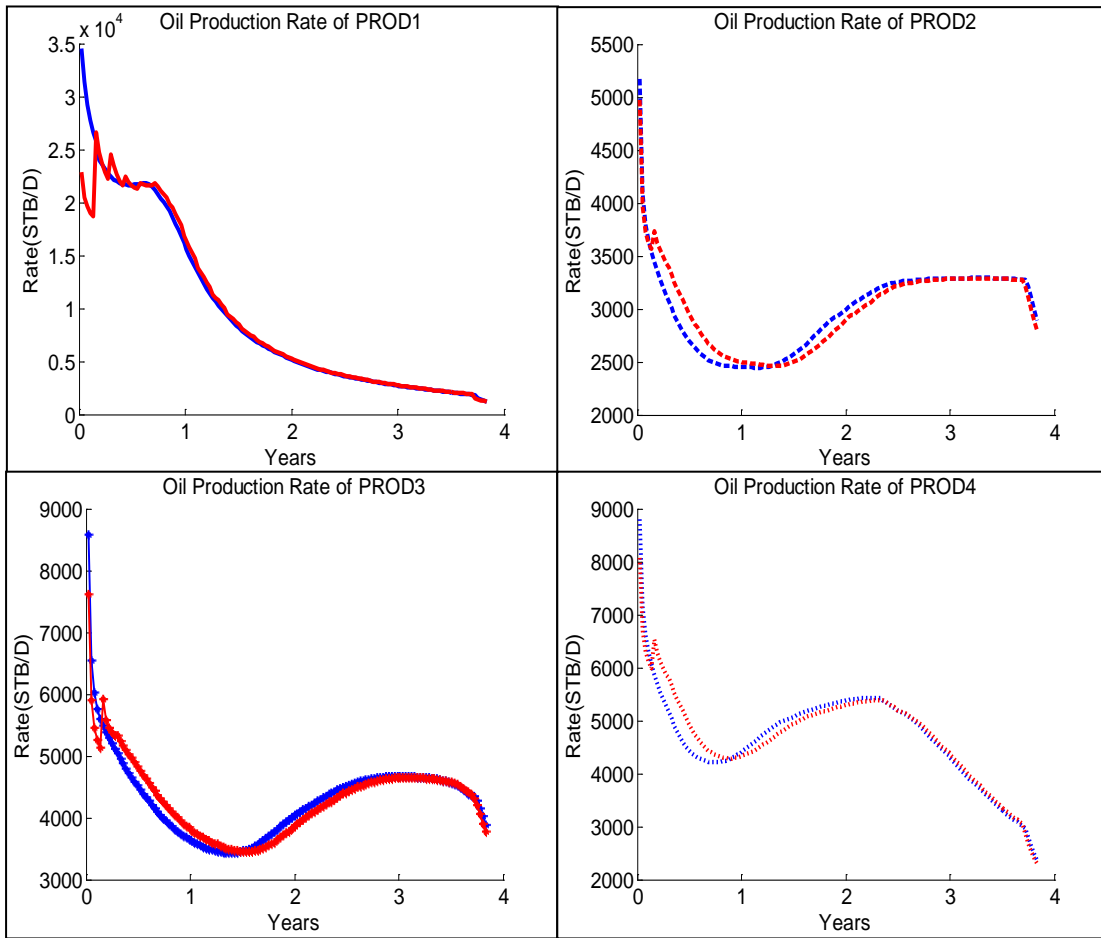


Figure 89: Comparison of explicit coupled and implicit coupled optimization oil production profiles for 5-spots pattern water flooding

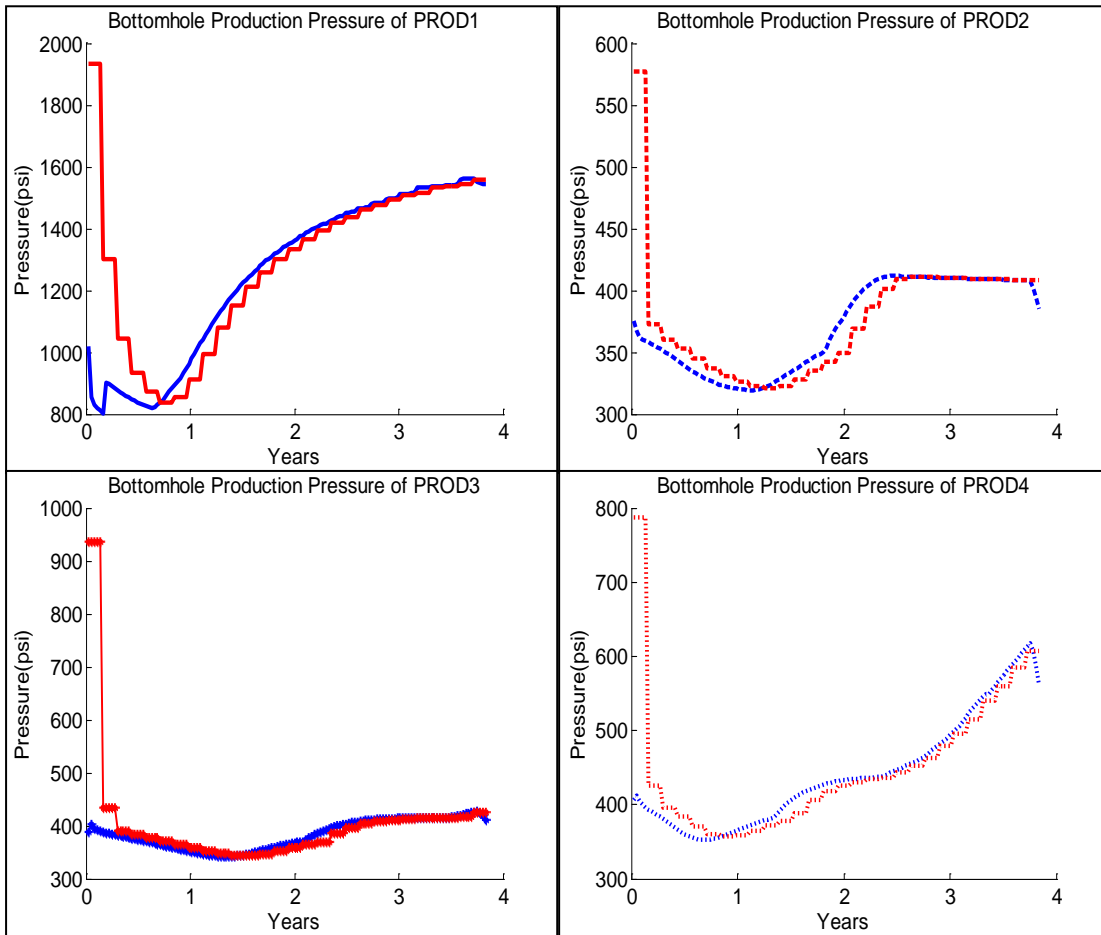


Figure 90: Comparison of explicit coupled and implicit coupled optimization bottomhole production pressure for 5-spots pattern water flooding

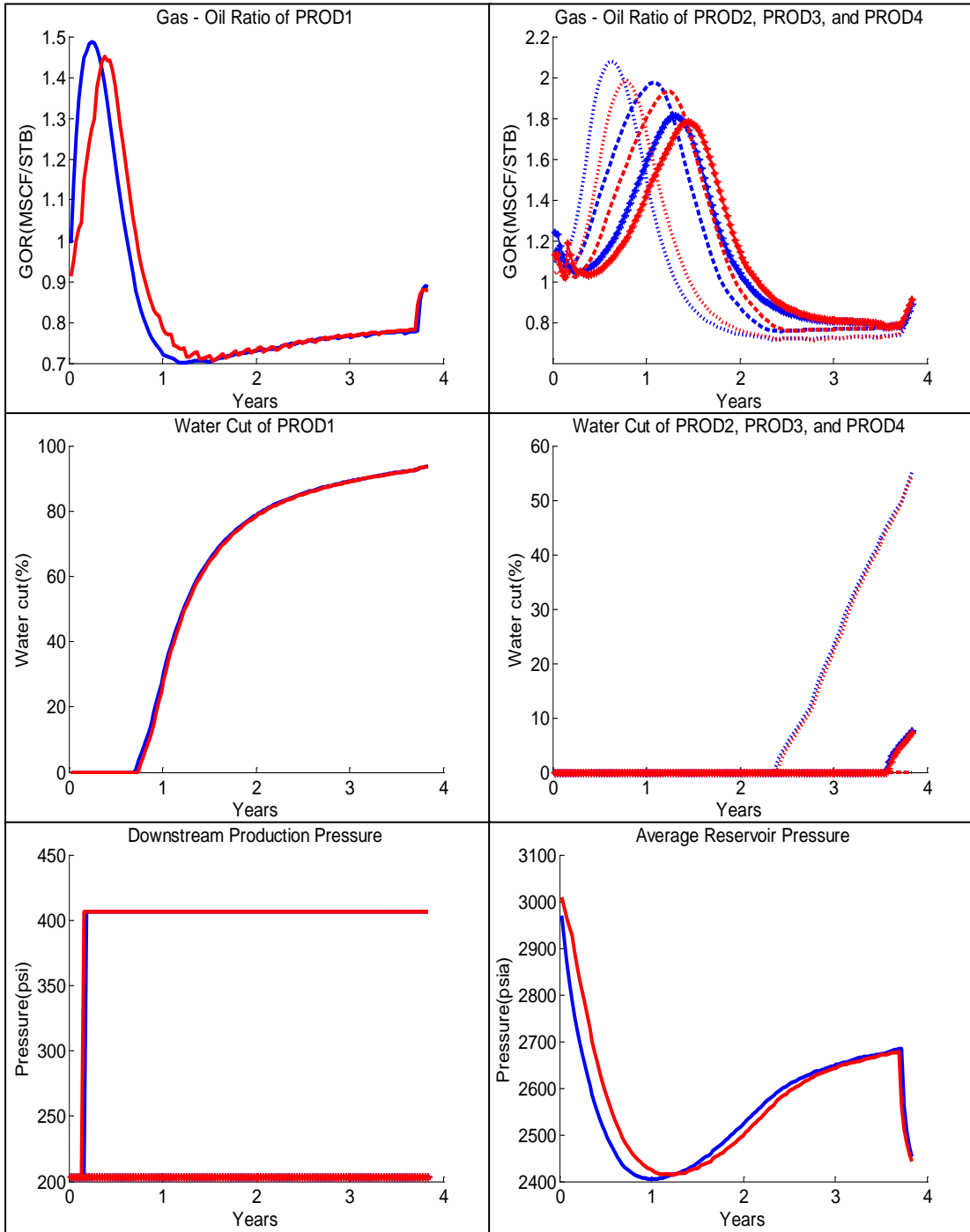


Figure 91: Comparison of explicit coupled and implicit coupled optimization GOR, water cut, and pressure for 5-spots pattern water flooding

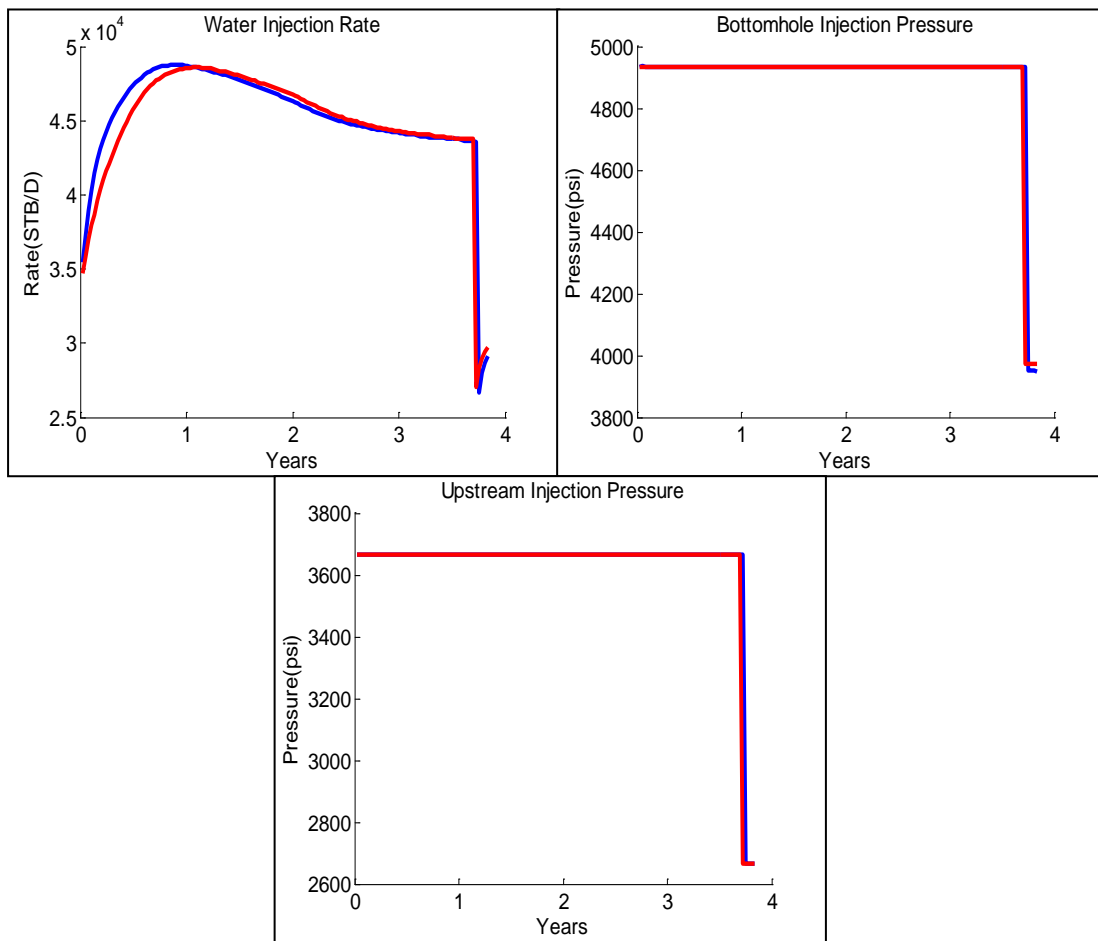


Figure 92: Comparison of explicit coupled and implicit coupled optimization water injection profile for 5-spots pattern water flooding

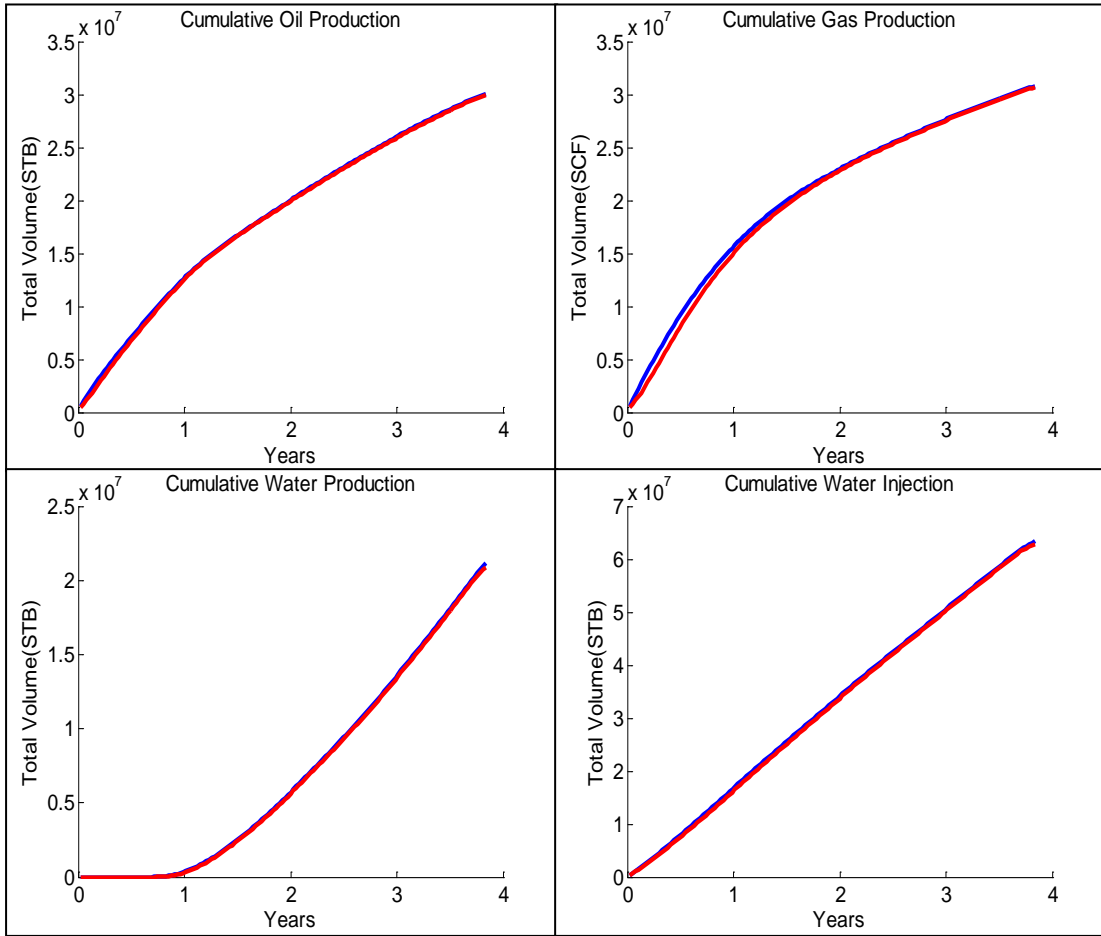


Figure 93: Comparison of explicit coupled and implicit coupled optimization cumulative production and injection volume for 5-spots pattern water flooding

From the result of comparison of explicit coupling and implicit coupling optimization, it shows that for both direct line drive water flooding and 5-spots pattern water flooding cases the upstream injection pressure and downstream production pressure control resulting from using explicit coupling and implicit coupling are quite identical. This leads to an idea to use the upstream injection pressure and bottomhole production pressure control results from production optimization using explicit coupling model and then use the control to run the implicit coupling model to calculate the oil, gas, and water production and water injection profile. The advantage of using the explicit coupling model to do the production optimization instead of implicit coupling is because the explicit coupling model requires less computational effort than implicit coupling model. The Table 21 summarizes the computational time using in production optimization. From the Table 21, we can conclude that the explicit coupling case use less CPU time in production optimization than implicit coupling case about 12-14 %.

Production strategies	Explicit Coupling Case	Implicit Coupling Case
Direct line drive water flooding	2086 sec	2380 sec
5-Spots pattern water flooding	2500 sec	2800 sec

Table 21: Summary of computational time using in production optimization

6.5. Optimization Using Explicit Coupling Model - Prediction Using Implicit Coupling Model

This section will show the result of optimization using explicit coupling model to run the production optimization and implicit coupling model to run the production prediction of direct line drive water flooding and 5-spots pattern water flooding. The optimization using explicit coupling model - Prediction using implicit coupling model method will be called explicit-implicit coupled optimization.

6.5.1. Direct Line Drive Water Flooding

The Figures 94 and 95 show the comparison of explicit-implicit coupled and implicit coupled optimization production profiles and injection profiles for direct line drive water flooding. The blue line represents the case of implicit coupled optimization while the red line represents explicit-implicit coupled optimization. It can be seen that there is difference in the timing that the downstream production pressure and upstream injection pressure is changed from maximum value to minimum value. However, it causes just only small impact on overall production and injection profile. It can be said that the production and injection profiles of the two different coupling cases are almost identical. The Figure 96 shows that cumulative production & injection and average reservoir pressure of the two different coupling schemes are also identical. The NPV of explicit-implicit coupled optimization is about 11.2 billion USD which is identical to optimized NPV of implicit coupling.

6.5.2. 5-Spots Pattern Water Flooding

The comparison of explicit-implicit coupled and implicit coupled optimization production profiles and injection profiles for 5-spots pattern water flooding can be found in Figures 97, 98, 99 and 100. The blue line represents the case of implicit coupled optimization while the red line represents explicit-implicit coupled optimization. The oil production profiles and bottomhole production pressure profiles of each production wells are shown in the Figures 97 and 98 which show no difference between the two coupling cases. Moreover, the gas-oil ratio, water cut, average reservoir pressure and water injection profiles of the two coupling cases are very similar. This because the control of explicit-implicit coupled and implicit coupled optimization is pretty much the same. The NPV of explicit-implicit coupled optimization is about 26.27 billion USD and it is identical to optimized NPV of implicit coupled case.

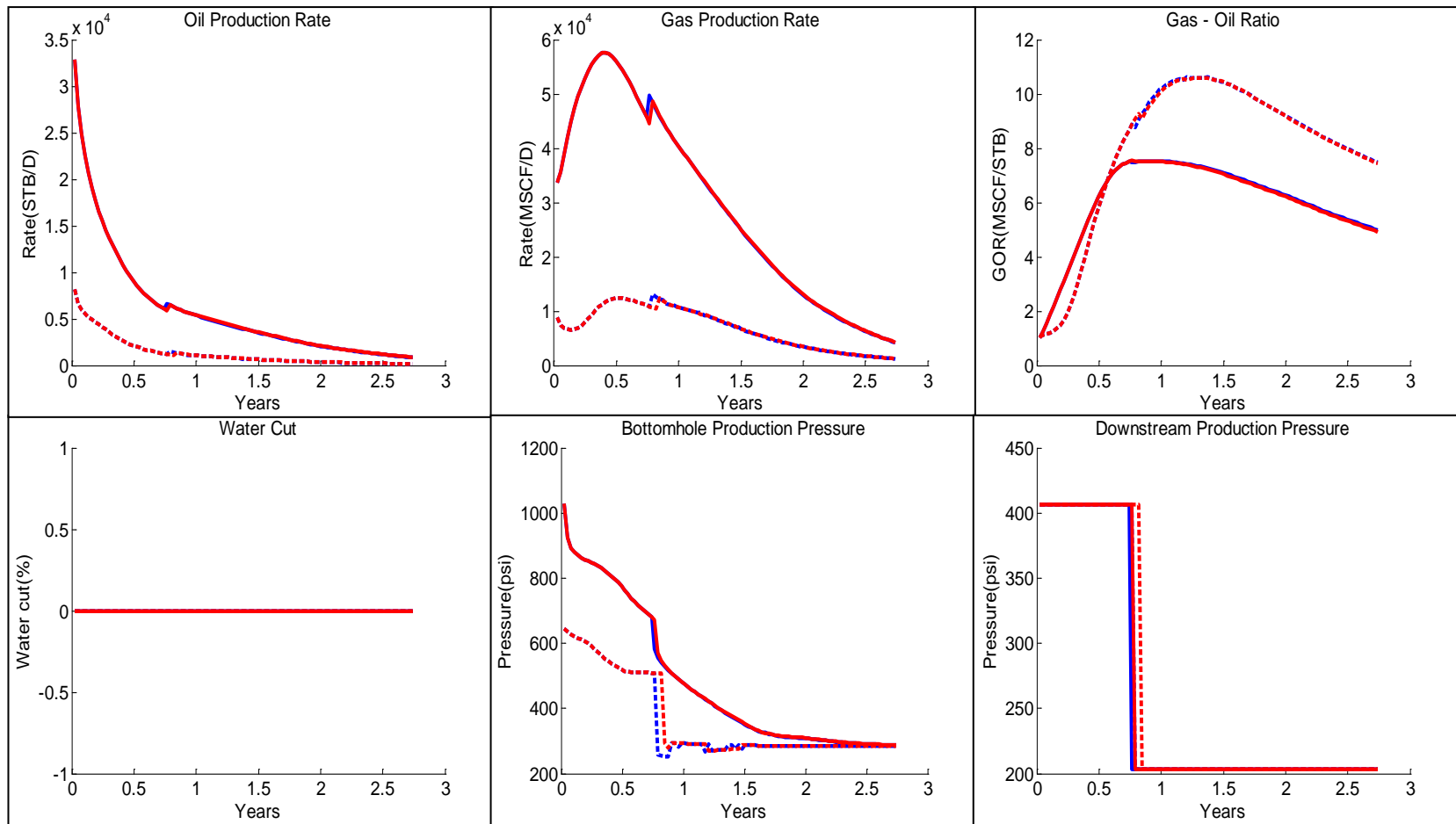


Figure 94: Comparison of explicit-implicit coupled and implicit coupled optimization production profiles for the case of direct line drive water flooding

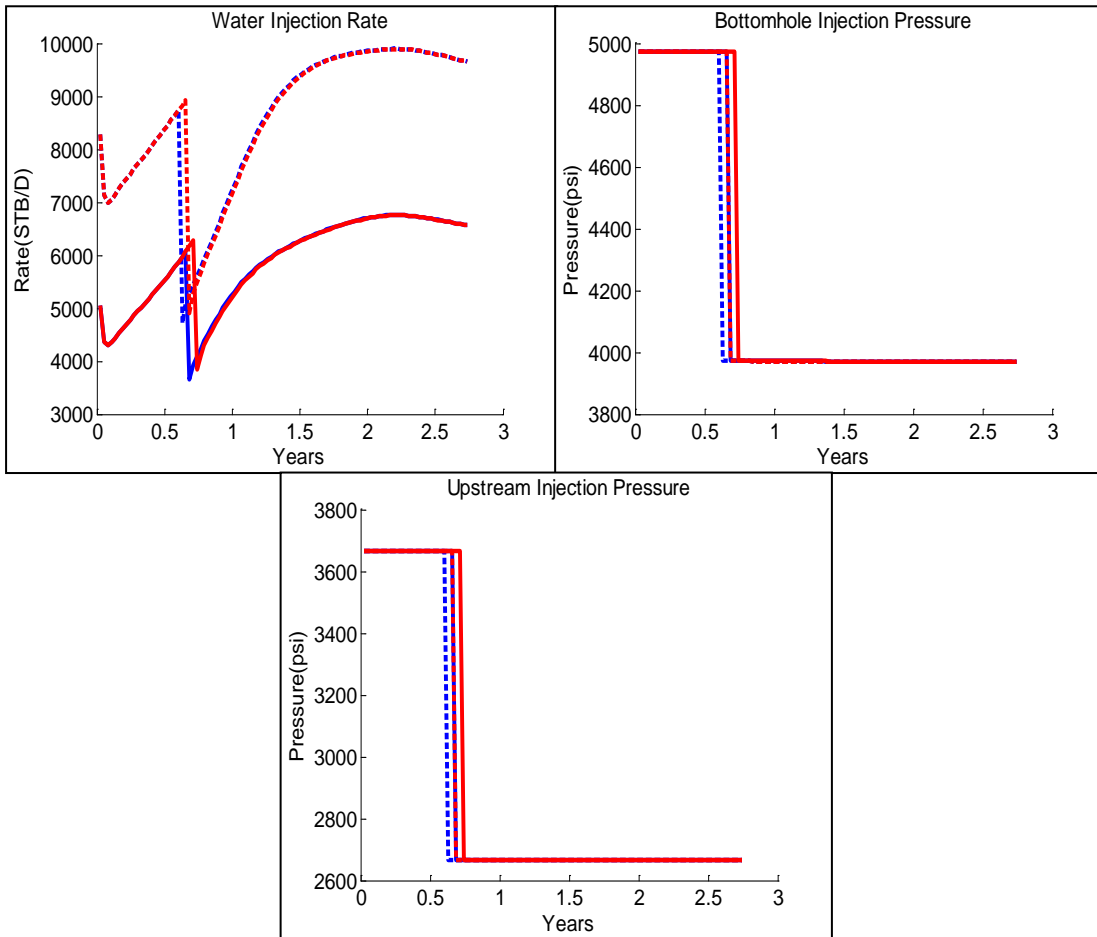


Figure 95: Comparison of explicit-implicit coupled and implicit coupled optimization injection profiles for the case of direct line drive water flooding

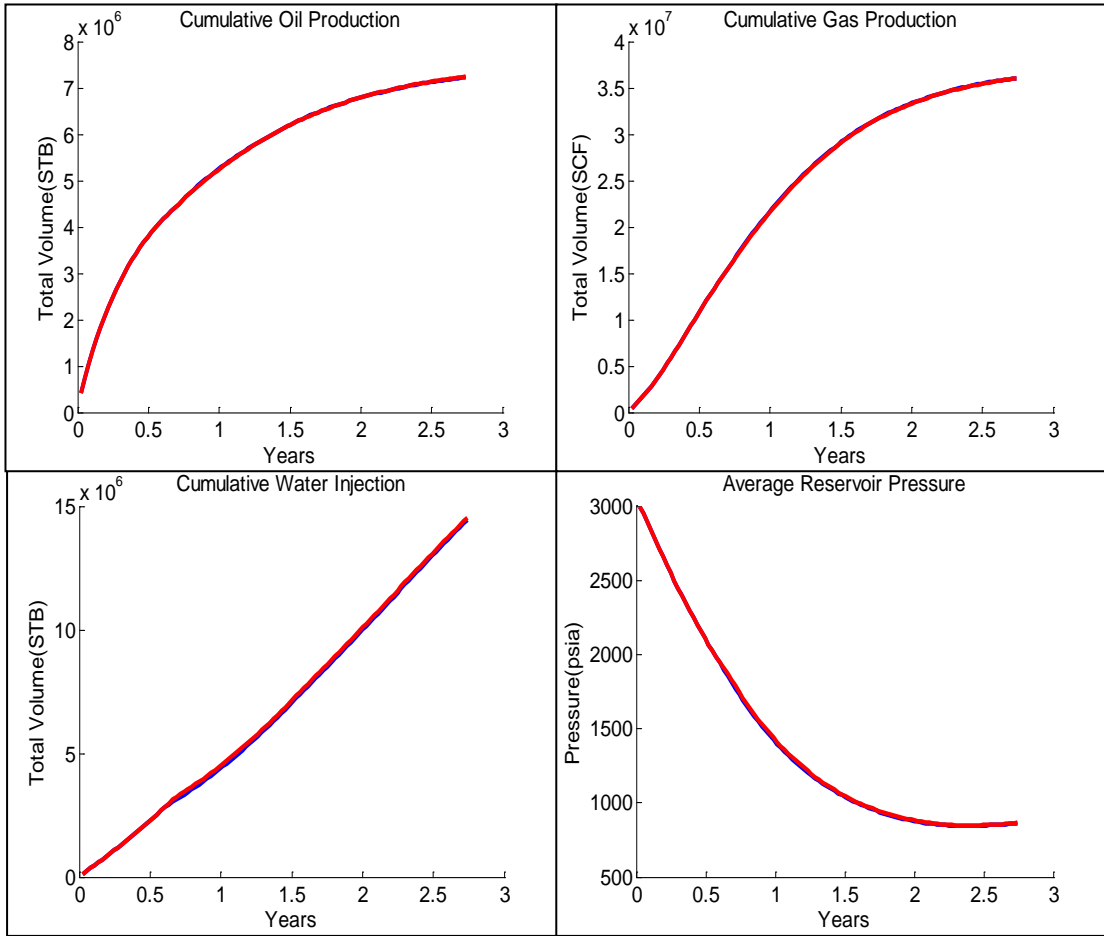


Figure 96: Comparison of explicit-implicit coupled and implicit coupled cumulative production & injection volume and average reservoir pressure for the case of direct line drive water flooding

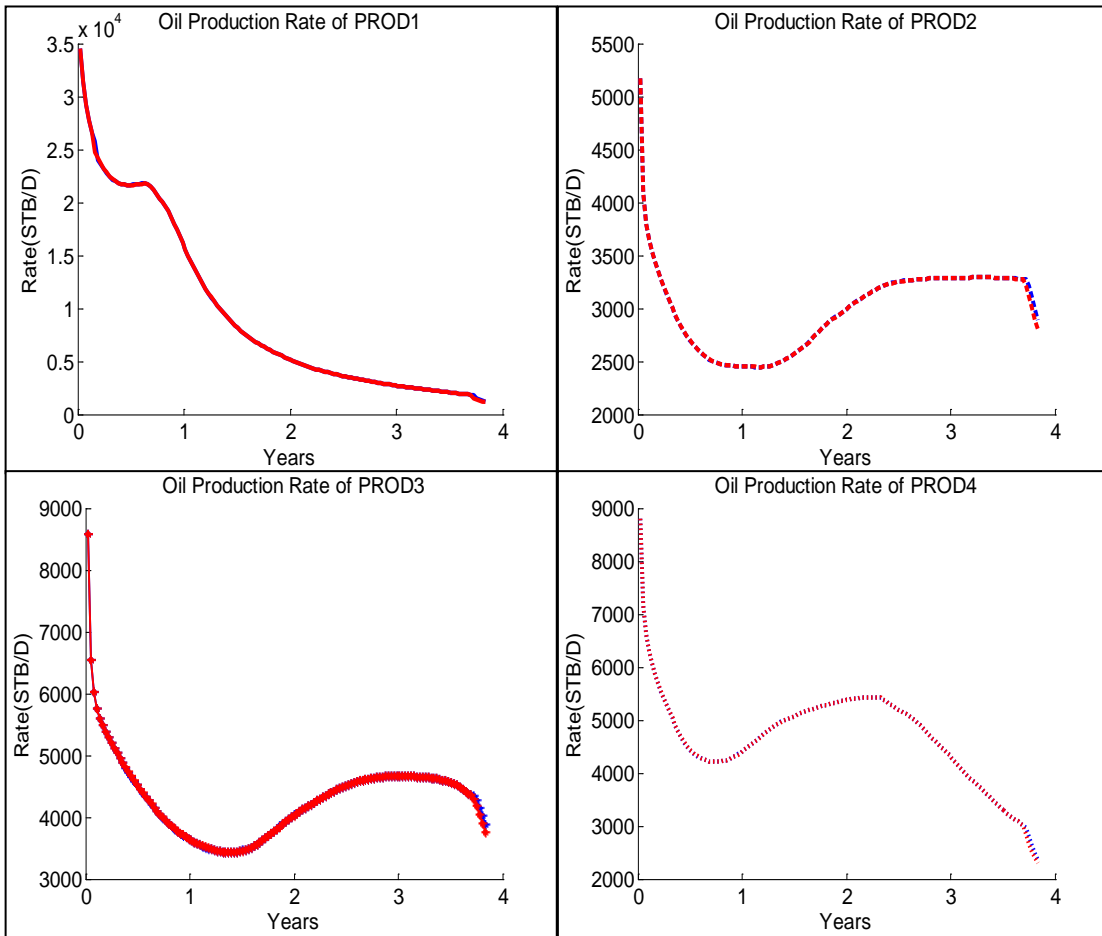


Figure 97: Comparison of explicit-implicit coupled and implicit coupled optimization oil production profiles for the case of 5-spots pattern water flooding

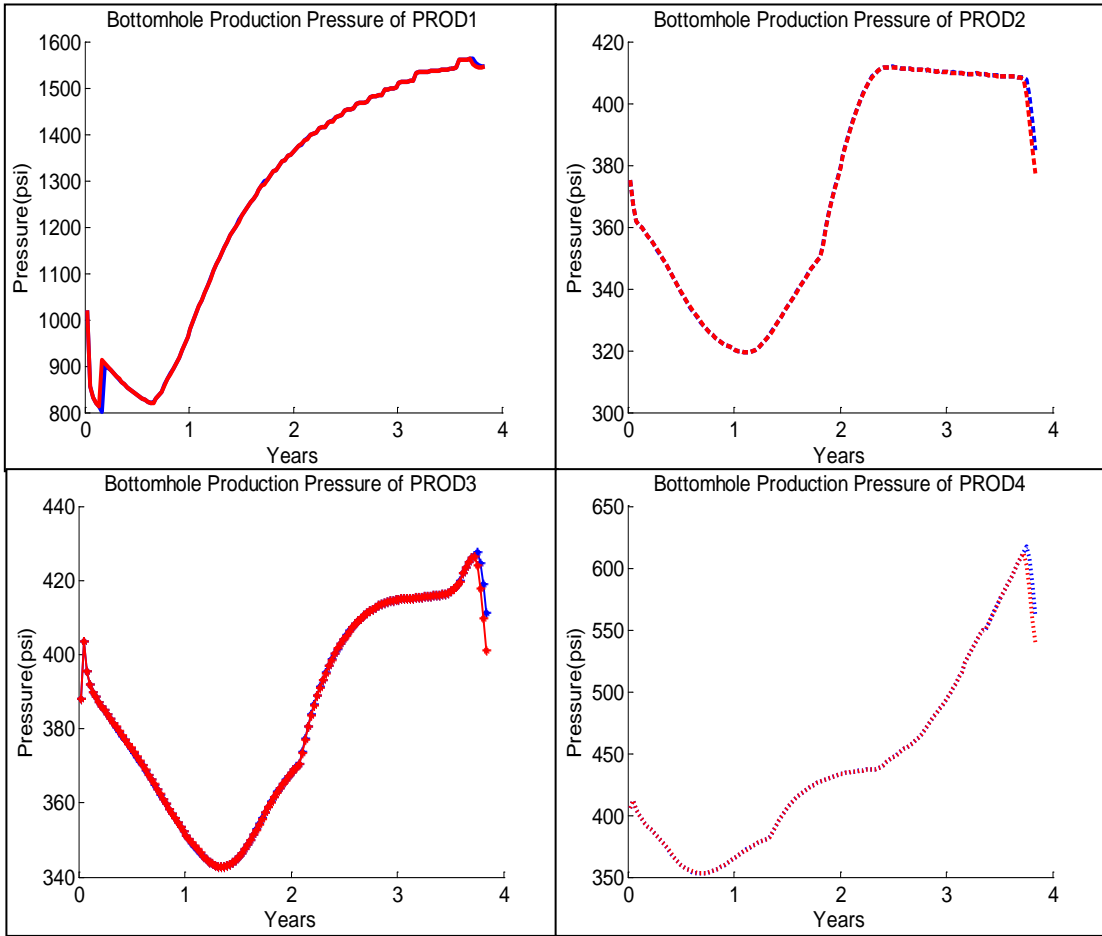


Figure 98: Comparison of explicit-implicit coupled and implicit coupled optimization bottomhole production pressure profiles for the case of 5-spots pattern water flooding

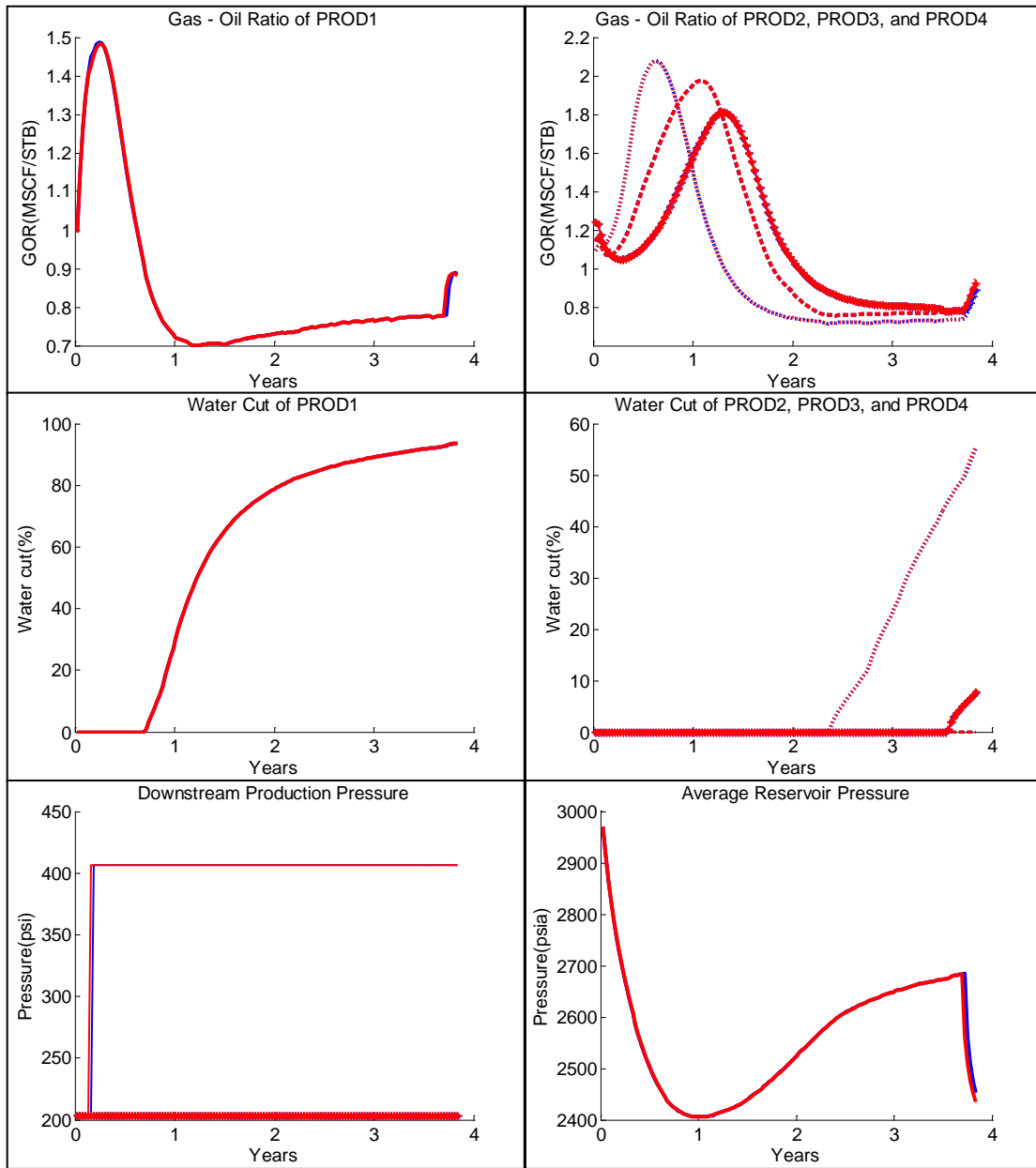


Figure 99: Comparison of explicit-implicit coupled and implicit coupled optimization production profiles for the case 5-spots pattern water flooding

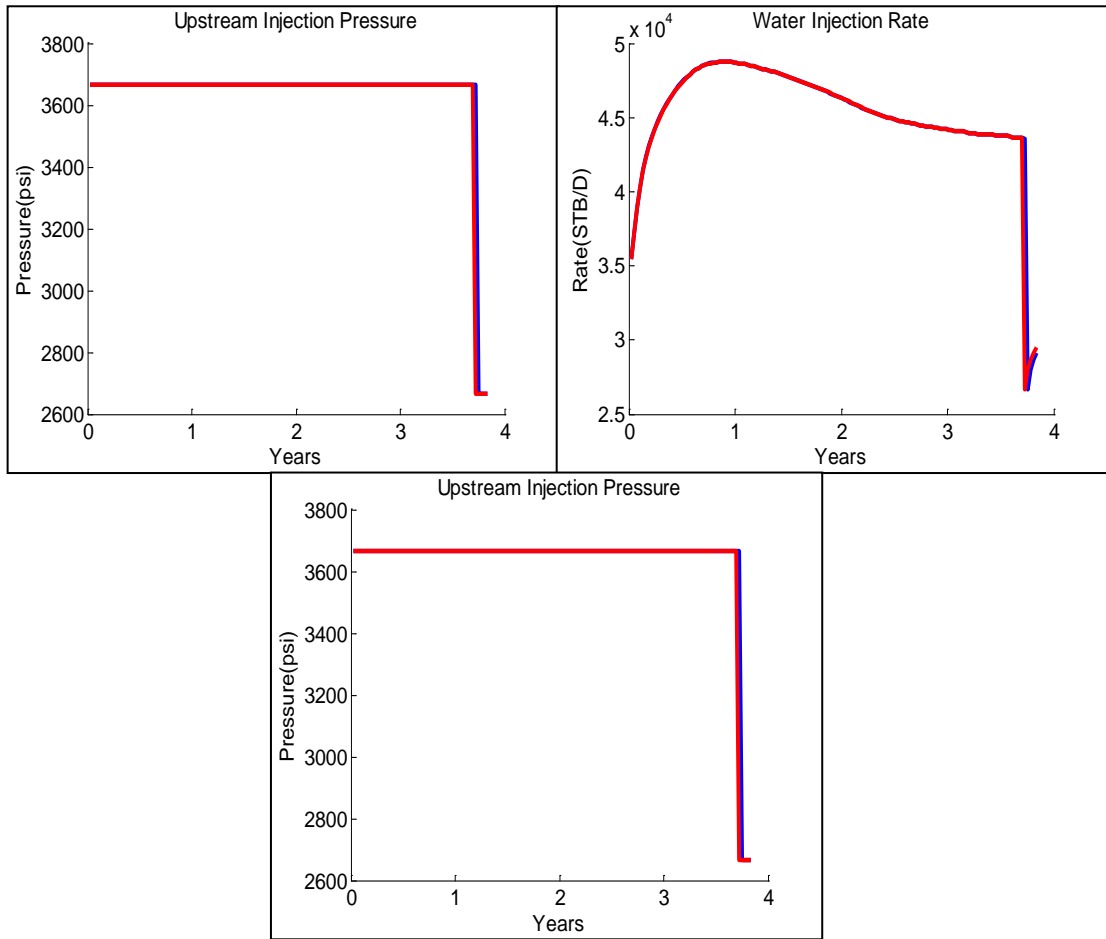


Figure 100: Comparison of explicit-implicit coupled and implicit coupled optimization injection profiles for the case 5-spots pattern water flooding

7. CONCLUSIONS AND RECOMENDATIONS

7.1 Summary

In standard framework of production optimization, the process aims to optimize the system of production that is scoped at the reservoir only. However, in practice, the system of production is the combination of reservoir and production facility. Hence, the understanding of fluid flow characteristic in the reservoir thru the flow in pipe is the one of important element in production optimization. This can be taken into account in the production optimization process by using coupled surface and subsurface model.

Normally, the surface and subsurface flow are modeled separately. However, in the past, there are several research study related to coupling surface and subsurface model. The research can be divided into two main groups. The first group is the research about advanced well modeling and another group is the coupled surface and subsurface model research. The detail of each research can be found in the CHAPTER 2.

In oil & gas industry, there are three main methods to couple surface and subsurface model; explicit coupling, implicit coupling, and fully implicit coupling. The procedure for explicit and implicit coupling is quite similar. The major difference between explicit coupling and implicit coupling is that the explicit coupling balances surface and subsurface model at the time step level while the implicit coupling do it at Newton's iteration level. Another approach to do coupling is the fully implicit coupling. The fully implicit coupling procedure is completely different from the previous two type of coupling such that the two systems of equations of surface and subsurface flow are

formulated as a single system of equation and it will be solved simultaneously in every Newton's iteration.

In order to investigate the coupling mechanism, we divide this research into two main phases. In the first phase of the study, we investigated the so-called coupling using the forward model whereas in the 2nd phase we attached the forward model into an optimization framework. We used several tools to investigate the various coupling mechanism in surface/subsurface dynamics. We started with the ECLIPSE100 with Network Option to study the effect of the coupling mechanism on the forward problem, that is, the reservoir simulation problem. However, we switched to the MATLAB® based reservoir simulation toolbox (MRST) for the production optimization process. To this end, we modified several of the function in MRST to suit our framework.

In the 1st phase of study, the coupling schemes that have been considered here are the explicit coupling for every time step, explicit coupling for every fixed period of time and implicit coupling. The results show in section 4 that most of the cases used in the implicit coupling and explicit coupling for every time step give the same production and injection profile. The results of the first phase also show that lived oil PVT clearly yield difference result between explicit coupling for every fixed period of time and implicit coupling. In addition, comparing between homogeneous low permeability and high permeability, the difference of production and injection profiles among the different coupling scheme of the high permeability case are more obvious than the case of low permeability. In terms of heterogeneity effect, the reservoir tends to impact more the

production and injection profile of different coupling scheme than the homogeneous reservoir.

In the second phase of this study, the modified MRST is used to run production optimization on selected fluid and reservoir properties and production scenarios. From the first phase of this study, the reservoir properties and fluid properties that give clear difference between explicit and implicit coupling scheme are heterogeneous high permeability reservoir and lived oil PVT fluid. Consequently, in order to investigate how the coupling schemes can affect the production optimization result, the reservoir that has heterogeneity and high permeability with lived oil PVT is selected. The production scenarios considered here are direct line drive water flooding and 5-spots pattern water flooding. For both production scenario cases, there is at least one production well that is deliberately locate in the high permeability zone in order to emphasize the effect of the high permeability.

The results for production optimization using explicit and implicit couplings for direct line drive water, and 5-spots pattern water flooding show that the gradient-based optimization and gradient calculation using adjoint model can improve the economical parameters, namely NPV by improving the upstream injection pressure and downstream production pressure controls.

The production optimization using the standalone subsurface model and coupled surface and subsurface model using implicit coupling scheme are also ran on both production scenarios in order to investigate the result of production optimization with and without surface facility model response. The results show that the production

optimization without consideration of surface facility model response gives an optimistic optimization result because the production optimization by using bottomhole production/injection pressure as control does not consider the effect of production and injection fluid such as gas-oil ratio and water cut. This leads to unrealistic bottomhole production pressure and inaccurate estimation of lower and upper bound of bottomhole production and injection pressure.

The optimized controls for the direct line drive water flooding of explicit and implicit coupling are quite the same. There is a small difference in the timing that the upstream injection pressure and downstream production pressure changed from maximum value to minimum value. However, the bottomhole pressures of explicit and implicit coupling are not completely inline. The bottomhole production pressure of explicit case is higher than implicit case in the early period of production as surface and subsurface model are not fully balanced. After that the bottomhole production pressure of the explicit case still higher than the implicit case but they have quite the same trend because gas-oil ratio profile which influence the outflow performance relationship and reservoir pressure which influence the inflow performance relationship of the both implicit and explicit cases are relatively similar. In general, it can be said that not only the optimized injection and production profile but also the optimized NPV from implicit and explicit coupling are fairly the same for the case that water flooding has small influence on pressure maintenance.

For the case of the 5-spots pattern water flooding, there is just a small difference in optimized control about the timing of changing in term of maximum and minimum

pressure control. This problem represents the case that water injection has a high influence on reservoir pressure. The difference of injection profile causes the shifting of reservoir pressure and gas-oil ratio profiles between implicit and explicit coupling cases. Since gas-oil ratio profiles influence the outflow performance relationship, the bottomhole production pressures of implicit and explicit coupling cases are also shifted and resulting in different oil production profile. Although the production profiles seem to be different, the optimized NPV from explicit and implicit coupling case has a small difference.

Although, in the case that water flooding plays a major role in the reservoir pressure support (5-spots pattern water flooding), the different coupling scheme can affect the production and injection profile. However, the difference is not significant enough to effect the value of optimized NPV. The rationale for this is that the NPV is a function of the production and injection volume. There is a strong relationship between reservoir pressure and production/ injection volume. It can be seen from the comparison of average reservoir pressure of implicit and explicit coupling in two different water flooding strategies that the pressure from the two coupling scheme is different in the early and middle time of production. However, the pressure is getting closer in the last time step. When the reservoir pressure is getting closer, it implies that the total mass in and out of the reservoir of the two cases is supposed to be approximately the same. Hence, the total production and injection volume is supposed to be the same and resulting in indifferent optimized NPV.

From the comparison of implicit and explicit coupling optimization result, it can be seen that the optimized controls from implicit and explicit coupling for both production scenarios are somewhat the same. This leads to an idea of using explicit coupling model for production optimization and then uses the optimized controls to run the prediction by using implicit coupling model in order to reduce the computational time but still get an accurate production & injection profiles and optimal NPV. The study shows that the optimization using explicit coupling - prediction using implicit coupling results are identical to the optimization results using implicit coupling.

7.2 Future Works

In the next paragraphs, a few suggestions will be given regarding the future work of this project.

In order to test the findings of this research to a more realistic scenario, real field data and more complete reservoir model need to be incorporated in to the optimization framework. Furthermore, in the real production field, the production scenario and constraint might be more complicated from the production scenarios and constraint that have been considered here. The production scenarios that we consider here is just a single unit of water flooding pattern while in a more realistic field, the production scenario might be consist of multiple unit of water flooding pattern. In an actual production field, the production constraint might be involve multiple objective such as pressure limit and maximum allowable water cut.

This research can be developed further by considering other parameters in the coupling mechanism. For example the type of balancing algorithm and point of coupling can be changed during simulation. As mentioned in section 5, the balancing algorithm that we used here is the Fast PI balancing algorithm which represents the IPR by linear model. Apart from Fast PI balancing algorithm, there are several balancing algorithm that calculate IPR differently. In terms of point of coupling, the point of coupling used here is at bottomhole of the wells while in practice, the point of coupling can be varied from bottomhole to the tubing head of the wells, depending on the suitability of the application and availability of the software. By including these two coupling parameters into further studies, we strongly believe that it will lead to more comprehensive conclusion of the research.

REFERENCES

- Beggs, H.D. 2003. *Production Optimization Using Nodal Analysis*, second edition. Tulsa, Oklahoma: OGCI and Petroskills Publication.
- Chen, Z., Huan, G., and Ma, Y. 2006. *Computational Methods for Multiphase Flows in Porous Media*, Dallas, Texas: Society for Industrial and Applied Mathematic
- Dempsey, J.R., Patterson, J.K., Coats, K.H. et al. 1971. An Efficient Model for Evaluating Gas Field Gathering System Design. *SPE Journal of Petroleum Technology* **23** (9): 1067-1073. 00003161.
- Economides, M.J., Hill, A.D., and Ehlig-Economides, C., 1993. *Petroleum Production Systems*, Upper Saddle River, New Jersey: Prentice Hall
- Emanuel, A.S. and Ranney, J.C. 1981. Studies of Offshore Reservoir with an Interfaced Reservoir/Piping Network Simulator. *SPE Journal of Petroleum Technology* **33** (3): 399-406. 00008331.
- Ertekin, T., Abou-Kassem, J.H., King, G.R., 2001. *Basic Applied Reservoir Simulation*, Richardson, Texas: Textbook Series, SPE.
- Fang, W.Y. and Lo, K.K. 1996. A Generalized Well-Management Scheme for Reservoir Simulation. *SPE Reservoir Engineering* **11** (2): 116-120. 00029124.
- Gonzalez, F.E., Lucas, A.K., Bertoldi, L.G.P. et al. 2010. A Fully Compositional Integrated Asset Model for a Gas-Condensate Field. Presented at the SPE Annual Technical Conference and Exhibition. SPE-134141-MS.

- Hayder, E.M., Dahan, M., and Dossary, M.N. 2006. Production Optimization through Coupled Facility/Reservoir Simulation. Presented at the Intelligent Energy Conference and Exhibition. SPE-100027-MS.
- Hepguler, G., Barua, S., and Bard, W. 1997. Integration of a Field Surface and Production Network with a Reservoir Simulator. *SPE Computer Applications* 9 (3): 88-92. 00038937.
- Holmes, J.A. 1983. Enhancements to the Strongly Coupled, Fully Implicit Well Model: Wellbore Crossflow Modeling and Collective Well Control. Presented at the SPE Reservoir Simulation Symposium. 00012259.
- Holmes, J.A., Barkve, T., and Lund, O. 1998. Application of a Multisegment Well Model to Simulate Flow in Advanced Wells. Presented at the European Petroleum Conference. 00050646.
- Litvak, M.L. and Darlow, B.L. 1995. Surface Network and Well Tubinghead Pressure Constraints in Compositional Simulation. Presented at the SPE Reservoir Simulation Symposium. 00029125.
- Okafor, C.C. 2011. Breaking the Frontiers for Effective Flow Assurance Using Integrated Asset Models (Iam). Presented at the SPE Arctic and Extreme Environments Conference and Exhibition. SPE-149537-MS.
- Stone, T.W., Edmunds, N.R., and Kristoff, B.J. 1989. A Comprehensive Wellbore/Reservoir Simulator. Presented at the SPE Symposium on Reservoir Simulation. 00018419.

- Trick, M.D. 1998. A Different Approach to Coupling a Reservoir Simulator with a Surface Facilities Model. Presented at the SPE Gas Technology Symposium. 00040001.
- Ursini, F., Rossi, R., and Pagliari, F. 2010. Forecasting Reservoir Management through Integrated Asset Modelling. Presented at the North Africa Technical Conference and Exhibition. SPE-128165-MS.
- Wickens, L.M. and Jonge, G.J.d. 2006. Increasing Confidence in Production Forecasting through Risk-Based Integrated Asset Modelling, Captain Field Case Study. Presented at the SPE Europec/EAGE Annual Conference and Exhibition. SPE-99937-MS.